DOCTOR OF PHILOSOPHY

The functional characterisation of TEX19 in human cancer cells and stem cells to explore clinical potential

Hazazi, Ali

Award date:
2017

Awarding institution:
Bangor University

PRIFYSGOL
BANGOR
UNIVERSITY

The functional characterisation of *TEX19* in human cancer cells and stem cells to explore clinical potential

Ph.D. Thesis 2017

Ali Mohammed Hazazi

Declaration and Consent

Details of the Work

I hereby agree to deposit the following item in the digital repository maintained by Bangor University and/or in any other repository authorized for use by Bangor University.

Author Name: Ali Mohammed Hazazi

Title: The functional characterisation of *TEX19* in human cancer cells and stem cells to explore clinical potential.

Supervisor/Department: DR. Ramsay McFarlane / Dr. Jane Wakeman / SBS/SMS

Funding body (if any): Security Forces Hospital, Kingdom of Saudi Arabia

Qualification/Degree obtained: PhD

This item is a product of my own research endeavours and is covered by the agreement below in which the item is referred to as "the Work". It is identical in content to that deposited in the Library, subject to point 4 below.

Non-exclusive Rights

Rights granted to the digital repository through this agreement are entirely non-exclusive. I am free to publish the Work in its present version or future versions elsewhere.

I agree that Bangor University may electronically store, copy or translate the Work to any approved medium or format for the purpose of future preservation and accessibility. Bangor University is not under any obligation to reproduce or display the Work in the same formats or resolutions in which it was originally deposited.

Bangor University Digital Repository

I understand that work deposited in the digital repository will be accessible to a wide variety of people and institutions, including automated agents and search engines via the World Wide Web.

I understand that once the Work is deposited, the item and its metadata may be incorporated into public access catalogues or services, national databases of electronic theses and dissertations such as the British Library's EThOS or any service provided by the National Library of Wales.

I understand that the Work may be made available via the National Library of Wales Online Electronic Theses Service under the declared terms and conditions of use (http://www.llgc.org.uk/index.php). I agree that as part of this service the National Library of Wales may electronically store, copy or convert the Work to any approved medium or format for the purpose of future preservation and accessibility. The National Library of Wales is not under any obligation to reproduce or display the Work in the same formats or resolutions in which it was originally deposited.

Statement 1:

This work has not previously been accepted in substance for any degree and is not being concurrently submitted in candidature for any degree unless as agreed by the University for approved dual awards.

Signed ……..

Date: ……

Statement 2:

This thesis is the result of my own investigations, except where otherwise stated. Where correction services have been used, the extent and nature of the correction is clearly marked in a footnote(s).

All other sources are acknowledged by footnotes and/or a bibliography.

Signed …….

Date …….

Statement 3:

I hereby give consent for my thesis, if accepted, to be available for photocopying, for inter-library loan and for electronic storage (subject to any constraints as defined in statement 4), and for the title and summary to be made available to outside organisations.

Signed …….

Date …….

NB: Candidates on whose behalf a bar on access has been approved by the Academic Registry should use the following version of Statement 3:

Statement 3 (bar):

I hereby give consent for my thesis, if accepted, to be available for photocopying, for inter-library loans and for electronic storage (subject to any constraints as defined in statement 4), after expiry of a bar on access.

Signed .....

Date .....

Statement 4:

I agree to deposit an electronic copy of my thesis (the Work) in the Bangor University (BU) Institutional Digital Repository, the British Library ETHOS system, and/or in any other repository authorized for use by Bangor University and where necessary have gained the required permissions for the use of third party material.

In addition to the above I also agree to the following:

1. That I am the author or have the authority of the author(s) to make this agreement and do hereby give Bangor University the right to make available the Work in the way described above.
2. That the electronic copy of the Work deposited in the digital repository and covered by this agreement, is identical in content to the paper copy of the Work deposited in the Bangor University Library, subject to point 4 below.
3. That I have exercised reasonable care to ensure that the Work is original and, to the best of my knowledge, does not breach any laws – including those relating to defamation, libel and copyright.
4. That I have, in instances where the intellectual property of other authors or copyright holders is included in the Work, and where appropriate, gained explicit permission for the inclusion of that material in the Work, and in the electronic form of the Work as accessed through the open access digital repository, *or* that I have identified and removed that material for which adequate and appropriate permission has not been obtained and which will be inaccessible via the digital repository.
5. That Bangor University does not hold any obligation to take legal action on behalf of the Depositor, or other rights holders, in the event of a breach of intellectual property rights, or any other right, in the material deposited.
6. That I will indemnify and keep indemnified Bangor University and the National Library of Wales from and against any loss, liability, claim or damage, including without limitation any related legal fees and court costs (on a full indemnity bases), related to any breach by myself of any term of this agreement.

Signature: ……

Date: ……

Abstract

The study of human embryonic stem cells (hESCs) and cancer cells *in vitro* is useful for exploring the behaviour of cells employed in the development of regenerative medicine and clinical applications. Testis expressed 19 (*TEX19)* is a specific human germ/stem cell gene identified as cancer testis antigen (CTA) gene that has recently emerged as a potential therapeutic drug target. CTA gene expression is normally restricted to human germline tissues, and these genes are activated in a wide range of tumour cells and cancer stem cells, hence, their intrinsic characteristics mark them as excellent potential cancer-specific biomarkers and promising drug/immunotherapeutic targets. CTA gene expression has been linked with stemness, but their function in stem cells has not been fully explored.

The findings of this study confirmed that *TEX19* is a CTA gene that is expressed in the testes and in numerous cancer types. Additionally it was demonstrated that human *TEX19* is expressed in hESCs and Induced pluripotent stem cells (iPSCs). TEX19 has dual cellular localisation, namely in the nucleus/cytoplasm, and may have a dynamic localisation in cancer cells. TEX19 is demonstrated to be a candidate oncogenic driver with a potential function in enhancing cancer cell proliferation and the self-renewal of human cancer cells *in vitro*; hence, it could contribute to influencing clinical outcomes. Furthermore, evidence is provided that TEX19 potentially acts as a transcriptional regulator by altering the transcript levels of multiple genes in distinct human cancer cells. TEX19 also regulates the mRNA levels of crucial stem cell marker genes in hESCs, *NANOG* in particular. These data also show that the loss of pluripotency in different human embryonic stem (hES) cell lines upon differentiation modifies the *TEX19* mRNA levels. Finally, the study demonstrates that TEX19 is required to control transposable element (TE) transcript levels in cancer cells and hESCs. Taking these findings together, the observations from cancer cells and hESCs suggest that *TEX19* is a stemness regulatory factor with possible application as a cancer biomarker/therapeutic target.

Acknowledgments

I am thrilled to have had the opportunity to complete this work. I am extremely grateful to Allah for giving me the power and patience to reach this stage. On this occasion, I offer my especial thanks to Dr Ramsay McFarlane for his supervision, tremendous assistance and unwavering support. In addition, I am thankful to Dr Jane Wakeman for sharing her experience and acting as my co-supervisor. I would also like to express my appreciation for the efforts of Mr Jason S. Williams and Dr John Sammut in sectioning FFPE tissue and carrying out assessments in the IHC experiments. Thanks and gratitude are extended to Dr Ellen Vernon, Dr Jana Jezkova and Dr Vicente Planells-Palop for their usual assist during my Ph.D. journey. I am grateful to all members of the McFarlane laboratory in the Medical School, past and present, for the time we spent working together as a team. I would like to thank the stem cell centre members at Sheffield University, namely Professor Peter W. Andrews and Dr Paul J. Gokhale, for their generous guesting and cooperation, as well as Dr Mark Jones for assisting with the FACS work. I would also like to thank Dr Lee Parry at the European Cancer Stem Cell Research Institute, Cardiff University. In addition, I deeply appreciate the support provided by Dr Hind Al Humaidan, who gave me the opportunity to practice the clinical applications of stem cells therapy at King Faisal Specialist Hospital in Riyadh. I would also like to extend my deepest thanks to the Department of Education Affairs at the Security Forces Hospital in Riyadh for offering me this prestigious scholarship and for their constant encouragement. Thanks to my close friend, Dr Faisal Alzahrani, for always being ready with encouraging words. Finally, at this moment, I cannot forget to express my huge gratitude to my family and my lovely daughter, Rawan, for standing together and supporting me in my steps towards excellence.

Thank you all

Ali Hazazi

Dedication

I would like to take advantage of this wonderful opportunity to dedicate my thesis to the Government of the kingdom of Saudi Arabia, which is conquering obstacles and working hard to advance the Country and ensure that it has a great future. Furthermore, I would also like to extend this dedication to the Security Forces Hospital due to the Hospital's unlimited efforts to cultivate medical services and make a meaningful contribution to the medical field for employees of the Ministry of Interior. I hope this effort contributes knowledge that helps to advance the vision of the clinical field in kingdom of Saudi Arabia.

Abbreviation

3'	Three prime end of DNA
5'	Five prime end of DNA
AML	Acute myeloid leukemia
ASCs	Adult stem cells
ACT	Beta Actin
bp	Base pair (s)
bFGF	Basic fibroblast growth factor
BRCA1	Breast cancer susceptibility 1
BRCA2	Breast cancer susceptibility 2
BSA	Bovine serum albumin
BTB	Blood-testis barrier
°C	Degrees Centigrade
cDNA	Complementary DNA
CNS	Central nervous system
CSCB	Centre of Stem Cell Biology
CSCs	Cancer stem cells
CTAs	Cancer-testis antigens
Da	Dalton
DAPI	4',6-diamidino-2-phenylindole
dH2O	Distilled water
DMEM	Dulbecco's Modified Eagle's Medium
DMSO	Dimethyl sulphoxide
DNA	Deoxyribonucleic acid
DPBS	Dulbecco's phosphate buffered saline
DSBs	Double-strand breaks
EDTA	Ethylenediaminetetraacetic acid
ELDA	Extreme limiting dilution analysis
ESCs	Embryonic stem cells
EST	Expressed sequence tag
FACS	Fluorescence-activated cell sorting

FBS	Foetal bovine serum
GAPDH	Glyceraldehyde 3-phosphate dehydrogenase
HBV	Hepatitis B virus
HCC	Hepatocellular carcinoma
HERVs	Human endogenous retrovirus
hESCs	human embryonic stem cells
HMBA	Hexamethylene bisacetamide
HSCs	Haematopoietic stem cells
HSCT	hematopoietic stem cell transplantation
IF	Immunofluorescence
IHC	Immunohistochemistry
iPSCs	Induced pluripotent stem cells
KDa	Kilodalton
MEFs	Mouse embryonic fibroblasts
mESCs	Mouse embryonic stem cells
mL	Milliliter
mM	Millimolar
mRNA	Messenger RNA
MSCs	Mesenchymal stem cells
ng	Nanogram
NAT	Normal adjacent tissues
NEAA	Non-Essential Amino Acids Solution
Oct4	Octamer-binding transcription factor 4
PCR	Polymerase chain reaction
PIWI	P-element induced wimpy testis genes
PIWIL	PIWI-like RNA-mediated gene silencing
pmol	Picomole
PSA	Prostate-specific antigen
PVDF	Polyvinylidene difluoride
RNA	Ribonucleic acid
RT-PCR	Reverse transcription-polymerase chain reaction
RT-qPCR	Quantitative, real time-polymerase chain reaction
SDS-PAGE	Sodium dodecyl Sulphate-polyacrylamide gel electrophoresis

SEREX	Serological screening of expression cDNA library
siRNA	Small interfering RNA
TAAs	Tumour associated antigens
TBE	Tris-borate-EDTA
TEs	Transposable Elements
TEX19	Testis expressed 19
Tris	Tris (hydroxymethyl) aminomethane
μg	Microgram
μL	Microliter
WB	Western blot
WHO	World Health Organization

List of Contents

List of Figures

List of Tables

Chapter1
Introduction

1. Introduction

1.1 The nature of cancer in humans

1.1.1 A general overview

Despite the fact that many deadly diseases have been eliminated either through vaccination or treatment, cancer, which was identified more than 3,000 years ago in the remains of humans, is still one of the world's deadliest diseases (Kelland, 2014). In fact, cancer is one of the major causes of death worldwide, particularly in developed and economically advantaged countries (Jemal et al., 2011). Despite the marked progress that has been made in the fight against this disease, cancer mortality rates remain high (Siegel et al., 2013).

A worldwide estimation by WHO provided evidence that cancer is killing more people than stroke and heart disease. Similarly, data indicates that cancer is 25% more harmful to men than to woman. In particular, lung cancer is diagnosed more frequently than breast, prostate, liver, stomach, colorectal cancer and other cancers. Breast cancer was diagnosed as the second killer and tops the list in women. Global Statistics for 2012 showed accelerated morbidity rates, with 14.1 million newly diagnosed cancer cases and a mortality rate in cancer patients of 8.2 million (Ferlay et al., 2015). Moreover, there are likely to be 20 million cancer cases by 2025 due to demographic and epidemiological changes in the world (Bray, 2014).

One in eight deaths worldwide is due to cancer, which includes more than 100 different diseases with miscellaneous risk factors and epidemiology. Cancer, which can initiate from any organ or cell type in the body, is characterised by the uncontrolled division of cells. In many cases, these cells can also invade normal tissues and distant organs in a development called metastasis. Epigenetic modification and DNA sequence mutation are also responsible to a large degree for the initiation of tumours by driving cancerous cell proliferation (Stratton et al., 2009a; Sharma et al., 2010; Brábek et al., 2010; Tomasetti et al., 2013; Wodarz & Zauber, 2015).

1.1.2 Causes and types of cancer

Determining the causes of cancer is complicated, but several factors may be implicated, including viruses (Parka et al., 2016), chemicals, radiation (Burger et al., 2013) and smoking (Washio et al., 2016). Genetic factors, environmental factors, occupational factors, life style and obesity are also strongly associated with the occurrence of cancer (Negri Jr et al., 2016; Martin-Moreno et al., 2008; Song & Giovannucci, 2015).

Age is also considered a contributory factor, and men over the age of 40 are susceptible to bowel and prostate cancer. On the other hand, women may develop breast cancer around the age of 40, but this is most likely from the age of 50 on (Autier, 2016). Data from the United Kingdom indicates that 50% of cancer patients are diagnosed at approximately 70 years of age, while 52% die when they are ≥75 years old, suggesting a relationship between age and cancer morbidity and mortality (Moller et al., 2011). Alcohol consumption has been recognised as one of the major causes of female breast cancer (Hirko et al., 2016) and colorectal cancer, particularly in Europe. Previously, alcohol was only considered a factor in cancers of the oral cavity, oesophagus and liver (Schütze et al., 2011). Moreover, death due to alcohol consumption increased globally from 3.6% to 5.5% in all cancer cases between the period from 2002 to 2012 (Praud et al., 2016).

Tumours are mainly categorised as benign growths or malignant cancers. Benign tumours are non-cancerous, with a slow growth rate, and do not usually transfer to other tissues. In contrast, malignant tumours are cancerous and commonly migrate to other parts of the human body in a process known as invasion-metastasis (Figure 1-1). Malignant tumours are dangerous, particularly when they occur in the vital organs (Souhami & Tobias, 2005; Valastyan & Weinberg, 2011).

Cancerous diseases are divided into different classes based on cell type or the organ of origin. For example, leukaemia is a blood cell cancer (Park et al., 2016), while a sarcoma is a type of cancer that originates from the mesenchymal connective tissues and occurs in muscles, cartilage and blood vessels (Sato et al., 2016). Bowel cancer arises from the colon or rectum (Kisiel et al., 2016). Blastomas are another type of cancer, which derives from immature tissues (Story & Johnston, 2016).

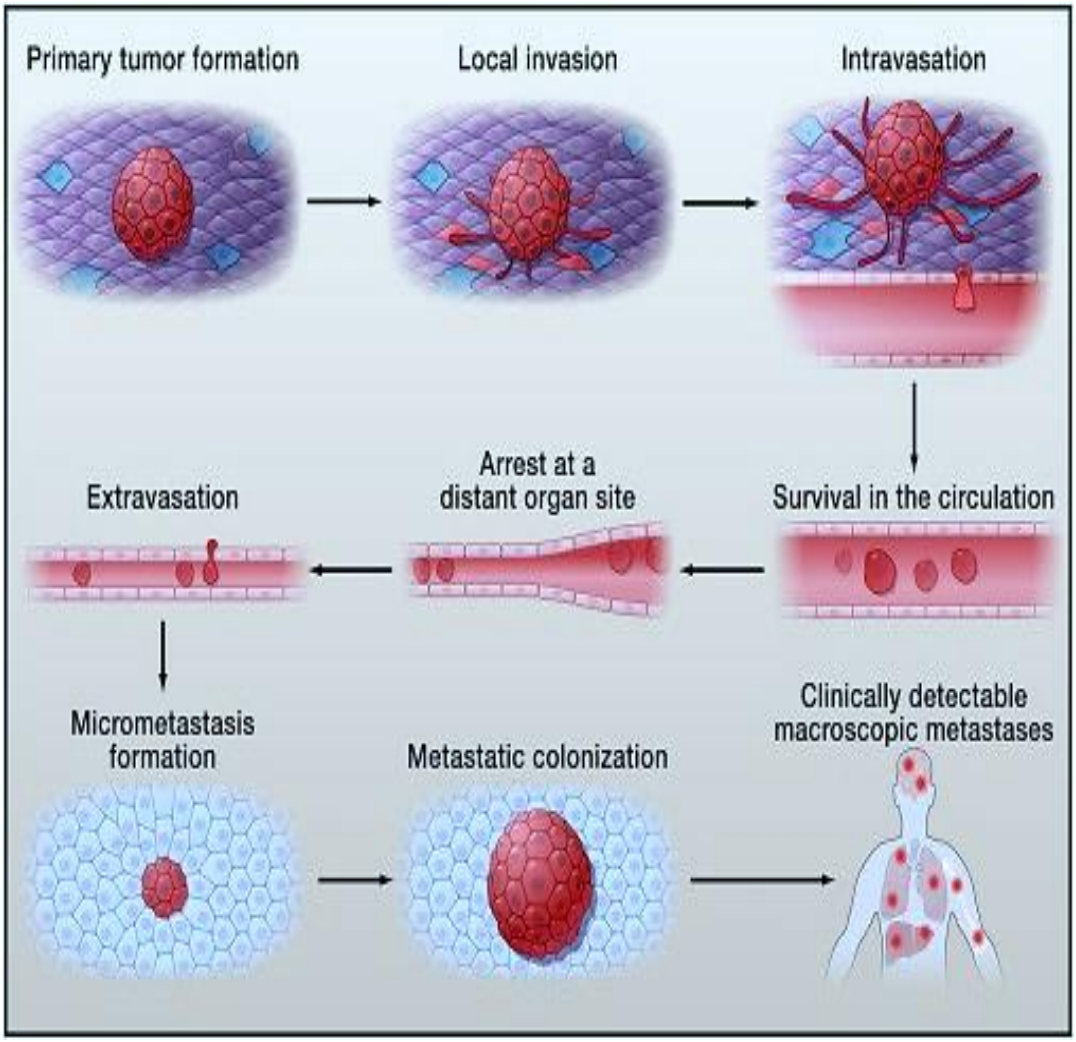

Figure 1-1 Invasion and metastasis in the human body.
The process of invasion-metastasis accommodates a sequence of steps whereby tumour cells are transported to other distant sites. These cancerous cells leave their primary location and start penetrating neighbouring tissues in a process known as local invasion. The tumour cells then commence the intravasation step, during which they invade the blood vessels and are transported by the blood circulation to distant tissues. In the extravasation step, the tumour cells then lodge in the small vessels of those tissues and attack them. The formation of a tiny colony of tumour cells is frequently designated a micrometastasis, and eventually, the last step, in which that colony develops into a colony of macroscopic size, is known as "metastatic colonisation" (Valastyan & Weinberg, 2011).

1.1.3 Biomarkers in cancer

Cancer biomarkers are defined as substances or processes that indicate the presence of cancer. They are secreted by the tumours in the body and can be detected as biological molecules in the blood, body fluids and tissues. They also serve as signals that indicate how the body is responding to cancer medication. Cancer biomarkers also play an important role in the disease's state by facilitating prediction, detection, diagnosis and prognosis. Tumour markers are distinctive for each type of cancer, and various factors such as tumour heterogeneity, occurrence and effectiveness influence their formation (Joshi et al., 2016; Mishra & Verma, 2010).

Alpha-fetoprotein (AFP) is one of the most notable cancer biomarkers and has been used efficiently for a long time to detect hepatocellular carcinoma (HCC) (Lai et al., 2012). However, new clinical studies have highlighted the importance of testing AFP, P53 and AFP-L3 together as efficient cancer biomarkers for HCC diagnosis in patients (Abdel-Aziz et al., 2016). Similarly, carcinoembryonic antigen (CEA) is considered the most common biomarker for colon cancer (Tiernan et al., 2013) and is also a sensitive biomarker for rectal adenocarcinoma screening (Makarova-Rusher et al., 2016). A positive test for the *BRCA1* and *BRCA2* gene mutation is linked with breast cancer in particular, but also with ovarian cancer (Kuchenbaecker et al., 2016). Prostate-specific antigen (PSA) is a significant and prognostic biomarker for prostate cancer (Kirby, 2014; Heidenreich et al., 2014), and C19-9 is a detectable and very sensitive biomarker for patients suffering from pancreatic cancer (Luo et al., 2016).

In light of the above, consideration of cancer biomarkers has become fundamental in the field of medicine because of their significance to detect cancer in early stage. Biomarkers can also aid in measuring the response of cancer patients to treatment doses. While not all cancer biomarkers have high sensitivity, and only a few are specific in terms of cancer detection, screening with these biomarkers should be mandatory in certain cases in order to reduce cancer morbidity (Karley et al., 2011; Mishra & Verma, 2010; Wu & Qu, 2015).

1.1.4 Hallmarks of tumorigenesis development

The hallmarks of cancer are the factors that are recognised as being essential for the formation of malignant tumours. These factors are specific to cancers and enable them to survive, disseminate and proliferate. In general, cancer cells are characterised by six traits or hallmarks. One of these is self-sufficiency in terms of growth signals, which means that the division of cancer cells occurs in the absence of growth signals. In contrast, the normal cells are controlled by external growth signals, which play a critical role in regulating cell division. Insensitivity to anti-growth signals is another cancer hallmark, as is evasion of apoptosis, where cancer cells avoid the programmed cell death mechanism (apoptosis) that is essential for the removal of damaged cells. Bypassing this mechanism provides an opportunity for cancer cells to progress. Another hallmark of cancer is unlimited replicative potential, where tumour cells escape the cell death that normally occurs after a certain number of divisions; in other words, normal cells undergo only a limited number of replications. A further trait of cancer is the formation of blood vessels that deliver oxygen and nutrients to cancer cells through a process known as sustained angiogenesis. In addition, cancer cells can escape from their sites of origin and invade neighbouring tissues or adjacent organs in a process known as metastasis, which is the sixth known cancer hallmark (Hanahan & Weinberg, 2000).

In 2011, Hanahan and Weinberg added four more hallmarks of cancer. These involve the genome instability responsible for producing the genetic variety and inflammation that foster various hallmark functions. Specifically, evasion of the immune system and metabolic pathway abnormalities are proposed as additions to the list of cancer hallmarks (See Figure1.2) (Hanahan & Weinberg, 2011).

Despite the fact that Sonnenschein and Soto (2013) generally agree with the proposed hallmarks of cancer, they developed another critical study in a bid to elucidate the complicated pathway signalling system produced by cancer cells and not to minimise the idea of cancer in a group of proliferating cells. A linking of mRNA splice factors with metastasis and cancer development based on sequence methodologies has also been reported (Oltean & Bates, 2014). This paves the way for the aberrant alternative splicing of human genes to be proposed as an additional cancer hallmark (See

Figure1.3), whereby a single gene can code various proteins during the process of gene expression (Ladomery, 2013).

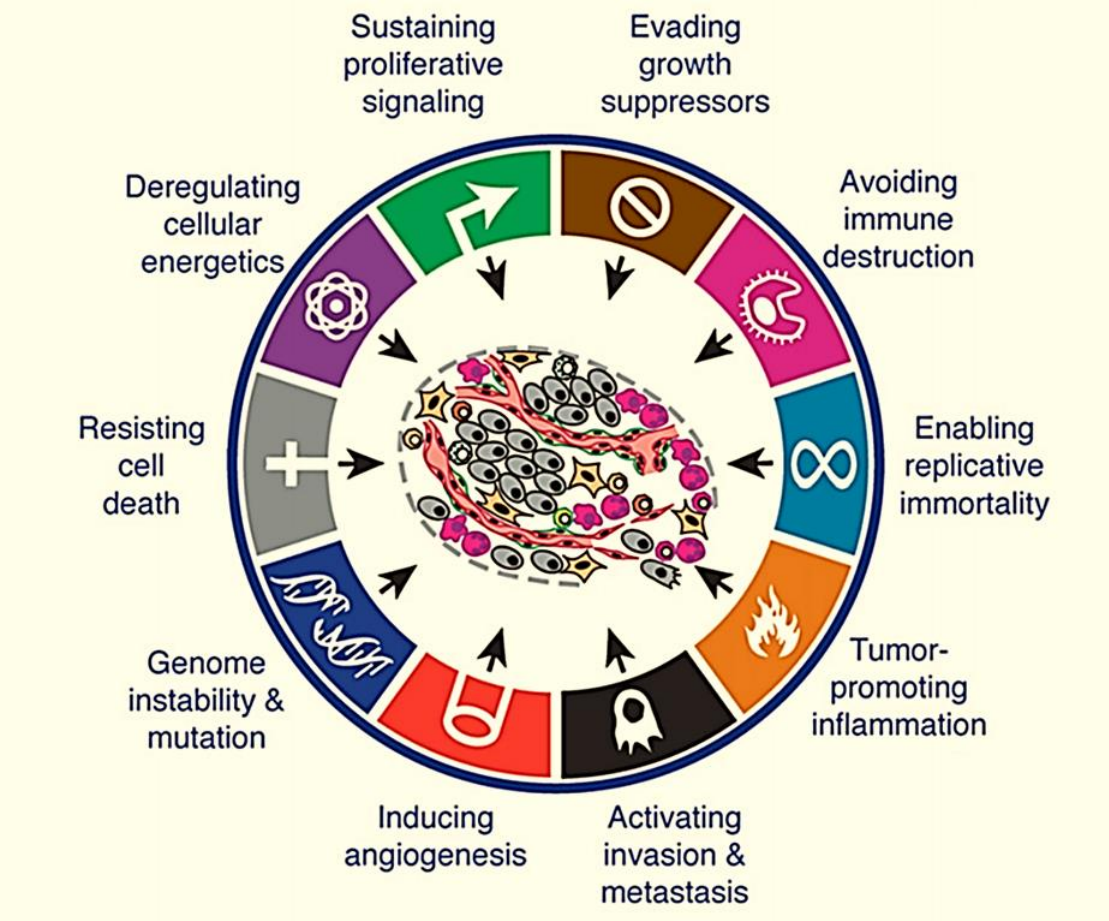

Figure 1-2 Original cancer hallmarks.
Hanahan and Weinberg's proposed elucidation of the first and second generation cancer hallmarks in the development of tumorigenesis (Hanahan & Weinberg, 2000; Hanahan & Weinberg, 2011).

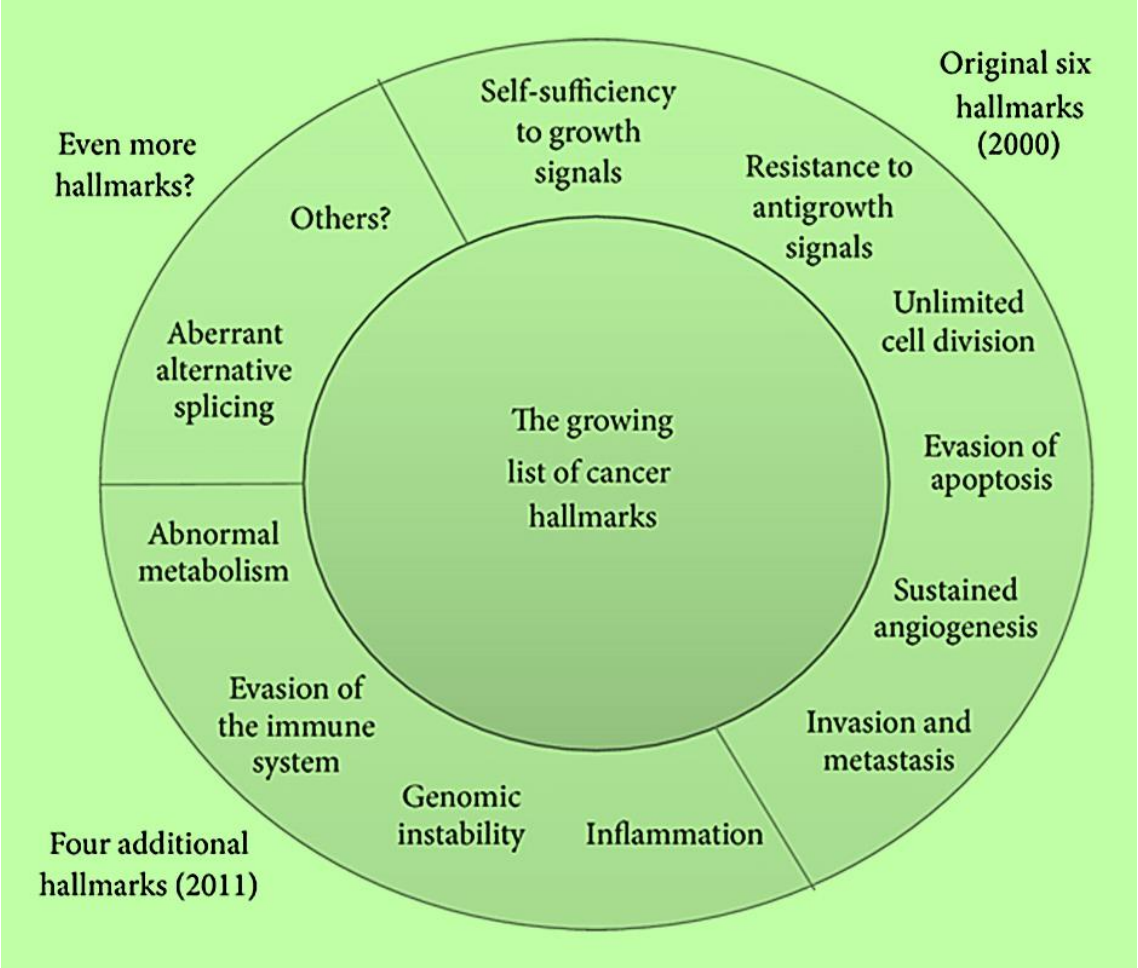

Figure 1-3 Additional cancer hallmarks.
Ladomery proposed aberrant alternative splicing as a further cancer hallmark. (Ladomery, 2013).

1.2 Influence of genomic stability on cancer

In-depth studies of tumorigenesis formation have indicated that three categories of gene are involved. Tumour suppressor genes, oncogenes and genomic stability genes which are implicated in regulating the process of chromosome segregation and DNA repair. However, cell proliferation is precisely regulated, and these three gene types contribute to cancer hallmarks. Alterations in oncogene and tumour suppressor gene expression are the leading causes of interrupted cell division and the subsequent formation of cancers. Oncogenes promote cell growth and have the potential to cause cancer, while tumour suppressor genes inhibit cell growth and promote apoptosis. A combination of oncogene expression at a high level and dysfunction or mutation of the tumour suppressor genes can trigger oncogenesis (Kim, 2015; Morris & Chan, 2015; Ferguson, et al. 2015; Negrini et al., 2010a; Vogelstein & Kinzler, 2004; Hanahan & Weinberg, 2011).

1.2.1 Tumour suppressor genes in tumorigenesis

Tumour suppressor genes (TSGs) are genes that have the ability to protect cells from the path to cancer. The dysfunction and mutation of TSGs are a likely cause of normal cells reaching the cancer stage. TSGs play a significant role in maintaining the cell cycle and apoptosis, a process in which they maintain the gene expression responsible for the continuation of the cell cycle. Otherwise the cell cycle does not stop, which leads to uncontrolled cell division and ultimately, the development of cancer (Thoma et al., 2011; Weinberg, 2013). *TP53* is one of the most important tumour suppressor genes linked with fighting cancer, and genetic alterations in *TP53* have been detected in 50% of cancer cases. *TP53* has been shown to play a critical role in commencing the inhibition of the cell cycle, in antiangiogenesis processes and in maintaining programmed cell death. A reduction in its function also leads to metastasis (Zhang et al., 2015; Surget et al., 2014). The deactivation of *TP53* has frequently been detected in a range of cancers including colon cancer (Prabhu et al., 2016) and acute myeloid leukaemia (AML) (Seipel et al., 2016). Active *TP53* supports differentiation of the stem cells and the progenitor cells through specific pathways and regulated differentiation. Conversely, its absence results in the continuation of stem cell replication, which leads to oncogenic epigenetic pathways being maintained/activated (Levine et al., 2016).

1.2.2 Oncogenes and cancer initiation

Oncogenes facilitate the continuation of uncontrolled cell proliferation and prevent the activation of apoptosis. In essence, oncogenes are frequently mutated genes, and they can be expressed at a high level in tumours (Bagci & Kurtgöz, 2015; Croce, 2008). Correspondingly, other oncogenes, such as cancer testis antigen (CTA) genes, are not mutated genes but derive an immunogenic expression in cancer patients (Whitehurst, 2014; Yang et al., 2015). Furthermore, the proto-oncogene is a gene that has the ability to change into oncogenes under specific conditions, such as mutation. Several factors can activate oncogenes, including mutations in the gene, chromosomal translocation and gene amplification (Bagci & Kurtgöz, 2015; Croce, 2008).

Mutation in the oncogenes change the structure of the encoded proteins in a way that alters their activity. The *Ras* oncogenes family, involving the *KRAS, HRAS* and *NRAS* genes, is an example of the oncogenes. (Croce, 2008; Fernández-Medarde & Santos, 2011). The mutation in different oncogenes has led to different types of carcinoma; for example, the mutation of the *KRAS* oncogene has been found to result in bowel, pancreatic and lung cancer (Rodenhuis, 1992), whereas myelodysplastic syndrome and acute myelogenous leukaemia have been detected in the case of mutations in *NRAS* oncogenes (Beaupre & Kurzrock, 1999). In addition, the *BRAF* gene is an example of a proto-oncogene that has been activated in different carcinomas, specifically, in 18% of bowel cancers, 59% of melanomas and 14% of liver carcinomas (Davies et al., 2002; Bagci & Kurtgöz, 2015; Solit et al., 2006).

Abnormalities in hereditary material and mutations generated by agents that damage DNA are known to influence cancer formation. Chromosome translocation is one of the genetic abnormalities linked with certain types of cancer, such as chronic myeloid leukaemia (CML), which arises from a mutual translocation between chromosomes 9 and 22 and is also known as Philadelphia translocation (Stratton et al.,2009b). Chromosome instability (CIN) leads to congenital abnormalities such as Down syndrome, and also plays a role in the promotion or suppression of tumour progression (Pfau & Amon, 2012). Likewise, chromosomal translocation can produce a mutation in the *EWSR1* gene, causing it to become an oncogene, and this subsequently leads to Ewing sarcoma in children (Slotkin et al., 2016). Gene amplification has a role in

initiating and developing oncogenes in solid tumours by increasing or doubling gene numbers, for example, the *ERBB2* gene in breast cancer (Bagci & Kurtgöz, 2015).

1.2.3 Genome stability genes

Genome stability genes are a set of genes that have been found to play a role in terms of maintaining genetic modifications and regulating DNA errors. Likewise, these genes also serve a dynamic purpose in chromosome segregation. However, alterations or genetic changes in these genes have been shown to initiate tumours in the body (Negrini, Gorgoulis & Halazonetis, 2010a). For example, *NBS1* gene is implicated and required in DNA double-strand break (DSB) repair (Sharma et al., 2015), and the mutation of this gene is associated with Nijmegen breakage syndrome (NBS), which is a congenital disorder (Tauchi, 2000). Moreover, the over expression of this gene is linked with prostate cancer (Berlin et al., 2014), oesophageal carcinoma (Kuo et al., 2012) and liver cancer (Wang et al., 2014). Furthermore, *BRCA1* and *BRCA2* are tumour suppressor genes that sustain a function in DNA repair and genome stability, and they are activated in breast / ovarian cancers, for which their activation serves as a risk indicator (Yoshida & Miki, 2004; Trego et al., 2016). Reduced function of the mouse double minute 2 homolog (MDM2), which is a protein encoded by the *MDM2* gene in the human, has been linked with the inhibition of DSB DNA repair. The *MDM2* gene has been found to be over expressed in certain type of cancers as an oncogene factor, while being down regulated in other tumours. This suggests that the *MDM2* gene behaves like a tumour suppressor gene and like an oncogene, depending on the relevant cellular setting (Maluszek, 2015).

1.3 Tumour-associated antigens (TAAs)

Tumour-associated antigens (TAAs) are capable of activating the immune system by producing antigenic determinants (epitopes) that are distinguishable by the immune system. TAAs can be exploited in cancer immunotherapy as they are produced in tumour cells but not in healthy cells (Krishnadas et al., 2013). The identification of novel TAAs is important to develop the field of cancer immunotherapy (Zavala & Kalergis, 2015). Various known TAAs are classified into different groups, including cancer testis antigens (CTAs), self-antigens (Savage et al., 2014) and viral antigens (Kelderman & Kvistborg, 2016). CTAs are a major group of TAAs. They are encoded

by genes that are characterised by their expression in cancer cells and germline tissues, not in other healthy somatic cells. In cancer, these developmental antigens are also produced in several kinds of malignant tumours as tumour-associated genes become active (Gjerstorff et al., 2015; Krishnadas et al., 2013; Mooney et al., 2016). Another group of TAAs are self-antigens, which are proteins that are over produced in cancer cells compared with healthy cells. TPD52 is an example of a tumour self-antigen that is frequently identified in various human malignant tumours (Bright et al., 2014). In addition, the family of self-antigens includes another type of antigen known as neo-antigens, which are produced due to new mutations in the genes normally expressed in healthy tissue. Since neo-antigens are newly formed, they are not recognised by the immune system (Lu & Robbins, 2016; Savage et al; 2014). Finally, viral antigens are proteins that are mainly derived from infections by oncogenic viruses. Such proteins are produced inside cancerous cells and form antigenic peptides that become recognisable by T cells (Kelderman & Kvistborg, 2016; Vigneron, 2015). For example, hepatitis B surface antigens (HBsAg) are associated with the development of hepatocellular carcinoma caused by infection from the hepatitis B virus. HBsAg can also accumulate in cirrhosis of the liver, so may not be a tight cancer- specific marker (Chu & Liaw, 2016).

1.3.1 Cancer testis antigen genes

CTAs are group of proteins encoded by genes whose expression is silenced in normal healthy somatic tissue and largely restricted to the tissues of the testis. These genes are found to be expressed in a wide range of tumour cells and cancer stem-like cells, and their intrinsic characteristics mark them as a promising therapeutic target (Whitehurst, 2014; Yang et al., 2015).Chen et al. (1997) were the first to coin the term "cancer testis antigen genes", which are also known as cancer germline antigen genes (Chen et al., 1997). CTAs can also act as neo-antigens in cancer cells due to the lack of expression of MHC class I antigens in germ cells, which subsequently causes the complex recognition of germ cell antigens by cytotoxic T-cells. Therefore, CTA proteins have high immunogenicity in cancer patients (Hirohashi et al., 2016).

In 1991, T-cell epitope cloning became the primary technique used to identify the first CTA gene family, named melanoma antigen-1 (*MAGE-A1*), from melanoma patients

(van der Bruggen et al., 1991). In the following years, other CTA genes, such as *MAGE-A2*, *MAGE-A3* and *GAGE-1*, were identified by applying similar methods (Chomez et al., 2001; De Backer et al., 1999; Gaugler et al., 1994). SEREX (serological analysis of recombinant cDNA expression libraries) technique was the next approach developed to discover further CTA genes. This technique has the capability to enable the analysis of immune response to tumour antigens. The approach entails the screening and serological analysis of the cDNA expression libraries of human tumours, with autologous sera from cancer patients (Sahin et al; 1997). The description of this method has proved beneficial in terms of classifying further CTA genes, including *NY-ESO-1* (Chen et al., 1997), *SSX* (Tureci et al., 1998) and *SCP1* (Tureci et al., 1998). In addition, new clinically relevant CT genes have been identified using bioinformatics approaches that designated meiosis-specific CT antigen genes (meiCT) (Feichtinger et al., 2012; Sammut et al., 2014). Correspondingly, cooperative schemes, such as the Cancer Genome Atlas (TCGA), have identified hundreds of CTA genes from expression profiles for large numbers of cancer patients (Kandoth et al., 2013; Lawrence et al., 2014; Vogelstein et al., 2013; Wang et al., 2016).

1.3.2 CTA gene classification

Multiple advanced strategies have identified more than 70 CTA gene families (Fratta et al., 2011). These different genes are classified into X-CTA and non-X-CTA genes (Simpson et al., 2005). The CTA genes that are localised on the X chromosome are termed X-CTA genes and are organised in well-defined clusters. X-CTA genes have been found to make up 10% of the total genes on the X chromosome. Examples of X-CTA genes include members such as *MAGE-A*, *MAGE-8*, *XAGE-2*, *MAGE-A3* and *NY-ESO-1* (Caballero & Chen, 2009; Simpson et al., 2005; Stevenson et al., 2007). Correspondingly, the autosomal chromosomes contain the CTA genes that are termed as non-X-CTA genes, which are generally distributed in singal copies (Simpson et al., 2005). *SCP-1* and *HORMD1* are examples of non X-CTA genes (Chen et al., 2005; Tureci et al., 1998). The different localisation for both X-CTA and non-X-CTA genes could suggest distinctive function (Caballero & Chen, 2009).

The classification of the identified CTA genes has been further extended into four groups, according to the expression profile in normal and malignant tissues: (i) CTA

genes with highly restricted expression in cancers, adult testis and placenta; this group is considered to be testis-restricted; (ii) CTA genes showing expression only in cancers, adult testis, central nervous system (CNS); this group is considered to be testis-CNS-restricted; (iii) CTA genes expressed in cancers and the adult testis, with expression in no more than two normal tissues; this group is considered to be testis-selective; (iv) CTA genes showing expression in the cancers, adult testis, CNS tissues, with expression in no more than two normal tissues; this group is considered to be CNS-selective (Hofmann et al., 2008).

1.3.3 CTA gene functions

The role and function of the majority of identified CTA genes is not yet fully understood. That said, various studies have indicated possible functions of these genes in tumorigenesis (Caballero & Chen, 2009; Fratta et al., 2011; Sulek et al., 2016). The functioning of particular CTA genes is thought to contribute to associate the cellular process in germ line. For example, synaptonemal complex protein 1 (SYCP1) has an important role in meiosis and meiotic crossover formation and *SYCP1* deletion has been associated with sterility (de Vries et al., 2005; Schramm et al., 2011; Tureci et al., 1998). In addition, the meiosis specific cohesin complex proteins, RAD21L and SMC1β, are involved in the regulation of meiotic recombination and meiotic sister chromatid cohesion (Ishiguro et al., 2011; Lee & Hirano, 2011; Ward et al., 2016). SPO11, another CTA, is a meiosis-specific protein that creates DNA double-strand breaks (DSBs) required for the initiation of meiotic homologue recombination (Yamada and Ohta, 2013). MAGE family members have been determined to regulate the ubiquitination of proteins, and their deviant expression in cancer cells alters the signalling pathway and cellular progression through ubiquitination (Weon and Potts, 2015). For example, MAGE-A1 is involved in controlling cellular signalling pathways (Ghafouri-Fard and Modarressi, 2009). In addition, some CTAs can regulate others; for instance, the transcription factor BORIS has been found to regulate expression of the *MAGE* gene family (Schwarzenbach et al., 2014; Vatolin et al., 2005). Meanwhile, the function of some CTA genes has been determined to induce cell proliferation and act as a proto-oncogene, such as the *PIWIL2* gene (Cheng et al., 2011). The depletion of *MAGE-A* expression induces the recruitment of tumour suppressors such as P53, to target promoters (Marcar et al., 2010a) and elevates the expression of downstream

genes (Marcar et al., 2010b; Nardiello et al., 2011; Weon & Potts, 2015). In human melanoma, the upregulation of the CTA gene *CAGE* has been found to stimulate apoptotic evasion, allowing tumour development to take place (Kim et al., 2010). Correspondingly, the upregulated expression of *TSGA10* disturbs the hypoxia-inducible factor (HIF)-1α and drive the development of angiogenesis (Mansouri et al., 2016). Expression and deletion approaches have shown the function of the majority of CTAs in spermatogenesis (Whitehurst, 2014).

1.3.4 CTA gene expression

The expression of the majority of X-CTA genes takes place in the spermatogonia cells of the normal testis prior to spermatogenesis. However, the expression of some X-CTA members has also been detected in placenta cells. The expression of non X-CTA genes has been reported to occur in the late phase of germ cell differentiation (Simpson et al., 2005; Stevenson et al., 2007). In line with these studies, the expression of CTA genes is not found in somatic tissues. Evaluation of messenger RNA, for numerous CTA genes, has elucidated their limited expression in non-germ line tissues, such as those of the spleen, liver and pancreas. However, these genes have also been classified as CTA genes where the analysis of their expression level has stipulated that it is lower than 1%, compared to their expression in normal testes (Caballero and Chen, 2009). In addition, immunohistochemistry has revealed that some CTA genes were found to be regularly expressed in foetal ovarian tissues (Nelson et al., 2007). Experimental studies have indicated a behaviour whereby CTA genes are co-expressed in the same positive tumour to a high degree in the later stages of tumour development (Caballero and Chen, 2009). Various cancers have been identified as being addicted to the *MAGE* family for viability (Weon and Potts, 2015). In clinical follow-up, individual genes, such as *DKKL*, *PLU-1* and *MAGEA3*, have been reported to be over-expressed in colorectal cancer and correlated with disease progression (Tarnowski et al., 2016). Nevertheless, the unique expression of CTA genes has attracted attention in terms of their application in cancer immunotherapy and their use as stratification markers, as reflected in the many clinical trials that are currently underway (Rousseaux et al., 2013, Salmaninejad et al., 2016).

1.3.5 The clinical applications of CTAs

1.3.5.1 CTA genes as potential diagnostic biomarkers

The use of several strategies has revealed the potential of CTAs to act as tumour and diagnostic markers in a range of cancer types (Wang et al., 2016). The analysis of the CTA SPAG9 antibody in blood samples, has unveiled a significantly high production of this protein in patients who are developing lung cancer, compared to the normal tissues, suggesting the aptness of SPAG9 as a candidate diagnostic marker for said cancer (Ren et al., 2016). In colorectal cancer, the novel CTA gene *AKAP4* was expressed in the majority of 200 clinical samples of various stages and grades. This indicates the potential use of *AKAP4* expression for the early diagnosis of colorectal cancer (Jagadish et al., 2016). In prostate cancer, a positive correlation has been demonstrated between the clinical and pathological parameters, including patient age, PSA level and tumour stage, and the expression of the CTA gene *BORIS*. In addition, the BORIS protein is present in aggressive prostate tumours and reported as a candidate diagnostic marker for prostate cancer (Cheema et al., 2014). The evaluation of the CTA NY-ESO1 by immunohistochemistry in synovial sarcomas, gastrointestinal stromal tumours, spindle cell sarcomas and other sarcomas has illuminated a particular CTA profile for different cancers with similar morphologies. Correspondingly, *NY-ESO1* has been reported to be strongly expressed in 76% of tumours that are positive for synovial sarcomas. In contrast, the other tumours evaluated displayed either extremely low or negative expression of *NY-ESO1*. Therefore, CTA genes can be deployed to distinguish malignant tissues and may become clinically useful in terms of cancer diagnosis (Lai et al., 2012).

1.3.5.2 CTA genes in immunotherapy

Immunotherapy employs the immune system to fight the tumours. Active and passive immunotherapy are the two main approaches used against cancer (Baxter, 2014). The majority of patients who develop cancerous diseases frequently undergo conventional therapies in clinics, including radiation, chemotherapy and surgery. These clinical therapies are effective for the elimination of primary tumours. However, they are less efficacious when the tumour cells are disseminated and progress the metastatic diffusion of the disease. Immunotherapy is a promising approach, due to its exploitation

of substances that restore the body's immune system or induce it to eradicate cancer cells (Mellman et al., 2011; Schuster et al., 2006; Vigneron, 2015).

The testes are in an immunologically privileged tissue. This distinctive feature is mediated in part by the blood-testis barrier (BTB), along with the silent expression factors for the MHC I class in testicular germ cells, subsequently tolerated the introduction of CTA antigen genes without stimulating the immune response (Hirohashi et al., 2016; Jager et al., 1998; Tarnowski et al., 2016). Accordingly, CTA proteins are immunogenic and their recognition by the immune system can develop the immunotherapy approach (Caballero & Chen, 2009; Tarnowski et al., 2016). The peptides of CTA proteins can generate the immune response with the assistance of other immuno-stimulatory factors, which play a role in maintaining, enriching and strengthening the response (Meek and Marcar, 2012). Melero et al., (2014) have described the generation steps of this immune response (see Figure 1.4).

1.3.5.2.1 The role of CTA genes in active immunotherapy

Active immunotherapy has the capability to stimulate the immune system in order to induce individual responses against a cancer or other disease. The elicitation of the immune system may be non-specific where agents such as cytokines generate a general immune response. In contrast, the specific active immunotherapy triggers the immune system using therapeutic vaccines to distinguish and eradicate cancer cells that have specific antigens on their surfaces (Baxter, 2014). However, therapeutic vaccine trials have been evaluated in patients developing melanoma cancer, using CTA genes such as *NY-ESO-1* and *MAGE-A3*, and these genes have been found to contribute to the regression of the tumour nodules (Caballero and Chen, 2009). The CTA SP17 vaccination provided a successful trial *in vivo* for preventing ovarian cancer in mammals (Chiriva et al., 2010). The analysis of various tumours, including lung non-small cancer, colon cancer, melanoma, breast cancer, multiple myeloma and ovarian cancer, has illustrated the high expression of *MAGE* genes family. This means that the design of vaccines for this family can aid in preventing incidences of various malignant tumours (Weon and Potts, 2015).

1.3.5.2.2 The role of CTA genes in passive immunotherapy

In passive immunotherapy, the immune components or external antibodies initiate the elicitation of the immune response. Forms of passive immunisation include adoptive T-cell therapy and monoclonal antibodies (Baxter, 2014). The uses of gene engineering in lymphocyte T-cells have mediated tumour regression in patients developing metastatic cancer (Bonini & Mondino, 2015; Restifo et al., 2012). In T-cell therapy, the lymphocyte T-cell is isolated from patients, then subjected to a culturing and enrichment process *in vitro* to express the desired tumour antigens, followed by the re-infusion of the T-cell into the patient (Bonini & Mondino, 2015; Restifo et al., 2012). Correspondingly, the gene-engineered T-cells have demonstrated promising progress in targeting CTA antigens. For example, the isolation of autologous CD4+ T-cells from patients developing metastatic melanoma cancer was carried out *in vitro* for expansion and enrichment, in order to target the CTA NY-ESO-1, these cells were re-infused back into the patient. Patient monitoring revealed the cessation of the development of either the pulmonary or nodal tumours. Interestingly, after this successful treatment, the patients were declared cancer-free two years later (Hunder et al., 2008). In addition, the induction of NY-ESO-1 in the isolated CD8+ T-cells has increased the response of the immune system in detecting tumour cells in patients developing acute myeloid leukaemia (Srivastava et al., 2016).

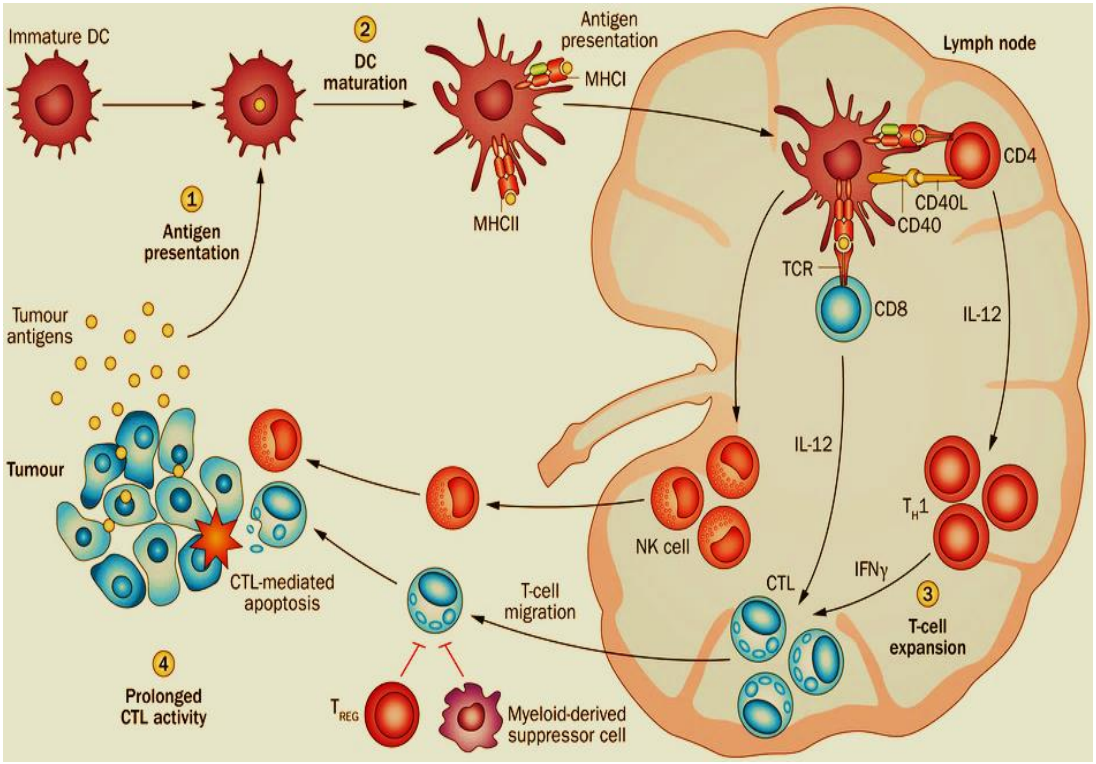

Figure 1-4 Generation of immune response alongside the tumour antigens.
The process of generating an immune response involves multiple steps: (1) Tumour cells can release the tumour antigens or the body can be immunised to elicit the immune response. This step can be activated by the CTAs. (2) Tumour cells can promote the maturation factors for the anti-dendritic cells in which this influence can be targeted. (3) The lymphocyte T-cell can be isolated, expanded and modified to identify the desired CTAs. (4) Clinical studies have reported the potential effect of checkpoint modifiers in sustaining the immune response through interaction with immunosuppressive mechanisms (Melero et al., 2014).

1.4 Pluripotent stem cells and cancer development

1.4.1 Stem cells overview

The term stem cell was first used in 1868 by Ernst Haeckel, who supported Charles Darwin's theory of evolution. The German term “Stammzelle” was used to describe them and they were thought to gives rise to all cells of the organism (Haeckel, 1874). Stem cells are unique in that they have the ability to become different types of cells. They are distinguished from other cells by two main features: first, the potential for self-renewal; and second, the ability to remain as stem cells or differentiate under controlled conditions into specialised cells after numerous cycles of cell division (Ullah et al., 2016). The specialised cells can form different organs, tissues, or specific cells, and play specific functions in the body. Repairing tissues is an example of a stem cell function in human development. Recent investigations have uncovered the potential use of stem cell in therapy for complicated diseases through regenerative medicine (Goodell et al., 2015; Ramalho-Santos & Willenbring, 2007; Stoltz et al., 2015).

1.4.2 Stem cells classification and characteristics

Self-renewal is the most distinct feature of stem cells. Stem cells are generally classified based on their potency. For example, the totipotent stem cells generated after egg fertilization (zygote) as a single cell have the ability to form all types of cells, organs, and extraembryonic tissues, which form placenta to develop the foetus (see Figure 1.5) (Surani & Tischler, 2012). After an 8-stage cell division, totipotent stem cells specialize into pluripotent stem cells, and these can generate all cell types except for placenta cells. Pluripotent cells develop embryonic stem cells, which can generate the three germ layers endoderm, mesoderm, and ectoderm (Condic, 2013; Keller & Gadue, 2016; Surani & Tischler, 2012). These cells continue to divide and specialize further into multipotent stem cells, which can generate a limited range of cells within a tissue lineage, such as haematopoietic stem cells (blood cells). Furthermore, stem cells can differentiate into oligopotent cells, which develop into few cell types such as myeloid cells, and unipotent cells, which differentiate into only one cell type. However, the multipotent, oligopotent, and unipotent stem cells are also identified as adult stem cells (Condic, 2013; Mitalipov & Wolf, 2009; Scholer, 2004; Surani & Tischler, 2012).

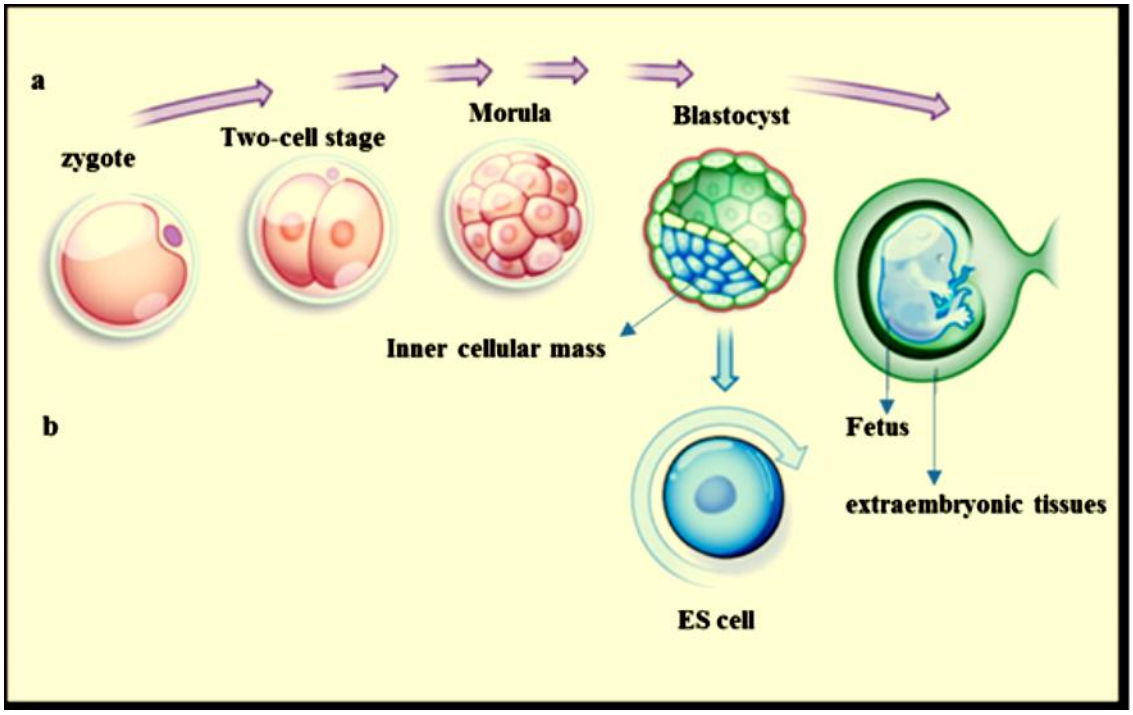

Figure 1-5 The development of embryonic stem cells.
(a) The embryo development after the egg fertilisation (Zygote). (b) The derivation of embryonic stem cells from the inner cellular mass after developing the blastocyst stage (Surani & Tischler, 2012).

1.4.3 Embryonic stem cells

The first successful trial to identify embryonic stem cells (ESCs) was recorded in 1981 in mice (Evans & Kaufman, 1981). The first derivation of human embryonic stem cells (hESCs) occurred in 1998 using IVF reproductive technology from the inner cell mass of blastocysts of fertilized oocytes *in vitro* (Thomson et al., 1998). hESCs have the ability to generate the three germ layers, which are formed in a process known as gastrulation. The three germ layers encompass ectoderm, mesoderm, and endoderm, and these layers are known as primary germ cells (Keller & Gadue, 2016). Each germ cell layer gives rise to a specific tissue. Ectoderm germ cell layers form skin, nervous system, and adrenal tissues. Mesoderm germ cell layers generate skeletal muscles, epithelia tissues, and haematopoietic cells. Endoderm germ layers give rise to the pancreases, liver, and respiratory system (Keller & Gadue, 2016). Since the isolation of hESCs, a number of protocols have been used to culture these cells *in vitro,* and mouse embryonic fibroblasts are generally used to initiate culturing *in vitro*. Matrigel and vitronectin with specific factors maintain the pluripotency and are used as a feeder free system. Furthermore, testing genetic integrity using karyotyping and whole genome

sequencing is required to ensure normal cells karyotype is maintained in hESCs cultures. (Braam et al., 2008; Damdimopoulou et al., 2016).

Embryonic stem cells have been proposed for clinical trials for decades and their functions in treating complicated diseases and replacing cells seem highly promising. Several factors, such as their plasticity led to great concern over their use and safety (Schwartz et al., 2015). In Parkinson disease, hESCs grafting was performed in animal models to generate dopamine, which acts as a precursor to pass messages to the nerve cells. The trial was encouraging for a clinical trial under safe and efficient conditions (Tabar, 2016). Furthermore, hESCs helped enhance hepatocyte maturation and proliferation in patients with liver cirrhosis by Notch pathway inhibition and activation of Wnt and ERK pathways (Chen et al., 2016). Moreover, clinical research of hESCs has developed models for glaucoma drugs and set up possibilities of using cellular therapy for people who have lost their vision (Chamling et al., 2016).

1.4.4 Adult stem cells

Adult stem cells (ASCs) are also known as somatic stem cells and their potency types are identified as multipotent, oligopotent, and unipotent. These types of cells have the ability to specialise into major cells of specific tissues or organs. Hematopoietic stem cells, mesenchymal stem cells, liver stem cells, skin stem cells, and pancreatic stem cells are all examples of the multipotent stem cells. Hematopoietic and Mesenchymal stem cells are the most investigated adult stem cells due to their positive and promising roles in regenerative medicine (Clevers, 2015; Nussler & Sajadian, 2014; Woo et al., 2016). ASCs possess vital self-renewal properties and have essential functions in repairing damaged tissues or replacing dead and damaged cells in specific tissues or organs (Passier & Mummery, 2003). ASC populations are established in particular environments known as niches in undifferentiated state. These niches prevent the depletion of ASCs, save them from outside damaging stimuli, and keep them in inactive situations until receiving proper activation signals. Based on a specific tissue demands, ASCs become active by signalling and start proliferation. They migrate from the niches, differentiate to replace deteriorated cells or repair damaged tissue cells, and sustain organ function and structure. ASCs are also, found to heal minor injuries in numerous

organs, such as bone marrow, kidney, intestine, and liver (Jiang et al., 2002; Montagnani et al., 2016; Passier & Mummery, 2003; Scadden, 2006; Woo et al., 2016).

1.4.4.1 Haematopoietic stem cells

Haematopoietic stem cells (HSCs) are an example of adult stem cells. They differentiate and develop all mature functional blood cells encompassing the myeloid and lymphoid cells in the circulatory system. The differentiation of the myeloid and lymphoid linage drives via the haematopoiesis process, and they mainly occupy the bone marrow (BM) (Seita & Weissman, 2010; Clarke & Frampton, 2016; Henschler, 2016). The myeloid cell line gives rise to particular blood cells including Basophils, Neutrophils, Eosinophils, Macrophages, Erythrocytes, Monocytes, and platelets, while the lymphoid lineage forms natural killer cells, T-lymphocytes, and B-lymphocytes (Till & McCulloch, 1961). Both cytokines and BMP-4 factors promote the differentiation process of HSCs (Chadwick et al., 2003). Since the isolation of human HSCs (Baum et al., 1992), CD34 surface marker has been the most important feature and surface marker used to identify human HSCs (Civin et al., 1984). Moreover, the CD34 surface antigen is down-regulated expression as long the human HSCs differentiate into hematopoietic progenitors, and this points an important function for CD34 to maintain human HSCs (Andrews et al., 1989). The power of human HSCs to produce abundant lines of blood cells has led to clinical and crucial breakthroughs in hematopoietic stem cell transplantation (HSCT) to cure complex diseases such as haematological malignancies, including acute myeloid leukaemia (AML), chronic myeloid leukaemia (CML), Hodgkin's lymphoma (HL), and Multiple myeloma. Additionally, HSCTs have made a major contribution to rebuilding damaged bone marrow and are known to cure diseases such as sickle cell anaemia and thalassemia (Felfly& Haddad, 2014; Park et al., 2015; Passweg et al., 2016).

Autologous and allogeneic are the main HSCT graft types. In an autologous procedure, the patient donates stem cells from his or her own blood before proceeding with chemotherapy, and subsequently those cells are returned to the patient after treatment. In contrast, in an allogenic HSCT, stem cells are harvested from an HLA- or ABO-matched relative or non-relative donor. Incompatible antigens result in transplant hyper rejection and engraftment failure. The autologous graft type is generally used to cure a

cancer not damaging the bone marrow, such as lymphoma, and this transplant has a limited percentage of rejection as the body can recognise the transplanted cells (Grube et al., 2016; Park et al., 2015). Conversely, clinicians in certain cases, such as leukaemia, use allogenic transplants to repair bone marrow failure. While this type of transplant is routinely used and has become a conventional treatment, the struggle to obtain a full HLA match can make it difficult to proceed with the allogenic graft. In addition, with allogenic HSCTs there is the risk of developing acute and/or chronic Graft versus Host Disease (GVHD) which result in transplant rejection (Grube et al., 2016; Shono et al., 2016).

When there is no fully matched donor or there is difficulty in obtaining human HSCs, the umbilical cord blood derived from new-borns becomes a remarkable alternative source of human HSCs that can be used to cure hematologic malignancies. Furthermore, cord blood stem cells are less immunogenic and more immature than stem cells harvested from adults, which offers them better regenerative aptitudes with minor incidences of Graft versus Host disease (de Lima et al., 2012; Delaney et al., 2010; Tiwari et al., 2016).

1.4.4.2 Mesenchymal stem cells (MSCs)

MSCs, also known as stromal cells, are multipotent and a further example of adult stem cells. MSCs are derived from the germ layer mesoderm and differentiate to give rise to bones, cartilage, muscles, and fat (Ding et al., 2011; Kalervo Väänänen, 2005). In addition, they are known as skeletal stem cells as they generate skeletal tissues (Bianco et al., 2006; Bianco & Robey, 2015). Human MSCs exist mainly in bone marrow, but they are also known to have a limited presence in the umbilical cord (Bieback & Netsch, 2016). Specific transcription factors and regulatory genes act in controlled functions and trigger the MSCs to differentiate to multiple linages (Dennis et al., 2001). In addition, the MSCs perform active and physiological tasks to maintain the niches of haematopoietic stem cells and regulate the emergence of a hematopoietic microenvironment (Bianco, 2014). The clinical application of MSCs becomes the closest use for stem cells in transplant after haematopoietic stem cells, as MSCs have emerged as a promising therapy to repair damaged cartilage or replace bone tissues.

However, engraftment of these types of cells in injured tissues was determined with small numbers of transplanted cells (Motavaf et al., 2016; Walmsley et al., 2016).

1.4.5 Induced pluripotent stem cells (iPSCs)

In 2006, somatic cell genetic reprogramming generated an exceptional type of stem cells known as induced pluripotent stem cells (iPSCs), and was a seminal breakthrough in the stem cells field. Four transcription factor genes, *Oct4*, *c-Myc*, *Klf4*, and *Sox2*, were introduced to mouse fibroblast cells via viral transduction and have generated iPSCs under embryonic conditions (Takahashi & Yamanaka, 2006). Likewise, the four exact transcription factors induced the reprogramming of somatic cells using the same technique and factors as in 2006 to yield human iPSCs from adult human fibroblasts (Takahashi et al., 2007). In both mice and humans, the transcription factor Nanog was not required for programming induction. The benchmarks and properties of iPSCs meet the defining criteria in embryonic stem cells in growth properties and morphology, and express ESC gene markers. These cells developed the main characteristics of stem cells to recruit self-renewal and could contribute to all linage from the three germ layers (Takahashi & Yamanaka, 2006; Takahashi et al., 2007). Though iPSCs discovery is fundamental, some challenges, such as genomic insertion, can occur and disrupt the application in regenerative medicine. *c-Myc* was reported to be expressed in 70% of cancer diseases (Kuttler & Mai, 2006) and has been used in iPSCs programming to achieve pluripotency. This transcription factor may act as an oncogene and can form cancer when used in trial therapies, so alternative approaches are required in order to produce safer iPSCs (Selvaraj et al., 2010). In addition, the induction of some transcription factors behave as oncogenes and break down the function of tumour suppressor genes such *TP53*. These mediate DNA damage, which results in reprogramming limitations and promotes tumour formation (Marión et al., 2009).

The use of viral vector for iPSCs is another threat as it may cause mutation and minimize both research and clinical applications (Medvedev et al., 2010). Solutions for these challenges are available, as it was possible to perform iPSCs reprogramming in mice and humans without *c-Myc*, termed as non-*c-Myc* iPSCs, and this efficiently reduces the probability of creating tumours (Nakagawa et al., 2008). Likewise, applying the technique of Episomal Reprogramming and using non-integrating episomal vectors

was an alternative to viral vector integration and yielded free transgene sequences (Yu et al., 2009). Furthermore, this technique does not induce iPSCs reprogramming efficacy as the influence as genomic viral integration (Hu, 2014).The remarkable self-renewal and differentiating features of iPSCs provide crucial consideration for their enrolment in clinical treatments and medical research, but reprogramming factors still provide concern about their utility (Okita & Yamanaka, 2011). Additionally, iPSCs research contributes in modelling disease (Fukuda, 2016), human organ transplant (Takebe et al., 2013), organ synthesis, tissue repair, treating vascular disease (Park et al., 2014), and blood cell formation (Singh et al., 2015).

1.4.6 Stem Cell Transcription Factors and Regulators

The self-renewal and differentiation to adult types of pluripotent stem cells are undoubtedly associated with various transcription factors, including OCT4, NANOG, and SOX2, and act as a substantial employment and regulatory complex in order to maintain pluripotency and control other pluripotency factors (Saunders et al., 2013; Wang et al., 2012; Rizzino & Wuebben, 2016).

OCT4 is a core transcription factor play a critical task in the embryonic development and stem cell pluripotency. In the early stage of embryogenesis, the restricted *OCT4* expression is identified in an embryo's inner cellular mass, which generates all three germ layers and embryonic stem cells. *OCT4* is also found to be expressed in the outer layers of embryos and becomes down regulated upon trophectoderm differentiation (Rizzino & Wuebben, 2016; Shi & Jin, 2010). OCT4 is necessary for the primordial germ cells and essential for providing potency for stem cells. Its expression level is linked with a stemness feature and pluripotency. Remarkably, the destiny of embryonic stem cells is determined by *OCT4* expression level. The power of OCT4 transcription factors extends to regulate other stem cell transcription factors including NANOG and SOX2 (Jez et al., 2014; Kehler et al., 2004; Okamoto et al., 1990; Rosner et al., 1990; Scholer et al., 1990; Scarola et al., 2015; Shi & Jin, 2010; Wu & Schöler, 2014).

NANOG is another important transcription factor in maintaining embryonic stem cells and it is involved in self-renewal and differentiation pathways (Silva et al., 2009; Novo et al., 2016). OCT4 transcription factor is required in the early stages of embryo

development, while a vital function for NANOG arises in the next phase of embryonic cell specification after blastocyst development (Cavaleri & Schöler, 2003). The inner cell mass of blastocysts requires NANOG for its construction and the dysfunction or absence of NANOG has been reported with lack of potency, developing cell differentiation, and yielded failed survival rates for germ and ESCs (Chambers et al., 2007; Chambers et al., 2003; De Mot et al., 2016). In ESC populations, *NANOG* expression can be upregulated or downregulated, which is associated with differentiation properties and the ESC population heterogeneity. Additionally, over expression is not interrelated with the cell cycle phase and the expression level of *OCT4* or *SOX2* (Hastreiter & Schroeder, 2016).

SOX2 is a central transcription factor that interacts with OCT4 in a complex and is required to maintain the ESCs and pluripotency. *SOX2* is expressed in the morula (post zygote ball of cells, prior to blastocyst stage) and its expression becomes restricted in the inner cellular mass upon blastocyst formation (Rizzino & Wuebben, 2016). Restricted *SOX2* expression has been detected in the epiblast and not in primitive extraembryonic endoderm (PrE) after the inner cellular mass develops to them in late blastocyst. Moreover, neural stem cells have expressed *SOX2* in high levels. Depletion of SOX2 has led to cell lethality. Both SOX2 and OCT4 co-operate to control pluripotency (Rizzino & Wuebben, 2016; She & Yang, 2015).

OCT4, SOX2, and NANOG are the main transcription factors regulating pluripotent stem cells. At the same time, they are controlling and activating expression levels of other different genes, which subsequently maintain cell potency. The stem cells also are regulated by other various transcription factors (Young, 2011), such as LIF-Stat3, which is involved in self-renewal (Ye et al., 2016), and FOXD3, which is a major factor in developing the pluripotent state (Krishnakumar et al., 2016).

In the adult stem cells, GATA2 is a critical protein to regulate the development of haematopoietic stem cells and its insufficiency interrupts proliferation and affects survival rates (Li et al., 2016b). Likewise, BMI1 is an essential stem cell regulator that maintains the multipotent and mesenchymal stem cells in humans, and the process of downregulating BMI1 resulted in both increased cell death and self-renewal reduction (Jung & A Nolta, 2016).

1.4.7 Stability of stem cell transcription factors in human cancer

Stem cell transcription factor instability is linked with cancer development and progression in different organs and tissues. Statistical data has shown high expressions of *OCT4* in 27% of diverse cancer types when likened to normal tissues. Upregulation of the *OCT4* level was detected in multiple cancers, including in renal, lung, brain, ovary, and testicular cancers. In blood cancers, the percentage of *OCT4* overexpression was reported in 25% of patients developing chronic lymphocytic leukaemia. (Schoenhals et al., 2009). Higher *OCT4* expression represents a predictor in prostate cancer prognosis (Kosaka et al., 2016). Likewise, elevation of *NANOG* expression was found in oral squamous cell carcinoma (Fu et al., 2016). Nuclear expression has been correlated with high development of cancer in ovaries, which delivers the high prospect for *NANOG* expression to be a biomarker for ovarian cancer (Siu et al., 2013). The overexpression has also been linked with poor prognosis in breast and bowel cancers (Meng et al., 2010; Nagata et al., 2014). The abundant expression of *SOX2* is present in solid tumours and bioinformatics analysis has detected high *SOX2* expression in nearly 20% of malignant tumours examined (Schoenhals et al., 2009). The over expression is also detected with prostate cancer (Guzel et al., 2014) and patients suffering from squamous cell carcinomas in both the head and neck. However, targeting cancer cells with positive *SOX2* expression could be a novel approach to cure head and neck squamous cell carcinomas (Lee et al., 2014). As such, pluripotent stem cell markers can be remarkable biomarkers of tumorigenesis, such as expression levels of *SOX2* and *OCT4*, is critical to identifying oral squamous cancers in early stages (Fu et al., 2016).

1.5 Cancer stem cells

1.5.1 Cancer stem cells in tumour initiation

The behaviour and biology of cancer stem cells (CSCs) is a highly active research area because of their propensity and ability to differentiate into tumour cells. CSCs are present in many cancers and have the main characteristic of self-renewal. Tumour formation and cancer cell initiation are thought to occur due to the influence of CSCs signalling and pathways. The concept of CSC's origin and their power to influence

tumour cell initiation is not fully understood, but is fundamental in terms of cancer therapy (Rahman et al., 2016).

Different hypotheses try to reveal the derivation of CSCs. Epigenetic alterations contributes to regulate CSCs in terms of histone modification and DNA methylation, which, subsequent in tumour development, metastases and difficulty in therapy response (Muñoz et al., 2012; Ravasio et al., 2016). In addition, mutation in differentiated cells yields the ability to drive them back to a stem cell-like state (Friedmann-Morvinski & Verma, 2014). The theory of mutation in adult stem cells to form tumours has also been proposed due to their nature dynamics. Correspondingly, ASCs obtain frequent cell division in synchronism with their long life span, which makes these cells subject to mutation and subsequently forms tumours (López-Lázaro, 2015a; López-Lázaro, 2015b). Additionally, the migration of progenitor cells (adult stem cells with limited differentiation) to an incorrect location can drive the existence of CSCs (Nguyen et al., 2012). The balanced signalling pathways for Wnt, Hedgehog, and Notch regulate the various normal stem cell properties, such as survival, apoptosis, self-renewal, and differentiation. Nevertheless, dysregulation, or over activation, for these crucial signalling pathways contributes to the survival of CSC populations (Cirri & Chiarugi, 2012; O'Leary et al., 2016).

It is known that CSCs inhabit specific microenvironments known as niches. These specialised areas play critical roles in regulating CSC functions, and keep them away from immune cells. Additionally, they assist tumour cell initiation and generate metastases. However, targeting and understanding niches relevant to a specific type of cancer may help in approaching new therapies (Plaks, Kong & Werb, 2015).

1.5.2 Cancer stem cells and stem cells

CSCs share common characteristics with normal stem cells, such as a self-renewal capacity and differentiation capabilities. Both of them produce telomerase, which is essential for their life span (Rahman et al., 2016). In addition, similar signalling pathways, such as Wnt, BMI-1, Notch, and Sonic Hedgehog, help maintain their self-renewal. Normal stem cells and CSCs determine versus properties such as normal karyotype for normal stem cells while CSCs develops abnormal karyotype. Self-

renewal and differentiation are highly regulated in normal stem cells and highly dysregulated in CSCs (Rahman et al., 2016). The transcription factors CSCs express are typically core transcription factors of normal stem cells, such as OCT4, SOX2, and NANOG. Transcription factors, such as BMI1, which is involved in self-renewal, and Yin Yang 1 (*YY1*), which is commonly expressed in different types of cancer, have a marked role in assessing the function of CSCs transcription factors (Kaufhold et al., 2016).

1.5.3 CSCs identification strategy

Identification of CSCs among cancer cell populations is critical. Nevertheless, different strategies have been used for CSCs isolation and identification. One major strategy to identify CSCs is based on the expression of cell surface markers and intracellular markers by developing designated antibodies targeting cell population markers using fluorescence activated cell sorting (FACS) (Chen et al., 2013). In 1997, the expression level $CD34^{+}$ $CD38^{-}$ was the initial surface marker phenotype and had given outstanding elucidation of CSCs and leukemic stem cells (LSCs) in particular. Haematopoietic stem cells (HSCs) are positive for CD34 and CD38 in normal condition while LSCs not express the CD38 surface marker, which subsequently distinguishes between normal and leukemic cells (Dick, 1997). Likewise, CD133 and CD44 are important CSCs surface biomarker examples and are correlated with numerous cancer types (Ajani, et al. 2015). CSCs surface marker phenotype CD133 was reported as a putative marker in different human cancer types and its identification is critical to detect multiple cancers (Mak et al., 2014). The high expression of CD133 was significant in tumour cells derived from colorectal cancer and has been shown to be a vital link in terms of colorectal cancer survival rates (Wang et al., 2016). Overexpression of CD133 was also, reported with 51.4% of patients with diffuse-type gastric cancer and signalling pathway activation in Notch is thought to contribute to maintaining CD133 induction (Konishi et al., 2016). CD44 is another CSCs surface marker that is linked to metastasis in human breast tumours (McFarlane et al., 2015) and elevates in epithelial tumours, such as head and neck cancers (Prince et al., 2007). Furthermore, a set of CSCs surface markers together encompass CD133+, $\alpha 2\beta 1^{high}$, and CD44+ are employed as a powerful tool in prostate tumour investigation (Collins et al., 2005). Proper CSC determination can

provide a potent screening for malignant tumours that can assess prognosis and determine drug strategy (Chen et al., 2013).

1.5.4 CSCs and chemotherapy strategy

There is a known link between the CSCs and the reproduction of tumour cells through the activation of numerous mechanisms responsible for the dysregulation of signalling pathways and apoptosis, which causes chemotherapy resistance (Vidal et al., 2014). Nevertheless, the application of anti-CSC agents along with chemotherapy is a fundamental key to eradicating tumour cells and CSCs (see Figure. 1.6), such as the combination of both Cyclopamine and Imatinib to target chronic myeloid leukaemia. Cyclopamine compound targets CSCs while Imatinib eradicates cancer cells. The trial of this combined therapy is still under pre-clinical investigation (Vidal et al., 2014).

The reside area of CSCs (niches) is found to sustain the life span of CSCs, as these microenvironments consist of extracellular matrix components, cell surface signalling molecules, and vascular and inflammatory cells. However, a number of studies propose to target the signalling pathways and niches supporting the dynamics of CSCs, which may work in parallel with chemotherapy to eliminate tumour cells (Borovski et al., 2011; Hanahan & Coussens, 2012; Vidal et al., 2014). However, expression levels of CSCs surface markers can encourage the strategy of chemotherapy by providing an indication of cancer types and prognosis (Rahman et al., 2016).

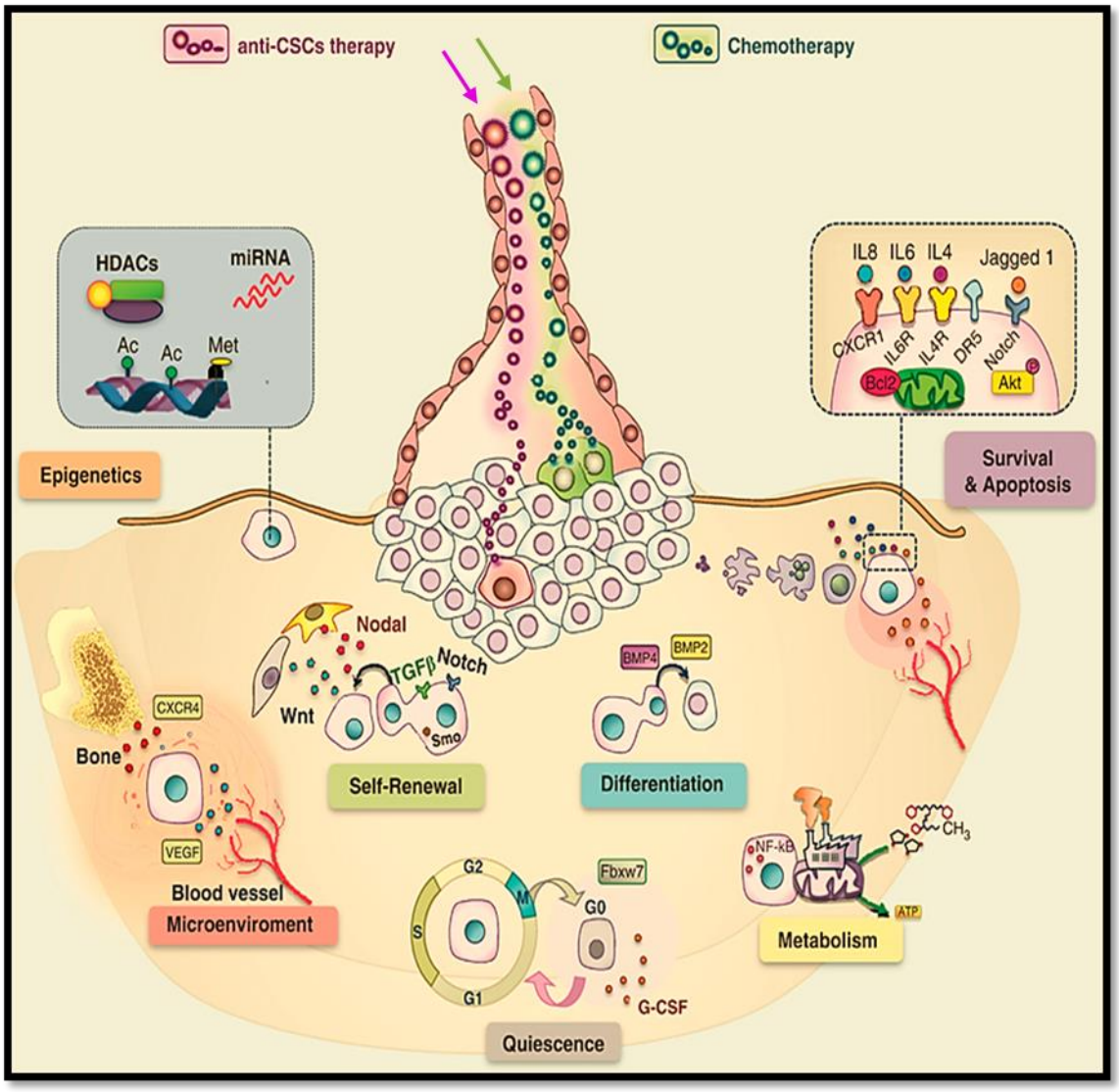

Figure 1-6 The mechanism response of cancer stem cells to chemotherapy.
The scheme describes the targeting of cancer stem cells and tumour cells with a combination of both conventional therapy (green) and anti-CSC agents targeting specific pathways (purple), and is highly proposed to eradicate tumour cell compartments (Vidal et al., 2014).

1.6 Testis expressed 19 (*TEX19*)

1.6.1 *TEX19* as a marker of pluripotency

Tex19 is a specific gene in mammals, initially discovered in the germ cells of mice (Kuntz et al., 2008; Wang et al., 2001). In rodents, duplication of the *Tex19* orthologue has generated pair paralogues in mice and rats, known as *Tex19.1* and *Tex19.2*, whereas a single gene is present in humans. Both *Tex19.1* and *Tex19.2* are located on chromosome 11, while the human *TEX19* is located on chromosome 17 (see Figure 1.7). Human *TEX19* and murine *Tex19.1* are linked to a number of genes, including *Sectm1*, *CD7* and *UTS2R*. In addition, in both humans and mice, *Tex19* genes are found to be oriented similarly in line with the centromere and separated from the *UTS2R* locus by similar distance. This supports the idea that human *TEX19* is closely related to murine *Tex19.1* and suggests that it is the human gene orthologue for the *Tex19.1* form (Kuntz et al., 2008).

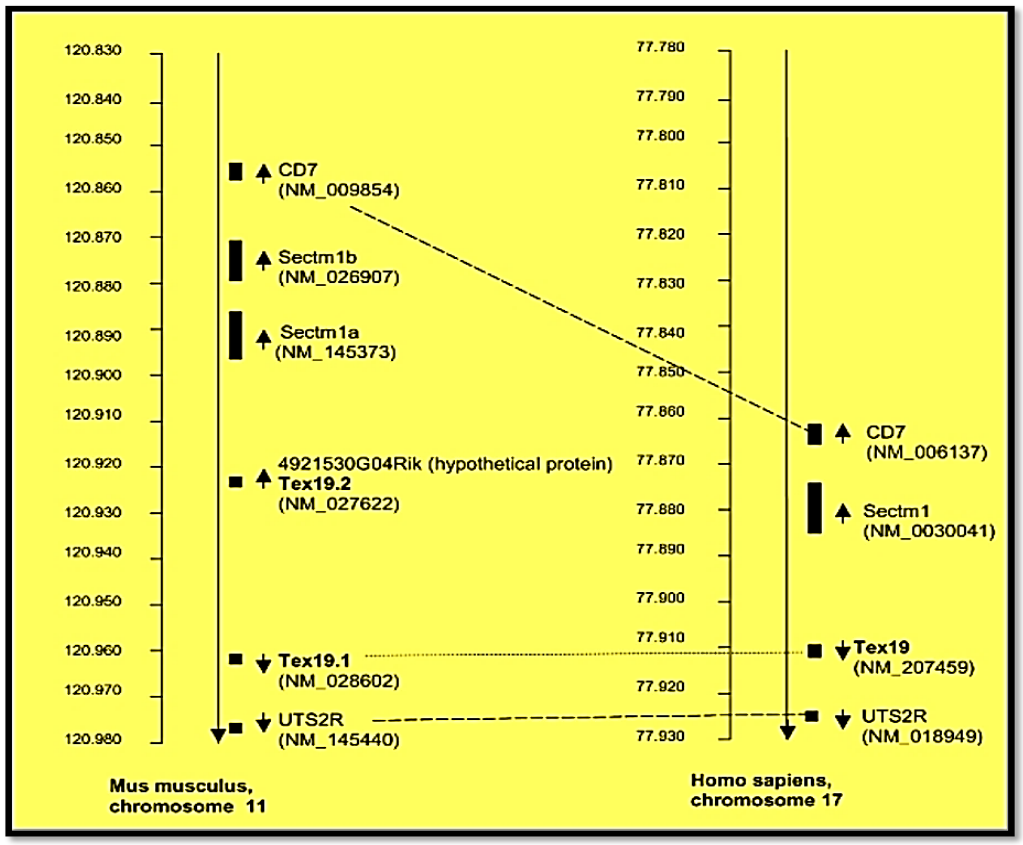

Figure 1-7 Arrangement of the genomic location for *Tex19* genes.
Human *TEX19* is located on chromosome 17, while both paralogue genes *Tex19.1* and *Tex19.2* are located on chromosome 11. Compared to the paralogue gene *Tex19.2*, the human orthologue gene *Tex19.1* is closer to the human *TEX19* gene, being oriented in a similar direction (Kuntz et al., 2008).

The detected expression for the two paralogues differs. The expression of *Tex19.2* has been found to be negative in early embryogenesis, being reported as specifically detected in male somatic gonad lineage and female germ cells. In contrast, murine *Tex19.1* is detected in early embryo and pluripotent stem cells in mice and later becomes restricted to male germ cells (Kuntz et al., 2008). Interestingly, this paralogue has been found to express similarly to the stem cell marker *Oct4,* and its expression decreases upon embryonic stem cell differentiation. In addition, human *TEX19* expression has been found to be similar to that of murine *Tex19.1,* with specific expressions in the testes and undifferentiated embryonic stem cells (Kuntz et al., 2008). In human tissues, *TEX19* expression has been identified in placental cells and in testis tissue in adults (Celebi et al., 2012). A recent study found TEX19 protein only in testis tissue, not in normal tissues (Zhong et al., 2016).

The function of *Tex19* genes in mammals and humans is still unclear and poorly understood. However, murine *Tex19.1* expression was found to be parallel to *Oct4* gene expression (Kuntz et al., 2008). *Oct4* is expressed in unfertilised oocytes, and detected in the inner cellular mass, which gives rise to embryonic stem cells. In addition, it is indispensable in generating pluripotency in stem cells (Nichols et al., 1998; Niwa et al., 2000). Correspondingly, *Tex19.1* expression was detected in unfertilised eggs, zygotes, inner cellular masses, and embryos, and was maternally inherited as other pluripotent markers (Kuntz et al., 2008). Consistent with this observation, *Tex19.1* gene might be a transcription factor in self-renewal regulation and stem cell pluripotency. In contrast, *Tex19.2* expression is different from murine *Tex19.1,* which suggest different function during the embryo development (Kuntz et al., 2008). Other studies have indicated a remarkable function for Tex19.1, in which its loss results in postponement of embryonic development (Reichmann et al., 2013). Tex19.1 deletion is found to cause defects in spermatogenesis and meiotic chromosomal synapsis, (Yang et al., 2010). As such, Tex19.1 deletion produces infertility in males as well as impairs spermatogenesis (Öllinger et al., 2008); its existence is essential for spermatogenesis and required for placenta development (Tarabay et al., 2013).

Studies have indicated the potential function for Tex19.1 in transposable elements regulation. In the early stage of spermatogenesis, Tex19.1 deletion in testes has provided consistent change in genes that are encoded for meiotic recombination, such as *REC8, SPO11,* and *Smc1β,* and synaptonemal complex genes involve *Sycp1, Sycp2, and Sycp3* (Öllinger et al., 2008). In contrast, a significant upregulation change has been determined in long terminal repeats (LTRs)-retrotransposon *MMERVK10C*. However, this elevation in *MMERVK10C* element may drive spermatogenesis defects (Öllinger et al., 2008). Further study has supported the role of Tex19.1 in repressing retrotransposon in placenta in the female. The deletion of Tex19.1 in placenta cells elevates expression of long interspersed nuclear element (*LINE-1*). This elevation can contribute to retrotransposons deregulation, which is subsequent to placenta dysfunction (Reichmann et al., 2013). This finding establishes that, Tex19.1 is part of a regulated mechanism in the germ line to control transposable elements and sustain genomic balance through consecutive generation (Öllinger et al., 2008; Reichmann et al., 2013). Recent studies have suggested the function of *TEX19* to supress transposable elements could be linked to the function of the flanking gene, Secreted and transmembrane1 gene (*Sectm1*), which is also involved in regulating retrotransposon activity (see Figure 1.8) (Bianchetti et al., 2015).

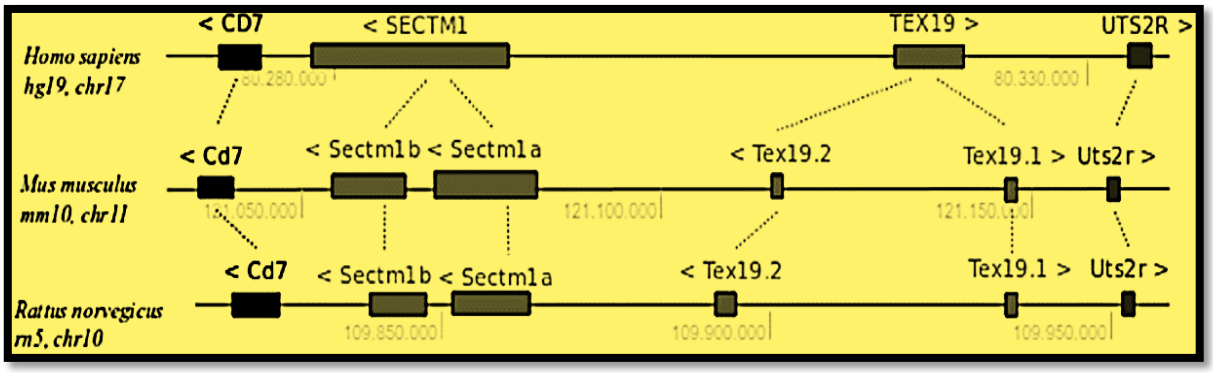

Figure 1-8 representational diagram showing the Synteny of *Tex19* and *Sectm1* genes in mammals.

1.6.2 *TEX19* as a CTA gene and potential cancer biomarker

TEX19 is a specific human gene that was first identified as a novel meiosis-related CTA gene in 2012 (Feichtinger et al., 2012). The identification of this CTA gene was based on two approaches: first, a manual literature search for human genes reported as having specific expression in meiosis; and second, bioinformatics analysis to find specific human meiosis genes (Feichtinger et al., 2012) based on individual studies that reported cross-species expression in humans and mammals. However, this individual study assigned human orthologues to specific testis genes in mice to yield human testis genes which might be meiosis-specific (Chalmel et al., 2007; Feichtinger et al., 2012). The sequence data and information from expressed sequence tag (EST) libraries was assigned to exclude genes having negative expressions in testes and the central nervous system and genes not found in cancer EST libraries. Then, the candidate genes were subjected to further validation by RT-PCR, and the expression patterns yielded were analysed and subjected to cross-comparison in a meta-analysis. This statistical analysis involved microarray data obtained from cancer patients (Feichtinger et al., 2012). Based on the CTA gene classification described by Hofmann et al. (2008), *TEX19* was classified as a cancer-selective CTA gene, and its expression pattern was determined in normal testis and thymus tissues. More significantly, *TEX19* has shown remarkable expression in several different cancer cells. However, the explanation for determined expression in the thymus could be a physiological process, including age-related atrophy changes in thymus tissue (Feichtinger et al., 2012).

To date, few studies have addressed whether *TEX19* is a CTA gene. However, recently, Zhong et al. (2016) evaluated the expression of *TEX19* in multiple bladder carcinoma samples and other normal human tissues, confirming the results of a study by Feichtinger et al. (2012) elucidating the restricted expression of *TEX19* in testes and cancer tissues. However, this CTA gene was positive in 60% of bladder carcinoma samples and reported to have high expression levels in high-grade tumours. These findings encourage further investigation into whether *TEX19* drives cancer-cell progression or expresses as an oncogene and into use of this CTA gene in immune therapy (Feichtinger et al., 2012; Zhong et al., 2016).

1.7 The project aims

The overreaching aim of this project is to elucidate the functional role (s) of *TEX19* in cancer and human stem cells. The specific goals of this project are as follows:

1- To investigate the expression of *TEX19* at the cellular and tissue levels in both normal and cancer tissues, as well as in distinct cancer cell lines, to re-evaluate whether the *TEX19* is a definitive CTA gene.
2- To investigate the expression of *TEX19* in human induced pluripotent stem cells (iPSCs) and human embryonic stem cells (hESCs) to assess whether *TEX19* expression is restricted to pluripotent stem cells and if it has a role in conferring stemness features.
3- To analyse the cellular localisation of TEX19 in normal tissues, cancer tissues, cancer cells, and cancer stem-like cells.
4- To study the effect of *TEX19* depletion in pluripotent embryonal carcinoma cells and other distinct cancer cells to determine if *TEX19* is required to influence the proliferation of cancer cells.
5- To assess the expression levels of a wide range of genes following *TEX19* depletion to determine whether TEX19 functions in transcriptional regulation
6- To determine whether TEX19 regulates transposable elements in both cancer and human embryonic stem cells.
7- To determine if TEX19 function is linked to the function of embryonic stem cell marker genes, including *OCT4*, *NANOG*, and *SOX2*.

Chapter 2

Materials and Methods

2. Materials and methods

2.1 The origins and sources of human cells

The SW480, HCT116, LOVO, 1321N1, MCF7, G361 and COLO800 cancer cell lines were supplied by the European Collection of Cell Cultures (https://www.phe-culturecollections.org.uk/collections/ecacc.aspx). The cancer cell line H460 was purchased from the American Type Culture Collection (https://www.atcc.org). The A2780 cancer cell line was gifted by Prof. P. Workman (Cancer Research UK Centre for Cancer Therapeutics, Surrey, UK). The NTERA2 cell line was generously provided by Prof. P.W. Andrews from the Centre of Stem Cell Biology (CSCB) at the University of Sheffield. The cancer cell line PE014 was obtained from Cancer Research Technology, Ltd. All cancer cell lines went through an authentication test at least once per annum, conducted by LGC Standard Services in the UK, to verify each cell line (Tracking numbers 710236782 and 710418378).

2.2 Growing and culturing human cells

Human cancer cells were cultured in different media based on the particular cancer cell line. The medium for each cell line was supplemented with 10% foetal bovine serum (FBS), purchased from Thermo Scientific (#10270). The optimal temperature for cell growth was 37°C in a humidified incubator, using sterile dH_2O for the humidity. Variable conditions of CO_2 were set up based on the cell type. All cell lines were cultured in 5% CO_2 except for the NTERA2 cell line, which was maintained in 10% CO_2. The proliferation conditions for the cells, along with the different media, are outlined in Table 2.1. A LookOut® Mycoplasma PCR Detection Kit was purchased from Sigma Aldrich (#MP0035) and used according to the manufacturer's procedure. This check was conducted regularly on all cell lines to ensure that the cultures were always free of mycoplasma contamination.

Table 2-1 The culture conditions for human cancer cells used in this study

Cell line	Type of cancer	Medium	Supplier	CAT#	CO_2 %
SW480	Colon adenocarcinoma	DMEM+ GLUTAMAX™	Thermo Scientific	61965-026	5%
HCT116	Colon carcinoma	McCoy's 5A medium+ GLUTAMAX™	Thermo Scientific	36600-021	5%
LOVO	Colon adenocarcinoma	Ham's F12 + GLUTAMAX™	Thermo Scientific,	31765-027	5%
1321N1	Brain astrocytoma	DMEM+ GLUTAMAX™	Thermo Scientific	61965-026	5%
MCF7	Breast adenocarcinoma	DMEM+ GLUTAMAX™	Thermo Scientific	61965-026	5%
PE014	Ovarian Adenocarcinoma	RPMI 1640 + GLUTAMAX™	Thermo Scientific	61870-010	5%
A2780	ovarian carcinoma	DMEM+ GLUTAMAX™	Thermo Scientific	61965-026	5%
NTERA2	Embryonal carcinoma	DMEM+ GLUTAMAX™	Thermo Scientific	61965-026	10%
H460	Lung carcinoma	RPMI 1640 + GLUTAMAX™	Thermo Scientific	61870-010	5%
G361	Malignant melanoma	McCoy's 5A medium+ GLUTAMAX™	Thermo Scientific	36600-021	5%
COLO800	Melanoma	RPMI 1640 + GLUTAMAX™	Thermo Scientific	61870-010	5%

2.3 The process of thawing human cells

The cells were transferred from liquid nitrogen storage and placed to thaw in a clean water bath containing sterile dH_2O for no more than 90 seconds. The thawed cells were added to 10 mL of complete medium in a sterile 15 mL conical tube with gentle mixing by pipetting for 10 seconds, and the conical tube was then centrifuged for approximately 3 minutes at 400x*g*. The medium was removed, 10 mL of the complete medium was added, and the cells were mixed by pipetting for 20 seconds. A 5 mL sample of the medium containing the cells was then transferred to each of two T25 flasks. The flasks were incubated in a humidified incubator at the desired temperature and CO_2 level (see Table 2.1).

2.4 Passaging and maintenance of human cells

The cells were thawed and incubated for 24 hours and then examined using light microscopy to confirm the correct morphology and cell confluence. The two 25 mL flasks were then moved to the hood for transfer into T75 flasks. The culture medium was removed from each T25 flask and the cells were washed with 1X DPBS buffer (Thermo Scientific #14190-094). The DPBS buffer was aspirated, and a volume of trypsin-EDTA solution (Thermo Scientific #25300054) not exceeding 0.5 mL was added to each T25 flask. The cells were then incubated for approximately 5 minutes to ensure complete detachment of all cells. The two T25 flasks were then returned to the hood, and 5 mL of complete medium was added to deactivate the trypsin-EDTA solution. The medium in each T25 flask was collected into one sterile 15 mL conical tube and centrifuged for about 3 minutes at 400x*g*. The medium was aspirated and 13 mL of complete medium was added with gentle mixing, followed by transfer of the cells to a new T75 flask. The flask was then incubated with the optimal CO_2 percentage and temperature for that cell type until the cells reached 70–80% confluence. The cells were then passaged again into two or more T75 flasks, using the same procedure.

2.5 Human cell cryopreservation

Human cell banking solution was prepared by adding 1 mL DMSO (Sigma #D8418) to 9 mL FBS in a sterile 15 mL conical tube to make final concentration of 10% DMSO; this solution was designated as the cell freezing medium. Each single freezing needed

1mL of 10% DMSO solution; the rest of the freezing medium was stored at -20°C until further use. In order to progress to the banking step, the cells were grown in T75 flasks until 80% confluence. The medium was discarded and the cells were washed with 1X DPBS buffer and then trypsinised with 1mL of trypsin-EDTA solution for 5 minutes in the incubator. Subsequently, 10 mL of complete medium was added to the cells, and the mixture was transferred to a 15 mL conical tube and centrifuged for 5 minutes at 400x*g*. The medium was aspirated and the pellets were resuspended in 1mL of 10% DMSO. The resuspended pellets were transferred immediately to a cryopreservation vial labelled with the type of cells, passage number and date. The cells were stored for 24–48 hours at -80°C and then transferred to a liquid nitrogen tank for long-term storage.

2.6 Human cell counting

Cells were counted by collecting them in a sterile tube, suspending them in complete medium, and mixing by gentle pipetting. A 10 µL volume of suspended cells was mixed with 10 µL of Trypan blue dye (Gibco® #15250-061) and 10 µL of that mixture was transferred to the chamber of a cell counting slide (Bio-Rad; Cat: 145-0011). The slide was inserted in to an automatic cell counter (Bio-Rad; TC10^{TM}) to obtain the cell count.

2.7 The source and maintenance of human embryonic stem cells

The human embryonic stem cells (hESCs) in this research study were generously provided by Prof. Peter Andrews from the Centre of Stem Cell Biology at the University of Sheffield. The obtained human embryonic stem cells were the SHEF6, H9, H7S14 and H7S6 cell lines. The SHEF6, H9 and H7S14 primary cell lines had normal karyotypes, while the H7S6 cell line was reported to have an abnormal karyotype. The hESC culture was carried out for the SHEF6 line using mouse embryonic fibroblasts (MEFs) as feeder cells for cell culturing. By contrast, the SHEF6, H9, H7S14 and H7S6 primary cell lines were cultured using vitronectin as a feeder-free system at the Centre of Stem Cell Biology at the University of Sheffield.

2.8 The culture of mouse embryonic fibroblasts (MEFs)

2.8.1 The preparation of MEF cells medium

Mouse embryonic fibroblasts (Amsbio #GSC-6201M) were used as feeder cells to grow the hESCs that had been banked in liquid nitrogen. The MEFs were cultured in complete medium freshly prepared by combing DMED medium (Thermo Scientific #21969035) with 15% FBS (Thermo Scientific, Gibco #10270). Subsequently, the complete medium was filtered using disposable vacuum filter units (EMD Millipore #SCGP00525). The medium was used immediately or stored at -20°C.

2.8.2 Thawing and plating of MEF cells

The MEF cells were thawed in a clean water bath at 37°C for 90 seconds. A 1 mL volume of thawed cells was then added to 10 mL of complete medium in a sterile 15 conical tube, and this was centrifuged for 3 minutes at 400x*g*. Subsequently, the medium was removed and 10 mL of fresh complete medium was added. The cells were resuspended by gently pipetting up and down and 5 mL of the medium containing the resuspended cells was transferred to each of two T25 flasks. The cells were incubated in 5% CO_2 in a humidified incubator at 37°C. The cells were then left for 24 hours to adhere to the flask and be ready for use. The MEF cells were not allowed to grow in the incubator for more than 8 days; new MEF cells were prepared after that time.

2.9 The culture of human embryonic stem cells on feeder cells

The culturing of human embryonic stem cells (hESCs) on MEF cells after cryopreservation is essential. Culturing the hESCs on MEF cells requires refreshing of the complete medium. The complete medium for this culture was prepared by combining of 40 mL of DME/F-12 free serum media, 10 mL of KO serum, 250 µL of glutamine, 90.9 µL of β-mercaptoethanol, 0.5 mL of 1% NEAA and 2 µL of human bFGF. All these components were mixed thoroughly and the resulting medium was filtered (see Table 2.2 for more details). The hESC cells were removed from liquid nitrogen storage and thawed in a clean water bath at 37°C for 90 seconds. A 1 mL volume of cells was then added to 10 mL of the complete medium in a sterile tube and centrifuged for 3 minutes at 400x*g*. The medium was then discarded, 5 mL of complete medium was added, and the cells were resuspended. Subsequently, the medium in one

flask plated with MEF cells was discarded and the MEF cells were washed at least once with 1X DPBS. The complete medium containing the hESCs was then added to the T25 flask coated with MEF cells. The flask was then transferred to a humidified incubator with a 5% CO_2 atmosphere at 37°C to culture the hECSs. The medium was changed regularly and the hESCs were monitored every day. The cultures were split after the hESCs reached 70–80% confluence.

Table 2-2 Components of the medium used to culture the hESCs on feeder cells

Component	Stock concentration	Final concentration	1X	Source	CAT#
DME/F-12	---------	80%	40 mL	Sigma	D8437
Knock Out (KO) serum	---------	20%	10 mL	Thermo Scientific	10828010
Glutamine	200 mM	1 mM	250 µL	Thermo Scientific	25030024
β-mercaptoethanol	55 mM	0.1 mM	90.9 µL	Thermo Scientific	21985023
NEAA	100X	1%	0.5 mL	Thermo Scientific	11140050
Human bFGF	0.1 mg/mL	4 ng/mL	2 µL	Thermo Scientific	13256029

2.10 The passage of human embryonic stem cells on feeder cells

Three T25 flasks were plated with MEF cells, prepared as described in Section 2.8.2, at least a day before passage. The medium in these flasks was discarded, the cells were washed with 1X DPBS and 4 mL of complete hESC medium was added. The medium from a culture flask containing confluent hESCs was removed, the cells were washed with 1X DPBS, and 1 mL of collagenase (Thermo Scientific #17104019) was added. The cells were left for approximately 5–7 minutes in the incubator at the desired percentage of CO_2 and temperature. The collagenase was aspirated and 3 mL of hESC medium was added. Glass Beads were placed in the T25 flask with 3 mL of complete medium and the flask was gently shaken to detach the hESCs. A 1 mL of the cells was

then transferred to each of the 3 previously prepared flasks. The medium was changed regularly and the cells were monitored every day.

2.11 The banking of human embryonic stem cells

The medium of confluent flasks was discarded and the cells were washed with 1X DPBS. One millilitre of collagenase was added and left for approximately 5–7 minutes in the incubator at the desired percentage of CO_2 and temperature. The collagenase was removed and 3 mL of hESC cell medium was added. Beads were added to the T25 flask, which was then gently shaken to detach the cells. The cells were transferred to a sterile 15 mL conical tube and centrifuged for 3 minutes at 400x*g*. The medium was discarded and the cells were suspended in 1 mL cryopreservation medium (FreSR™-S, Stem Cell Technology #05859) and immediately transferred to cryopreservation tubes, stored at -80°C for 24 hours and then placed in liquid nitrogen. Freezing medium containing a combination of 10% DMSO and 90% Knockout (KO) serum was also used.

2.12 The culture of human embryonic stem cells on a feeder-free system

The hESCs were cultured on feeder-free system using vitronectin (#A14700) in T25 flasks and E8 medium (supplied by CSCB). Vitronectin is a recombinant human protein that supports the growth of hESCs with limited variability. The E8 medium was designed for the hESCs growing on feeder-free systems and is characterised by its support of these cells, so that they grow and expand with perfect morphology. Vitronectin was defrosted on ice and prepared by adding 100 mL of 1X DPBS buffer to 1 mL of vitronectin in a sterile tube and gently mixing. A 3 mL volume of the prepared vitronectin was added to the each T25 flask and the flasks were left at least 1 hour in the hood at room temperature before use. This allowed the vitronectin to coat the flask and become a feeder for the cells.

In order to culture the hESCs in feeder-free conditions, 4 mL of E8 medium was placed in four vitronectin-coated T25 flasks. The medium from hESCs grown on feeder cells (MEF) was discarded, the cells were washed with 1X DPBS, and 4 mL of E8 medium was added. The cells were scraped smooth with a sterile fine pipette tip (Alpha Labs

#LW4061). Subsequently, 1 mL of cells was transferred to the 4 flasks. The cells were then incubated in a humidified incubator with 5% CO_2 at 37°C. The medium was changed regularly and the cells were monitored every day. The culturing and splitting of hESC cultures was performed based on the nature of each experiment.

2.13 The passage of human embryonic stem cells on a feeder free system

Passage of the hESCs at a precise time is important to keep them in perfect morphology and to avoid cell differentiation and the occurrence of abnormal karyotypes. As soon as the hESCs reached confluence, the medium was discarded and the cells were washed with 1X DPBS. Next, 5 mL of E8 medium was added and the cells were scraped smooth with a sterile fine pipette tip. A 1 mL of cells was added to T25 flasks coated with vitronectin, and 4 mL of E8 medium was added and gently mixed to prevent the cells from localising in one place in the flask (The E8 medium could be added before the cells).

2.14 NTERA2 differentiation

A set of inducer agents, including retinoic acid and hexamethylene bisacetamide (HMBA), was applied to differentiate human embryonal carcinoma cells (NTERA2). The retinoic acid and HMBA medium was prepared by adding 3 mg/mL retinoic acid and 3 mM HMBA inducer to 500 mL of complete medium (DMEM+Glutamax^{TM} +10% FBS). DMSO medium was prepared as a control by adding 5 mL of DMSO to 500 mL of complete medium. The total RNA was extracted from the differentiated cells as described in Sections 2.16. The differentiation components condition are listed in Table 2.3. Experiments were repeated three times at least.

2.15 The differentiation of human embryonic stem cells (hESCs)

The hESCs were differentiated with 3 mg/mL of retinoic acid added to E6 medium at different selected timelines. The differentiation was carried out on a feeder-free system (vitronectin). The E6 medium is characterised by its support of somatic cells and the absence of bFGF factor, which is essential to maintain embryonic stem cells. As a result, the embryonic cells will differentiate and the retinoic acid will direct them to a

neuronal pathway. The total RNA was extracted from the differentiated cells as described in Sections 2.16. The differentiation components condition are listed in Table 2.3. Experiments were repeated three times at least.

Table 2-3 Differentiation inducers and media with the preparation conditions

Component	Source	Cat#	Preparation Conditions
DMEM+Glutamax™	Thermo Scientific	61965-026	Used for no more than 2 weeks.
Essential 6™ Medium	Thermo Scientific	A1516401	Used for no more than 2 weeks.
DMSO	Sigma	D8418	----------
Retinoic acid	Sigma	R2625	In darkness
HMBA	Sigma	224235	In darkness

2.16 The extraction of total RNA from human cells

The total RNA from human cells was isolated utilising the RNeasy Plus Mini kit (Qiagen, 74134). The culture medium was aspirated. The cells were washed with 1X DPBS buffer and then trypsinised with 1 mL of trypsin-EDTA. The trypsin-EDTA was aspirated and complete medium was added to the cells to deactivate trypsin. The cells were then collected in a sterile tube and centrifuged for 3 minutes at 400x*g*. The medium was aspirated and cells were suspended with 1X DPBS buffer, and then centrifuged for 3 minutes at 400x*g*. The wash buffer was aspirated and the pellets were re-suspended in 1 mL of 1X DPBS and transferred to a sterile Eppendorf tube. The cells were centrifuged for 3 minutes at 400x*g* and the wash buffer was aspirated. Subsequently, RLT Plus buffer was added to the pelleted cells at 350 µL for $<5 \times 10^6$ cells and 600 µL for 5×10^6 to 1×10^7 cells. The cells were vortexed with RLT Plus buffer for 30 seconds to obtain a homogenised lysate, which was then transferred to a gDNA Eliminator spin column placed in a 2 mL collection tube and centrifuged for 30 seconds at ≥1000x*g*. The column was discarded and the flow-through was saved. One volume of 70% ethanol was added to the collection tube (either 350 µL or 600 µL, based on the volume of RTL Plus added previously). Up to 700 µL of the sample was transferred to an RNeasy spin column placed in a 2 mL collection tube and centrifuged for 15 seconds

at ≥1000x*g* and the flow-through was discarded. A 700 µL volume of RW1 buffer was added and spun for 15 seconds at ≥1000x*g* and the flow-through was discarded. A first and second addition of 500 µL RPE buffer was spun for 15 seconds and 2 minutes, respectively, at ≥1000×g and the flow-through was discarded each time. The RNeasy spin column was placed in a new sterile Eppendorf tube and 30 µL of RNase-free water was added. The Eppendorf tube was centrifuged for 1 minute at ≥1000x*g* to elute the RNA. A NanoDrop ND-1000 spectrophotometer was used to assess the quality and quantity of the obtained RNA.

2.17 Total RNA isolation from human embryonic stem cells

The culture medium was aspirated and the cells were washed with 1X DPBS buffer. The cells were scraped with sterile beads in 5 mL 1X DPBS buffer. The cells were transferred to a 15 mL sterile conical tube and centrifuged at 400x*g* for 3 minutes. The wash buffer was aspirated and the cells were suspended in 1 mL of 1X DPBS and transferred to a sterile Eppendorf tube. The cells were centrifuged for 3 minutes at 400x*g* and the wash buffer was aspirated. RLT Plus buffer was added and RNA isolation followed the protocol described in Section 2.16.

2.18 The synthesis of complementary DNA (cDNA)

The total RNA from normal human tissues was purchased from Clontech (#636643) and total RNA from the cancer tissues was supplied by both Ambien and Clontech. The total RNA for number of cancer cells used in this study was generated in the McFarlane lab from cell cultures (see Table 2.1). The RNA from hESCs was extracted from cultures in the McFarlane lab and Prof. P.W. Andrews's lab at Sheffield University. The total RNA for induced pluripotent stem cells (iPSCs) and fibroblasts was produced from tissue culture in the McFarlane lab.

According to the manufacturer's instructions, 1µg of the total RNA was used to synthesise complementary DNA using SuperScript® III First-Strand Synthesis (Thermo Scientific #18080051). The quality of generated cDNA was assessed using the human *βACT* gene as an endogenous control. All components of the SuperScript® III First-Strand synthesis were defrosted on ice and then vortexed and centrifuged briefly. A 1 µg sample of total RNA from each sample was added to a sterile PCR tube,

followed by addition of 1 µL of 50 µM oligo (dT) and 1 µL of 10 µM dNTP. Subsequently, DEPC treated water was added to reach a final volume of 10 µL. The RNA mixture was vortexed and spun briefly, incubated in a PCR machine at 65°C for 5 minutes, and then placed on ice for at least 1 minute. During the RNA mixture incubation, the cDNA synthesis mix was prepared for each sample by combining the following components in a new sterile PCR tube: 2 µL of 10X RT buffer, 2 µL of 0.1 M DTT, 4 µL of 25 mM $MgCl_2$, 1 µL of RNase Out and finally 1 µL of SuperScript. The resulting 10 µL of cDNA synthesis mix was added to each RNA mixture and this reaction mix was incubated in the PCR machine for 50 minutes at 65°C and terminated at 85°C for 5 minutes. The PCR reaction mix was placed on ice for 1 minute, 1 µL of RNase H was added, and the mixture was incubated for 20 minutes at 37°C. The cDNA reaction products were diluted eight fold by addition of DEPC treated water and stored at -20°C until use.

2.19 Analysis of the polymerase chain reaction (PCR) products and agarose gel preparation

The sequences of genes of interest were obtained from the database of the National Centre for Biotechnology Information (http://www.ncbi.nlm.nih.gov/gene, while ensuring the spanning of at least one intron. The RT-PCR primers were designed using special software, including the Oligonucleotide Properties Calculator (http://biotools.nubic.northwestern.edu/OligoCalc.html) and Primer3 software http://primer3.ut.ee/. The synthesised primer sequences were supplied from the Eurofins MWG operon (https://www.eurofinsgenomics.eu/). The primers were diluted using sterile dH_2O following the manufacturer's instructions to a final concentration of 10 pmol. The sequences of the synthesised RT-PCR primers are detailed in Table 2.4.

The RT-PCR process was initiated by synthesising the complementary DNA, followed by PCR reaction amplification. The PCR reaction used BioMix Red (BioLine; BIO-25006). For each reaction, the following components were combined in a sterile PCR tube: 25 µL of BioMix Red, 1 µL of forward primer, 1 µL of reverse primer, 2 µL of diluted cDNA and sufficient RNase/DNase free water to make a final volume of 50 µL. The PCR reaction tube was vortexed, centrifuged briefly and then placed in the PCR machine (Techne TC-312 thermal cycler) for the amplification. The amplification

cycles were 96°C for 5 minutes as a pre-cycling step, followed by a denaturation step at 96°C for 30 seconds for 40 cycles. The annealing temperature was 55°C for 30 seconds and then extension at 72°C for 40 seconds. The PCR reaction ended with a final extension temperature at 72°C for 5 minutes. The PCR reaction mixture was loaded onto a prepared 1% agarose gel (MELFORD #9012-36-6), together with a HyperLadder™ (BIOLINE; BIO-33054) to estimate the yield product size. The agarose gel was prepared with 1X TE buffer (Alpha Laboratories #EL0080) and stained by adding 8 µL of peqGREEN dye (PEQLAB; PEQL37-5010). The gel electrophoreses unit was programmed to run at 400 mA and 120 V for 60 minutes. Experiments were repeated three times at least.

Table 2-4 The sequences for the designed RT-PCR primers and the expected product size

Gene	Primer	Sequence	Product Size (bp)
TEX19	Forward	5'- GTGCCCACATGAACAGAGAC -3'	344
	Reverse	5'- GACATGCCCTCTTCCTCATAC -3'	
OCT4	Forward	5'- CTGGAGAAGGAGAAGCTGGA -3'	509
	Reverse	5'- GCATAGTCGCTGCTTGATCG -3'	
NANOG	Forward	5'- CTGCTGAGATGCCTCACACG -3'	497
	Reverse	5'- GCTCCAGGTTGAATTGTTCC -3'	
SOX2	Forward	5'- GCAACCAGAAAAACAGCCCG -3'	590
	Reverse	5'- CGAGTAGGACATGCTGTAGG -3'	
βACT	Forward	5'- AGAAAATCTGGCACCACACC-3'	553
	Reverse	5'- AGGAAGGAAGGCTGGAAGAG -3'	

2.20 Sequencing PCR products

PCR product was cleaned up using PureLink™ Quick Gel Extraction and PCR Purification Combo Kit (Thermo Scientific #220001), according to the manufacturer's instructions. 300 ng of each purified PCR product was sent to Eurofins MWG for sequencing to confirm identity using primers from Table 2.4. The obtained sequencing results were aligned and blast against corresponding genes using blast tool https://blast.ncbi.nlm.nih.gov/Blast.

2.21 Procedure for the quantitative polymerase chain reaction (RT-qPCR).

The sequences for the RT-qPCR primers were obtained and designed utilising http://www.ncbi.nlm.nih.gov/tools/primer-blast/, https://primerdepot.nci.nih.gov/ and http://www.ensembl.org/index.html. 1X Tris-EDTA buffer solution (Sigma #T9285) was used to prepare the commercial primers according to the manufactures' instructions. The designed RT-qPCR primers are listed Table 2.5 and the commercial primers utilised in the quantitative PCR assays are listed in Table 2.6.

The quantitative polymerase chain reaction was carried out using GoTaq® RT-qPCR Master reagents (Promega #A6001), following the manufacturer's instructions. A 2 µL sample of diluted cDNA in a 20 µL final reaction volume were placed in each well of a Hard-Shell® 96-well plate (BioRad #9655) and each reaction was repeated in triplicate. The reaction amplification was performed at 95°C for 10 minutes for the pre-denaturation step, followed by denaturation at 95°C for 15 seconds for 40 cycles. The primer sequences were annealed at 60°C for 1 minute, followed by 60°C for 5 seconds, and then an extension step at 95°C for 5 seconds. After the completion of 40 cycles, the melt was analysed. In addition, two negative controls were used to ensure no contamination, and at least two reference genes were applied for normalisation. The quantitative PCR assays were achieved with a BioRad CFX analyser and the results were analysed using BioRad CFX Manager Software (version 2). In all RT-qPCR experiments, delta delta CT method was used for the calculation of RT-qPCR quantification. This method straight uses the threshold cycle (CT) data, which is

generated from RT-qPCR system to calculate the relative gene expression in reference and target samples, using a reference gene as the normalizer. The CT value is the cycle in which the detectable signal (fluorescence) can be achieved. For all experiments, dual endogenous reference genes were used at least. The obtained results by RT-qPCR were statistically examined using the t-test to yield any significant difference. All RT-qPCR Experiments were repeated three times at least.

Table 2-5 The designed sequences used for RT-qPCR primers in this study

Genes	Primer	Sequence	Amplicon Size (bp)
GPR137B	Forward	5'-GGGCAACCGGTATTTGAGTA-3'	90
GPR137B	Reverse	5'-ACCCTCACGCTGATGAACTT-3'	
ATG16L1	Forward	5'-GCATTGTCCAGCAGGAACTT-3'	108
ATG16L1	Reverse	5'-AAATGATTTTGCAAGCCGAA-3'	
DTWD1	Forward	5'-CGCCAAAAGCAAGTTTTTCT-3'	93
DTWD1	Reverse	5'-CACCTGGAACCAAACAAACA-3'	
MRS2	Forward	5'-GGCCACTTCCCATGAACATA-3'	98
MRS2	Reverse	5'-AATGGGAGTTGCTTTTGGAA-3'	
FAM117B	Forward	5'-TACTGGAGGGGCTTGAAGAA-3'	106
FAM117B	Reverse	5'-AGGTCTCCGGAGCAGAGC-3'	
LONRF1	Forward	5'-TCAGACAGTTCATCAGGCAGA-3'	119
LONRF1	Reverse	5'-GCACCATATTGTCCTCTTTGC-3'	
FAM98B	Forward	5'-AGATAATCCACCCTCTGCCG-3'	92
FAM98B	Reverse	5'-GAGACGTGCTGGACACACTG-3'	
ZCCHC2	Forward	5'-GGGAGTCTGATGATATGGACTG-3'	110
ZCCHC2	Reverse	5'-ACATCCTGACCTAGAGCCCA-3'	
ZBTB18	Forward	5'-TCGCTCAGACACTGTAGCAAA-3'	110
ZBTB18	Reverse	5'-CCAGCAGGACTCAGAGGAAA-3'	
INPP4B	Forward	5'-TTCTGGTAGGACACTGGTTCG-3'	107
INPP4B	Reverse	5'-CATTCCCATCTGAGTATCCCA-3'	
ARHGAP9	Forward	5'-GGCCACTCCTCTTTTCCTCT-3'	148
ARHGAP9	Reverse	5'-ACAATCGGCTGAGAATGAGAA-3'	
C4BPB	Forward	5'-TAGCCATGAACTGGATTCCC-3'	96
C4BPB	Reverse	5'-TCGGAGCCAGTGTCTAGAGG-3'	
CACNA1G	Forward	5'-AAAGAGGCTGGTGAAGACGA-3'	101
CACNA1G	Reverse	5'-TCCTGGTCAACACACTCAGC-3'	
PCDHB13	Forward	5'-ATGGAGACCAGGGATGTGAG-3'	102
PCDHB13	Reverse	5'-CGTCAGCGCTACAGACAGAG-3'	
GPR183	Forward	5'-TTCCCTGAGGAGTTGCAGAG-3'	95
GPR183	Reverse	5'-GACCCGAACGAGTCACTGAT-3'	
TFAP2E	Forward	5'-CCACCAGGCTGTCTTTGG-3'	101
TFAP2E	Reverse	5'-GGGAATGAGCCTCCTAGACC-3'	
CD274	Forward	5'-TGTCAGTGCTACACCAAGGC-3'	108
CD274	Reverse	5'-ACAGCTGAATTGGTCATCCC-3'	

DAAM2	Forward	5'-GATGCCCTAGGTCCTCATTG-3'	94
DAAM2	Reverse	5'-CATGCCCTGACTTTACCAGG-3'	
SPINK2	Forward	5'-TGCCACACACAGGGTTAAAG-3'	108
SPINK2	Reverse	5'-CAGCCTCTCTGATCCCTCAA-3'	
TRIM54	Forward	5'-GGACTGCCATAGAGGATTCG-3'	93
TRIM54	Reverse	5'-TCCAAACCAGTGGTGATCCT-3'	
CCNE1	Forward	5'-CCACACCTGACAAAGAAGATGATGAC-3'	84
CCNE1	Reverse	5'-GAGCCTCTGGATGGTGCAATAAT-3'	
CTSL2	Forward	5'-TTACATAGCCATTCGAGCCC-3'	91
CTSL2	Reverse	5'-TACGGCTTTGAAGGAGCAAA-3'	
CYFIP1	Forward	5'-AGGTCCACGTTGGACAGC-3'	106
CYFIP1	Reverse	5'-GCCAAGGAAACTCCCAGG-3'	
DIXOC1	Forward	5'-ACAGGTGCTGCTGACAGTTG-3'	107
DIXOC1	Reverse	5'-GGGTCAAGTCACCCAGAACT-3'	
FHL2	Forward	5'-GTGCCGGTCCTTGTAAGACA-3'	94
FHL2	Reverse	5'-GGTGTGCTTTGAGACCCTGT-3'	
GAR1	Forward	5'-CACCTGGAGGTCGAGGTAAA-3'	106
GAR1	Reverse	5'-TTGTCAGAAAACATGAAGGCT-3'	
MATA2	Forward	5'-CCGACGGCCTTATGCTCCT-3'	146
MATA2	Reverse	5'-CTGGGCCACCAGATCTTTGAC-3'	
MDC1	Forward	5'-AATGGCTGTGTAGCCAGGAC-3'	102
MDC1	Reverse	5'-CTTCATGTTGACTCCACCCC-3'	
MYB	Forward	5'-GCAGGTTCCCAGGTACTGCT-3'	107
MYB	Reverse	5'-GCACCAGCATCAGAAGATGA-3'	
MYL9	Forward	5'-CTTGCTGGACATCTTGGCTT-3'	106
MYL9	Reverse	5'-GGAGTCCAGACCCGACG-3'	
PTBP2	Forward	5'-TCGTCAGATCCTCTCTTCACG-3'	90
PTBP2	Reverse	5'-CTCGGTTCTTGTGAGCGAA-3'	
TRIM55	Forward	5'-GAATCAGCTCCACTGCCACT-3'	90
TRIM55	Reverse	5'-TGCACCTGCAGCTACTTCTC-3'	
PNLDC1	Forward	5'-TACCACCCCCTCATCTTTCA-3'	108
PNLDC1	Reverse	5'-TGGATGACTCTTCCTGGGAT-3'	
PROZ	Forward	5'-ACCACAGAAGTCTTTTCCTTCG-3'	91
PROZ	Reverse	5'-GGTGCTGACCTCTGAGAAGC-3'	
PAPPA2	Forward	5'-GGTGCCAGTTTGCTGTTCTA-3'	107
PAPPA2	Reverse	5'-CTGTGACAGTGATTAAGGAGCA-3'	
CAMK4	Forward	5'-AGCATAAGGCTTCTGGGTCC-3'	91
CAMK4	Reverse	5'-CGATTTCTTCGAGGTGGAGT-3'	
LGALS14	Forward	5'-TCGATGGGCAAAGTTGTAAA-3'	94
LGALS14	Reverse	5'-AGATGGCAAACCATTTGAGC-3'	
LY6G6C	Forward	5'-CAGGGACCTTGTAGCAGGAG-3'	90
LY6G6C	Reverse	5'-CCATGAAAGCCCTTATGCTG-3'	
GREM2	Forward	5'-CAGGGAAAGCTTCCAGAACA-3'	118
GREM2	Reverse	5'-CCCGCTGTGGACTAGAGAAC-3'	
XIRP1	Forward	5'-TGTTCAGCAGGGTAGAGGCT-3'	110
XIRP1	Reverse	5'-CAAGAACCTCCAGAGGAACG-3'	
LY96	Forward	5'-TCCCTTGAAGGAGAATGATATTG-3'	90
LY96	Reverse	5'-ATTTGCCGAGGATCTGATGA-3'	
DACT3	Forward	5'-GTAGGGCGCTGAGAAGGAC-3'	106
DACT3	Reverse	5'-CATCTATGCCAGTGAGAGGC-3'	

UPB1	Forward	5'-CTCGTACAGAAGGCAAAGGG-3'	110
UPB1	Reverse	5'-TCTGCCCTTCATAGACGCAT-3'	
KLKB1	Forward	5'-GTGAGAACCCTGGCAACATC-3'	102
KLKB1	Reverse	5'-TGGATTCTCACTGAAGCCCT-3'	
SEPT12	Forward	5'-ATCAGGTGCTCTTGGTCAGC-3'	96
SEPT12	Reverse	5'-GTGCTTTGACGAGGACATCA-3'	
MORN5	Forward	5'-TAGCCCTTTCGACAGGTACG-3'	100
MORN5	Reverse	5'-ACCCAGTCACGAGGGTAGTC-3'	
GPX5	Forward	5'-AAGTGCGATGGCCTCATAGT-3'	110
GPX5	Reverse	5'-CCCTTCTCCTAGCCTGCTTT-3'	
POU2F3	Forward	5'-ATGGCAGGTCCTTGACTCAG-3'	101
POU2F3	Reverse	5'-GGCCTAGATTTCAACAGGCA-3'	
CDHR2	Forward	5'-TCCCATAGGTCAGAGGGTCA-3'	90
CDHR2	Reverse	5'-CAGTGATCCTGCCTGAGGAC-3'	
TSN	Forward	5'-ACACAACAAATGCTGCCAAG-3'	96
TSN	Reverse	5'-TGAAGACCAAATTTCCTGCTG-3'	
VIL1	Forward	5'-ACACAGGTGGAGGTGCAGAAT-3'	79
VIL1	Reverse	5'-GGTTGGTCGCTGTCCACTTC-3'	
LINE-1	Forward	5'-AAATGGTGCTGGGAAAACTG-3'	209
LINE-1	Reverse	5'-GCCATTGCTTTTGGTGTTTT-3'	
SINE	Forward	5'-ACGAGGTCAGGAGATCGAGA-3'	173
SINE	Reverse	5'-GATCTCGGCTCACTGCAAG-3'	
HERV K gag	Forward	5'-CCCGACATTTGTCTTGGTCT-3'	178
HERV K gag	Reverse	5'-CCTGGGGAATCCTTCTCTTC-3'	
HERV K pro	Forward	5'-TGTTCCTCAGGGTTTTCAGG-3'	153
HERV K pro	Reverse	5'-CCCTGGAAGCAGAGAGACTG-3'	
HERV K pol	Forward	5'-TTGAGCCTTCGTTCTCACCT-3'	216
HERV K pol	Reverse	5'-CTGCCAGAGGGATGGTAAAA-3'	
HERV K env	Forward	5'-AAATTTGGTGCCAGGAACTG-3'	145
HERV K env	Reverse	5'-CCACATTTCCCCCTTTTCTT-3'	
HERV K HML2 rec	Forward	5'-ATGAACCCATCGGAGATGCA-3'	160
HERV K HML2 rec	Reverse	5'-AACAGAATCTCAAGGCAGAAGA-3'	
HERV K 107	Forward	5'-GAGAGCCTCCCACAGTTGAG-3'	172
HERV K 107	Reverse	5'-TTTGCCAGAATCTCCCAATC-3'	
HERV K 10	Forward	5'-GATAACGTGGGGGAGAGGTT-3'	156
HERV K 10	Reverse	5'-TCCATCCATGTGACTGGTGT-3'	

Table 2-6 Commercial RT-qPCR primers used in this study

Gene	Evaluate Name	Source	CAT#
GAPDH	Hs_GAPDH_2_SG	Qiagen	QT01192646
TUBA1C	Hs_TUBA1C_1_SG	Qiagen	QT00062720
YWHAZ	YWHAZ_1_SG	Qiagen	QT00087962
β-Actin	Hs_ACTB_1_SG	Qiagen	QT00095431
PAX6	Hs_PAX6_1_SG	Qiagen	QT00071169
POU5F1	Hs_POU5F1_1_SG	Qiagen	QT00210840
NANOG	Hs_NANOG_2_SG	Qiagen	QT01844808
SOX2	Hs_SOX2_1_SG	Qiagen	QT00237601
TEX19	Hs_TEX19_1_SG	Qiagen	QT00033047
PIWIL1	Hs_PIWIL1_1_SG	Qiagen	QT00064638
PIWIL2	Hs_PIWIL2_2_SG	Qiagen	QT01681085
PIWIL3	Hs_PIWIL3_1_SG	Qiagen	QT00071526
PIWIL4	Hs_PIWIL4_1_SG	Qiagen	QT00011074

2.22 Extraction of total protein from human cells

Confluent cells (Table 2.1) were detached with trypsin and washed with 1X DPBS. Complete medium was then added to stop the trypsin reaction. The cells were collected in a sterile conical 15 mL tube and centrifuged for 5 minutes at 400x*g*. The medium was then aspirated and the pellets were washed once using 1X DPBS buffer. The pellets were suspended in 1X DPBS, transferred to new Eppendorf tubes, and centrifuged for 3 minutes at 400x*g*. The wash was removed, 100–150 µL of M-PER lysis buffer (ThermoFisher #78503) was added and the cell pellets were homogenised by gently pipetting up and down. A 1 µL of protease inhibitor (Thermo Scientific #87785) was added for each 100 µL of M-PER lysis buffer. The lysed cell pellets were then set up on a shaker for 10 minutes at room temperature. Subsequently, the cell pellets were centrifuged in a cooled condition for 15 minutes at 1000x*g*. The supernatant (the protein) was transferred to a sterile Eppendorf tube and stored immediately at -80°C until needed. The lysates of human normal tissues were obtained as a commercial product and the protein amount was added according to the manufacturer's instructions (see Table 2.7).

Table 2-7 The sources of human normal lysates analysed by western blotting

Normal lysate	Source	CAT#	Loading amount
Testis	Abcam	Ab30257	20 µg
Skeletal muscle	Abcam	Ab29331	20 µg
Thymus	Abcam	Ab30146	20 µg
Colon	Abcam	Ab30051	20 µg
Small intestine	Abcam	Ab29276	20 µg
Ovary	Abcam	Ab30222	20 µg
Breast	Abcam	Ab30090	20 µg
Lung	Novus Biological	NBP2-27734	20 µg
Liver	Novus Biological	NBP2-29220	20 µg

2.23 Extraction of total protein from human embryonic stem cells

The culture medium was aspirated and the cells were washed with 1X DPBS buffer. The cells were scraped with sterile beads in 5 mL of 1X DPBS buffer. The cells were transferred to a sterile conical tube and centrifuged at 400x*g* for 3 minutes. The wash buffer was aspirated and the pellet was suspended in 1 mL of 1X DPBS and transferred to a sterile Eppendorf tube. The cells were centrifuged for 3 minutes at 400x*g* and the wash buffer was aspirated. Next, 100 µL of M-PER was added and the total protein isolation followed the protocol described in Section 2.22.

2.24 Protein concentration assessment

The amount of extracted protein was evaluated by the Pierce™ BCA Protein Assay Kit (Thermo #23225) to ensure equivalent protein level loading on the western blots. The kit was provided with a set of protein standards (prepared from bovine serum albumin) and working solutions A and B. The working reagent was prepared by combining 50 parts of Reagent A and one part of Reagent B, followed by gentle mixing and protecting from direct light. Next, 1 µL of each standard and protein sample was added individually to 200 µL of the prepared working reagent. The samples were covered with foil and incubated for 30 minutes at 37°C. A Nano-Drop ND-1000 spectrophotometer was used to assess the standard curve and the concentration of the yielded protein.

2.25 Western blotting analysis of proteins from human cells

Each sample was prepared using Bolt® Sample Reducing Agent (Thermo Scientific #B0009), Bolt® LDS Sample Buffer (Thermo Scientific #B0007) and 30 µg of the total extracted protein in an Eppendorf tube, following a brief vortex and spin. The samples were incubated for 10 minutes at 70°C and then loaded onto a commercial 15-well Bolt™ 4–12% Bis-Tris Plus Gel (Thermo Scientific #NW04125BOX). A Precision Plus Protein™ Dual Colour Standard (Bio-Rad #161-0374) was loaded alongside the protein sample to estimate the protein molecular weight. The Bolt MES SDS Buffer (Thermo Scientific #B0002) was prepared by dilution the concentrated reagent (20X) in dH2O to make a final volume of 1X for the western blot or protein separation. The electrophoresis unit was programmed at 165 V for 40 minutes. Following the protein separation, the protein was transferred to a PVDF membrane using a Trans-Blot®

Turbo™ RTA Mini PVDF Transfer Kit (Bio-Rad #1704272). Transfer buffer was prepared by composing 200 mL of 5x transfer buffer (BIO-RAD #10026938), 200 mL of absolute ethanol and 600 mL of nanopure water.

The PVDF membrane (pore size 0.2 μm) was activated in pure methanol for at least 2 minutes, following the manufacturer's instructions in the kit, and placed in distilled water and then in the transfer buffer until used. Two stacks were thoroughly wetted with transfer buffer. Next, the PVDF membrane was positioned on a wet stack, followed by the protein gel and another wet stack. Subsequently, the protein gel was transferred electrophoretically for 7 minutes utilising a Trans-Blot® Turbo™ Transfer System for rapid transfer with high efficiency. Once the protein was transferred to the PVDF membrane, a blocking step was then applied. The blocking solution was prepared with 5% dry milk in 1X DPBS/0.5% Tween 20. The membrane was placed in the blocking solution for at least 1 hour. Next, the membrane was probed with primary antibody and incubated overnight at 4°C. The PVDF membrane was washed 3 times with 1X DPBS/0.5%/Tween (Tween buffer) and then probed with the secondary antibody for 1 hour, followed by 3 washes with Tween buffer.Antibody detection and western blot analysis followed the Pierce ECL Plus Substrate (Thermo Fisher #32132) instructions. The CL-XPosure Film (Thermo Scientific #34091) used here is an outstanding photographic film for use with ECL substrates for horseradish peroxidase (HRP) and developing visualised bands using optimal exposure times. Primary and secondary antibodies are listed Tables 2.8 and 2.9. Experiments were repeated three times at least.

Table 2-8 The primary antibodies and optimal concentrations for the western blot analyses

Primary Antibody	Company	CAT#	Host	Application	Dilution
Anti-α-Tubulin	Sigma	T6074	Mouse	WB	1:5000
Anti-GAPDH	Santa Cruz	SC-365062	Mouse	WB	1:3000
Anti-TEX19	R&D	AF6319	Sheep	WB	1:200
Anti-MAGEC1	Abcam	Ab61404	Mouse	WB	1:500

Table 2-9 Secondary antibodies and the optimal concentration for the western blot analyses

Secondary Antibody	Company	CAT#	Target species	Application	Dilution
Anti-mouse	Cell Signalling	7076	Mouse	WB	1:3000
Anti-sheep	R&D	HAF016	Sheep	WB	1:20000

2.26 Knockdown in human cancer cells by siRNA

Human cancer cells in the confluence stage were seeded at 2×10^5 cells per well in a 6-well plate (Costar #3516) using complete medium (10% FBS added). The cells were then incubated overnight at the desired temperature and CO_2 percentage to allow attachment. The next day, fresh medium added. An siRNA was prepared in a sterile Eppendorf tube for each well by combining 100 μL of the appropriate serum-free medium, 6 μL Hiperfect Transfection Reagent (Qiagen #301705) and 1.2 μL 10 μM siRNA. For the targeted sequence genes, see Table 2.10. The mixture was vortexed, spun briefly, and then incubated for 15 minutes at room temperature. The mix was then added dropwise to each well, with gentle shaking. A negative non-interference control (Qiagen #1022076) was applied alongside the experimental tests to assess the effectiveness of siRNA knockdown. The cells were incubated and same procedure was carried out for further 2 days, to give 3 siRNA treatments in total. The cells were then harvested for RNA isolation or protein extraction. Experiments were repeated three times at least.

2.27 Knockdown in human embryonic stem cells by siRNA

Human embryonic stem cells were seeded at 1×10^6 cells in T25 flasks using E8 medium on a feeder-free system and incubated for 24 hours. The culture medium was then removed and replaced with fresh medium. A mixture of siRNA was prepared in a sterile Eppendorf tube for each flask by combining 100 μL of the medium, 8 μL of Hiperfect Transfection Reagent (Qiagen #301705) and 1.2 μL of 10 μM siRNA for the targeted sequence gene (see Table 2.10). The mixture was vortexed, spun briefly and then incubated for 15 minutes at ambient temperature. Next, the mix was added and each flask was shaken gently. A negative non-interference control (Qiagen #1022076) was

applied alongside the experimental samples to assess the effectiveness of the siRNA knockdown. The cells were then incubated and the same procedure was carried out for 3 more days at exactly the same time, to give 4 siRNA treatments in total. The cells were then harvested for RNA or protein analysis. Experiments were repeated three times at least.

Table 2-10 The target sequences of siRNA used for knockdown of human *TEX19* gene

Gene	Source & siRNA Name	CAT#	Target sequence
TEX19	**Qiagen Hs_FLJ35767_7**	**SI04247705**	**5'TTCAACATGGAGATCAGCTAA3'**
Non-interfering siRNA	**Qiagen Negative Control siRNA**	**1022076**	----------

2.28 Immunofluorescence (IF) protocol

2.28.1 Human cell seeding

Human cells were seeded on sterile coverslips at 1×10^5 cells per well in a 24-well plate (Chemglass Life Sciences; 12 mm; #CLS-1760-012) in complete medium. The cells were then incubated at the optimum temperature and CO_2 percentage until they reached 80% confluence.

2.28.2 Human cell fixation

The medium was aspirated and the cells were washed once with 1X DPBS. The cells were then fixed in 1 mL 4% paraformaldehyde (Thermo Scientific #28908) for 10 minutes. The paraformaldehyde fixing solution was removed and the cells were washed 3 times with 1X DPBS buffer at room temperature for 5 minutes with shaking. The washes were discarded and 1 mL 0.2% Triton was added to the cells as a permeabilisation agent. The cells were incubated in the hood for 10 minutes and the permeabilisation buffer was then discarded. The cells were again washed with 1X DPBS buffer 3 times for 5 minutes. The blocking buffer was prepared by combining 47.5 mL of 1X DPBS and 2.5 mL of FBS. The wash was aspirated and 1 mL of blocking

buffer was added to each well. The cells were incubated on a shaker for 1 hour at room temperature.

2.28.3 Antibodies and cell mounting

Following the incubation, the blocking solution was removed and the optimal concentration of primary antibody was added to each well (see Table 2.11). The primary antibody was diluted in a blocking solution and about 300 μL was transferred to each well. The primary antibody was added and the plate was incubated overnight at 4°C in the dark.

The primary antibody was removed and the cells were washed with 1X DPBS buffer 3 times for 10 minutes at room temperature; the plate was placed on a shaker for each wash. The optimal concertation of secondary antibody was then added to each well. The secondary antibody was diluted in a blocking solution and about 300 μL transferred to each well (see Table 2.12). The secondary antibody was incubated for approximately 2 hours at room temperature with foil covering the plate. All secondary antibodies were prepared in the dark and diluted with blocking solution. After the completion of secondary antibody incubation, the cells were washed with 1X DPBS 3 times for 10 minutes. Prolong® Gold Antifade Reagent with DAPI (Cell Signalling #8961) was utilised to mount the coverslips. A Zeiss LSM 710 confocal microscope was used to detect the immunofluorescence and the images were analysed using ZEN software. IF Experiments were repeated three times at least.

Table 2-11 Primary antibodies and the optimal concentrations for immunofluorescence assays.

Primary Antibody	Company	CAT#	Host	Clone	Dilution
Anti-α-Tubulin	Sigma	T6074	Mouse	Monoclonal	1:1000
Anti-TEX19	Abcam	ab185507	Rabbit	Polyclonal	1:500

Table 2-12 Secondary antibodies and the optimal concentrations for immunofluorescence assays.

Antibody	Dye/Label	Wavelength of light (nm)	Source &CAT#	Host	Species Reactivity	Dilution
Anti-mouse IgG (H+L)	Alexa Fluor® 568	578 / 603	Life Technologies A11031	Goat	Mouse	1:500
Anti-rabbit IgG (H+L)	Alexa Fluor® 488	495 / 519	Life Technologies A11034	Goat	Rabbit	1:500

2.29 Growth curves of human cell proliferation

The human cells were seeded in 6-well plates at 2×10^5 cells per well for the SW480 and H460 cell lines and 2.5×10^5 cells per well for the NTERA2 cell line. The incubation was carried out with the required CO_2 percentage and the optimal temperature, based on the cell line. After 24 hours, the cells were treated with *TEX19 siRNA* together with the negative non-interference control for each well, as described in section 2.26. On the next day, the cells were counted with an automatic cell counter and the total protein was extracted. Each count and protein isolation was performed in triplicate. The human cell proliferation was monitored by curve analysis for 8 days after siRNA treatment. Experiments were repeated three times at least.

2.30 Extreme limiting dilution analysis (ELDA) in human cells

SW480, H460 and NTERA2 cells were seeded in a 96-well plate (Costar; Corning 3474) and incubated at the required CO_2 enrichment and optimal temperature. The cells were plated at different cell numbers (1000, 100, 10 and 1 cell per 100 μL of complete media). A further 12 wells of repeats containing untreated cells and non-interfering siRNA were prepared alongside the *TEX19 siRNA* treated cells. On the next day, the medium was replaced with fresh medium. An siRNA mixture was prepared in a sterile Eppendorf tube for each well by combining 4.7 μL of the appropriate serum free medium, 0.3 μL of Hiperfect Transfection Reagent (Qiagen #301705) and 0.1 μL of 10 μM siRNA for the human *TEX19* gene. The mixture was vortexed, spun briefly, and then incubated for 15 minutes at room temperature. The mix was then added dropwise

to each well of the 24-well plate with gentle shaking. The cells were incubated for 10 days at the appropriate CO_2 percentage and temperature. The *TEX19 siRNA* treatment was carried out for the first 3 days alongside the non-interfering siRNA treatment. The cells were supplied with 50 µL of medium to maintain them during the long incubation. After 10 days, the positive cells in the wells were counted using a light microscope. The analysis of the self-renewal frequency was conducted using the ELDA web tool http://bioinf.wehi.edu.au/software/elda/. Experiments were repeated three times at least.

2.31 Immunohistochemistry (IHC)

Altered human cancer tissues and nearby normal tissues were obtained from different patients of both genders and various ages (see Table 2.13). Written consent was provided by each individual patient. In addition, the use of these samples was approved by the local research ethics committee (North Wales Research Ethics Committee – West). All the cancer and normal tissues were fixed in formalin and embedded in paraffin. The immunohistochemistry was conducted on 4 µm thick tissue sections. A Ventana Benchmark XT instrument was utilised for the automated staining following a standard Immunohistochemistry protocol. Polyclonal rabbit antibody purchased from Abcam (#185507) was used as primary antibody for the IHC application. Discovery Universal Secondary Antibody (Biotinylated Ig cocktail) from Roche (#760-4205) was used .The Ventana iCoreo slide scanner was utilised for capturing the digital images. Experiments were repeated three times at least.

Table 2-13 patient information and tumour staging

case	Gender	Age	Site	Differentiation	Duke's Stage	T	N	M	EVA
C45	M	90	Ascending	Poor	B	3	0	X	No
C35	F	77	Caecum	Moderate	B	3	0	X	No
C12	F	69	Transverse	Moderate	B	2	0	X	No

T-tumour, N-node, M-metastasis, EVA- extramural vascular invasion.

Chapter 3

Evaluation of *TEX19* expression in normal human tissues, cancer cells/tissues and stem cells

3. Evaluation of *TEX19* expression in normal human tissues, cancer cells/tissues and stem cells

3.1 Introduction

One of the major intrinsic features of CTA genes is their expression in tumour cells and silencing in normal somatic tissues (McFarlane et al., 2015). Expression of these genes is normally restricted to human germline tissues. However, their activation in somatic tissues can contribute to oncogenesis (Caballero & Chen, 2009; Fratta et al., 2011; Whitehurst, 2014). These genes are also termed cancer germline genes; their exceptional expression means that they can be employed as cancer biomarkers and new therapeutic targets (McFarlane et al., 2015). Some CTA genes have also been reported to be expressed in the placenta, foetus and ovary, as well as in immature cells, including trophoblasts and spermatogonia (Costa et al., 2007; Scanlan Simpson & Old, 2004). In addition, some CTA genes can be activated in other immune privileged tissue, such as the brain, in which their expression level is often lower than 1% of that in normal testes (Caballero & Chen, 2009; Fratta et al., 2011). The expression of some CTA genes has been detected in cancer stem-like cells, and these genes termed cancer/testis/stem genes (Ghafouri-Fard, 2015, Yamada et al., 2013).

The testis is an immune-privileged organ encompassing about 250 testicular lobules that are separated by tissue barriers; each lobule contains between one and three seminiferous tubules. The epithelium of the seminiferous tubules consists of germ cells and Sertoli cells. Germ cells produce sperm cells by the process known as spermatogenesis. Sertoli cells contribute to nourishing the developing sperm cells (Durairajanayagam et al., 2015; Jones & Lopez, 2013). In this vein, immunohistochemistry has shown that CTAs are clearly present in the testis, spermatogonia, primary spermatocytes and Sertoli cells in seminiferous tubules (Yang et al., 2005). Different CTAs show different patterns of staining, where some CTAs, such as MAGE-1 and MAGE-3, have shown strong cytoplasmic and variable nuclear staining (Jungbluth et al., 2000). In addition, nuclear pattern staining was detected for some CTAs, such as HORMAD1, while cytoplasmic only staining was shown for SPANX (Caballero & Chen, 2009).

RT-PCR analysis have revealed that CTA genes are expressed in different type of cancers. However, not all CTA genes are expressed at similar levels, and their detection is altered in different cancer types (Hofmann et al., 2008; Scanlan, Simpson & Old, 2004; Whitehurst, 2014). In cancers like melanoma, bladder cancer, hepatocellular carcinoma and non-small-cell lung cancer, CTA genes have been reported to have a high level of expression; meanwhile, moderate expression has been observed in prostate and breast cancer, and low expression has been found in bowel and renal cancer (Scanlan, Simpson & Old, 2004; Hofmann et al., 2008). However, this encourages the idea that CTA genes can play a significant role in effecting tumour progression, and they can be useful as targets in immunotherapy (Grizzi et al., 2015).

Until now, a limited amount of research has studied the expression of *TEX19* in mammals, or more specifically, in humans. In mice, *Tex19.1* gene has been expressed in both the placenta and adult testis. *Tex19.1* was found to be in a similar fashion expressed as *Oct4* in the early stage of embryonic development, and its expression decreases during differentiation; thus, its role as pluripotent marker was proposed (Kuntz et al., 2008). In human, *TEX19* was found to be expressed in testis and silenced in normal tissues except weak expression in thymus in some samples. In addition, *TEX19* found to be activated in distinct cancer types, and it has been identified as a CTA gene (Feichtinger et al., 2012). Furthermore, Zhong and co-workers (2016) confirmed the restricted expression of *TEX19* in the testis, and the presence of the protein in range of bladder carcinoma samples (Zhong et al., 2016).

The aim of the work described in this chapter is to study *TEX19* expression profiles with a view to determining whether it is a definitive CTA gene. A further aim is to investigate its expression in multiple pluripotent cells to determine whether *TEX19* could be a stem determining gene. An additional goal is to determine the cellular localisation for TEX19 protein to provide insight into protein function (s).

3.2 Results

3.2.1 Analysis of *TEX19* expression in human normal tissues and cancer cells

To evaluate the expression patterns of *TEX19*, RT-PCR analysis was carried out in 21 normal tissues. The cDNA of these normal tissues was synthesised from total RNA. In RT-PCR analysis, the *βACT* gene was used to assess the quality of synthesised cDNA and as a positive control for the cDNA. The expression of *TEX19* in multiple normal tissues was assessed, and it was detected only in the testis and very weakly in the thymus (Figure 3.1). The PCR products for both *TEX19* and *βACT* migrated to approximately the expected sizes (344 bp and 553 bp, respectively).

The expression study of *TEX19* was extended further for investigation in several cancer cell lines using RT-PCR. The cDNA was synthesised from total RNA. In the RT-PCR assay, screening of the *βACT* gene was used to assess the quality of synthesised cDNA and as a positive control for the generated cDNA. The results showed a wide range of expression for *TEX19* (Figure 3.2). A high expression signal was detected in colon adenocarcinoma (SW480 and LOVO), colon carcinoma (HCT116), liver carcinoma (HEP G2), cervical adenocarcinoma (HeLa-S3), ovarian carcinoma (A2780) and leukaemia (jurkat). Less apparent expression signal was detected in astrocytoma (1321N1), embryonal carcinoma (NTERA2), colon adenocarcinoma (HT29), colon carcinoma (T84), lung adenocarcinoma (H460), prostate adenocarcinoma (PC-3), breast carcinoma (MDA-MB-453 and MCF-7), ovary tumour, ovarian cancer (oestrogen receptor negative PE014), melanoma (G361, MM127, COLO800 and COLO857), epidermal carcinoma (A-431), Burkitt lymphoma (Raji) and leukaemia (K-562), although weak bands are associated in most cases.

Based on the results obtained from RT-PCR in normal and cancer cells, the investigation was carried out using RT-qPCR for further confirmation. The same cDNA as in the previous analysis was used to quantify the expression levels of *TEX19*. The values of the cycle threshold (Ct) were determined after amplifying *TEX19* to analyse the expression level. Ct values > 37 were considered negative expression. The *TEX19* expression levels in normal tissues shown by RT-qPCR were consistent with the results

obtained by RT-PCR. *TEX19* showed significant expression in the testis, with detectable Ct values = 30.13. Weak expression was detected in the thymus, with Ct values = 36.22; this was extremely close to the relative cut-off. In the rest of the samples, Ct values of either zero or > 37 were detected; this was considered negative expression (Figure 3.3 A & B).

The *TEX19* expression level was deteced by RT-qPCR in the most of cancer samples (Figure 3.4 A), which was consistent with the RT-PCR results. Positive expression was determined with Ct values < 37. *TEX19* showed significant expression in the testis, with detectable Ct values = 28.06. Cancer samples of SW480, HCT116, LOVO, HEP G2, A2780, K-562, Burkitt lymphoma (Raji) and leukaemia (jurkat) cells showed significant expression. The cancer samples detected with Ct values > 37 were considered to show negative expression (Figure 3.4 A & B).

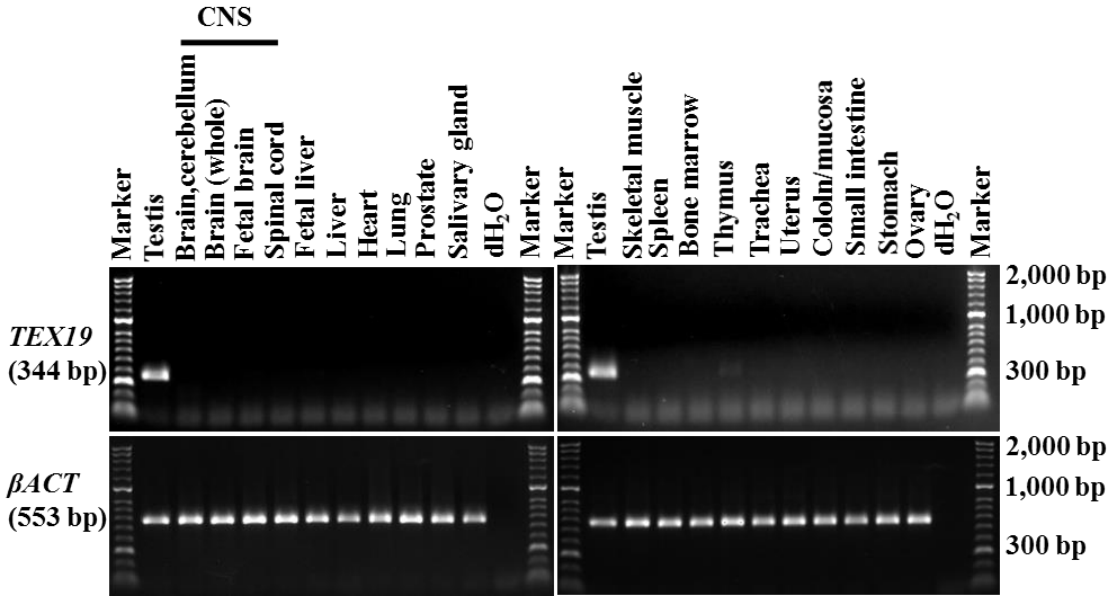

Figure 3-1 RT-PCR analysis of the *TEX19* gene expression in normal human tissues.
Agarose gels present the *TEX19* expression in normal human tissues. The expected PCR product size of *TEX19* is 344 bp. The expression profile of the *βACT* gene was used as a positive control for the cDNA samples synthesised from normal tissues. dH_2O was used as negative control. The PCR product of *βACT* has an expected size of 553 bp.

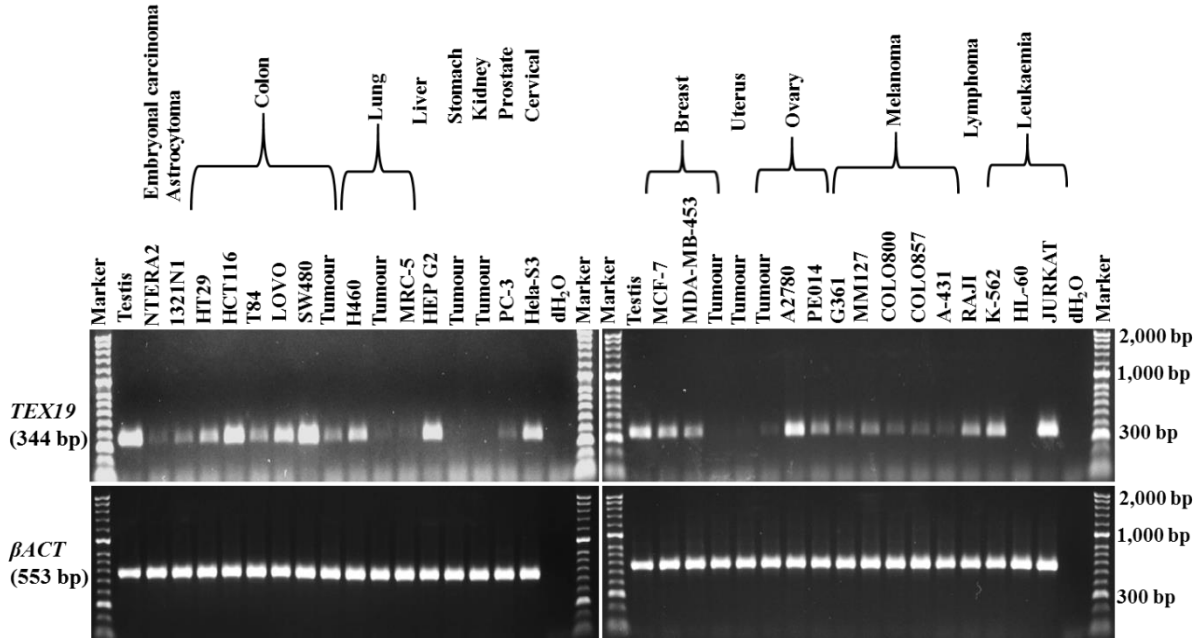

Figure 3-2 RT-PCR analysis of *TEX19* gene expression in human cancer cells.
Agarose gels present the *TEX19* expression in cancer cells. The expected PCR product size of *TEX19* is 344 bp. The expression profile of the *βACT* gene was used as a positive control for the cDNA samples synthesised from cancerous cells. dH_2O was used as negative control. The PCR product of *βACT* has an expected size of 553 bp.

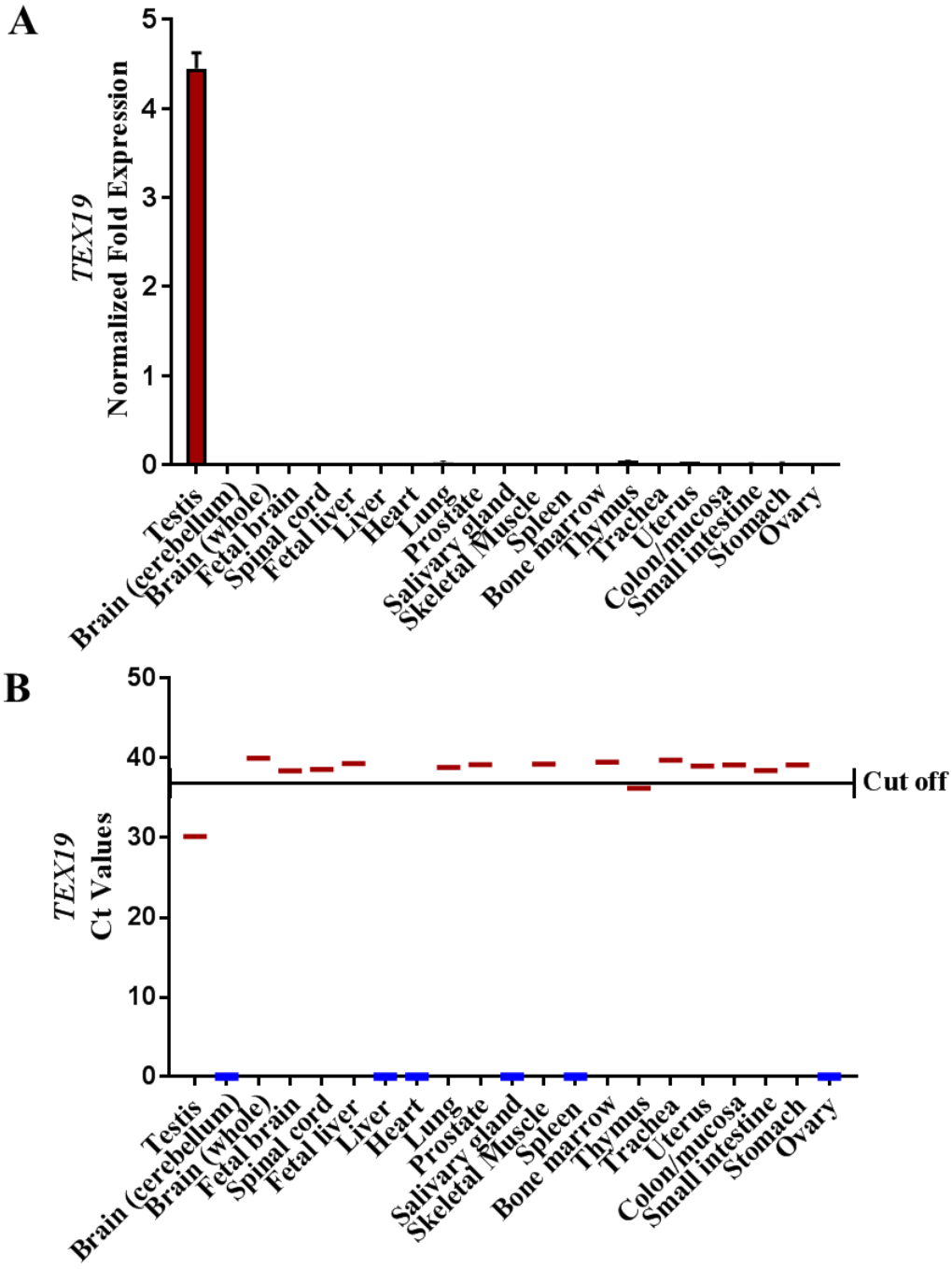

Figure 3-3 RT-qPCR analysis of the *TEX19* gene expression in normal human tissues.
(A) Bar chart presenting the expression levels of the *TEX19* gene in the testis and multiple normal tissues. The obtained data were normalised using a combination of two endogenous reference genes, *TUBA1C* and *GAPDH*. The error bars show the standard errors of the mean. (B) Chart presenting the calculated Ct values following *TEX19* cDNA amplification in normal tissues. Samples above the cut off line show with a Ct value > 37 and are considered to represent negative expression. Samples with no detectable *TEX19* expression have Ct values of zero and shown on the graph above as blue dashes.

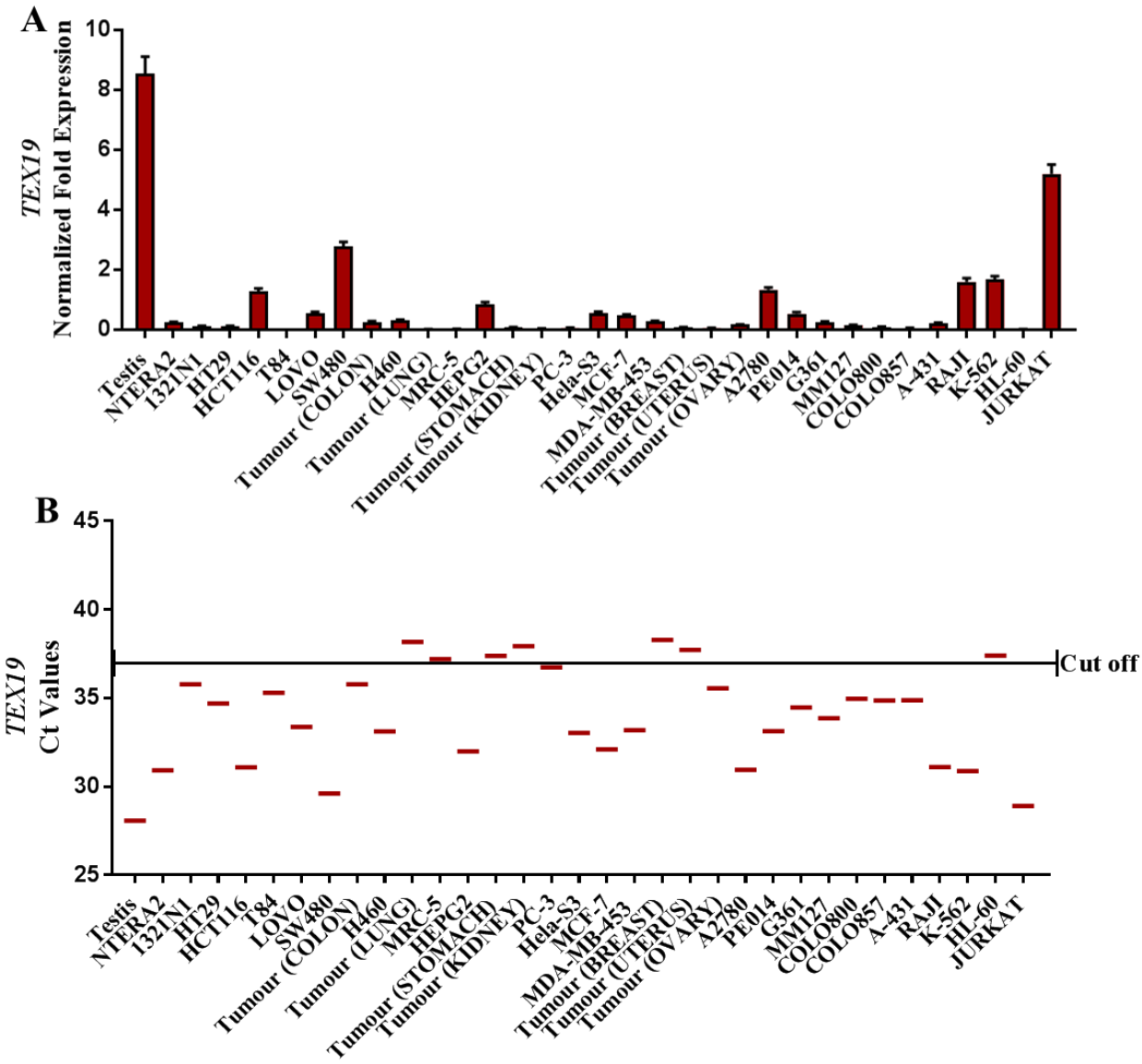

Figure 3-4 RT-qPCR analysis of the *TEX19* gene expression in human cancer cells.
(A) Bar chart presenting the expression levels of *TEX19* gene in the testis and numerous cancer cells. The obtained data were normalised using a combination of two endogenous reference genes, *TUBA1C* and *GAPDH*. The error bars show the standard errors of the mean. (B) Chart presenting the calculated Ct values following *TEX19* cDNA amplification in cancer cells. Samples above the cut-off line exhibit a Ct value > 37 and are considered to represent negative expression.

3.2.2 Analysis of TEX19 protein levels in normal human tissues and cancer cells

TEX19 protein level was assessed in multiple normal human tissues, human embryonic stem cells (hESCs), fibroblast cells by western blotting and distinct cancer cells using polyclonal antibody (R&D, #AF6319). In normal tissues, MAGEC1 was used as a CTA control. Two positive loading controls were used (anti-GAPDH and anti-α-Tubulin). The MAGEC1 protein migrated to approximately 124 KDa, as expected. Both loading controls migrated to the expected protein size (approximately 37 KDa and 50 KDa for anti-GAPDH and anti-α-Tubulin, respectively). The TEX19 protein size is predicted to be approximately 18.5 KDa, and it was found to migrate at approximately 24 KDa in this study. The approximate predicted size of the protein was indicated with an arrow (Figure 3.5 B and C). The band migrating below this is suggested to be a degradation product. TEX19 depletion verified the specificity of the used antibody (Figure 3.5 D).

In normal tissues, the presence of TEX19 was significantly detected in the testis, while very weak signals were found in the thymus (Figure 3.5 A). TEX19 protein was detected in hESCs; normal fibroblast exhibited negative results, as no signal was observed (Figure 3.5 B). In addition, the presence of TEX19 was detected in all cancer cell lines tested (Figure 3.5 C). Strong signals were observed in colon cancer (SW480 and HCT116), ovarian carcinoma (A2780), ovarian cancer (oestrogen receptor negative PE014), large-cell lung carcinoma (H460), breast carcinoma (MCF-7), malignant melanoma (G361) and leukaemia (JURKAT). Weaker signals were detected in embryonal carcinoma (NTERA2), astrocytoma (1321N1), cervical adenocarcinoma (HeLa-S3) and melanoma (COLO800).

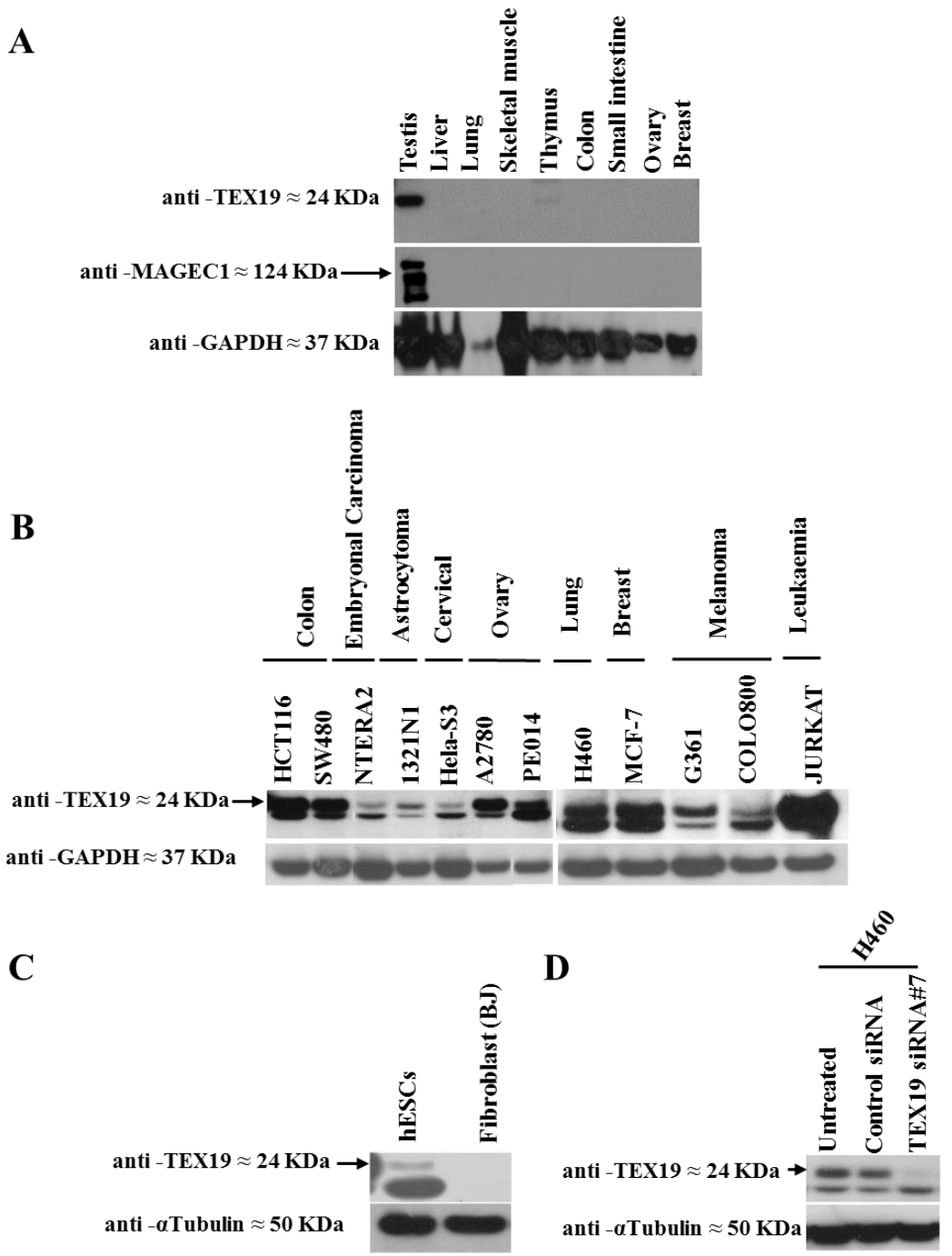

Figure 3-5 Western blot analysis of TEX19 protein levels in normal tissues, hESCs and distinct cancer cell lines.

(A) The results demonstrate the TEX19 protein levels in normal tissues, with a strong band in the testis and a very faint band in the thymus. MAGEC1 was used as a CTA control. GAPDH was used as a loading control. (B) TEX19 is present in all cancer cell lines. GAPDH was used as a loading control. (C) TEX19 is present in hESCs but not in fibroblasts. (D) TEX19 siRNA depletion in H460 showing anti-TEX19 antibody (R&D, #AF6319) specificity. Tubulin was used as a loading control.

3.2.3 Analysis of *TEX19* expression in human embryonic stem cells and induced pluripotent stem cells

The expression of human *TEX19* was investigated in hESCs and induced pluripotent stem cells (iPSCs) using RT-PCR and RT-qPCR. The RNA was generated in the McFarlane lab for both hESCs and iPSCs. Moreover, iPSCs were originally reprogrammed from human fibroblasts, and these fibroblasts were used as a negative control. Testis tissue were used as a positive control. Cancer stem cells (CSCs) and NTERA2 cells were used as a positive control representing stem cells that can express the stem cell marker genes *OCT4*, *NANOG* and *SOX2*. The SW480 cancer cell line presented high expression of *TEX19*. Using RT-PCR, *TEX19* was detected with significant expression in hESCs and iPSCs, while it was negative in fibroblasts (Figure 3.6 A). The *βACT* gene was used to assess the quality of synthesised cDNA and as a positive control for the generated cDNA. The PCR products for both *TEX19* and *βACT* migrated to approximately the expected sizes (344 bp and 553 bp, respectively). Furthermore, *OCT4*, *NANOG* and *SOX2* were detected in hESCs, iPSCs, CSCs and NTERA2 (Figure 3.6 B). The expression of stem cell markers verifies the pluripotency of these cells. Fibroblast cells did not express *OCT4*, *NANOG* and *SOX2*. PCR products for *OCT4*, *NANOG* and *SOX2* migrated to approximately the expected sizes (509 bp, 497 bp and 590 bp, respectively).

Based on the results obtained by RT-PCR, further confirmation was carried out using RT-qPCR in hESCs and iPSCs. CSCs and NTERA2 were used as a positive stem cell controls, and they expressed *OCT4*, *NANOG* and *SOX2*. Fibroblasts were used as a negative control for iPSCs. SW480 was included as a further cancer cell line express *TEX19*. The obtained results by RT-qPCR showed significant expression of *TEX19* in hESCs and iPSCs, while negative expression was detected in fibroblasts (Figure 3.7 A). These findings were consistent with the RT-PCR results. *OCT4*, *NANOG* and *SOX2* were expressed in hESCs, iPSCs and the positive control cells (NTERA2 and CSCs). Fibroblast cells did not express *OCT4*, *NANOG* and *SOX2*. *OCT4* and *SOX2* showed higher expression levels compared to *NANOG* in hESCs, iPSCs and NTERA2 cells (Figure 3.7 B, C and D).

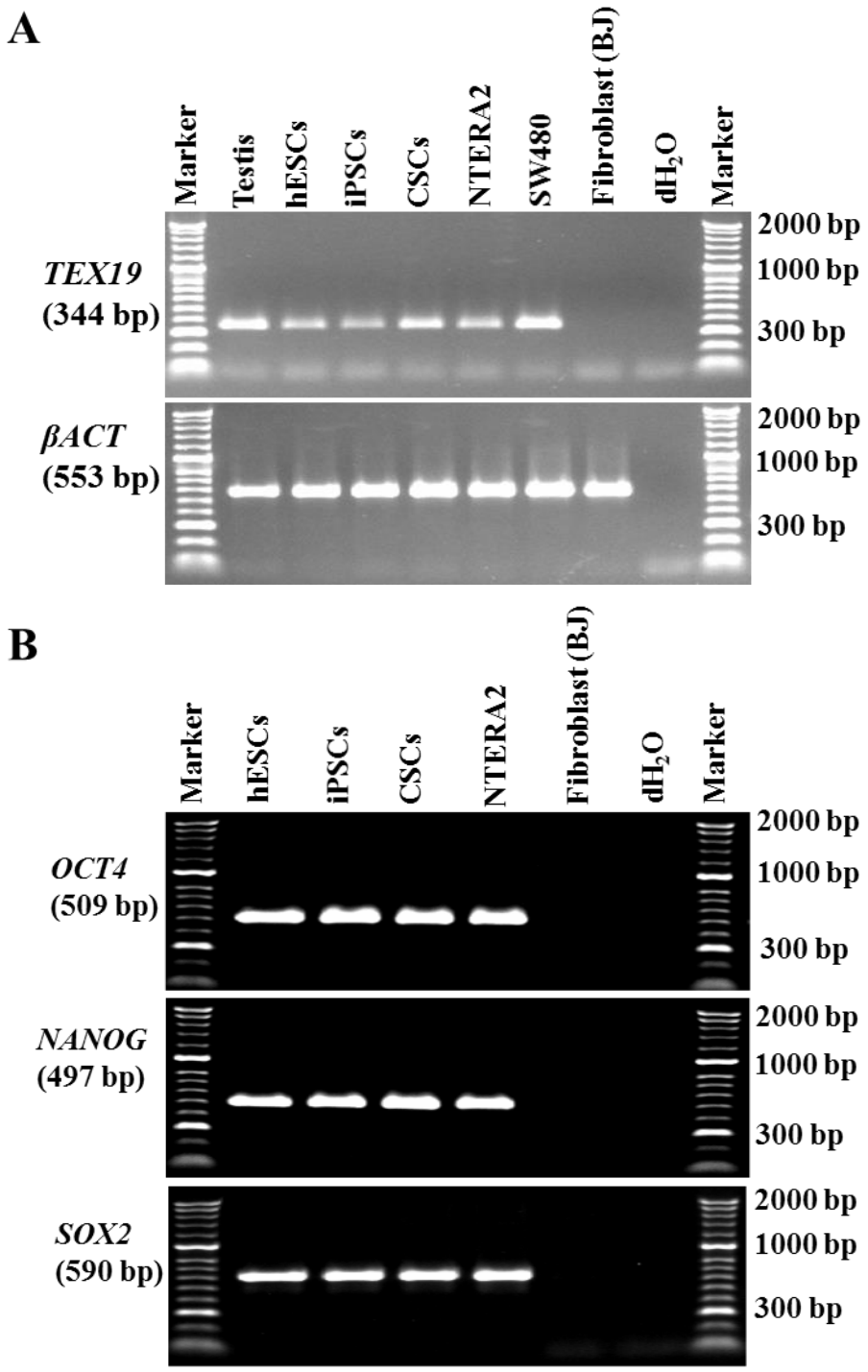

Figure 3-6 RT-PCR analysis of *TEX19* gene expression in hESCs and iPSCs.
(A) *TEX19* expression in hESCs and iPSCs. The expression profile of the *βACT* gene was used as a positive control for the synthesised cDNA. Testis tissue was used as a positive control. CSCs and NTERA2 were used as a positive stem cell control. fibroblast cells were used as a negative control for the iPSCs. SW480 was used as a cancer cell line. (B) Expressions of *OCT4*, *NANOG* and *SOX2* genes as stem cell markers. The PCR products were detected with the expected sizes (presented on the left).

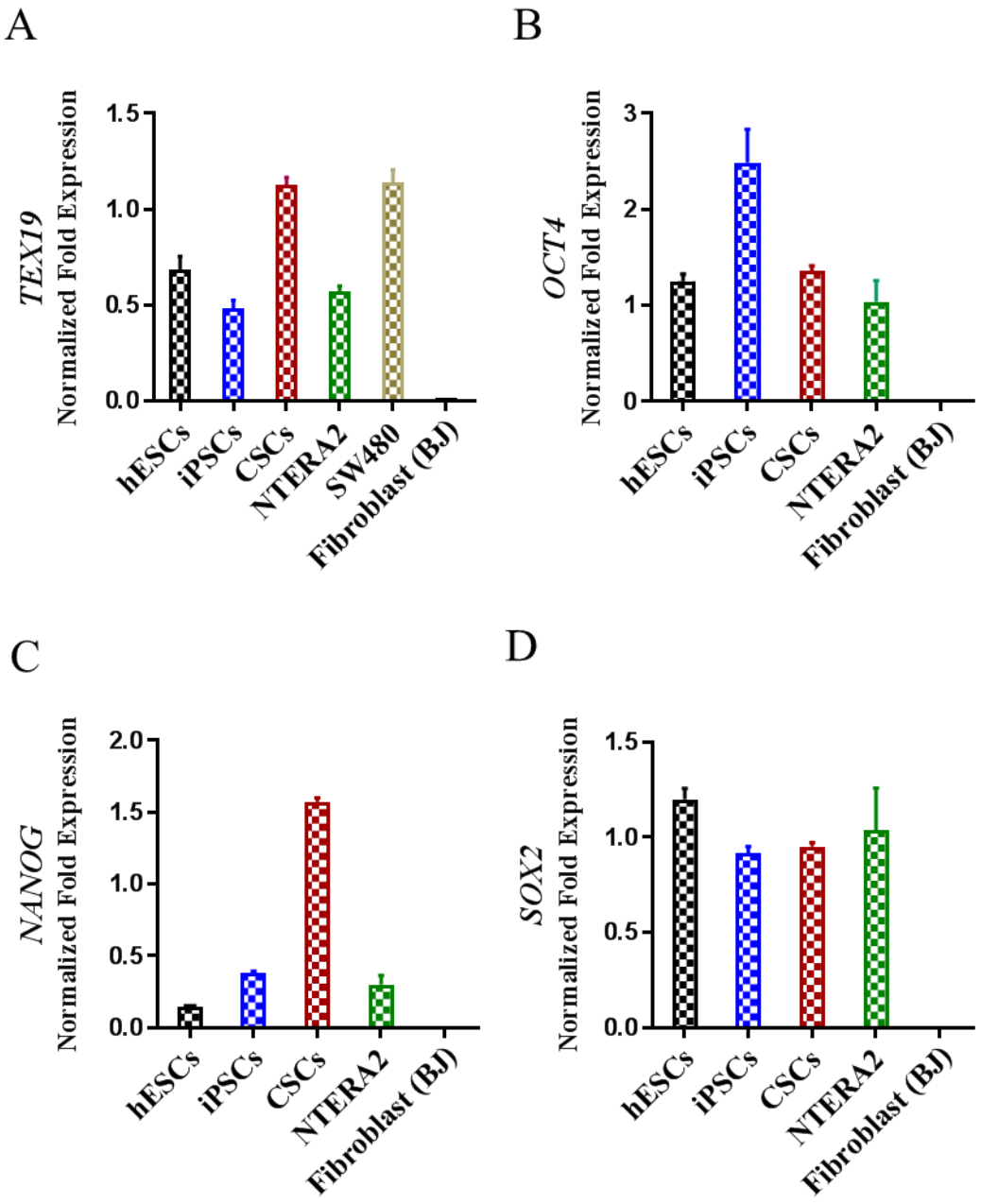

Figure 3-7 RT-qPCR analysis of the *TEX19* gene expression in hESCs and iPSCs.
(A) Bar chart presenting the expression levels of the *TEX19* gene in hESCs and iPSCs. CSCs and NTERA2 calls were used as positive stem cell controls. Fibroblast cells were used as a negative control for the iPSCs. SW480 was used as cancer cell line. (B) Bar chart showing the expression levels of the *OCT4* gene in hESCs, iPSCs, CSCs and NTERA2. (C) Bar chart demonstrating the expression levels of the *NANOG* gene in hESCs, iPSCs, CSCs and NTERA2. (D) Bar chart showing the expression levels of the *SOX2* gene in hESCs, iPSCs, CSCs and NTERA2 cells. *OCT4*, *NANOG* and *SOX2* genes were used as stem cell markers. The obtained data were normalised using a combination of two endogenous reference genes, *YWHAZ* and *GAPDH*. The error bars show the standard errors of the mean.

3.2.4 Analysis of *TEX19* expression in human differentiated cancer stem-like cells

As can be seen in Figures 3.6 and 3.7, *TEX19* was activated upon the reprogramming of iPSCs from human fibroblasts, while its detection was negative in fibroblasts. In line with this, *TEX19* expression was investigated during the differentiation period to determine whether *TEX19* expression is correlated with the stemness features. NTERA2 represents embryonal carcinoma, and this was used because it shares characteristic with stem cells due to the expression of the stem cells markers. NTERA2 cells were differentiated using two inducer agents, namely retinoic acid and HMBA. Two controls were used, namely untreated cells and DMSO. NTERA2 cells were differentiated for 10 days. Total RNA was extracted and the cDNA was synthesised for each day. To verify successful differentiation, *OCT4* was used as a stem cell marker. The transcript levels of both *OCT4* and *TEX19* were analysed according to differentiation time using RT-qPCR.

The differentiation of NTERA2 cells was successful. As can be seen in Figures 3.8 and 3.9 A and B, the mRNA levels of both *OCT4* and *TEX19* in untreated cells and DMSO remained constant as positive controls. The analysis of *OCT4* mRNA levels in the cells treated with retinoic acid showed a significant decline from day 2, and the *OCT4* transcript levels started to be unmeasurable at day 5 (Figure 3.10 B). This indicates that NTERA2 cells became differentiated. On days 2, 3 and 4, *OCT4* transcripts were detected with a significant reduction ($p<0.05$, $p<0.0001$ and $p<0.0001$, respectively). In addition, the analysis of *TEX19* mRNA levels showed significant reductions on all days except day 3 (Figure 3.10 A). The *p*-values were $p<0.001$ for days 1, 6, 7 and 9. For days 2, 5 and 8, the *p*-value<0.01. The *p*-value was $p<0.05$ for Day 4. The analysis of *OCT4* transcript levels in the cells treated with HMBA showed a significant decline from day 1, and the *OCT4* mRNA could not be detected from day 5 (Figure 3.11 B). This indicated successful differentiation. On days 1, 2, 3 and 4, *OCT4* transcripts were detected with a significant reduction ($p<0.05$, $p<0.01$, $p<0.0001$ and $p<0.0001$ respectively). In addition, the analysis of *TEX19* mRNA levels showed significant reductions on days 1, 9 and 10, $p<0.01$. Also, significant reductions were observed on days 5, 6 and 8, $p<0.05$ (Figure 3.11 A). These results suggest that *TEX19* is correlated with *OCT4* stem cell marker and linked with stemness features. Further work on this carried out in Chapter 5.

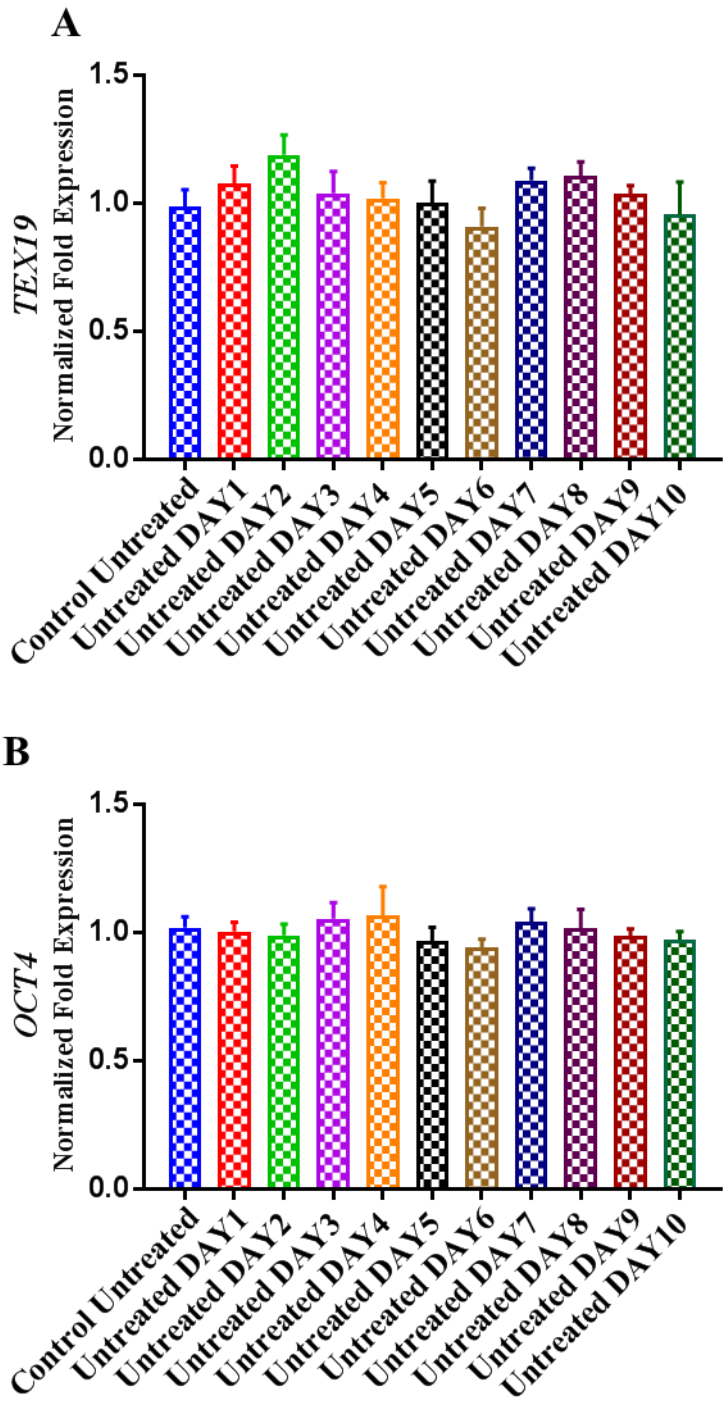

Figure 3-8 RT-qPCR analysis of the *TEX19* transcript levels in untreated NTERA2 cells.

(A) Bar chart presenting constant mRNA levels of *TEX19* gene in untreated NTERA2 cells for 10 days. (B) Bar chart showing constant mRNA levels of the *OCT4* gene in untreated NTERA2 cells for 10 days. *OCT4* was used as a stem cell marker. The obtained data were normalised using a combination of two endogenous reference genes, *TUBA1C* and *GAPDH*. The error bars show the standard errors of the mean.

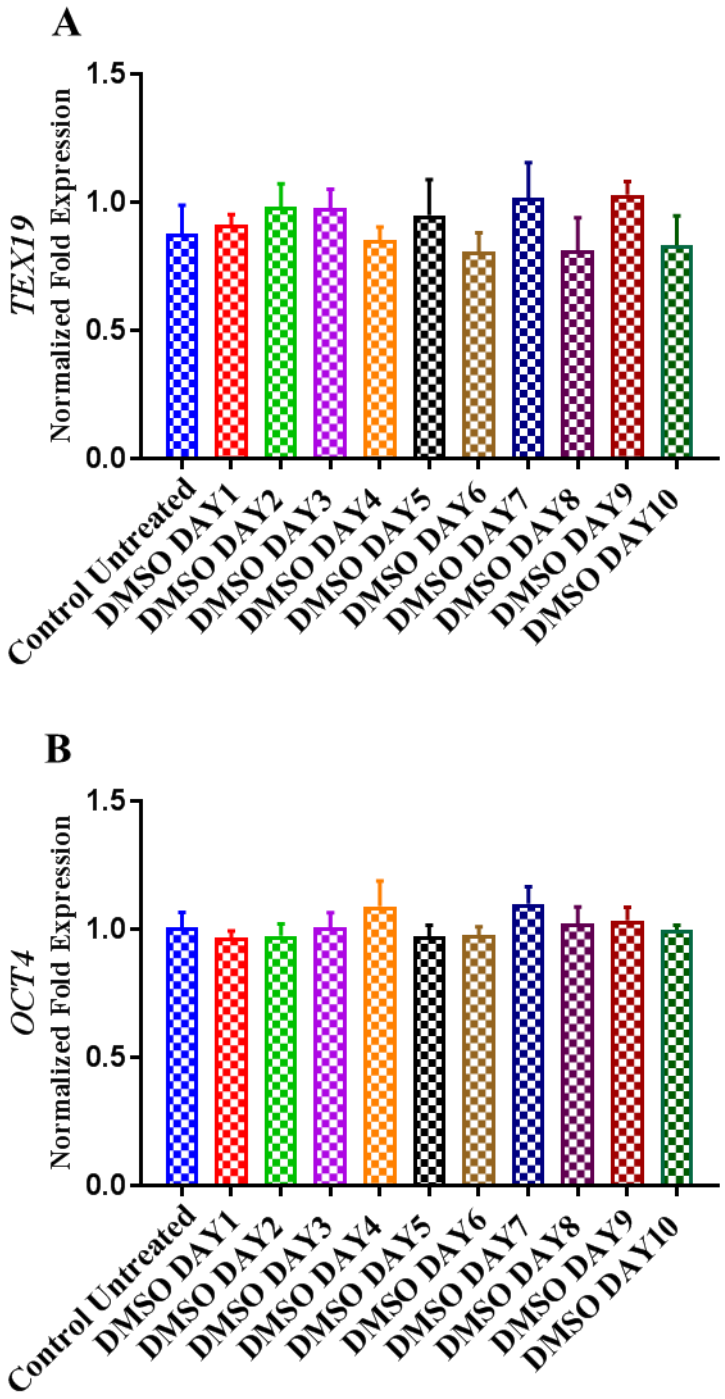

Figure 3-9 RT-qPCR analysis of the *TEX19* transcript levels in NTERA2 cells treated with DMSO.

(A) Bar chart presenting constant mRNA levels of *TEX19* gene in NTERA2 cells treated with DMSO for 10 days. (B) Bar chart showing constant mRNA levels of *OCT4* in NTERA2 cells over 10 days. The expression of *OCT4* was used as a stem cell marker. The obtained data were normalised using a combination of two endogenous reference genes, *TUBA1C* and *GAPDH*. The error bars show the standard errors of the mean.

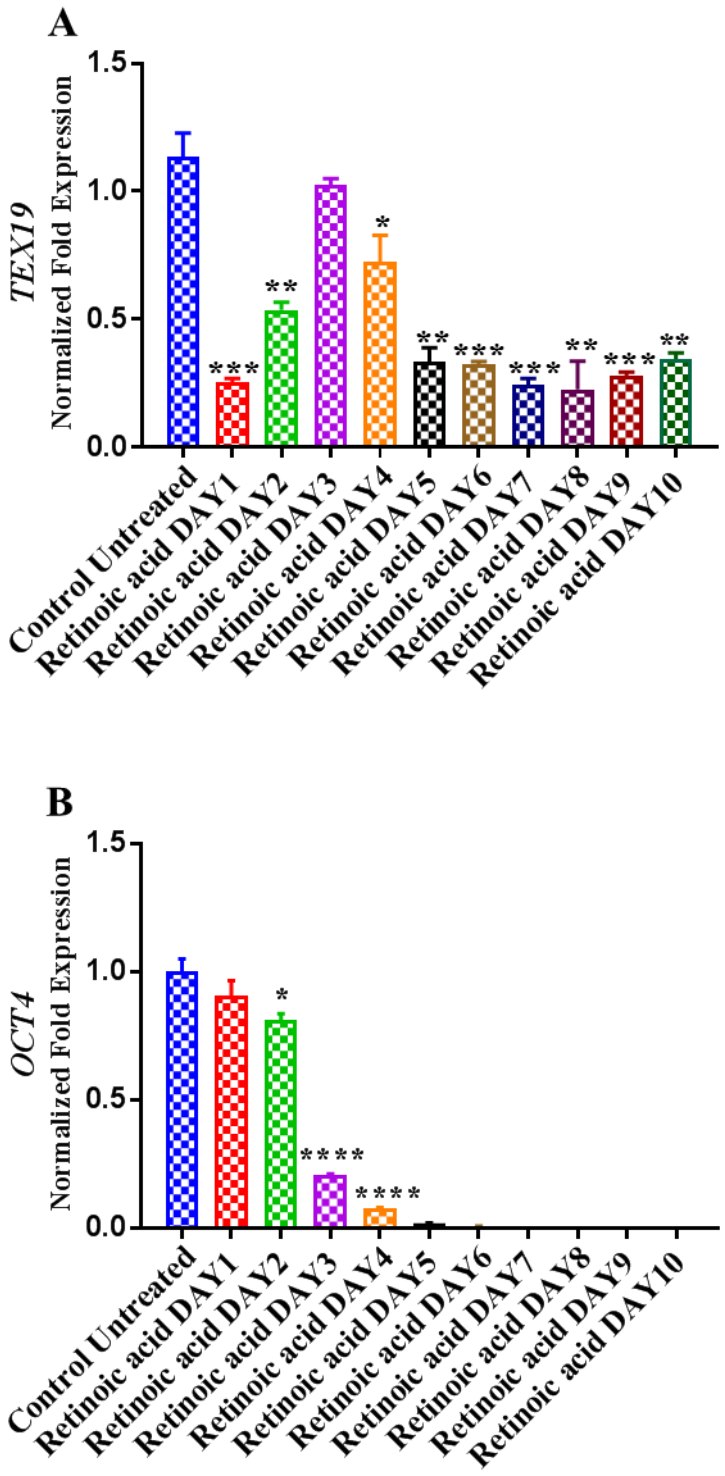

Figure 3-10 RT-qPCR analysis of the *TEX19* transcript levels in NTERA2 cells treated with retinoic acid.

(A) Bar chart presenting the mRNA levels of the *TEX19* gene in NTERA2 cells treated with retinoic acid for 10 days. Asterisks above the bars indicate *p*-values (*: $p<0.05$; **: $p<0.01$; ***: $p<0.001$). (B) Bar chart showing the mRNA levels of *OCT4* in NTERA2 cells over the 10 days of differentiation. The expression of the *OCT4* gene was used as a stem cell marker. Asterisks above the bars indicate *p*-values (*: $p<0.05$; ****: $p<0.0001$). The obtained data were normalised using a combination of two endogenous reference genes, *TUBA1C* and *GAPDH*. The error bars show the standard errors of the mean.

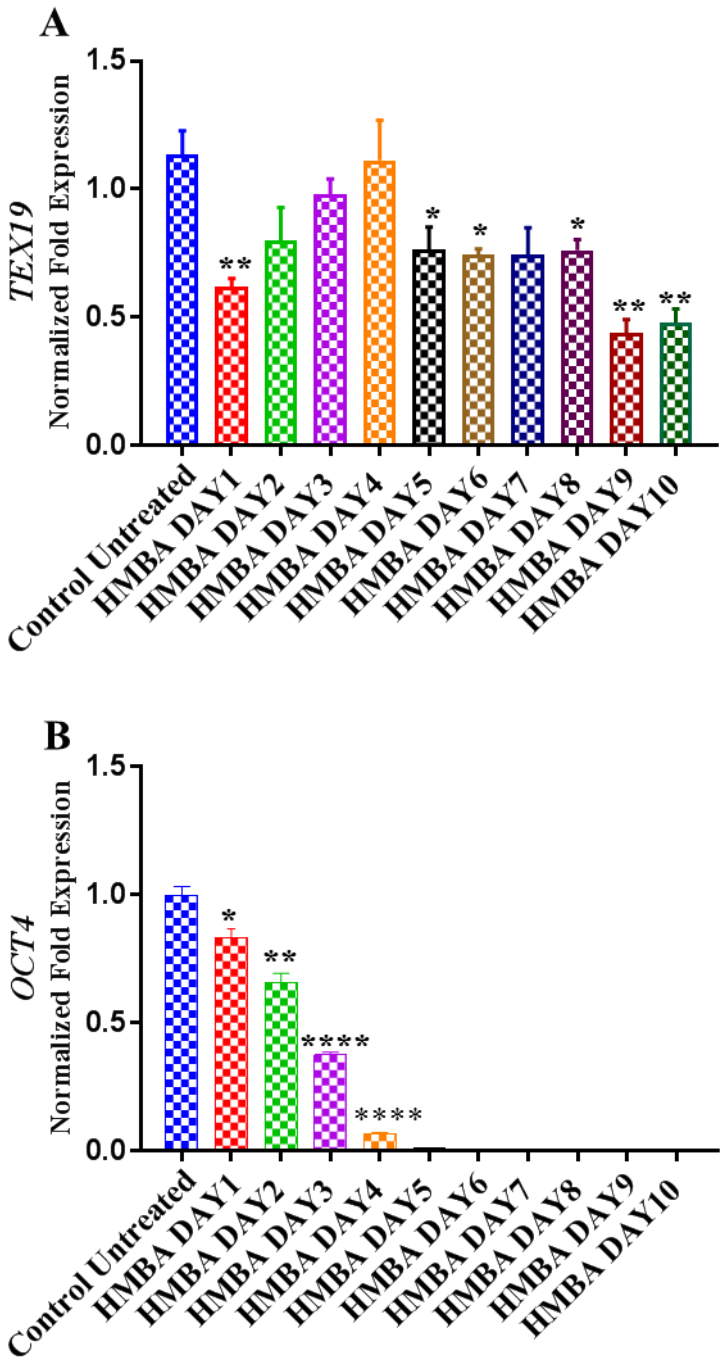

Figure 3-11 RT-qPCR analysis of the *TEX19* transcript levels in NTERA2 cells treated with HMBA.

(A) Bar chart presenting the mRNA levels of the *TEX19* gene in NTERA2 cells treated with HMBA for 10 days. Asterisks above the bars indicate *p*-values (*: $p<0.05$; **: $p<0.01$). (B) Bar chart showing the mRNA levels of *OCT4* in NTERA2 cells over 10 days of treatment. The expression of *OCT4* was used as a stem cell marker. Asterisks above the bars indicate *p*-values (*: $p<0.05$; **: $p<0.01$; ****: $p<0.0001$). The obtained data were normalised using a combination of two endogenous reference genes, *TUBA1C* and *GAPDH*. The error bars show the standard errors of the mean.

3.2.5 Immunohistochemistry staining analysis of TEX19 in clinically normal tissues and colonic tumours

Immunohistochemistry (IHC) staining was used to determine the tissue distribution of TEX19 in normal human colon and colonic tumours. IHC staining for tissues was carried out using the fully automated Ventana Benchmark XT staining system. A rabbit anti-TEX19 polyclonal antibody (Abcam, ab185507) was used to detect TEX19 protein in the examined tissues. Testis tissues were used as a positive CTA control. The negative control was used to demonstrate absence of non- specific secondary antibody staining in the tissues. The protein level of TEX19 was examined in testis, multiple normal human colon and colorectal tumour samples. Using the Abcam anti TEX19 antibody, IHC staining showed the detection of TEX19 in the normal testis, specifically in the cells surrounding the periphery of seminiferous tubules (Figure 3.12).

IHC staining of TEX19 was carried out in matched samples (normal adjacent tissue [NAT] and colon tumour tissues) in three colon cancer patients (patients #45, #35 and #12). One negative control was used per staining run of normal adjacent tissues (NAT) and colon tumour tissues (Figure 3.13). In patient #45, TEX19 showed weak staining at the top of the colonic crypt within the cytoplasm in NAT (Figure 3.14). Interestingly, very strong positive staining was detected in colon tumour tissue; the staining showed strong nuclear and weak cytoplasmic localisation for TEX19 (Figure 3.15). In patient #35, NAT exhibited moderate cytoplasmic staining at the top of the crypts (Figure 3.16). Strong nuclear staining was observed for TEX19 in the matched cancer tissue for this patient (Figure 3.17). In patient #12, TEX19 showed weak cytoplasmic staining at the top of the colonic crypt (Figure 3.18). Weak cytoplasmic staining for TEX19 was observed in the matched cancer tissue (Figure 3.19). Apart from patient #12, NAT and colon tumour tissue exhibited a clear difference in immunostaining for TEX19, further validating its utility as a cancer biomarker.

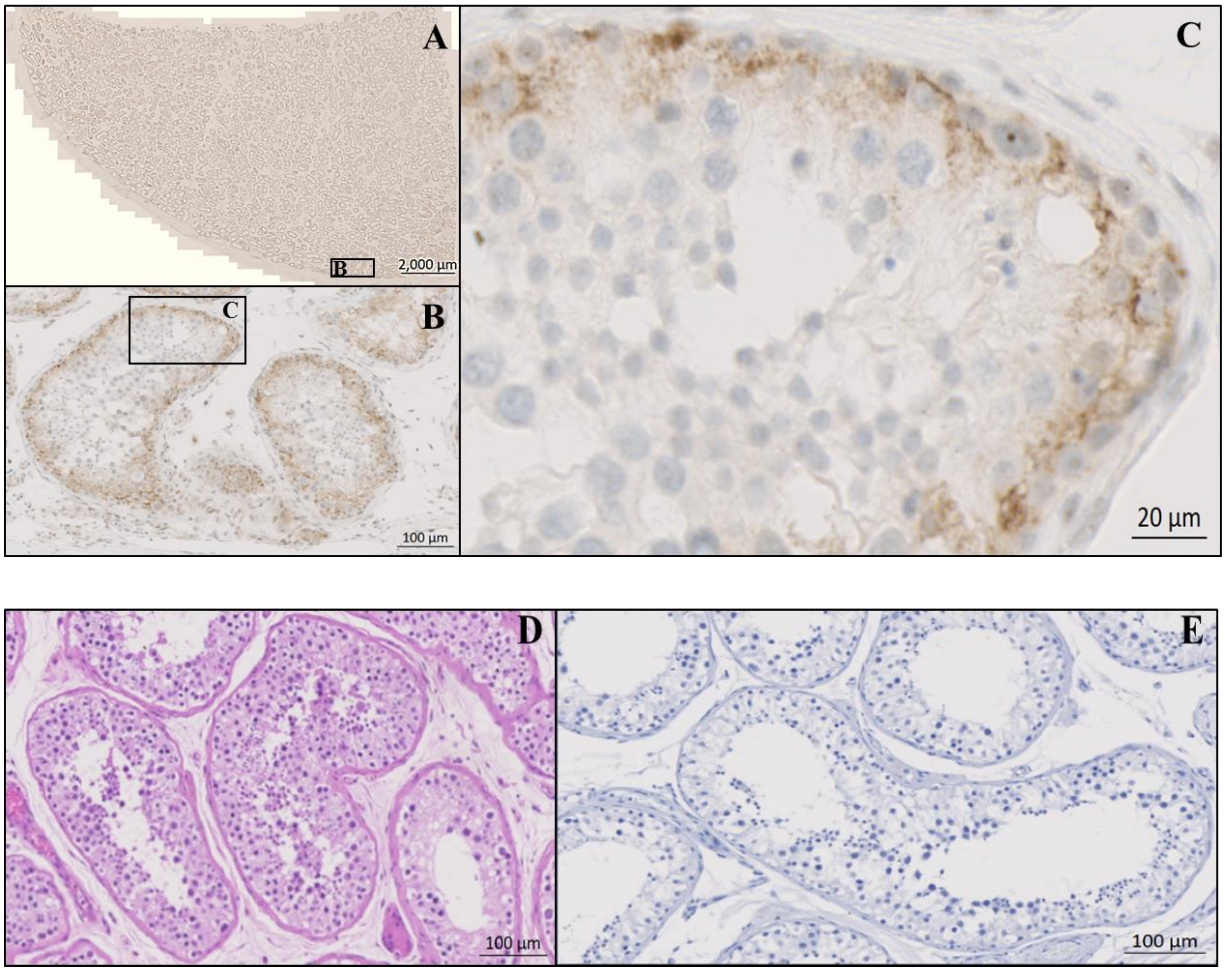

Figure 3-12 IHC staining of TEX19 protein using rabbit polyclonal antibody (Abcam, ab185507) in normal human testis tissue.
(A, B, C) IHC images presenting the cytoplasmic positive cells on the periphery of seminiferous tubules stained brown with anti-TEX19 antibody. Normal testis tissue was used as a positive control for CTAs. Positive cells demonstrate cytoplasmic staining. The magnifications are x0.5, x5 and x20, respectively. (D) H&E staining (x5). (E) Negative control (x5): secondary antibody only.

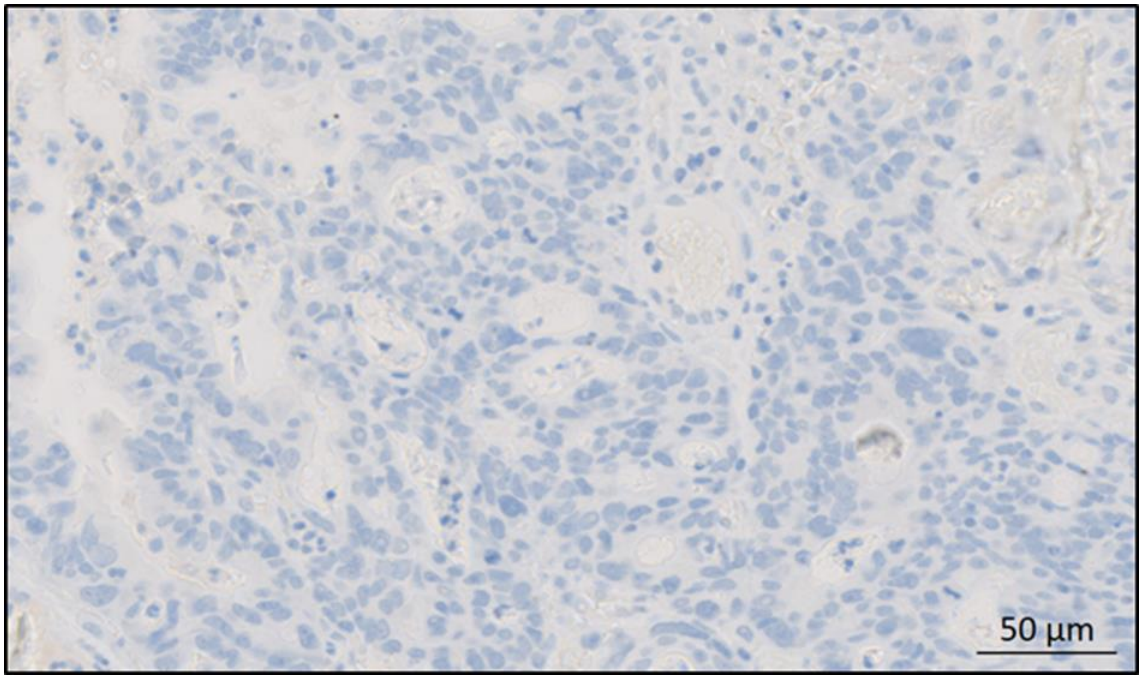

Figure 3-13 IHC negative control.
Image shows staining with secondary antibody only (Roche, #760-4205). One negative control slide was used per staining run of 3 normal adjacent tissues (NAT) and 3 colon tumour tissues. Image display negative staining in the tissue and the magnification is x10.

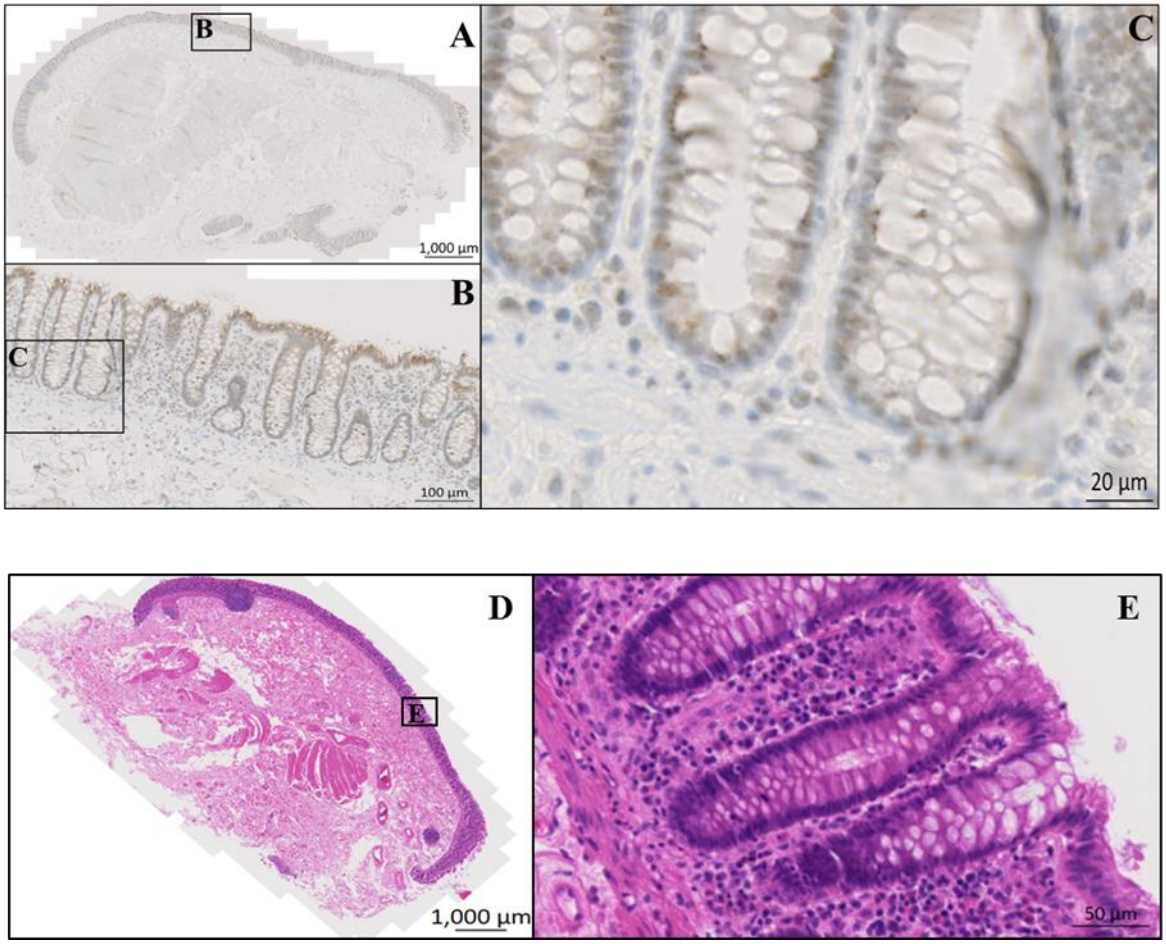

Figure 3-14 IHC staining of TEX19 protein in normal adjacent tissue (NAT) from colon cancer patient #45 using rabbit polyclonal antibody (Abcam, ab185507).
(A, B, C) Images show weak cytoplasmic staining with the TEX19 antibody. The magnifications are x0.5, x5 and x20 respectively. (B) Artefactual edge-effect staining at the top of colon crypts. (C) Weak cytoplasmic staining. (D, E) H&E staining of the normal colon crypt (x0.5 and x10, respectively).

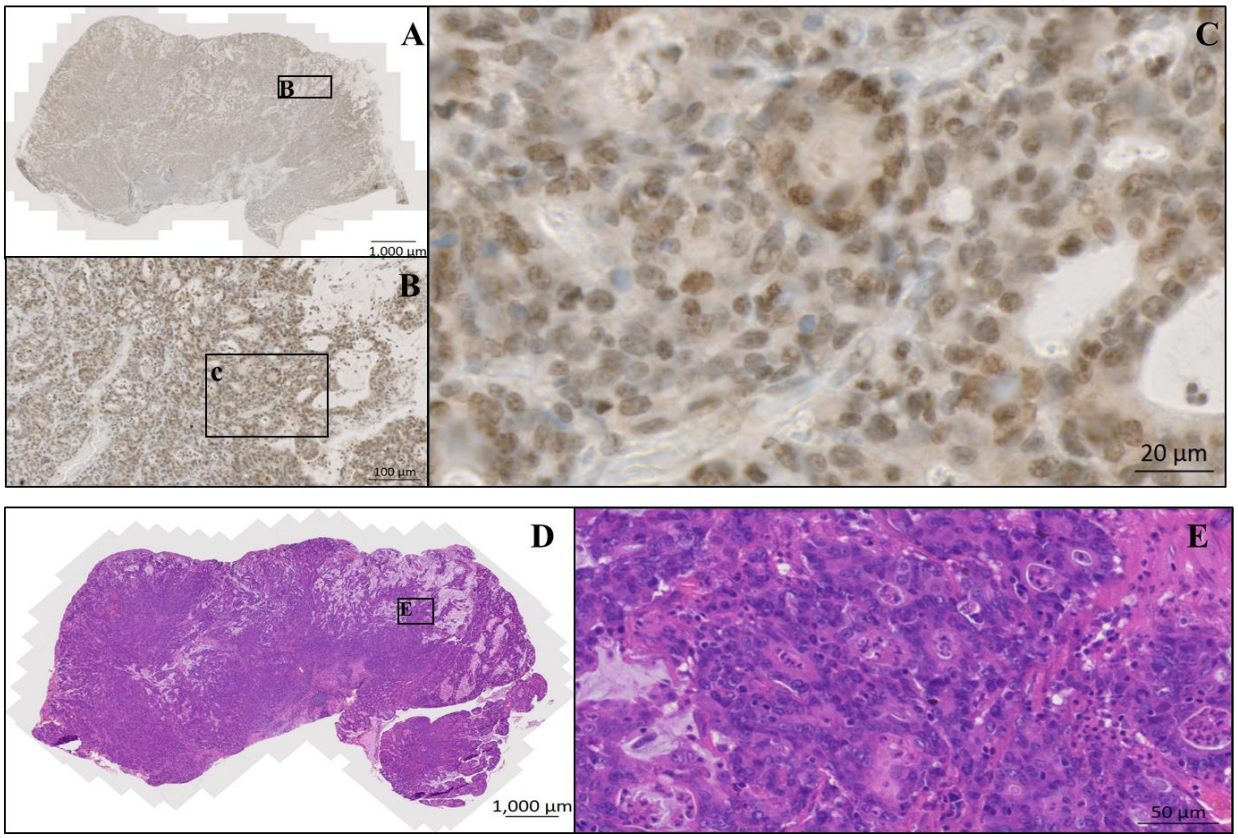

Figure 3-15 IHC staining of TEX19 protein in colon tumour tissue from colon cancer patient #45 using rabbit polyclonal antibody (Abcam, ab185507).
(A, B, C) Images display TEX19 antibody showing strong nuclear and weak cytoplasmic staining in colon tumour tissue. The magnifications are x0.5, x5 and x20, respectively. (C) Strong nuclear staining in the carcinoma area. (D, E) H&E staining of the colon carcinoma (x0.5 and x10, respectively).

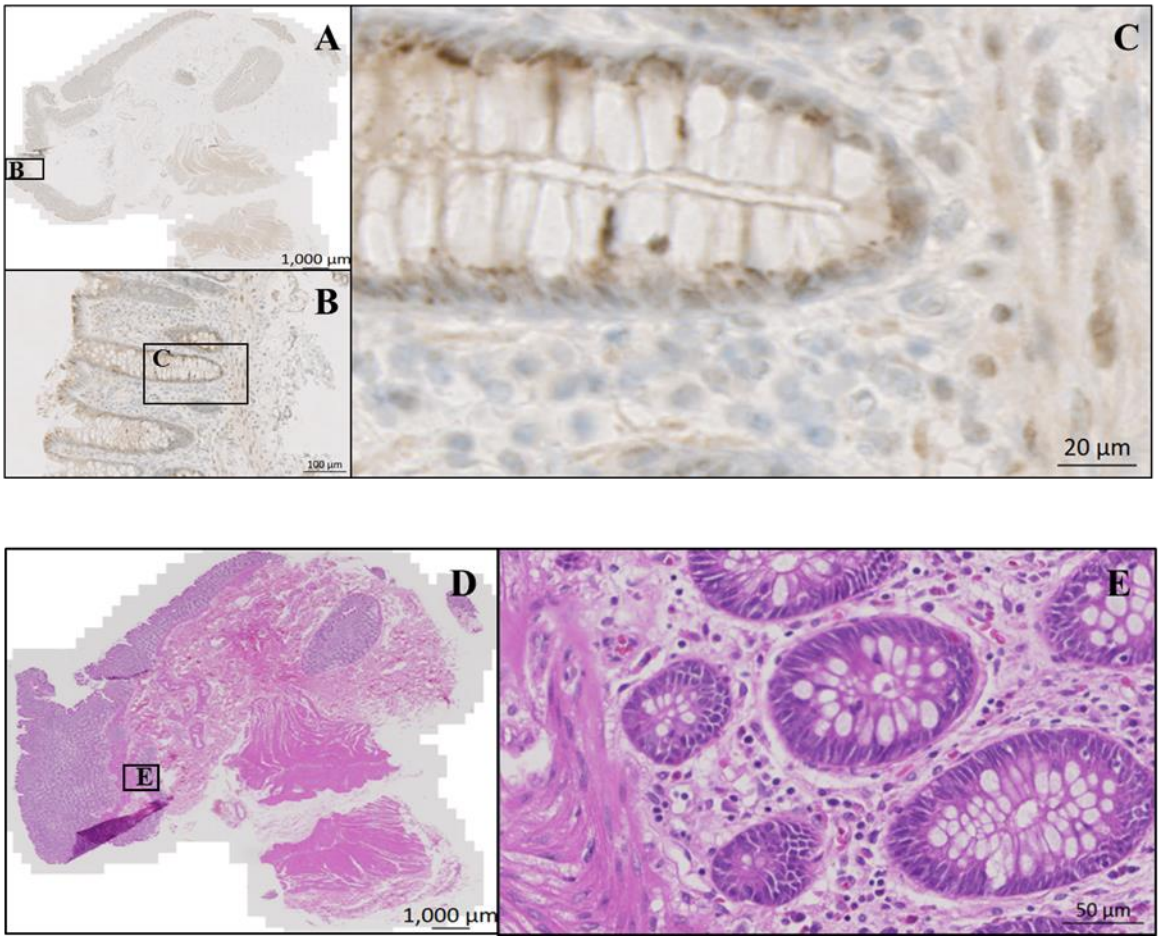

Figure 3-16 IHC staining of TEX19 protein in normal adjacent tissue (NAT) from colon cancer patient #35 using rabbit polyclonal antibody (Abcam, ab185507).
(A, B, C) Images show moderate cytoplasmic staining with the TEX19 antibody. The magnifications are x0.5, x5 and x20, respectively. (B) Artefactual edge-effect staining at the top of the colon crypts. (C) Moderate cytoplasmic staining. (D, E) H&E staining of the normal colon crypt (x0.5 and x10, respectively).

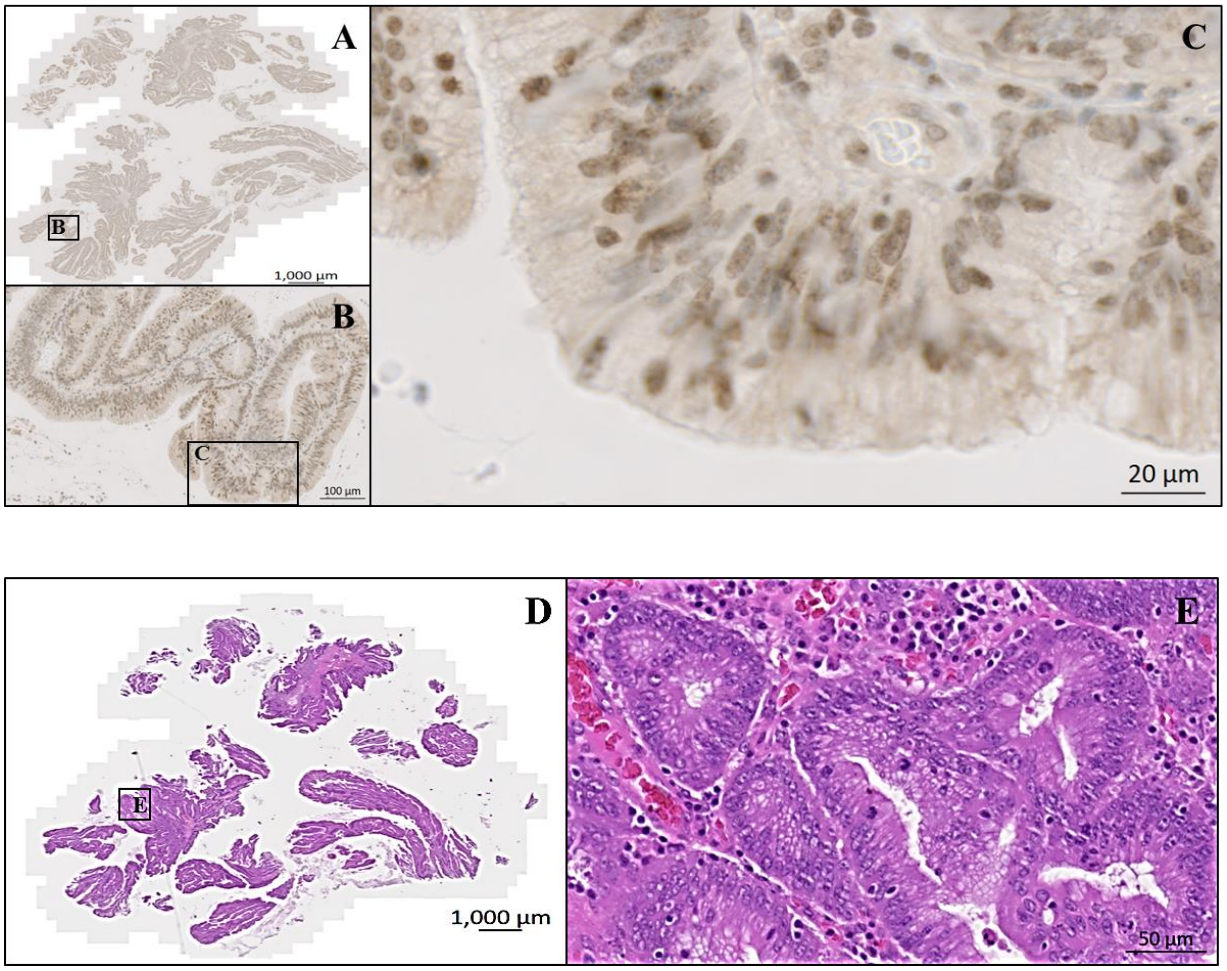

Figure 3-17 IHC staining of TEX19 protein in colon tumour tissue from colon cancer patient #35 using rabbit polyclonal antibody (Abcam, ab185507).
(A, B, C) Images show the TEX19 antibody's strong nuclear staining in colon tumour tissue. The magnifications are x0.5, x5 and x20, respectively. (C) Strong nuclear staining in the carcinoma area. (D, E) H&E staining of the colon carcinoma (x0.5 and x10, respectively).

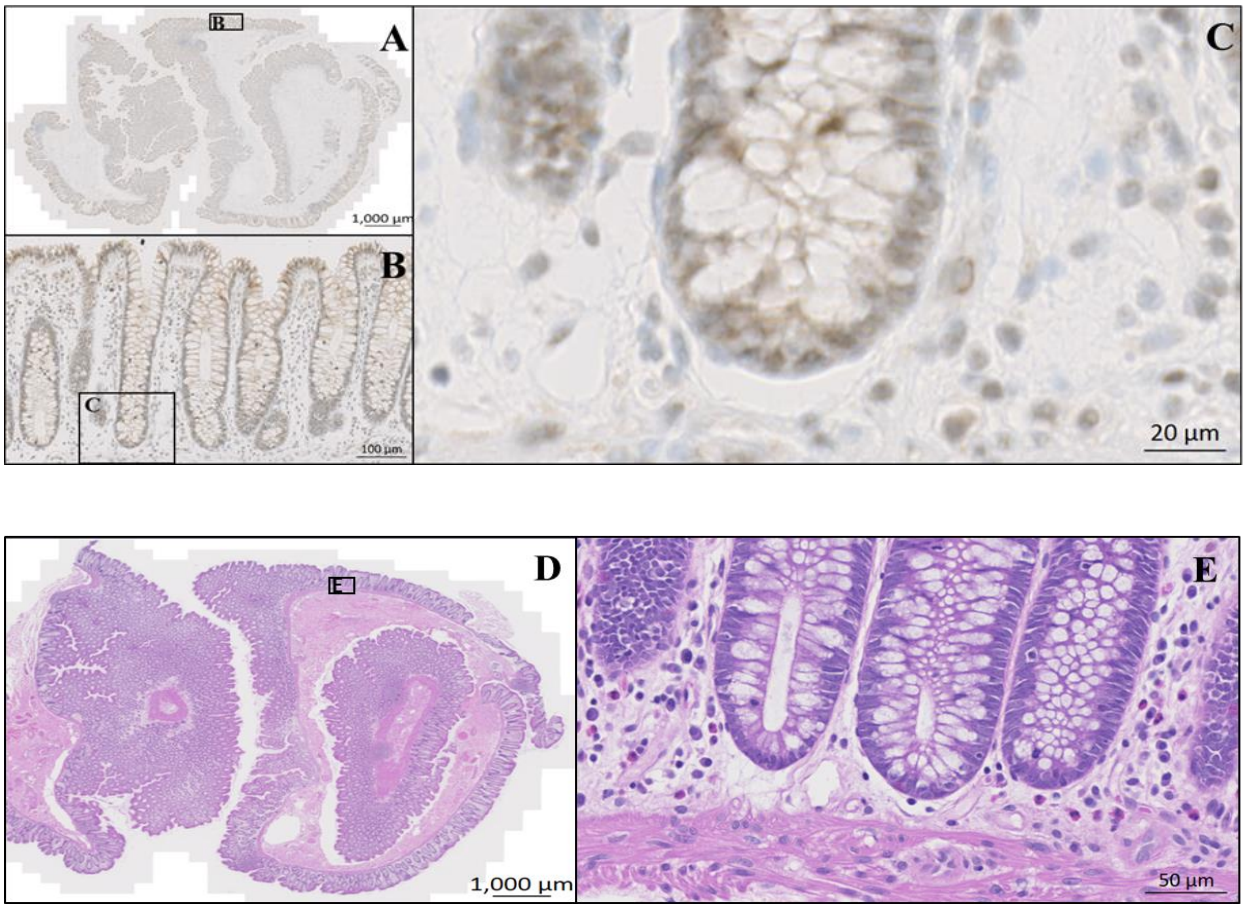

Figure 3-18 IHC staining of TEX19 protein in normal adjacent tissue (NAT) from colon cancer patient #12 using rabbit polyclonal antibody (Abcam, ab185507).
(A, B, C) Images show weak cytoplasmic staining with the TEX19 antibody. The magnifications are x0.5, x5 and x20, respectively. (B) Artefactual edge-effect staining at the top of colon crypts. (C) Weak cytoplasmic staining. (D, E) H&E staining of the normal colon crypt (x0.5 and x10, respectively).

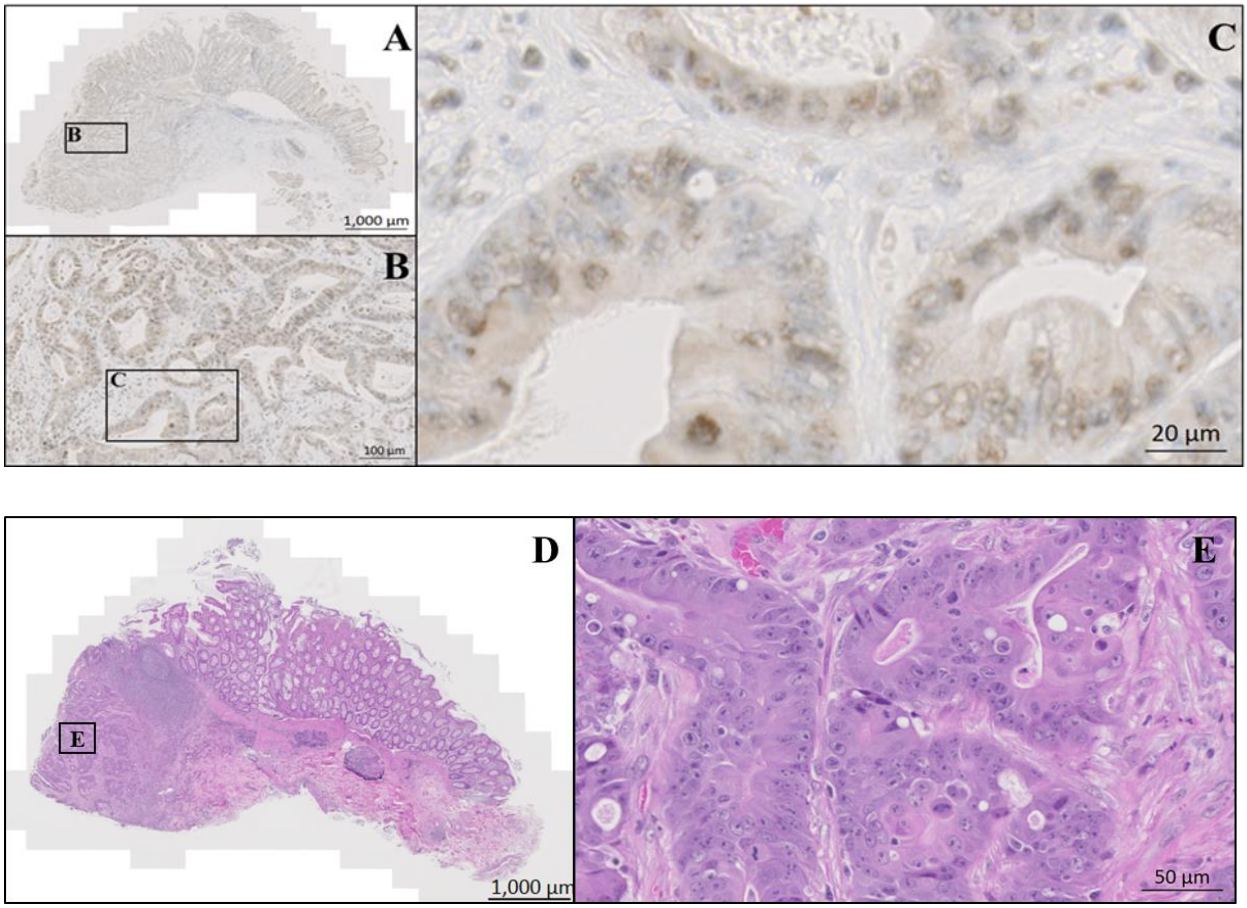

Figure 3-19 IHC staining of TEX19 protein in colon tumour tissue from colon cancer patient #12 using rabbit polyclonal antibody (Abcam, ab185507).
(A, B, C) Images show the TEX19 antibody's weak cytoplasmic staining in colon tumour tissue. The magnifications are x0.5, x5 and x20, respectively. (C) Weak cytoplasmic staining in the carcinoma area. (D, E) H&E staining of colon carcinoma (x0.5 and x10, respectively).

3.2.6 Immunofluorescence staining analysis of TEX19 in pluripotent embryonal carcinoma cells and cancer cells

Because *TEX19* was expressed in distinct cancer cells, indirect immunofluorescence (IF) was carried out to determine the protein cellular localisation. Three different cancer cell lines were examined for TEX19 localisation involving pluripotent embryonal carcinoma (NTERA2), colon adenocarcinoma (SW480) and large-cell lung carcinoma (H460). A rabbit polyclonal anti-TEX19 antibody (Abcam, ab185507) was used to detect TEX19 protein in the examined cancer cells. DAPI (blue) was used as nuclear staining, and α-tubulin was used as a positive control and cytoplasmic marker.

The analysis results of IF images demonstrated that TEX19 had dual or individual localisation. In NTERA2, the localisation of TEX19 was detected mainly in the nucleus, and no protein was detected in the cytoplasm (Figure 3.20). In H460, the IF staining showed TEX19 protein localised in or surrounding the nucleus (Figure 3.21). In SW480, the localisation of TEX19 was found in the nucleus and cytoplasm (Figure 3.22). The observation of different localisations could suggest that TEX19 acts as a dynamic protein, and its function could be based on its cellular localisation.

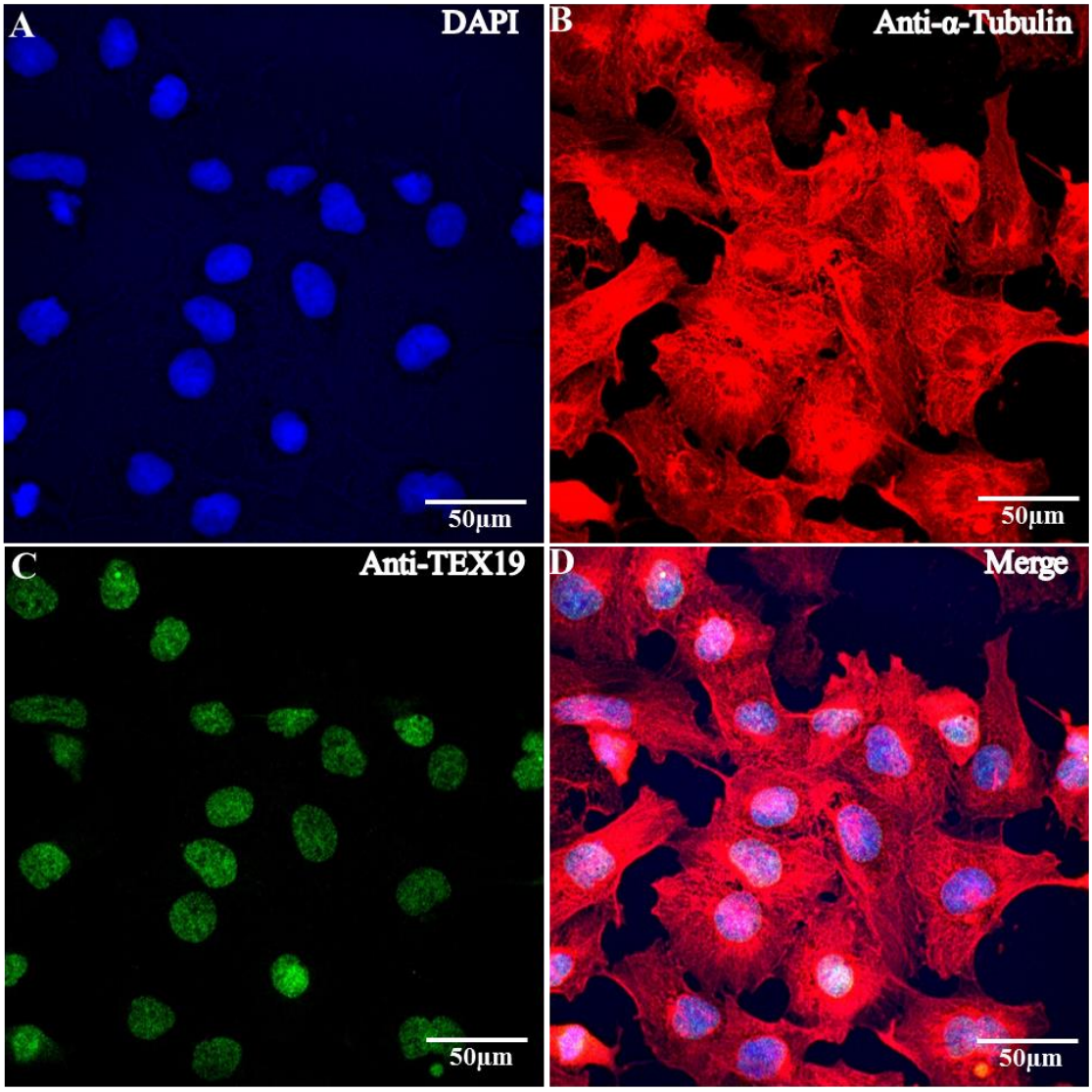

Figure 3-20 IF staining showing TEX19 protein localisation in NTERA2 cells.
Images demonstrate the IF staining for anti-α-Tubulin (SEGMA, T6074; 1:1000) and anti-TEX19 (Abcam, ab185507; 1:500) in NTERA2 cells. (A) DNA stained with DAPI (blue). (B) Staining of anti-α-Tubulin (red). (C) Staining of anti-TEX19 (green). (D) Staining of DAPI, anti-α-Tubulin and anti-TEX19 (blue, red and green). Images were analysed using a ZEISS LSM 710 confocal microscope.

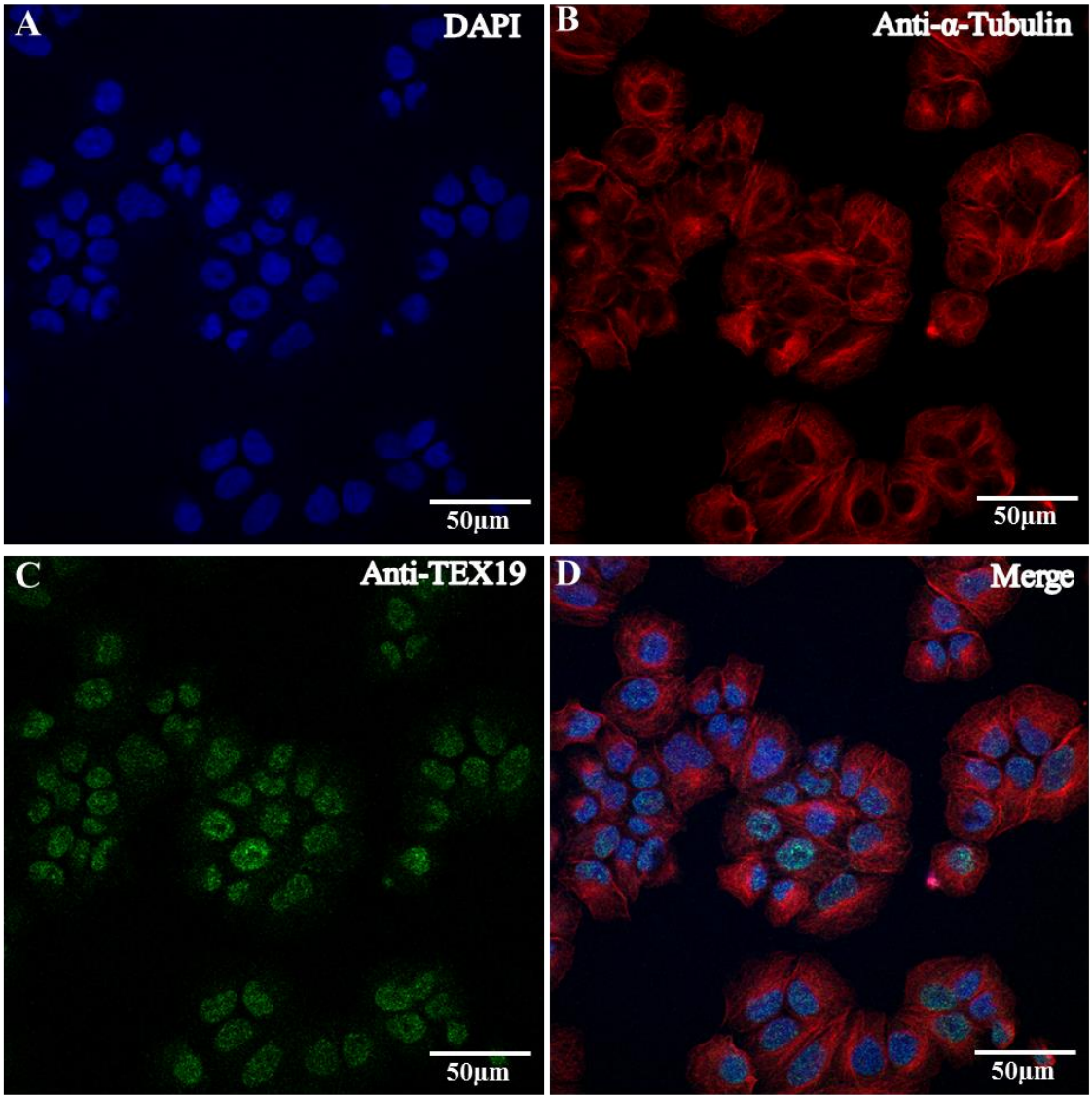

Figure 3-21 IF staining shows TEX19 protein localisation in H460 cells.
Images demonstrate the IF staining for anti-α-Tubulin (SEGMA, T6074; 1:1000) and anti-TEX19 (Abcam, ab185507; 1:500) in H460 cells. (A) DNA stained with DAPI (blue). (B) Staining of anti-α-Tubulin (red). (C) Staining of anti-TEX19 (green). (D) Staining of DAPI, anti-α-Tubulin and anti-TEX19 (blue, red and green). Images were analysed using a ZEISS LSM 710 confocal microscope.

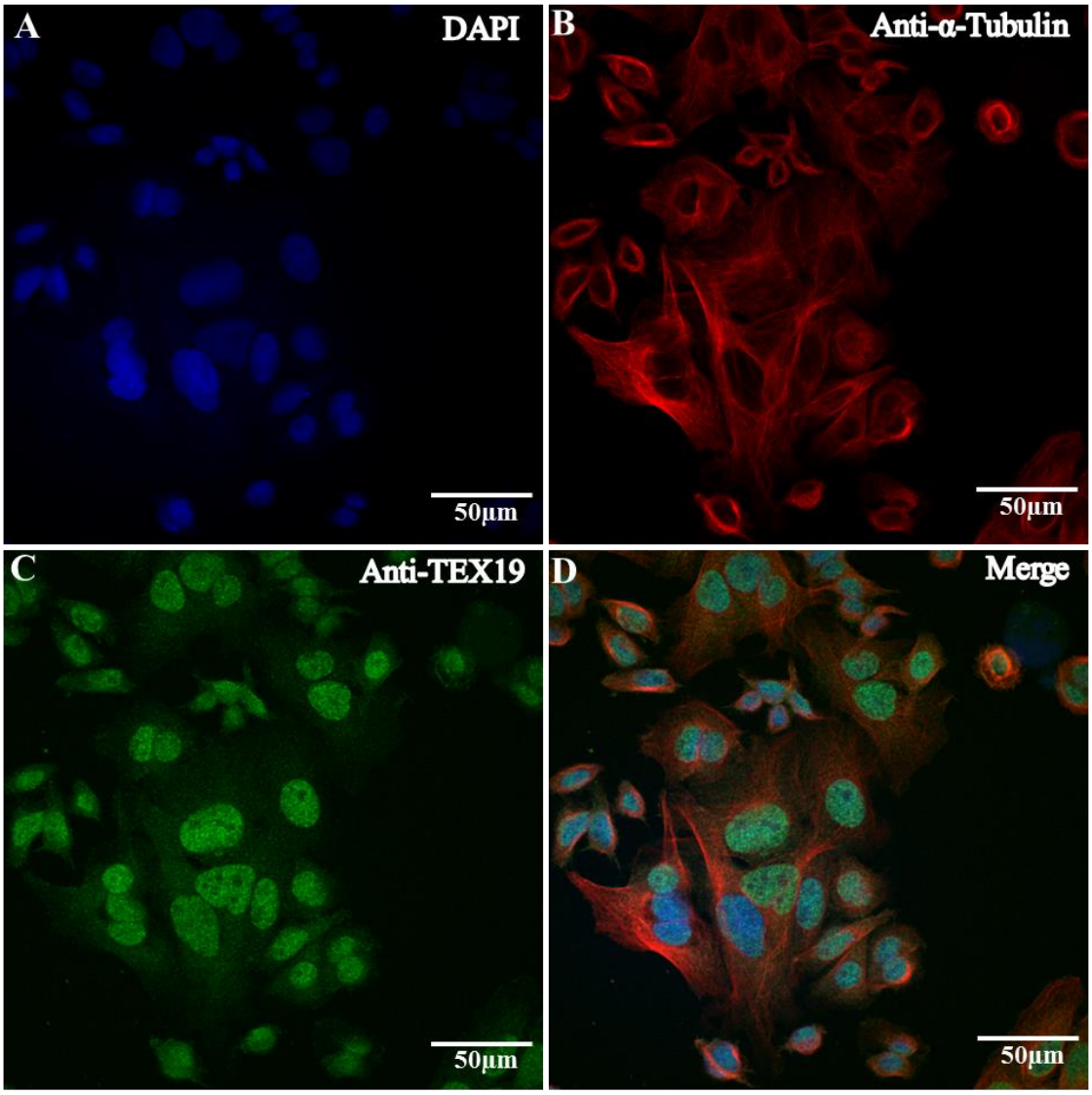

Figure 3-22 IF staining shows TEX19 protein localisation in SW480 cells.
Images demonstrate the IF staining for anti-α-Tubulin (SEGMA; T6074; 1:1000) and anti-TEX19 (Abcam, ab185507; 1:500) in SW480 cells. (A) DNA stained with DAPI (blue). (B) Staining of anti-α-Tubulin (red). (C) Staining of the anti-TEX19 (green). (D) Staining of DAPI, anti-α-Tubulin and anti-TEX19 (blue, red and green). Images were analysed using a ZEISS LSM 710 confocal microscope.

3.3 Discussion

The initial detection of *TEX19* in normal human tissues and cancer samples was achieved for the first time in 2012 using conventional RT-PCR screening; at this time, it was identified as A CTA gene (Feichtinger et al., 2012). In this study, *TEX19* expression was evaluated using RT-PCR and RT-qPCR in multiple normal tissues and cancer samples. The analysed results confirmed that *TEX19* expression is restricted to the testis tissues and expressed weakly in the thymus. However, Feichtinger et al. (2012) explained the weak expression in thymus by saying that the samples had atrophied, as they were obtained from deceased individuals. In addition, the detectable Ct values of *TEX19* in the thymus (36.22) were found to be very close to the determined cut off > 37. This may indicate the possibility that normally the healthy thymus does not express *TEX19*. Furthermore, the RT-qPCR analysis showed positive results for *TEX19* in 25 out of 32 cancer samples. The cancer samples did not express *TEX19* were those with Ct values > 37, as this was the cut off determined in this study. These cancer samples involve lung tumour, diploid lung (MRC-5), kidney tumour, stomach tumour, uterus tumour, breast tumour and promyelocytic leukaemia (HL-60) sample. This lack of measurable expression could be explained according to the heterogeneous nature of cancer. Correspondingly, the activation of *TEX19* in a wide range of cancer cells suggest its function in oncogenesis.

TEX19 protein was detected in various bladder cancer samples by using western blotting (Zhong et al., 2016). This chapter extended the study of TEX19 protein presence further. Moreover, the expected size for TEX19 protein is around 18.5 KDa, and the used antibody detected the protein at around 24 KDa. This is could be explained according to post-transcriptional modification of proteins. Correspondingly, Oba-Shinjo and his co-workers (2008) reported discrepancies in the presence of CTA protein and mRNA levels in tissues due to post-transcriptional modifications (Oba-Shinjo et al., 2008). The antibody used was found to be TEX19 specific based on siRNA depletion. The western blot analysis in normal tissues showed the presence of TEX19 in the testis and hESCs, while a very weak signal was detected in the thymus. As explained above, the presence of TEX19 protein in thymus may be due to tissue changes with age or sample deterioration (Feichtinger et al., 2012). In cancer cells, TEX19 was present in all tested samples. In this study, the presence of TEX19 protein was detected

with a single or dual band, and there was no clear reason for this; this result was not linked with the type of cells, passage number or confluency of cells. Additional research is required to comprehend this effect and assess whether it can be explained according to the post-transcriptional modification of proteins. This study revealed similar results to Zhong et al. (2016), where TEX19 protein present in multiple cancer samples. More importantly, the RT-PCR, RT-qPCR and western blot analyses showed high consistency in all obtained results. Taking these results together, this chapter has demonstrated that *TEX19* is a testis/cancer-selective CTA gene.

Mouse *Tex19.1* is a germline gene found to be expressed in ESCs and linked to the *Oct4* expression (Kuntz et al., 2008). No previous study has demonstrated this in humans. In the first stage, this chapter investigated *TEX19* expression in hESCs, iPSCs and differentiated cancer stem cells. Both RT-PCR and RT-qPCR analyses showed that *TEX19* is expressed in hESCs and iPSCs but not in fibroblasts. Along with stem cell markers (*OCT4*, *SOX2*, *NANOG*), *TEX19* is activated in iPSCs after their reprogramming from precursor fibroblasts. This observation highly suggests that *TEX19* plays a role in conferring stemness features, and this gene may behave as a stem cell transcription factor. This result was encouraging, and a further step was taken to investigate *TEX19* expression in human model stem cells (NTERA2) upon differentiation. In cells treated with retinoic acid, *TEX19* transcript levels significantly decreased upon the decline and cessation of *OCT4* except on day 3. This may indicate that *TEX19* expression is correlated with stem cell marker expression. In line with this, the consequential reduction and *OCT4* cessation in the cells treated with HMBA decreased *TEX19* mRNA levels on most tested days. The differentiation process did not cause silencing of the gene of interest, but it did suggest a high likelihood that *TEX19* expression is linked with stemness features. Based on this observation, more work was performed, and this is discussed in Chapter 5.

IHC analysis demonstrated TEX19 in the normal testis with positive staining restricted to the periphery of the seminiferous tubules, as expected of a CTA. This adds weight to TEX19's prospective immunogenic capacity. In normal colon tissues, TEX19 staining was observed mainly only on the edges of the section. Some NAT did exhibit some weak staining, however, this could be due to activation of TEX19 in this tissue adjacent to the tumour. Zhong and co-workers (2016) observed clear negative staining in normal

tissues with TEX19 positive staining restricted to the testis and 60% of the bladder cancer patients in their study. It would therefore be informative to stain normal tissue that was not adjacent to cancer tissue to establish whether *TEX19* is activated in these tissues or not. This may be an artefact due to sample dehydration during tissue conditioning, overstaining with primary antibody or antibody residue accumulating at the edge of the section (i.e. the edge effect). Matched samples (NAT and cancer tissue) revealed the strong presence of TEX19 in cancer tissues, as well as a clear difference between matched NAT and cancer tissues, particularly in patients #35 and #45. This differential staining further validates TEX19 as a promising cancer biomarker subject to IHC testing in a greater number of patients. The strong positive nuclear localisation of TEX19 indicates cancer-specific accumulation in the nucleus; this could signal a carcinogenic event. However, further IHC analysis is required to determine whether TEX19 can be used to discriminate between cancer and normal tissues *in vivo*.

Accurate protein localisation is necessary to ensure the normal function of the protein and integration with the biological function network. Abnormal protein localisation is linked to cancer formation and gene expression alternation (Hung & Link, 2011). IF analysis was carried out to elucidate cellular localisation in different cancer cells, and this was found to differ. In SW480, TEX19 was found in the cytoplasm and nucleus. In H460, TEX19 localised mainly in or around the nucleus. In (NTERA2), TEX19 was found exclusively in the nucleus. This variable localisation could prevent TEX19 from functioning correctly, and this effect may accumulate to develop into cancer. In addition, TEX19 may perform a dynamic function based on its localisation.

To summarize, the work in this chapter has confirmed that *TEX19* is a CTA gene through mRNA expression and protein level evaluation. In addition, the study revealed that *TEX19* is a stemness gene through its expression in hESCs and iPSCs, and it showed that the expression level decreases in the differentiation process. Both IHC and IF showed extensive nuclear localisation, suggesting a signal of oncogenesis acquired in the nucleus in only cancer cells. More in depth, this chapter encourages the study of whether TEX19 plays a role in cancer and stem cells.

Chapter 4

TEX19 influences proliferation and regulates gene expression in cancer stem-like cells and cancer cells

4. *TEX19* influences proliferation and regulates gene expression in cancer stem-like cells and cancer cells

4.1 Introduction

In cancer, cells proliferate out of control and accumulate without responding to the signals that control cellular growth. Over time, cancer cells and their progenitors succeed in evading programmed cell death and divide more rapidly. Moreover, these cells display high heterogeneity in different morphological and phenotypic features, such as proliferation and gene expression. Genetic and epigenetic alternations are the main factors responsible for the generation of heterogeneity in distinct tumour cells. However, such tumour heterogeneity can lead to different progressions of cancer cells and variable responses to therapy (Hirohashi et al., 2016; Marusyk & Polyak, 2010; Ouyang et al., 2012).

Different studies have shown a strong correlation between CTA genes expression and cell proliferation in a wide range of cancer cells. In line with this, Maxfield and co-workers (2015) performed a study demonstrating that CTA genes enhance cancer cell viability. They used silencing techniques, such as siRNA transfection, for multiple CTA genes in different cancer cells (Maxfield et al., 2015). For example, the depletion of *FATE1* expression reduced the viability to >30% for prostate cancer, breast cancer, sarcoma and melanoma cancer cells. The study also has demonstrated the depletion of *FATE1* mRNA caused a potent loss in viability in a colorectal cancer cell line HCT116. *ZNF165* is another CTA gene expressed in breast cancer cells, and its depletion reduced cell viability for these cells (Maxfield et al., 2015). Another study silenced *MAGEC2* using siRNA transfection in multiple melanoma cells; this study demonstrated that *MAGEC2* mRNA knockdown impairs the proliferation and viability in melanoma cells (Lajmi et al., 2015). A further study has illustrated that the overexpression of *MAGE-A1* can acts as an oncogene and subsequently promotes proliferation in multiple myeloma cells, while its knockdown inhibits the melanoma cell proliferation process (Wang et al., 2016). An additional study has reported the depletion of *NY-SAR-35* in human embryonic kidney (HEK) 293 cells using siRNA, led to cell proliferation suppression (Song et al., 2016). Shang and colleagues (2014) carried out *CT45A1*

overexpression and knockdown in a breast cancer cell line (MCF7) to evaluate *CT45A1* function. The overexpression of *CT45A1* led to upregulation of numerous oncogenic and metastatic genes. In addition, signalling pathways involving CREB and ERK became constitutively activated. Further, the consequence of *CT45A1* overexpression in MCF7 has increased tumorigenesis, invasion and metastasis. In contrast, knockdown of *CT45A1* led to a substantial reduction in the migration and invasion of MCF7 cancer cells (Shang et al., 2014). In sum, these studies indicate the potential significance of CTA genes in regulating cancer cell proliferation, and subsequently, the development of oncogenesis (Cheng, Wong & Cheng, 2011). Thus, CTAs may have a tumorigenic function, and their loss may become detrimental for cancer cell survival (Maxfield et al., 2015; Song et al., 2016).

Although the function of most CTAs is unknown, some play a role in regulating gene expression and signalling pathways (Whitehurst, 2014). In a cancer cell line (HCT116), depletion of *FATE1* was found to stabilise *BIK* gene expression; this gene is required for modulating apoptosis. Moreover, measurement of the results of *ZNF165* depletion in breast cancer showed elevation of *SMAD7, SMURF2* and *PMEPA1* mRNAs. In contrast, the overexpression of *ZNF165* was found to increase expression of the *WISP1* oncogene. Furthermore, in lung adenocarcinoma, the depletion of *IGF2BP3* attenuated the endogenous expression of HIF target genes. Ultimately, CTA genes could play direct or indirect roles in triggering oncogenic signalling cascades and influencing the expression of other genes (Maxfield et al., 2015).

In the previous chapter, the results showed that *TEX19* was activated in most of the tested cancer cells, and it was identified as a CTA gene. No previous study has reported a function for human *TEX19*. Moreover, it is not known whether *TEX19* is required for the proliferation, self-renewal, and control of gene expression in human cancer stem-like cells and cancer cells. This chapter aims to measure the effects following *TEX19* depletion in pluripotent embryonal carcinoma cells, lung cancer cells and colorectal cancer cells to establish whether *TEX19* expression enhances cancer cell proliferation or self-renewal. In addition, the study investigates whether *TEX19* depletion influences expression of other genes to determine if it functions in transcriptional regulation.

4.2 Results

4.2.1 Depletion of *TEX19* in cancer stem-like cells and cancer cells

The depletion of *TEX19* was carried out in cancer stem-like cells (NTERA2), lung cancer cells (H460) and colon adenocarcinoma (SW480). *TEX19* siRNA#7 was used for all experiments. Negative siRNA was employed as a control to assess *TEX19* depletion. The transfection of cells with *TEX19* siRNA#7 was carried out for 72 hours along with control siRNA (negative siRNA). Following the treatment, *TEX19* mRNA was evaluated via RT-qPCR to assess the depletion level. The measurement of mRNA *TEX19* showed significant depletion compared to the control in NTERA2 ($p<0.0001$; Figure 4.1 A), H460 ($p<0.001$; Figure 4.2 A) and SW480 cells ($p<0.0001$; Figure 4.3 A).

The depletion of TEX19 was verified by western blot analysis to confirm the obtained results yielded by RT-qPCR. Using anti-TEX19 polyclonal antibody (R&D, #AF6319), a TEX19 protein size of approximately 24 KDa was detected, which was higher than the expected size of 18.5 KDa. Single or dual bands were detected following western blotting analysis, and siRNA depletion verified the specificity of the antibody (discussed in Chapter 3). The increase in intensity of the lower molecular weight band following siRNA depletion suggests that this band is a TEX19 degradation product (Figure 4.1 B). This is supported by the fact co-workers did not observe this second band while using the same antibody in these cell lines (Planells-palop, PhD. Thesis, Bangor University). Moreover, the lower band was not observed in SW480 (Figure 4.3 B), suggesting a cell line specificity. Anti-α-Tubulin was used as a control to verify the proper protein loading, and this migrated to the expected protein size of 50 KDa. Compared to the untreated cells and control siRNA, the cells transfected with the *TEX19* siRNA#7 molecules showed a significant reduction in the TEX19 protein level in NTERA2 cells (Figure 4.1 B), H460 cells (Figure 4.2. B) and SW480 cells (Figure 4.3 B).

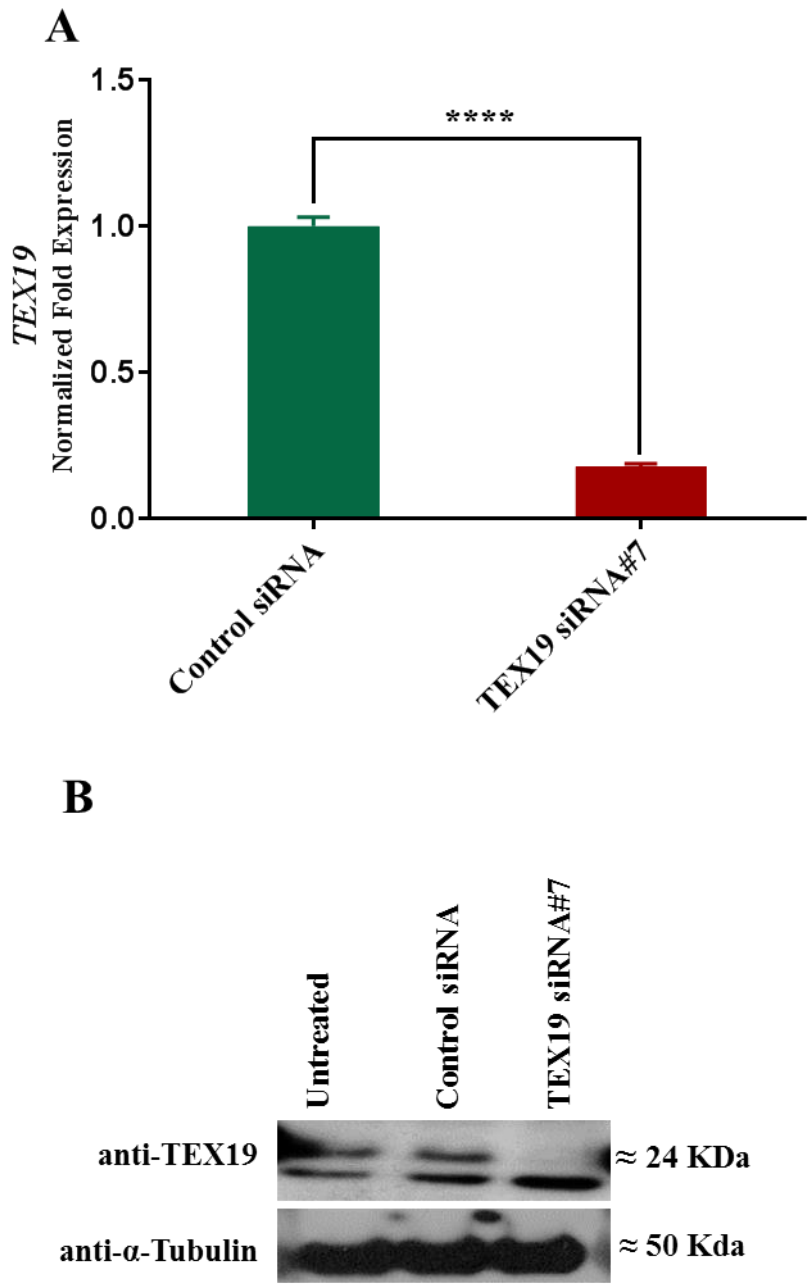

Figure 4-1 Depletion of *TEX19* in NTERA2 cells using siRNA#7.
(A) Bar charts presenting the analysis of *TEX19* expression by RT-qPCR in NTERA2 cells following depletion. NTERA2 cells transfected with *TEX19* siRNA molecules demonstrated a significant reduction in *TEX19* mRNA comparing to the control. Asterisks above the bar indicate the *p*-value (****: $p<0.0001$). *TUBA1C* and *GAPDH* were used for data normalisation. The error bars show the standard errors of the mean. (B) Western blotting analysis demonstrating the TEX19 protein level in NTERA2 following depletion. NTERA2 cells transfected with *TEX19* siRNA presented a significant reduction in the TEX19 protein level compared to untreated cells and control siRNA. Tubulin was used as a control to confirm equivalent loading in all wells.

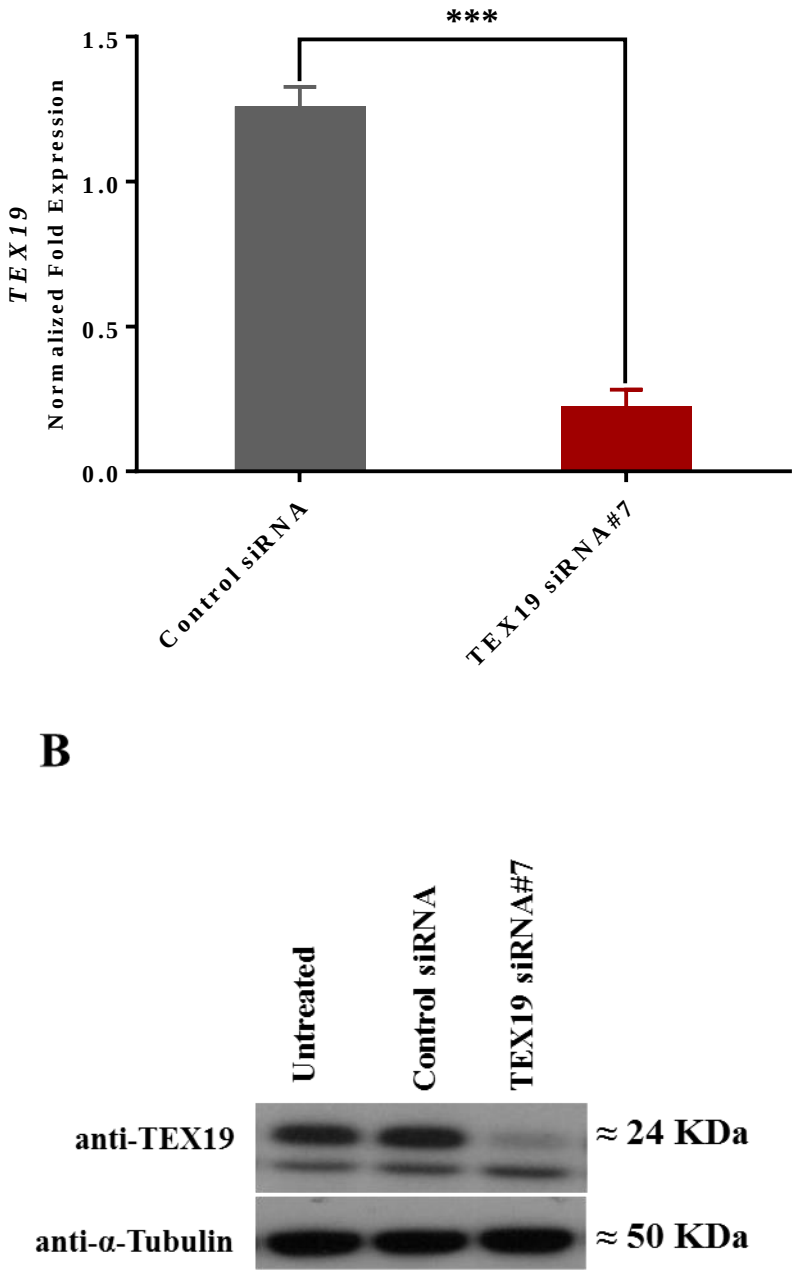

Figure 4-2 Depletion of *TEX19* in H460 cells using siRNA#7.
(A) Bar charts presenting the analysis of *TEX19* expression by RT-qPCR in H460 cells following depletion. H460 cells transfected with *TEX19* siRNA molecules demonstrated a significant reduction in *TEX19* mRNA compared to the control. Asterisks above the bar indicate the *p*-value (***: $p<0.001$). *TUBA1C* and *GAPDH* were used for data normalisation. The error bars show the standard errors of the mean. (B) Western blotting analysis demonstrating TEX19 protein level in H460 following depletion. H460 cells transfected with *TEX19* siRNA presented a significant reduction in the TEX19 protein level compared to untreated cells and control siRNA. Tubulin was used as a control to confirm equivalent loading in all wells.

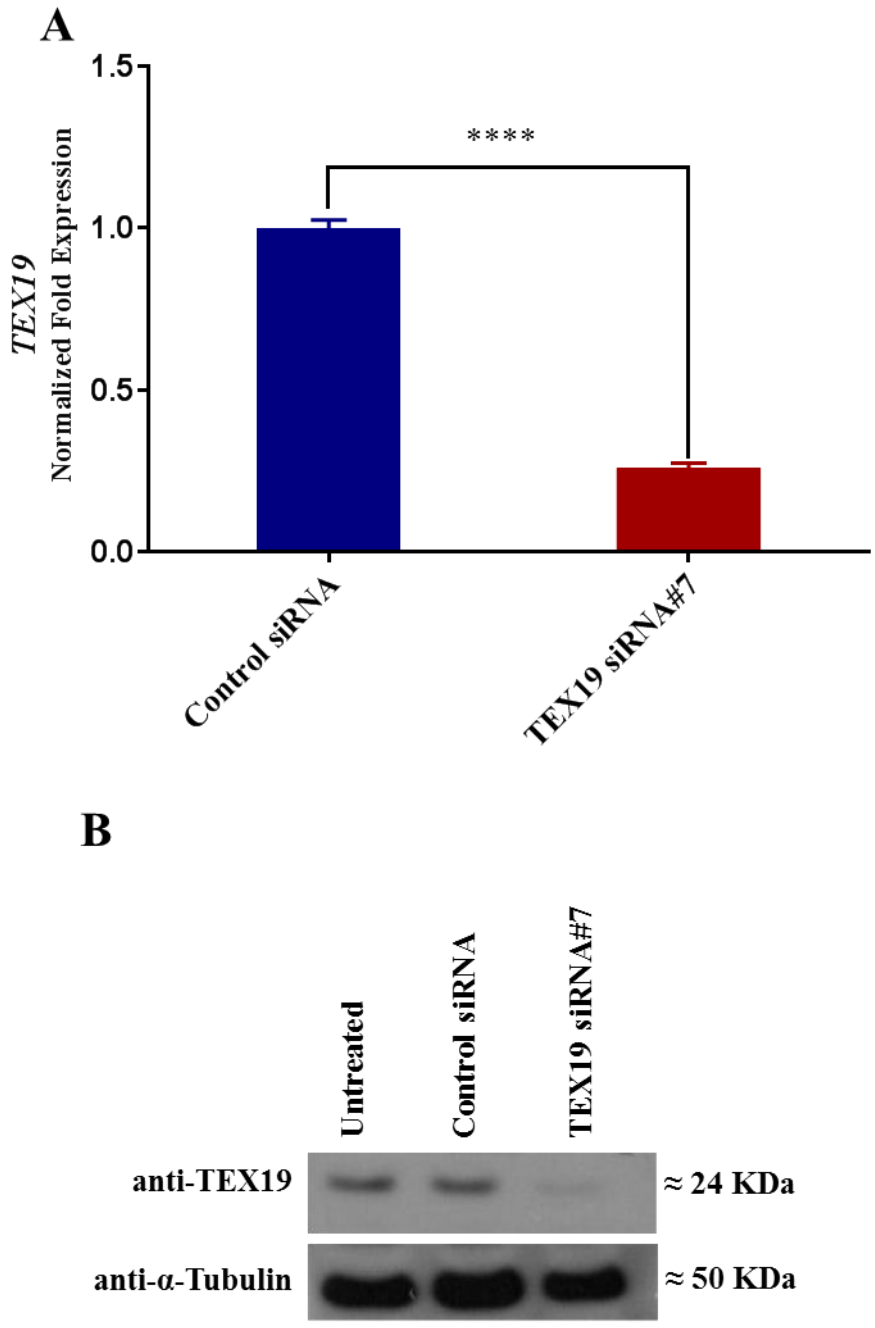

Figure 4-3 Depletion of *TEX19* in SW480 cells using siRNA#7.
(A) Bar charts presenting the analysis of *TEX19* expression by RT-qPCR in SW480 cells following depletion. SW480 cells transfected with *TEX19* siRNA molecules demonstrated a significant reduction in *TEX19* mRNA comparing to the control. Asterisks above the bar indicate the *p*-value (****: $p<0.0001$). *TUBA1C* and *GAPDH* were used for data normalisation. The error bars show the standard errors of the mean. (B) Western blotting analysis demonstrating TEX19 protein level in SW480 following depletion. SW480 cells transfected with *TEX19* siRNA presented a significant reduction in the TEX19 protein level compared to untreated cells and control siRNA. Tubulin was used as a control to confirm equivalent loading in all wells.

4.2.2 The effect of *TEX19* depletion on the proliferation of cancer stem-like cells and cancer cells

The successful depletion of *TEX19* was extended further to investigate whether *TEX19* is necessary for the proliferation of cancer stem-like cells and cancer cells. The experiments were carried out in NTERA2, H460 and SW480 cells. These cells were treated with *TEX19* siRNA#7 along with control siRNA (negative siRNA) for 8 days. Untreated cells and control siRNA cells were used as control for comparison with cells treated with *TEX19* siRNA to monitor proliferation.

In NTERA2 cells, the cells transfected with *TEX19* siRNA#7 showed significantly reduced cell numbers from day 3 ($p<0.01$) compared with untreated cells and control siRNA cells (Figure 4.4. A). From days 4–8, *TEX19* depletion resulted in a strong decline in proliferation ($p<0.0001$; Figure 4.4 A). Similarly, the depletion of *TEX19* in H460 cancer cells was found to result in significantly reduced proliferation starting from day 3 until day 8 ($p<0.0001$; Figure 4.5 A). In SW480 cells, the *TEX19* knockdown also significantly reduced cancer cell proliferation from days 3–8 ($p<0.0001$; Figure 4.6 A). Moreover, *TEX19* depletion in NTERA2 cells was found reduce cell proliferation even more compared to H460 and SW480 cancer cells.

Along with counting cells to determine the cell proliferation, the protein was extracted for each specific day and western blotting analysis was carried out to assess TEX19 protein level at different times. Untreated cells and control siRNA cells were used as control. In NTERA2 cells, TEX19 depletion showed significant protein reduction on days 2 and 3, and no high molecular weight protein was detected from day 4 (Figure 4.4 B). Correspondingly, TEX19 knockdown revealed significant protein reduction in H460 (Figure 4.5 B) and SW480 (Figure 4.6 B). Anti-α-Tubulin was used as a control to verify the proper protein loading, and this migrated to the expected protein size of 50 KDa. However, the significant reduction in TEX19 protein level was found to be consistent with the reduction in proliferation of cancer cells.

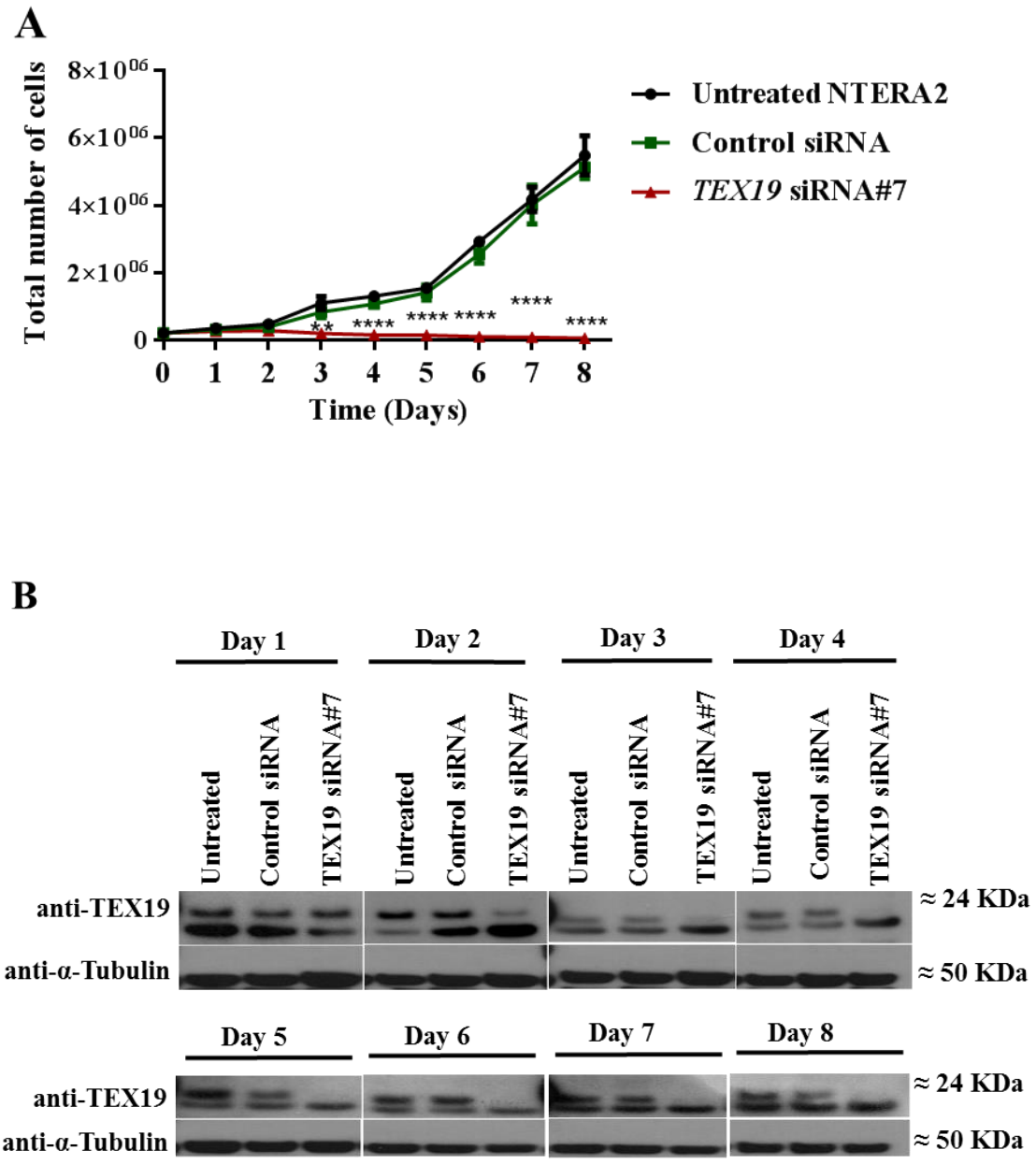

Figure 4-4 NTERA2 cells transfected with *TEX19* siRNA.
(A) Cell count curve demonstrating the proliferation of untreated NTERA2 cells, control siRNA cells and cells treated with *TEX19* siRNA#7 for 8 days. Untreated cells and control siRNA cells were used as control. Cells treated with *TEX19* siRNA#7 showed a substantial proliferation reduction compared to the controls. The error bars represent the standard deviation for the three replicates. Asterisks indicate *p*-values (**: $p<0.01$; ****: $p<0.0001$). (B) Analysis of western blot showing the TEX19 protein level upon NTERA2 cell proliferation. The results showed that cells treated with *TEX19* siRNA#7 demonstrated strong reduction in TEX19 protein level comparing to the controls. Tubulin was used as a control to confirm equivalent loading in all wells.

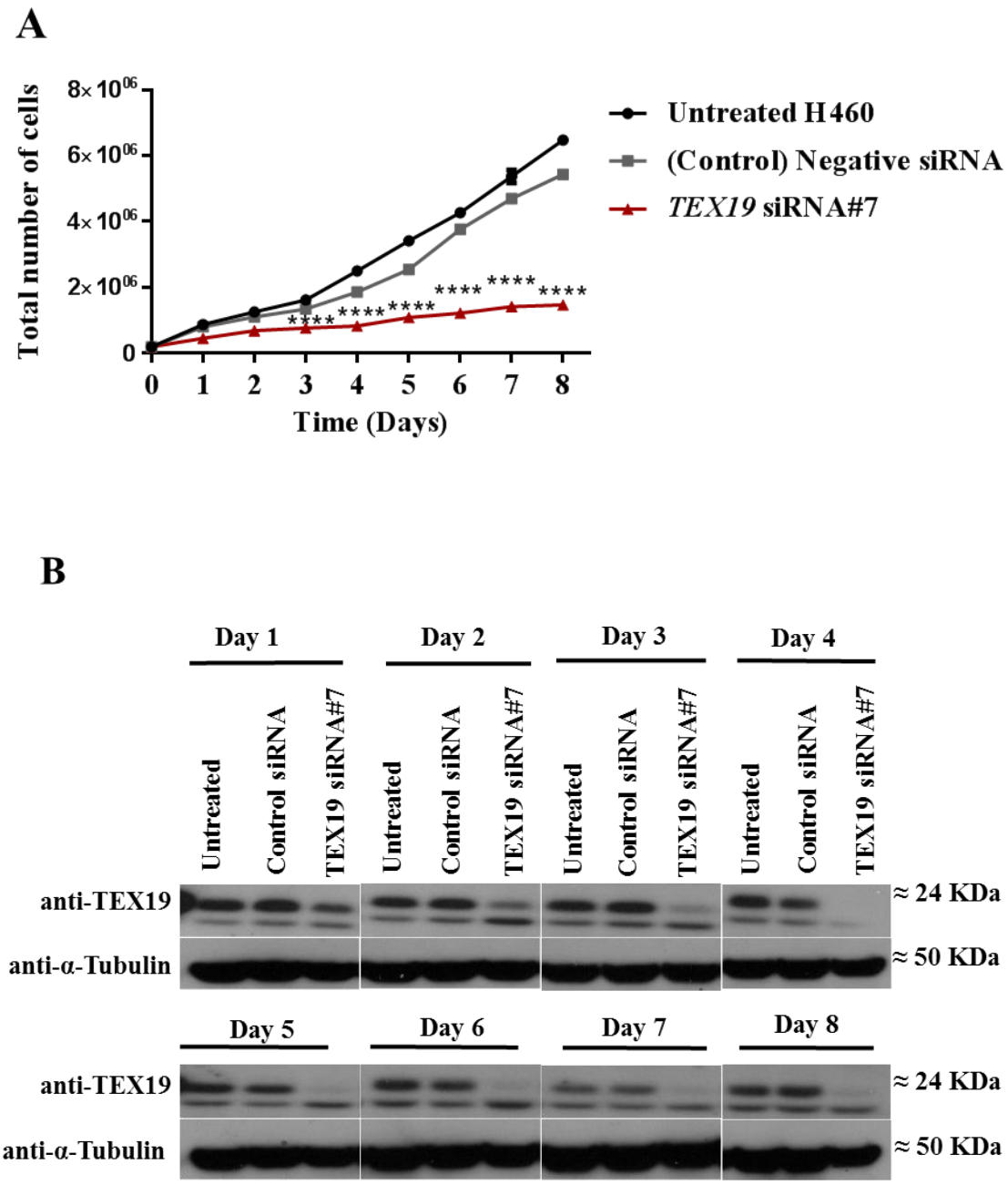

Figure 4-5 H460 cells transfected with *TEX19* siRNA.
(A) Cell count curve demonstrating the proliferation of untreated H460 cells, control siRNA cells and cells treated with *TEX19* siRNA#7 for 8 days. Untreated cells and control siRNA cells were used as control. Cells treated with *TEX19* siRNA#7 showed substantial proliferation reduction comparing to the controls. The error bars represent the standard deviation for the three replicates. Asterisks indicate the *p*-value (****: $p<0.0001$). (B) Analysis of western blot demonstrating the TEX19 protein level upon H460 cell proliferation. The results showed that cells treated with *TEX19* siRNA#7 demonstrated a strong reduction in TEX19 protein level compared to the controls. Tubulin was used as a control to confirm equivalent loading in all wells.

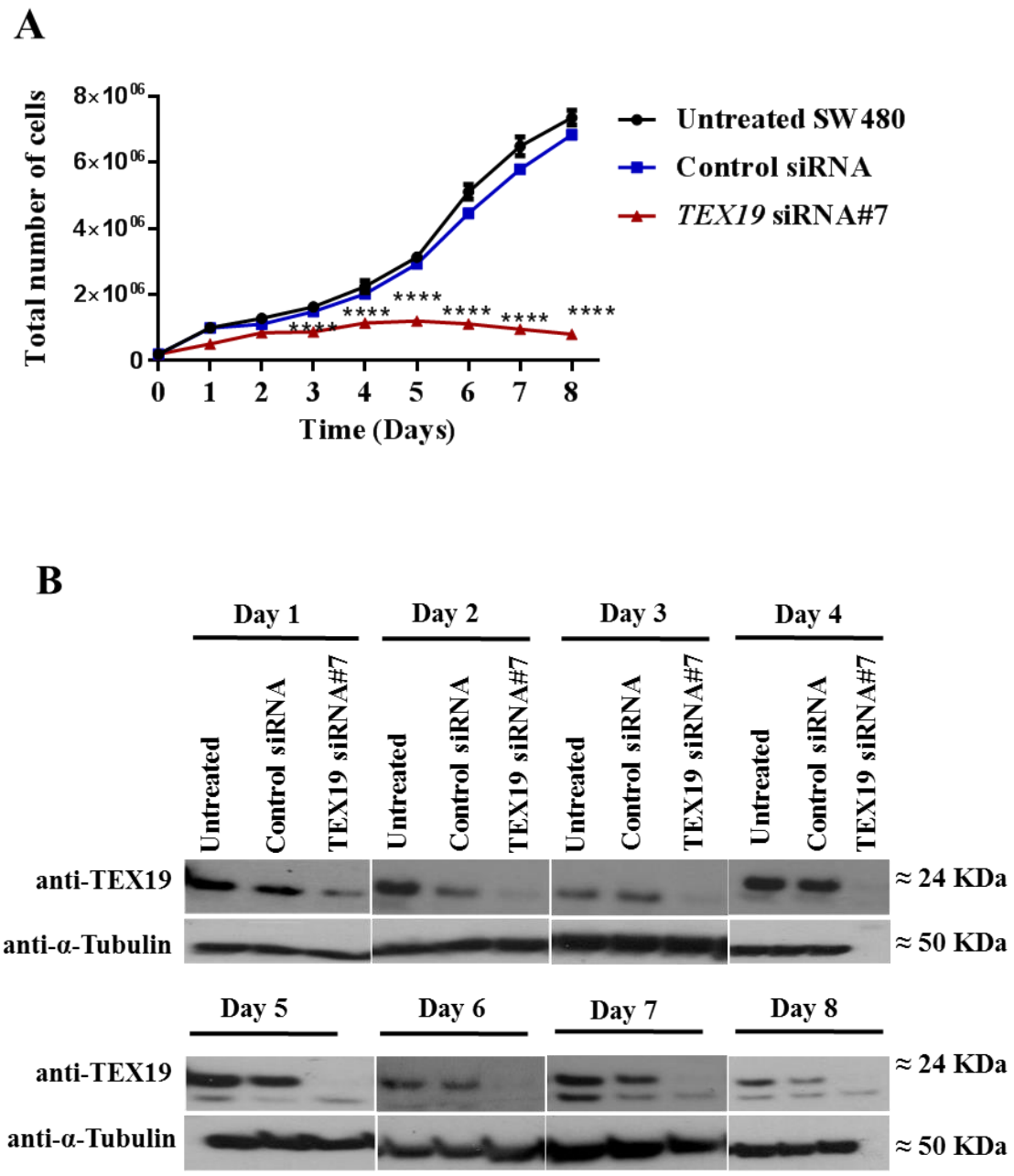

Figure 4-6 SW480 cells transfected with *TEX19* siRNA.
(A) Cell count curve demonstrating the proliferation of untreated SW480 cells, control siRNA cells and cells treated with *TEX19* siRNA#7 for 8 days. Untreated cells and control siRNA cells were used as control. Cells treated with *TEX19* siRNA#7 showed substantial prolifration reduction compared to the controls. The error bars represent the standard deviation for the three replicates. Asterisks indicate the *p*-value (****: $p<0.0001$). (B) Analysis of western blot demonstrating TEX19 protein level upon SW480 cell proliferation. The results showed that cells treated with *TEX19* siRNA#7 demonstrated a strong reduction in the TEX19 protein level compared to the controls. Tubulin was used as a control to confirm equivalent loading in all wells.

4.2.3 Assessment of the self-renewal potential of cancer stem-like cells and cancer cells using extreme limiting assay (ELDA).

The cell count curves showed a significant reduction in cancer cell proliferation following *TEX19* depletion. Therefore, further confirmation was carried out using ELDA assay to assess self-renewal potential of cancer stem-like cells and cancer cells following the transfection with *TEX19* siRNA#7. ELDA assay was carried out in NTERA2, H460 and SW480 cells. These cells were plated with different serial dilutions of 1000 cells, 100 cells, 10 cells and 1 cell per well for 10 days. Each serial dilution was carried out in 12 wells. NTERA2, H460 and SW480 cells were transfected with *TEX19* siRNA#7 along with siRNA control (negative siRNA). Untreated cells and control siRNA cells were used as control. In addition, images of both untreated cells and transfected cells were taken to determine the self-renewal effect following siRNA treatment. The analysis of ELDA assay in NTERA2 determined that the transfection with *TEX19* siRNA caused a significant renewal drop; no positive renewal was detected in the wells with serial dilutions of 100 cells, 10 cells or 1 cell (Figure 4.7 A). A comparison of this observation with untreated cells and negative siRNA cells indicated that *TEX19* depletion hugely reduced the self-renewal of NTERA2. Moreover, an example image of the cells also shows the effect of *TEX19* siRNA transfection on the renewal of cultured cells after 10 days (Figure 4.7 B). Correspondingly, in H460 cells, *TEX19* siRNA transfection hugely reduced the cancer cell self-renewal, where only one positive renewal was detected in dilutions of 100 cells and 10 cells, and two positive renewals were found in the dilution of 1 cell (Figure 4.9 A). An example of the imaged cells also shows the effect of *TEX19* siRNA transfection on the renewal of cultured cells after 10 days (Figure 4.9 B). In SW480 cells, the effect of *TEX19* siRNA transfection significantly decreased the cancer cell self-renewal, where only one positive renewal was detected in dilutions of 100 cells and 1 cell, and negative renewal was detected in the dilution of 10 cells (Figure 4.11 A). An example of the imaged cells also shows the effect of *TEX19* siRNA transfection on the renewal of cultured cells after 10 days (Figure 4.11 B). The ELDA analysis and pairwise tests illustrated the significant influence of *TEX19* depletion on cancer cell self-renewal at $p<0.0001$ in NTERA2 (Figure 4.8 A, B), H460 (Figure 4.10 A, B) and SW480 cells (Figure 4.12 A, B). The ELDA analyses for all tested cells were consistent with the results obtained

from the cell count curves, showing that *TEX19* influences the self-renewal of cancer stem-like cells and cancer cells.

A

Number of cells per well	Number of wells plated	NTERA2		
		Untreated	control siRNA	*TEX19* siRNA#7
Number of wells showing positive renewal after 10 days of siRNA transfection				
1000	12	12	12	8
100	12	11	11	0
10	12	12	11	0
1	12	11	10	0
Self-renewal frequency (95% CI)		1/7 (1/14-1/4)	1/8 (1/16-1/4)	1/1091 (1/2194-1/543)
P value	1.53e-56			

B

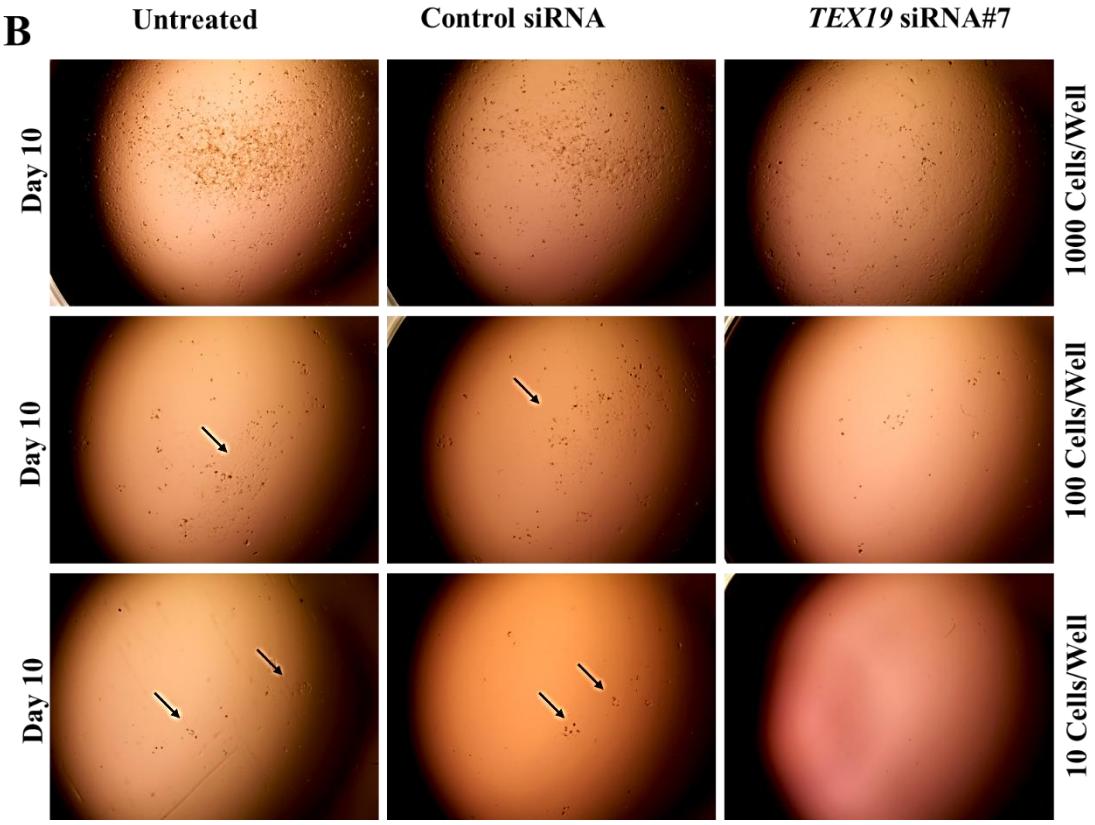

Figure 4-7 Effect of *TEX19* siRNA transfection on NTERA2 cell self-renewal determined by ELDA.
(A) ELDA assay examination after *TEX19* siRNA#7 treatment for 10 days demonstrating the number of wells showing positive renewal. ELDA assay was carried out by seeding with different numbers of cells (1000, 100, 10, 1 cells/ml) and showed positive renewal in all untreated cells and control siRNA cells. (B) Images demonstrating the renewal of NTERA2 cells after 10 days of transfection. Untreated cells and control siRNA cells were used as control and they showed no self-renewal effected comparing to transfected cells with *TEX19* siRNA#7.

A

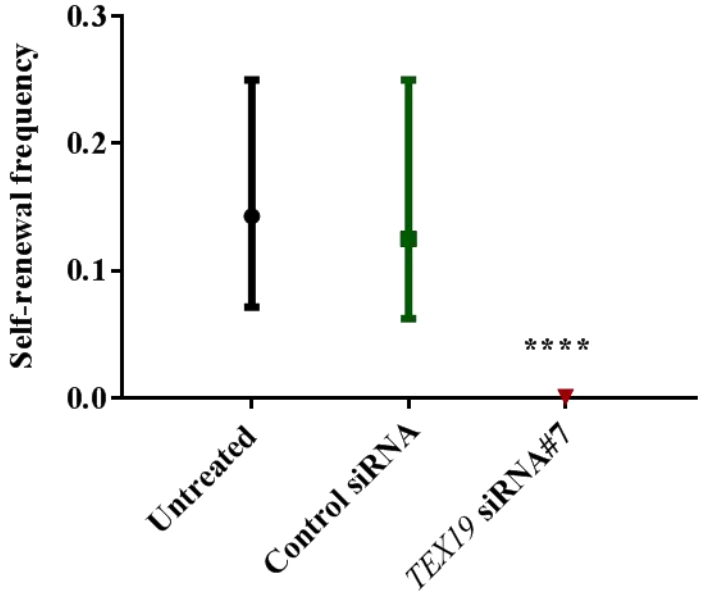

B

Pairwise tests for differences in NTERA2 self-renewal frequencies				
Group 1	**Group 2**	**Chisq**	**DF**	**Pr(>Chisq)**
Control siRNA	Untreated	0.213	1	0.644
Control siRNA	*TEX19* siRNA	151	1	8.84e-35
TEX19 siRNA	Untreated	166	1	5.77e-38

Figure 4-8 ELDA assay analysis after *TEX19* siRNA transfection in NTERA2 cells.
(A) Graph demonstrating the influence of *TEX19* siRNA#7 on NTERA2 self-renewal. Untreated cells and control siRNA cells showed no effect on their renewal. Cells treated with *TEX19* siRNA#7 exhibited a significant renewal reduction. Asterisks indicate the *p*-value (****: $p<0.0001$). (B) Analysis representing the pairwise comparison of transfected groups of NTERA2 cells. Chisq indicates Chi-square; DF indicates degrees of freedom; Pr (>Chisq) indicates the probability value. The pairwise comparison showed no effect on the renewal in untreated cells and control siRNA cells. NTERA2 cells treated with *TEX19* siRNA#7 exhibited a significant difference, with Pr (>Chisq) <0.0001.

A

Number of cells per well	Number of wells plated	H460		
		Untreated	control siRNA	*TEX19* siRNA#7
Number of wells showing positive renewal after 10 days of siRNA transfection				
1000	12	12	12	11
100	12	11	10	1
10	12	11	11	1
1	12	11	11	2
Self-renewal frequency (95% CI)		1/7 (1/15-1/4)	1/12 (1/25-1/6)	1/370 (1/701-1/196)
P value	1.33e-31			

B

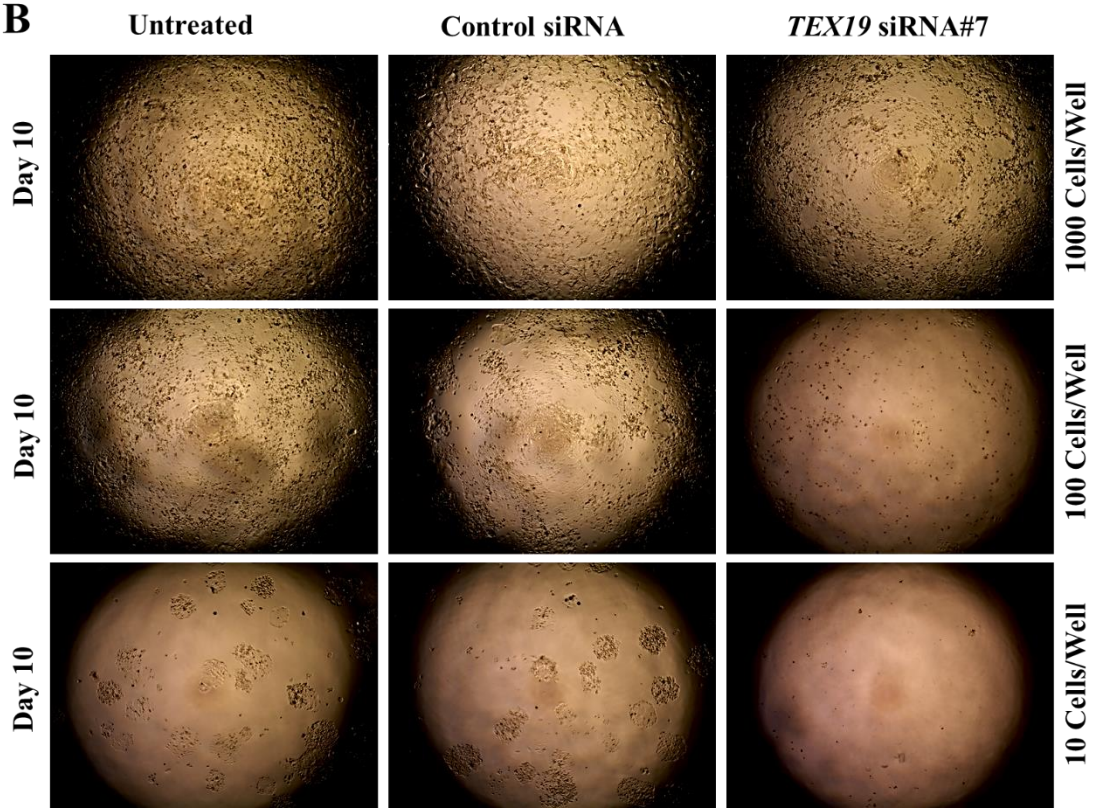

Figure 4-9 Effect of *TEX19* siRNA transfection on H460 cell self-renewal determined by ELDA.

(A) ELDA assay examination after *TEX19* siRNA treatment for 10 days demonstrating the number of wells showing positive renewal. ELDA assay was carried out by seeding with different numbers of cells (1000, 100, 10, 1 cells/ml) and showed positive renewal in all untreated cells and control siRNA cells. (B) Images demonstrating the renewal of H460 cells after 10 days of transfection. Untreated cells and control siRNA cells were used as control and they showed no self-renewal effected comparing to transfected cells with *TEX19* siRNA#7.

A

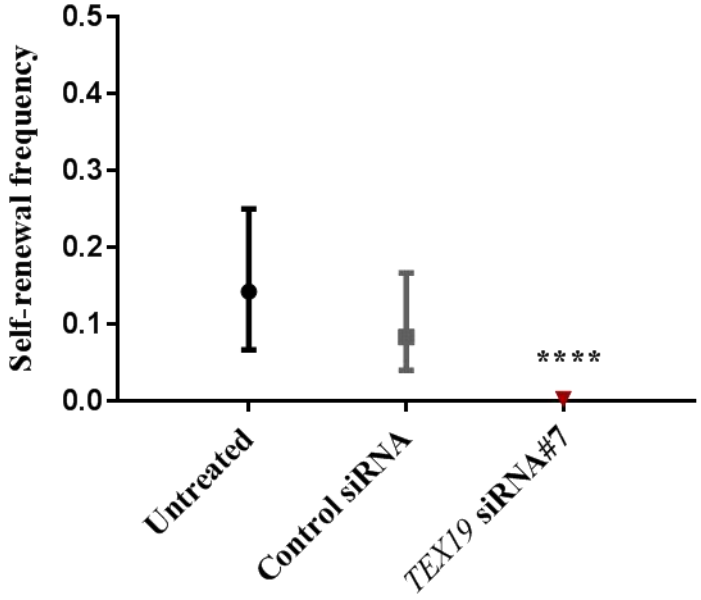

B

Pairwise tests for differences in H460 self-renewal frequencies				
Group 1	**Group 2**	**Chisq**	**DF**	**Pr(>Chisq)**
Control siRNA	**Untreated**	**2.64**	**1**	**0.104**
Control siRNA	***TEX19* siRNA**	**83**	**1**	**7.94e-20**
***TEX19* siRNA**	**Untreated**	**102**	**1**	**4.46e-24**

Figure 4-10 ELDA assay analysis after *TEX19* siRNA transfection in H460 cells.
(A) Graph demonstrating the influence of *TEX19* siRNA#7 on H460 self-renewal. Untreated cells and control siRNA cells showed no effect on their renewal. Cells treated with *TEX19* siRNA#7 exhibited a significant renewal reduction. Asterisks indicate the *p*-value (****: $p<0.0001$). (B) Analysis representing the pairwise comparison of transfected groups of H460 cells. Chisq indicates Chi-square; DF indicates degrees of freedom; Pr (>Chisq) indicates the probability value. The pairwise comparison showed no effect on the renewal in untreated cells and control siRNA cells. H460 cells treated with *TEX19* siRNA#7 exhibited a significant difference, with Pr (>Chisq) <0.0001.

A

Number of cells per well	Number of wells plated	SW480		
		Untreated	control siRNA	*TEX19* siRNA#7
Number of wells showing positive renewal after 10 days of siRNA transfection				
1000	12	12	12	10
100	12	11	10	1
10	12	10	10	0
1	12	11	11	1
Self-renewal frequency (95% CI)		1/8 (1/16-1/4))	1/13 (1/27-1/6)	1/575 (1/1073-1/308)
P value	6.53e-38			

B

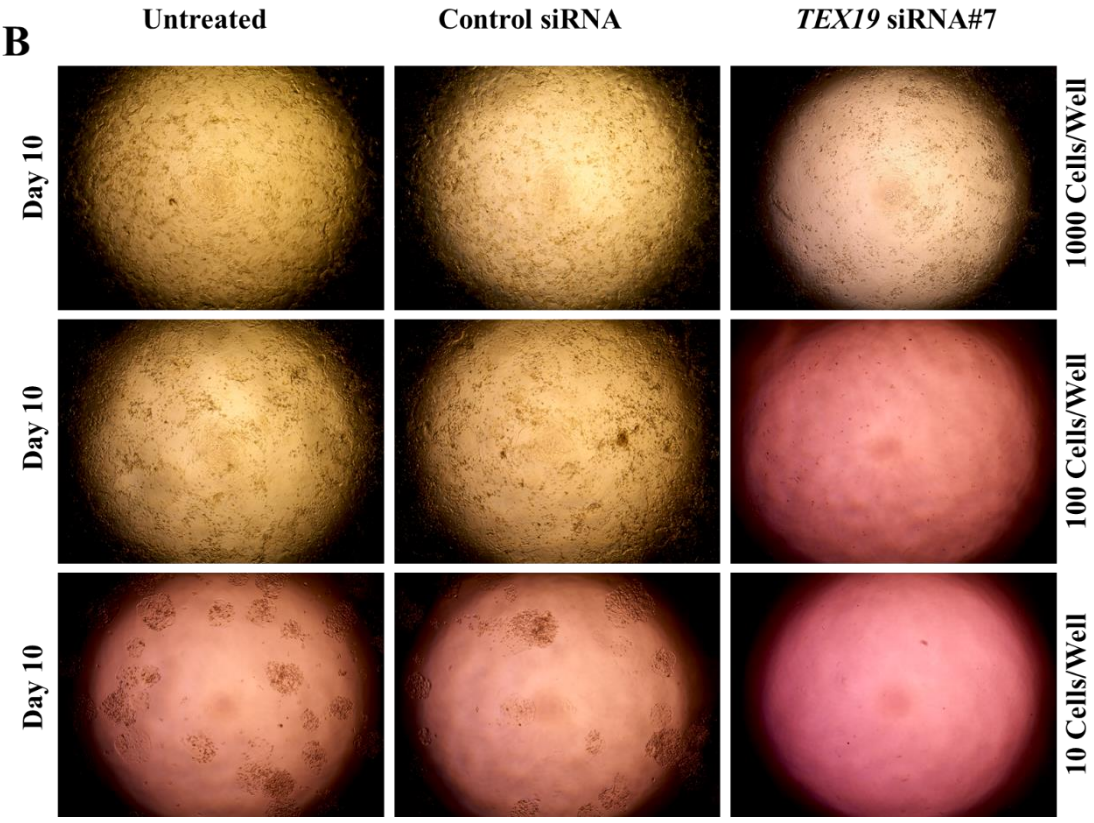

Figure 4-11 Effect of *TEX19* siRNA transfection on SW480 cell self-renewal determined by ELDA.

(A) ELDA assay examination after *TEX19* siRNA treatment for 10 days demonstrating the number of wells showing positive renewal. ELDA assay was carried out by seeding with different numbers of cells (1000, 100, 10, 1 cells/ml) and showed positive renewal in all untreated cells and control siRNA cells. (B) Images demonstrating the renewal of SW480 cells after 10 days of transfection. Untreated cells and control siRNA cells were used as positive control and they showed no self-renewal effected comparing to transfected cells with *TEX19* siRNA#7.

A

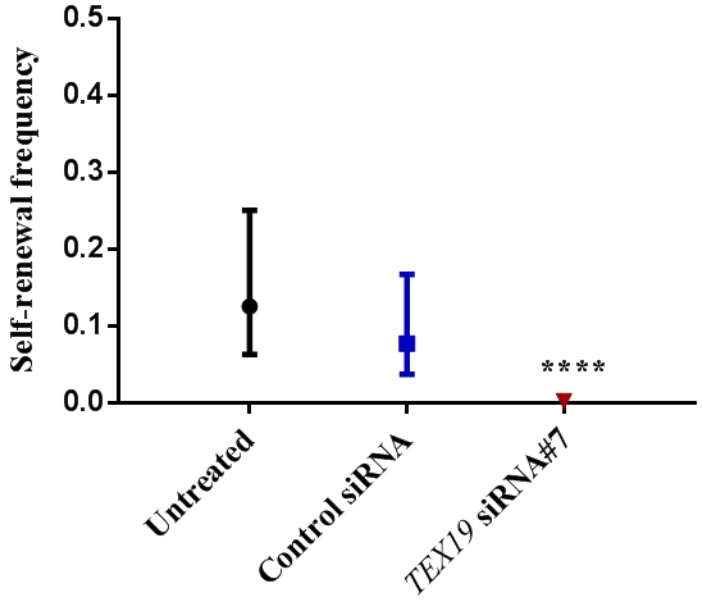

B

Pairwise tests for differences in SW480 self-renewal frequencies				
Group 1	**Group 2**	**Chisq**	**DF**	**Pr(>Chisq)**
Control siRNA	Untreated	2.35	1	0.125
Control siRNA	*TEX19* siRNA	100	1	1.24e-23
TEX19 siRNA	Untreated	119	1	8.37e-28

Figure 4-12 ELDA assay analysis after *TEX19* siRNA transfection in SW480 cells.
(A) Graph demonstrating the influence of *TEX19* siRNA#7 on SW480 self-renewal. Untreated cells and control siRNA cells showed no effect on their renewal. Cells treated with *TEX19* siRNA#7 exhibited a significant renewal reduction. Asterisks indicate the *p*-value (****: $p<0.0001$). (B) Analysis representing the pairwise comparison of transfected groups of SW480 cells. Chisq indicates Chi-square; DF indicates degrees of freedom; Pr (>Chisq) indicates the probability value. The pairwise comparison showed no effect on the renewal in untreated cells and control siRNA cells. SW480 cells treated with *TEX19* siRNA#7 exhibited a significant difference, with Pr (>Chisq) <0.0001.

4.2.4 *TEX19* depletion regulate gene expression in cancer stem-like cells and cancer cells

To explore the influence of *TEX19* depletion on gene expression, multiple genes were selected based on RNA sequencing data (Planells-palop, PhD. Thesis, Bangor University). This experiment was previously carried out in SW480 cells using *TEX19* siRNA#6 in the McFarlane laboratory. *TEX19* mRNA depletion resulted in the identification of a cohort of 80 genes with altered transcript levels response to *TEX19* siRNA#6 treatment. In this study, 46 genes (Figure 4.13) were selected to validate their expression via RT-qPCR following *TEX19* siRNA#7 transfection in NTERA2, H460 and SW480 cells to identify common genes with consistent alternation expression in response to *TEX19* transcript depletion. Moreover, some of these genes were selected due to their links to spermatogenesis, meiosis and cell proliferation.

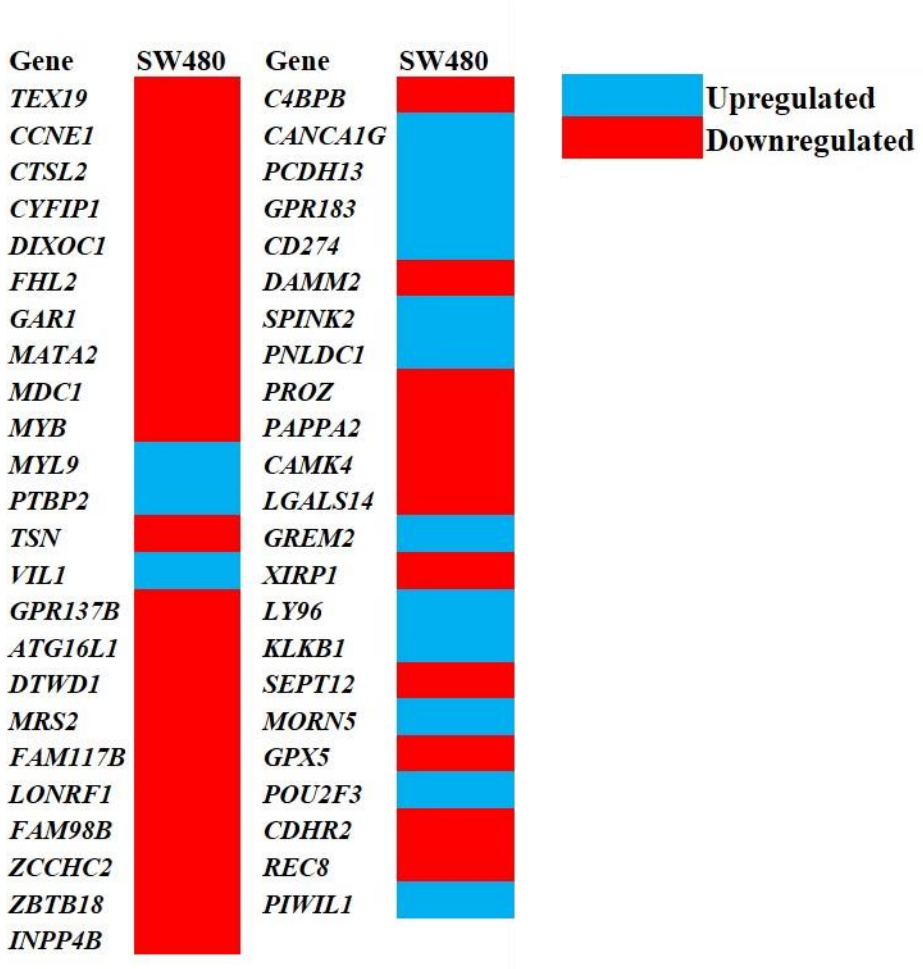

Figure 4-13 Genes of interest selected based on RNA sequencing data.
The scheme illustrates 46 genes that were found with altered transcript levels following transfection of SW480 with *TEX19* siRNA#6.

The measurement of mRNA was performed via RT-qPCR for the selected genes after *TEX19* transcript knockdown, and this showed altered mRNA levels in cancer stem-like cells and cancer cells. The analysed data were normalised to *TUBA1C* and *GAPDH*. Moreover, the control siRNA (negative siRNA) was applied as control for *TEX19* knockdown. In NTERA2 cells, the depletion of *TEX19* mRNA changed the transcript levels for a limited number of genes, namely *GRAP137B* and *SEPT12*, compared to the control (Figure 4.14). However, no significant changes were observed for the rest of the investigated genes. Both *GRAP137B* and *SEPT12* were downregulated (p<0.01).

In H460 cells, *TEX19* transcript depletion altered mRNA levels of multiple genes, most of which were downregulated (Figure 4.15). The following genes showed significantly decreased mRNA levels (p<0.05): *CYFIP1*, *MYB*, *MYL9*, *TSN* and *PCDHB13*. Similarly, the transcript levels of *GAR1*, *MATA2*, *MDC1*, *VIL1*, *GPR137B*, *FAM98B*, *ZCCHC2*, *CACNA1G* and *CD274* were significantly reduced (p<0.01). In addition, the transcript levels of *FAM117B*, *PAPPA2* and *SEPT12* were more inhibited compared to the previously mentioned downregulated genes (p<0.001). In contrast, *PIWIL1* and *LY96* mRNA levels were significantly elevated compared to the control (p<0.01 and p<0.001, respectively). However, the analysis showed no significant change for the other investigated genes.

Carrying on the investigation in SW480 revealed the influence of *TEX19* transcript depletion on controlling the expression of numerous genes. However, most of these genes were upregulated comparing with the control (Figure 4.16). The *MDC1*, *MYL9*, *PTBP2*, *ATG16L1*, *LONRF1*, *FAM98B*, *ZBTB18*, *DAMM2*, *PROZ*, *KLKB1* and *REC8* genes showed significantly increased mRNA levels (p<0.05). Similarly, the transcript levels of *CTSL2*, *CYFIP1*, *DIXOC1*, *FHL2*, *MATA2*, *VIL1*, *MRS2*, *FAM117B*, *ZCCHC2*, *CACNA1G*, *SPINK2*, *PNLDC1*, *CAMK4*, *GPX5*, *POU2F3* and *CDHR2* were significantly elevated (p<0.01). In addition, the mRNA levels of *PCDHB13*, *CD274*, *XIRP1*, *LY96* and *PIWIL1* were more elevated compared to the previously mentioned upregulated genes (p<0.001). In contrast, mRNA levels of *GAR1* and *LGALS14* were significantly downregulated compared to the control (p<0.01). However, the transcript levels showed no significant change for the rest of the investigated genes.

Taking these results together, the reducing of *TEX19* mRNA level influenced multiple genes with altered transcript levels. Moreover, most investigated genes were upregulated in SW480, while they were downregulated in H460 when *TEX19* was depleted. More importantly, no common gene was identified with consistent expression in the NTERA2, H460 and SW480, but some genes were observed to have consistent expression in two different cell lines. Genes involving *PIWIL1* and *LY96* showed elevated transcript levels in SW480 and H460. *GAR1* mRNA level was observed to be downregulated in H460 and SW480 cells. Finally, *GPR137B* and *SEPT12* mRNA levels were inhibited in NTERA2 and H460 cells.

In the context of the comparison to RNA sequence data, the RT-qPCR results obtained after *TEX19* siRNA#7 transfection were not fully consistent with the RNA sequencing results for SW480 cells transfected with *TEX19* siRNA#6. Depletion of *TEX19* in SW480 using *TEX19* siRNA#6 and siRNA#7 revealed genes with consistently downregulated mRNA levels, namely *GAR1* and *LGALS14*. In contrast, *MYL9*, *PTBP2*, *CANCA1G*, *PCDH13*, *CD274*, *PNLDC1*, *LY96*, *POU2F3*, *SPINK2*, *KLKB1* and *PIWIL1* were found to have consistently upregulated transcript levels. Correspondingly, comparing the sequencing results to the obtained results following *TEX19* depletion in H460, several genes were observed with consistently downregulated mRNA levels, including *CYFIP1*, *GAR1*, *MATA2*, *MDC1*, *MYB*, *TSN*, *GPR137B*, *FAM117B*, *FAM98B*, *ZCCHC2*, *PAPPA2* and *SEPT12*. In contrast, the *LY96* and *PIWIL1* genes revealed consistently upregulated mRNA levels. Finally, in NTERA2, only two genes – *GPR137B* and *SEPT12* – exhibited consistently downregulated transcript levels when compared to the RNA sequencing results. Remarkably, *PIWIL1* and *LY96* transcript levels were found to be elevated in SW480 and H460, and this was consistent with the RNA sequencing results. In contrast, *GAR1* mRNA level was found to be downregulated in SW480 and H460, and this was consistent with the RNA sequencing results. Likewise, *SEPT12* and *GPR137B* mRNA levels were found to be downregulated in NTERA2 and H460, and the results for these genes were consistent with the RNA sequencing data. More importantly, *PIWIL1*, *LY96*, *GAR1*, *GPR137B* and *SEPT12* were found to be more controlled by *TEX19* expression compared to other genes; their expressions were consistent in two cancer cell lines and similar to the RNA sequencing data (Figure 4.17).

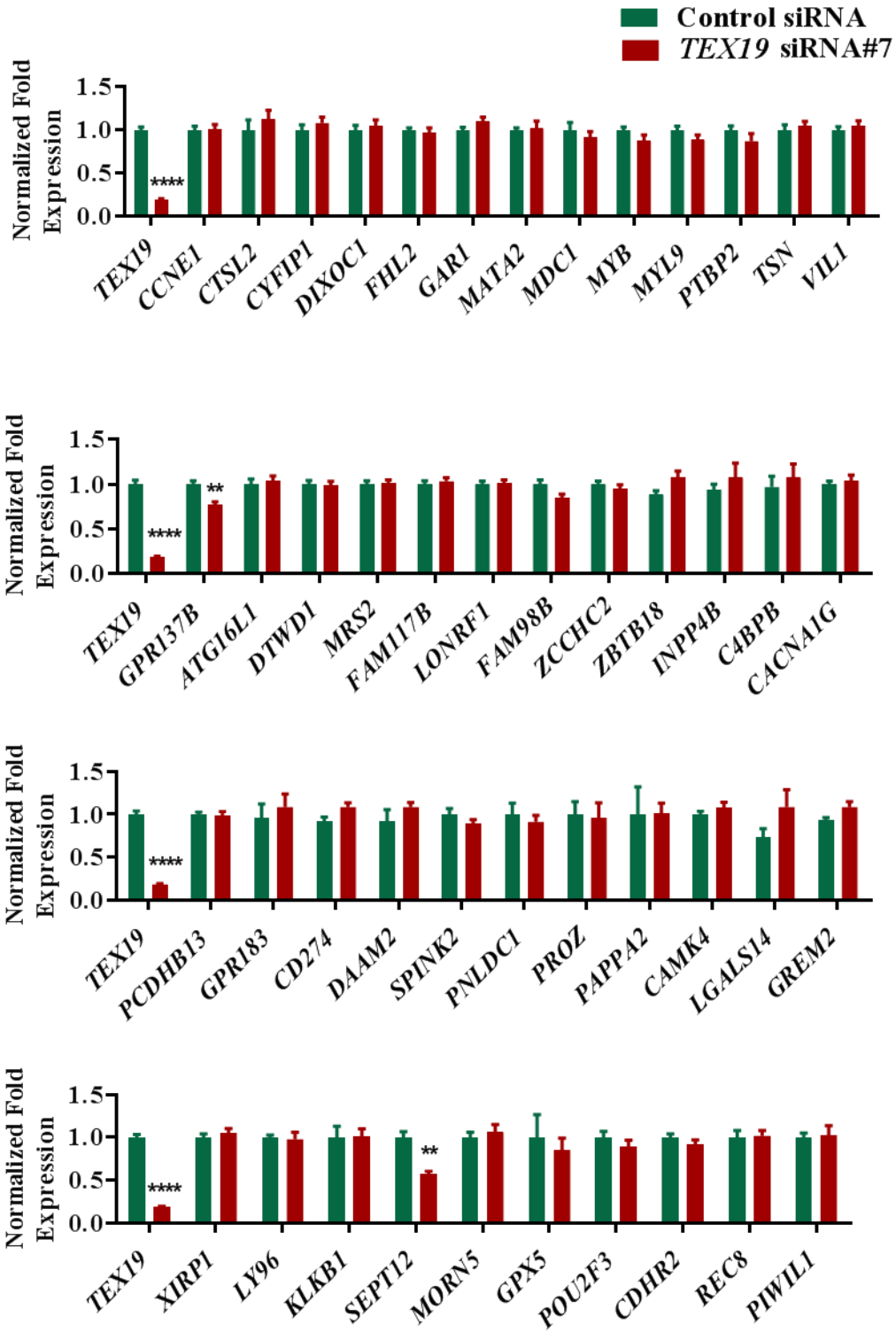

Figure 4-14 RT-qPCR analysis of genes of interest following *TEX19* transcript depletion in NTERA2 cells.

Targets were selected from differentially expressed genes obtained from the RNA sequencing results following *TEX19* depletion in SW480 cells using *TEX19* siRNA#6. NTERA2 cells were transfected with *TEX19* siRNA#7 and the results were compared to control siRNA. The findings demonstrate significant *TEX19* depletion altered mRNA levels for a limited number of genes of interest. Asterisks above the bar indicate *p*-values (**: $p<0.01$; ****: $p<0.0001$). *TUBA1C* and *GAPDH* were used for data normalisation. The error bars show the standard errors of the mean.

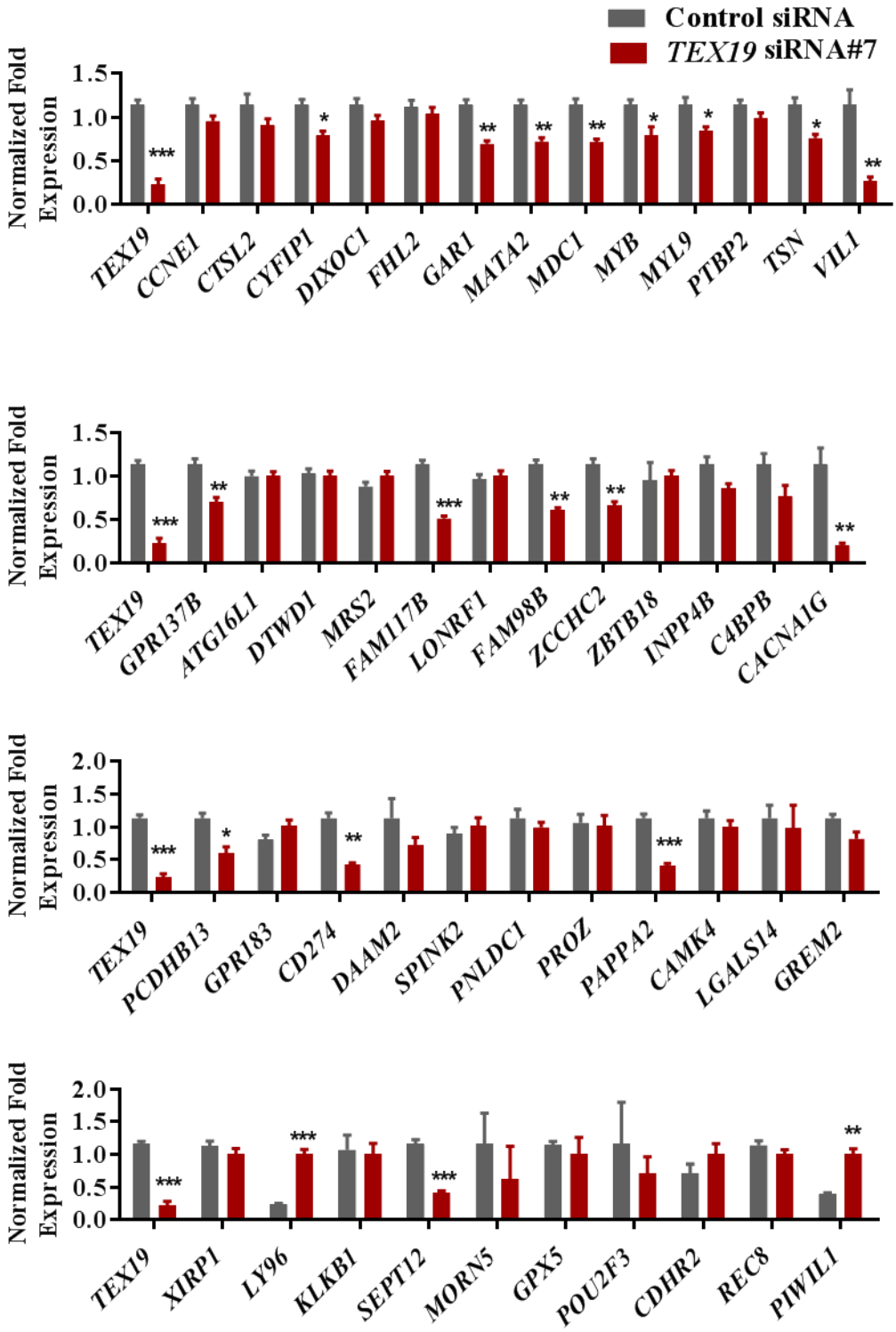

Figure 4-15 RT-qPCR analysis of genes of interest following *TEX19* transcript depletion in H460 cells.

Targets were selected from differentially expressed genes obtained from the RNA sequencing results following *TEX19* depletion in SW480 cells using *TEX19* siRNA#6. H460 cells were transfected with *TEX19* siRNA#7 and the results were compared to control siRNA. The results demonstrate significant *TEX19* depletion altered mRNA levels for multiple genes of interest. Asterisks above the bar indicate *p*-values (*: $p<0.05$; **: $p<0.01$***: $p<0.001$). *TUBA1C* and *GAPDH* were used for data normalisation. The error bars show the standard errors of the mean.

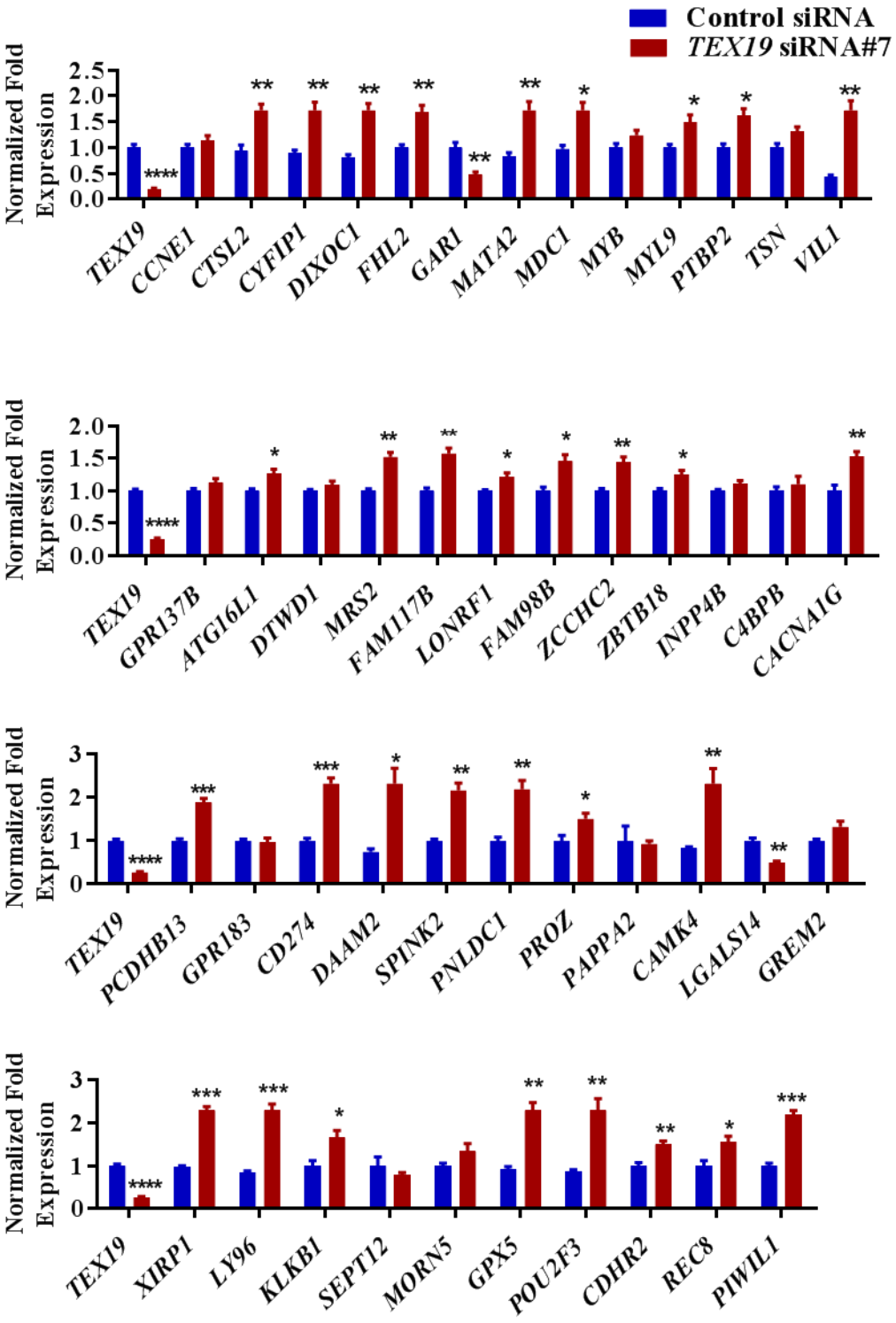

Figure 4-16 RT-qPCR analysis of genes of interest following *TEX19* transcript depletion in SW480 cells.

Targets were selected from differentially expressed genes obtained from the RNA sequencing results following *TEX19* depletion in SW480 cells using *TEX19* siRNA#6. SW480 cells were transfected with *TEX19* siRNA#7 and the results were compared to control siRNA. The findings demonstrate significant *TEX19* depletion altered the mRNA levels for several genes of interest. Asterisks above the bar indicate *p*-values (*: $p<0.05$; **: $p<0.01$***: $p<0.001$; ****: $p<0.0001$). *TUBA1C* and *GAPDH* were used for data normalisation. The error bars show the standard errors of the mean.

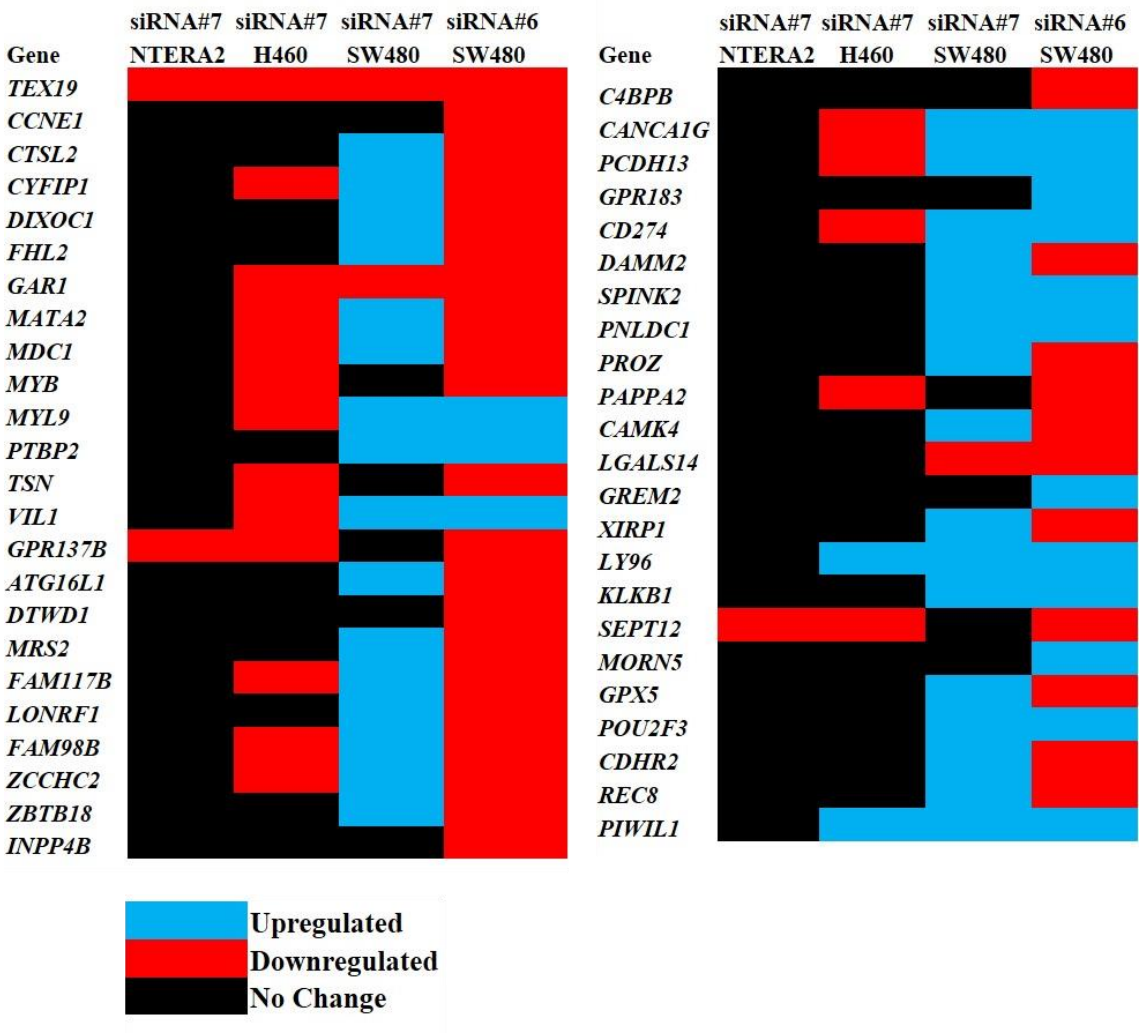

Figure 4-17 Assessment of expression for genes of interest following *TEX19* depletion.
The scheme illustrates the comparison of 46 differentially expressed genes following *TEX19* depletion. NTERA2, H460 and SW480 cells were transfected with *TEX19* siRNA#7. The results obtained from RNA sequencing data are presented with siRNA#6 for comparison of gene expression among the analysed data.

4.2.5 *TEX19* depletion regulates *PIWI* genes expression

PIWIL1 gene transcript level was observed to be significantly elevated in the RNA sequencing results. However, using different *TEX19* siRNA exhibited stable results in SW480 and H460 cells. In line with this, the consistency of *PIWIL1* expression in RNA sequencing data and in this study motivated the investigation of a set of genes belonging to the PIWI family to determine whether *TEX19* is involved in regulation of the PIWI pathway. To accomplish this, expressions of *PIWIL1*, *PIWIL2*, *PIWIL3* and *PIWIL4* were investigated after *TEX19* transcript depletion using *TEX19* siRNA#7.

Analysis of the mRNA levels of *PIWI* gene transcripts via RT-qPCR showed that they were different in cancer stem-like cells and cancer cells. Depletion of *TEX19* transcript in NTERA2 revealed elevated mRNA level in *PIWIL2* ($p<0.05$). Likewise, the analysis showed no significant change for *PIWIL1*, *PIWIL3* and *PIWIL4* (Figure 4.18 A). In H460 cells, *TEX19* transcript depletion upregulated the transcript level of *PIWIL1* ($p<0.01$). In contrast, the mRNA level of *PIWIL4* was significantly downregulated ($p<0.01$). Both *PIWIL2* and *PIWIL3* were negatively expressed (Figure 4.18 B). In SW480 cells, *TEX19* knockdown considerably upregulated *PIWIL1*, *PIWIL2* and *PIWIL4* ($p<0.001$, $p<0.01$ and $p<0.01$, respectively). SW480 cells were found to express no measurable level of *PIWIL3* (Figure 4.18 C).

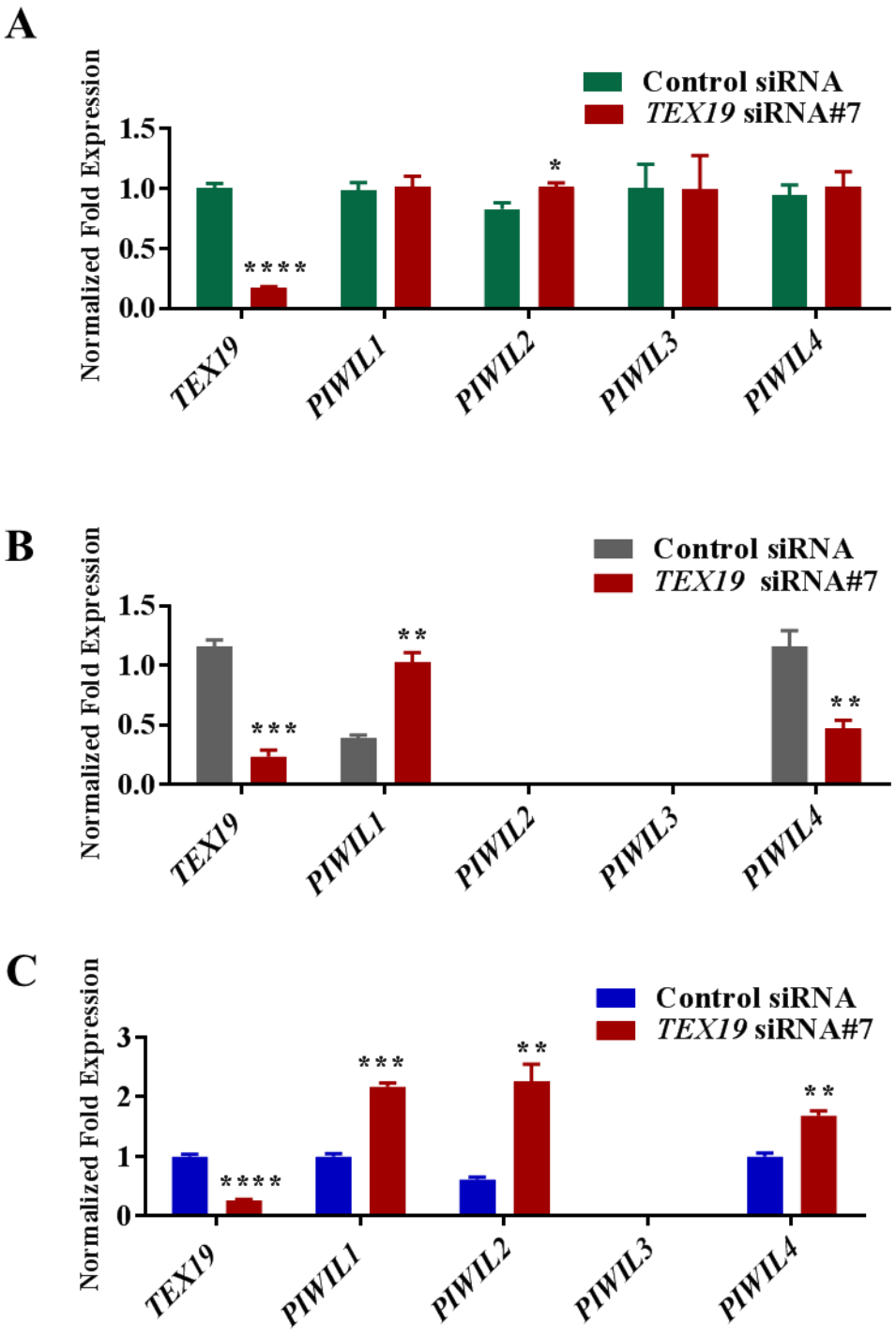

Figure 4-18 RT-qPCR analysis of mRNA levels of *PIWI* genes following *TEX19* transcript depletion.

Bar chart presenting the mRNA levels of the *PIWI* genes after transfection with *TEX19* siRNA#7. The results show significant *TEX19* transcript knockdown. (A) NTERA2 cells, (B) H460 cells, (C) SW480 cells. Asterisks above the bars indicate *p*-values (*: $p<0.05$; **: $p<0.01$***: $p<0.001$; ****: $p<0.0001$). *TUBA1C* and *GAPDH* were used for data normalisation. The error bars show the standard errors of the mean.

4.3 Discussion

4.3.1 *TEX19* depletion modulates proliferation and self-renewal

The function of CTA genes has been found to contribute to different biological features of cancers (Gjerstorff al., 2015; Fratta et al., 2011), such as metastasis and maintaining the proliferation of cancer cells (Greve et al., 2015; Por et al., 2010). In line with this, there is an urgent need to elucidate the role of CTA genes in enhancing proliferation and achieving cancer cells self-renewal. In this study, Depletion of *TEX19* in NTERA2, H460 and SW480 exhibited a significant reduction in the *TEX19* mRNA and TEX19 protein levels, signifying the efficiency of using *TEX19* siRNA. Western blotting analysis verified TEX19 knockdown, showing either a single or dual band. This observation was explained earlier in the previous chapter, which showed that it might be due to post-transcription protein modification.

The establishment of growth curves for cancer cells is effective when it comes to monitoring and evaluating the changes following biological treatment (Assanga & Lujan, 2013). Based on the cell count curves in this study, *TEX19* knockdown exhibited significant reductions in cell proliferation in the examined cancer stem-like cells and cancer cells, although these were observed at different levels. The analysis of the cell count curves suggested that the loss of *TEX19* inhibited proliferation to a greater extent in NTERA2 cells compared with SW480 and H460 cells. This could be explained by the variance in the doubling time of cancer cells, where the cell division of both SW480 and H460 was faster than that of NTERA2. Moreover, the screening of mRNA expression in the previous chapter showed that SW480 and H460 express *TEX19* to a greater extent than NTERA2 does. This could be interpreted as showing that the *TEX19* expression level is implicated in enhancing the proliferation rate.

ELDA assay is a widely used technique to compare groups of depleted cells using different serial dilutions and displaying the changes in the cell responses following biological treatment or molecule transfection (Groth, 1982; Hu & Smyth, 2009; Taswell, 1987). Applying ELDA assay to determine the effect of *TEX19* knockdown revealed a huge effect in all different dilutions (1 cell, 10 cells and 100 cells) in all tested cancer cells, suggesting the enrolment of TEX19 in cancer cell self-renewal. For the dilution of 1000 cells observed, a limited effect was observed; this could be due to

the number of seeded cells and the amount of siRNA treatment, as well as the rapidity of cell recovery. ELDA assay analysis exhibit similar results to those of cell count curves analysis, where *TEX19* depletion inhibited NTERA2 self-renewal more than the other cancer cells, suggesting that the high expression of *TEX19* could effectively enhance self-renewal. Correspondingly, the analysed results in the cell count curves and ELDA assay supported the idea that CTA genes provide a proliferative and self-renewal advantage for cancer cells. However, taking all these observations together, it can be inferred that TEX19 could act as oncogenic driver. More specifically, *TEX19* expression may be required to enhance self-renewal in cancer cells and cancer stem-like cells; its deactivation may participate in the discontinuity of cancer. Hence, *TEX19* could contribute as a promising therapeutic target in cancer treatment.

4.3.2 *TEX19* regulates gene expression

The RT-qPCR analysis of genes of interest verified the effects of *TEX19* depletion on most of those genes. This suggests a role of TEX19 in terms of controlling different genes' expressions either directly or indirectly and TEX19 may play as a transcriptional regulator. Re-evaluation of the set of selected differentially expressed genes was carried out to determine whether the changes in expression were cancer-cell specific. Using different siRNA, the gene expressions obtained were not fully consistent with those obtained from RNA sequencing data. This could be explained by suggesting that different siRNAs yield different levels of gene knockdown, and thus, they may have different consequences. Moreover, no common gene exhibited consistent expression in the three tested cancer cells, raising the question of why *TEX19* depletion did not yield similar expression changes in the three cancer cell lines. This could be explained in terms of the heterogeneity and different origins of cancer cells, since SW480 cells are derived from colon adenocarcinoma, H460 cells are derived from lung carcinoma and NTERA2 cells are derived from embryonal carcinoma. Remarkably, genes like *GAR1*, *GPR137B*, *SEPT12*, *LY96* and *PIWIL1* were observed to have consistent expression in two cancer cells, and these expression levels matched the RNA sequencing results, indicating a potential function of TEX19 in controlling the expression of these genes.

The *GAR1* gene encodes H/ACA ribonucleoprotein complex subunit 1 protein. This protein is essential for biogenesis of ribosomal ribonucleic acid (rRNA), and it is required for telomere maintenance (Dragon et al., 2000; Kiss et al., 2010; Wang & Meier, 2004). Moreover, mutation in *GAR1* is associated with diseases, including dyskeratosis congenita (Mason & Bessler, 2011) and aplastic anaemia (Orkin et al., 2014). The results showed that *TEX19* depletion influenced the mRNA level of *GAR1*, where it was downregulated in H460 and SW480; this was similar to the findings in the RNA sequence data. This observation indicates that *TEX19* mRNA reduction alters *GAR1* transcript level, which may disrupt its function. *GPR137B* is another influenced gene found with reduced mRNA level in NTERA2, H460 and RNA sequence data. Remarkably, silencing *GPR137B* using non-interfering siRNA inhibited the proliferation of pancreatic cancer cells (Cui et al., 2015), malignant glioma cells (Zong et al., 2014) and colon cancer cells (Zhang et al., 2014). Taking these findings together, it can be suggested that reducing *TEX19* level may be used a considerable tool to supress *GPR137B* expression. Moreover, *SEPT12* is a CTA gene (Feichtinger et al., 2012) required for spermatogenesis (Lai et al., 2016), and its loss is implicated in male infertility (Kuo et al., 2012b). The results showed downregulation of *SEPT12* mRNA levels in NTERA2, H460 and SW480 RNA sequence data, suggesting that this gene requires TEX19 to control its expression. A reduction in *TEX19* mRNA upregulated *LY96* in SW480, H460 and RNA sequence data. *LY96* is also known as the *MD-2* gene. It encodes lymphocyte antigen 96 protein, which interacts with toll-like receptor 4 (TLR4), thereby contributing to the innate immune system activation. *LY96* has been found to be linked with distant metastasis in colorectal carcinoma tissue and lymph node metastasis (Ohnishi et al., 2003; Xu et al., 2011). However, *TEX19* modulated LY96 expression, and further work is required to understand whether there is interaction between them.

The *PIWI* genes (*PIWIL1-PIWIL4*) are involved in the maintenance of spermatogenesis and play a role in the meiosis of germline stem cells. In addition, the genetic variation in these genes is anticipated to harm normal spermatogenesis (Gu et al., 2010; Robles et al., 2016). The results showed negative expression of *PIWIL3* in H460 and SW480; furthermore, *PIWIL2* was found not expressed in H460. This may be due to the heterogeneity in cancer cell lines. Remarkably, all *PIWI* genes were found to be expressed in embryonal carcinoma (NTERA2); this implies their predominant

expression in cells exhibiting developmental properties similar to those of the early embryo. *TEX19* knockdown revealed an influence in controlling *PIWIL1*, *PIWIL2* and *PIWIL4* expression in different cancer cells. To synthesise these findings, reduction of *TEX19* mRNA influenced the *PIWI* gene transcripts at different levels in cancer stem-like cells and cancer cells, suggesting a role of TEX19 in maintaining the PIWI pathway.

To summarise the results presented in this chapter, *TEX19* is a gene that can act as an oncogenic drive, providing a proliferative and self-renewal asset for human cancer stem-like cells and cancer cells. More importantly, *TEX19* expression has been suggested to be required for controlling the expression of several genes in distinct human cancer cells. Further research should be conducted to determine whether *TEX19* acts as an oncogene and a transcription factor gene.

Chapter 5

The role of *TEX19* in human embryonic stem cells (hESCs)

5. The role of *TEX19* in human embryonic stem cells (hESCs)

5.1 Introduction

Studying human embryonic stem cells (hESCs) *in vitro* is a useful tool for exploring early human development and identifying the source of cells that contribute to the development of regenerative medicine (Gaskell et al., 2016; Keller, 2005; Shufaro & Reubinoff, 2004). hESCs are unique pluripotent cells that are derived from the inner cell mass of blastocysts that form multicellular organisms. hESCs have intrinsic features, such as their ability to self-renew and differentiate into a wide range of cell types (Gaskell et al., 2016; Keller & Gadue, 2016). Due to this comprehensive differentiation, hESCs are potential prospects as useful sources in tissue engineering and transplantation (Langer & Vacanti, 2016; Shirai & Mandai, 2016). Three major transcription factor genes, *OCT4*, *NANOG* and *SOX2*, are essential and responsible for the maintaining pluripotency in hESCs (Boyer et al., 2005). In addition, *OCT4*, *NANOG* and *SOX2* are molecular stem cell markers that are preferentially express in hESCs (Abeyta et al., 2004; Sato et al., 2003), and the reduction in their expression results in them losing their pluripotency and stemness features (Singh et al., 2016).

Expression of *OCT4* and *NANOG* are frequently used as markers for indicating undifferentiated hESCs (Lai et al., 2015). The depletion of *OCT4 in vitro* has led to dramatic differentiation in hESCs proving that it is essential for providing pluripotency for hESCs (Zafarana et al., 2009). Likewise, downregulation of *NANOG* has resulted in reduction in the expression of *OCT4* and hESCs differentiation, thereby elucidating that both *OCT4* and *NANOG* are fundamentally required to prevent hESCs from losing their stemness properties (Hyslop et al., 2005). *SOX2* is another marker required for pluripotency, and its expression has been most frequently linked with stem cells and precursor cells. Depletion of *SOX2* has led to morphological changes in hESCs, indicating the differentiated state of those cells. Moreover, *SOX2* knockdown has been found to significantly downregulate the expression of *OCT4* and *NANOG*, thereby indicating that *SOX2* plays a critical role in maintaining pluripotency and controlling the expression for other stem cell markers (Fong et al., 2008). In addition to their crucial

function for maintaining pluripotency, *OCT4*, *NANOG* and *SOX2* are also implicated in regulating several transcription factor genes, such as *PAX6*, *HOXB1* and *MYF5*, which are required for the differentiation of hESCs, (Boyer et al., 2005). In line with stem cell markers, hESCs express a number of cell surface markers, including TRA-1-8, TRA-1-60, SSEA3 and SSEA4, but not SSEA1. These surface markers are also known as surface antigen phenotypes; they play a key role in the characterisation of hESCs and they are used to define pluripotent and differentiated cell types (Draper et al., 2002; Wright & Andrews, 2009).

The expression profile of CTA genes has been suggested to be linked to normal stem cell biology. During the development of embryo, epiblasts generate primordial germ cells have some activated CTA genes, and these genes are later inactivated as germ cells that undergo differentiation (Costa et al., 2007). Nevertheless, this restricted expression suggests that these genes play an important role during early embryogenesis (Costa et al., 2007; Cronwright et al., 2005; Ghafouri-Fard, 2015). Moreover, *SSX* (Sarcoma, Synovial, X-Chromosome) is a CTA gene found with downregulated expression after the differentiation of mesenchymal stem cells, thereby suggesting its expression as a stem cell marker (Cronwright et al., 2005). However, the function of CTA genes in stem cells has not been fully explored, and the role of these genes in stem cell biology is being actively investigated (Akers et al., 2010).

In Chapter 3, *TEX19* was reported as a CTA gene and it was found to be expressed in cancer stem-like cells, hESCs and iPSCs, but not in fibroblasts, thereby suggesting that it plays a role in stem cells. In mESCs, *Tex19.1* has been reported as a marker for pluripotency as its expression has been found to be associated with *Oct4* expression upon mESCs differentiation (Kuntz et al., 2008). No previous study has elucidated the function of TEX19 in hESCs. Analogous to this, this chapter aims to further investigate the presence of *TEX19* in different human embryonic stem (hES) cell lines. Moreover, this work aims to determine whether or not TEX19 is linked to the normal biology of hESCs, and if it can act as a stem cell marker.

5.2 Results

5.2.1 Analysis of *TEX19* expression in human embryonic stem cell lines

TEX19 expression was investigated in different human embryonic stem (hES) cell lines via RT-PCR. These hES cell lines include SHEF6, H9 and H7S14, which are normal karyotypes, and H7S6, which has an abnormal karyotype. H7S6 has the addition of a derivative of Chromosome 1, addition of 17q and a duplication of 20q CNV (20q11.21). cDNA from these hES cell lines was synthesised from the total RNA, and *βACT* RT-PCR was carried out to assess the quality of the cDNA. RT-PCR analysis revealed a detectable expression signal of *TEX19* in all of the examined hES cell lines (Figure 5.1). The PCR products for both *TEX19* and *βACT* migrated to the expected sizes (344 bp and 553 bp, respectively).

Based on the analysed hES cell line results obtained via RT-PCR, an investigation was carried out using RT-qPCR for further confirmation. In line with this, the expression of stem cell marker genes *OCT4*, *NANAOG* and *SOX2* was also checked to ensure that the hES cell lines were expressing the pluripotency markers. The RT-qPCR analysis results showed that SHEF6, H9, H7S14 and H7S6 all express a significant level of *TEX19* (Figure 5.2 A). H7S6 expressed *TEX19* more than the other hES cell lines. Correspondingly, all of the tested hES cell lines expressed the essential pluripotent stem cell markers *OCT4*, *NANOG* and *SOX2* (Figure 5.2 B, C, D).

In parallel with the molecular markers, the surface markers for the hES cell lines were checked in SHEF6. This step was done to monitor any changes that might have occurred, because the SHEF6 where cultured in the McFarlane lab and then transferred to the Andrews lab for the experiments. SSEA3, SSEA4 and TRA-1-60 are hESC surface markers; they were examined using flow cytometry, and the results showed positive detection (Figure 5.3).

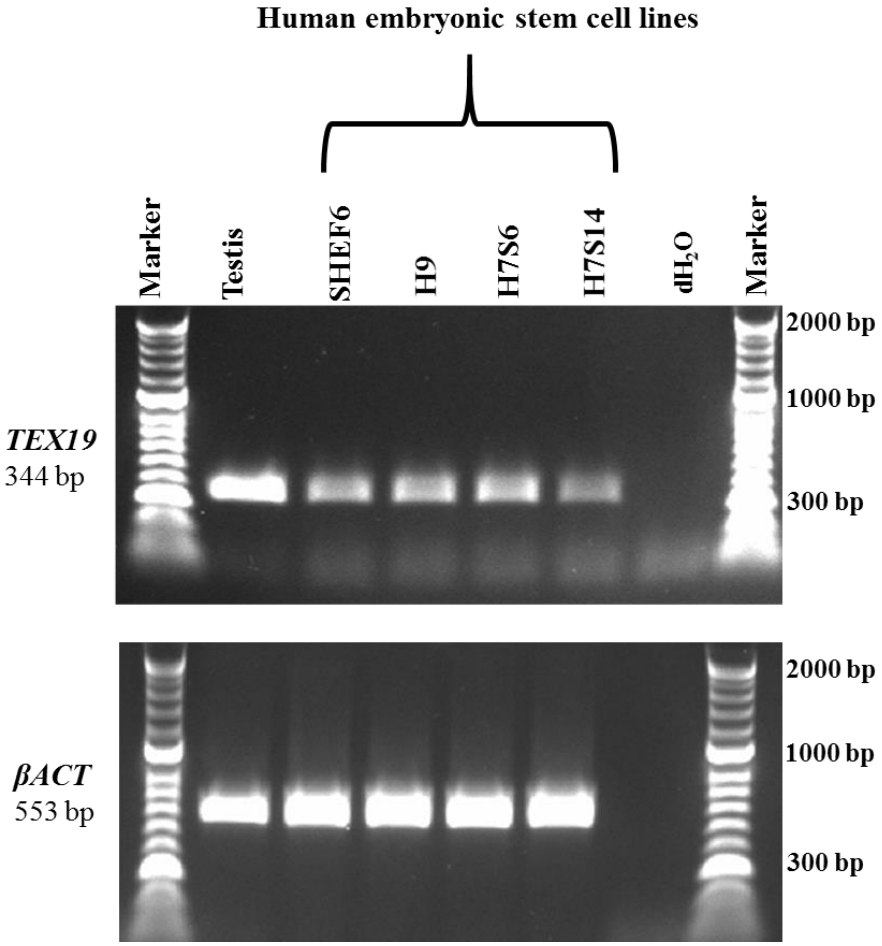

Figure 5-1 RT-PCR analysis of *TEX19* gene expression in hES cell lines.
Agarose gels present the *TEX19* expression in distinct hES cell lines. The expression profile of the *βACT* gene was used as a positive control for the synthesised cDNA. Testis tissue was used as a positive control. dH_2O was used as negative control. The PCR products were detected with the expected sizes (presented on the left).

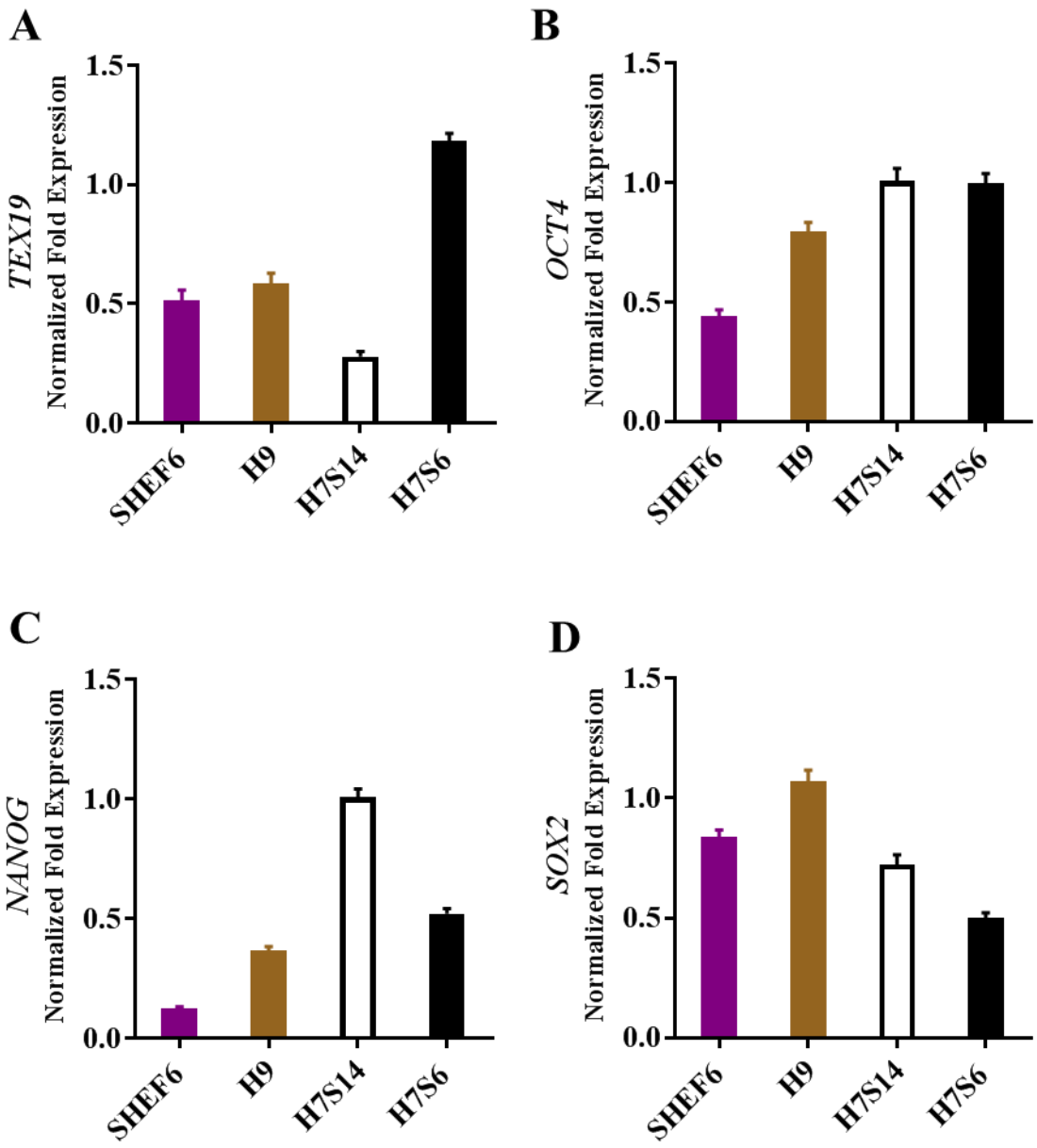

Figure 5-2 RT-qPCR analysis of the *TEX19* gene expression in distinct hES cell lines.
(A) Bar chart presenting the expression levels of the *TEX19* gene in hES cell lines. (B) Bar chart showing the expression levels of the *OCT4* gene in hESC. (C) Bar chart demonstrating the expression levels of the *NANOG* gene in the hES cell lines. (D) Bar chart showing the expression levels of the *SOX2* gene in the hES cell lines. *OCT4*, *NANOG* and *SOX2* genes were used as molecular stem cell markers. The obtained data were normalised using a combination of two endogenous reference genes, *YWHAZ* and *Actin*. The error bars show the standard errors of the mean.

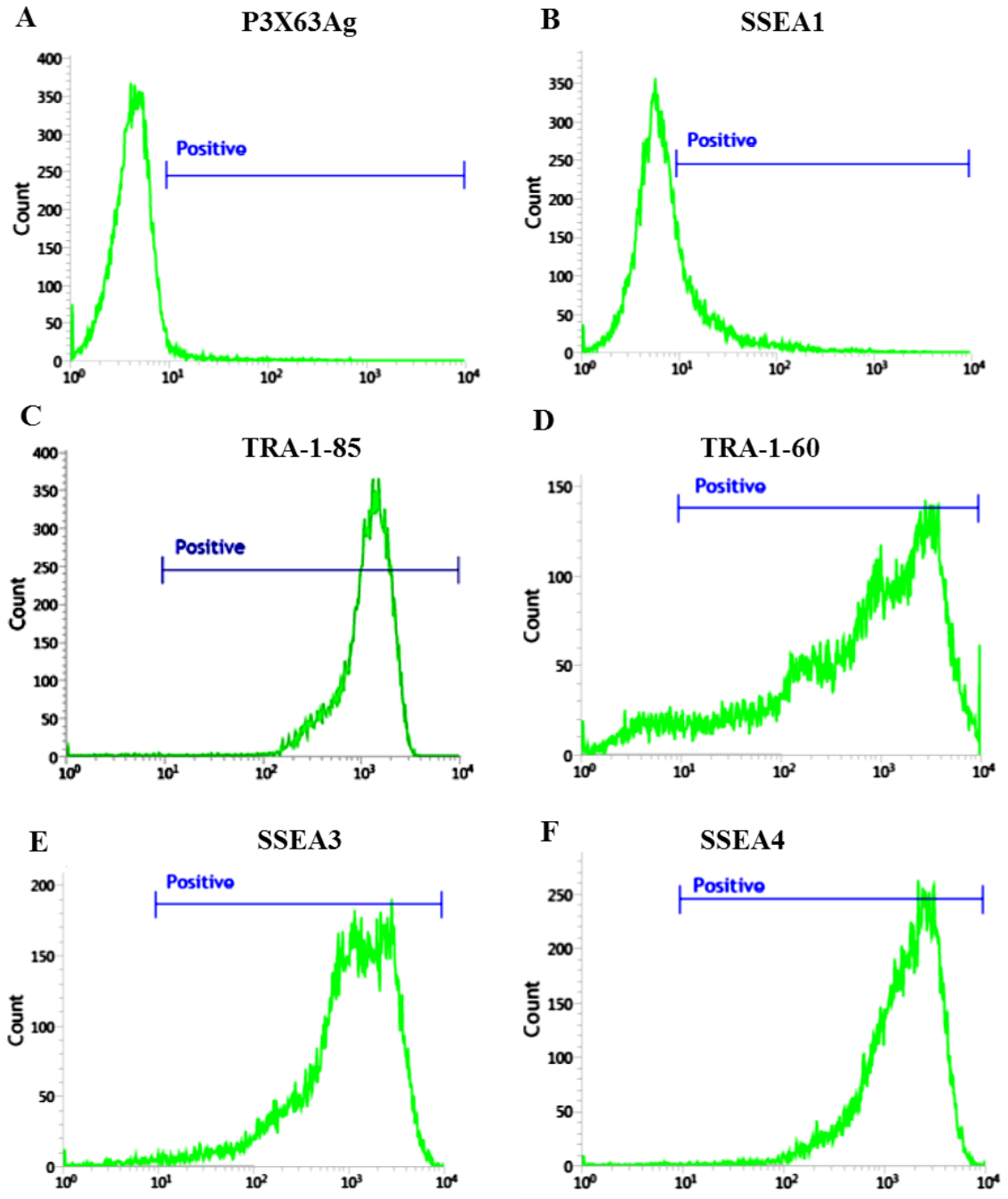

Figure 5-3 FACS analysis of cell surface makers in SHEF6.
Flow cytometric profile of surface antigen phenotypes in the untreated hES cell line (SHEF6). (A) P3X63AG indicates the negative gate, and it was used as the negative control. (B) SSEA1 was used as the differentiation marker. (C) TRA1-85 was used as a positive control for human cells. (D) TRA1-60 is a hESC surface marker, and it was used as the positive control. (E, F) SSEA3 and SSE4 are hESC surface markers. Y is the relative cell count. X is the fluorescent intensity.

5.2.2 Depletion of *TEX19* in human embryonic stem cell lines

In order to explore whether TEX19 plays a function in hESCs, the depletion of *TEX19* was carried out in different hES cell lines: SHEF6, H9, H7S14 and H7S6. *TEX19* siRNA#7 was used to perform all the experiments. Negative siRNA was used as a control to assess *TEX19* depletion. The transfection of cells with *TEX19* siRNA#7 was carried out for four days along with the control siRNA (negative siRNA). Following completion of the treatment, the cDNA was generated from total RNA, and *TEX19* mRNA was evaluated via RT-qPCR to assess the depletion level. The measurement of *TEX19* mRNA showed significant depletion in comparison to the control in all the hES cell lines except for H7S14. A significant depletion was observed in the following hES cell lines: SHEF6 ($p<0.01$), as shown in Figure 5.4.A, H9 ($p<0.01$), as shown in Figure 5.4.B and H7S6 ($p<0.0001$), as shown in Figure 5.4.D. The *P* value was not statistically significant in H7S14 (Figure 5.4.C).

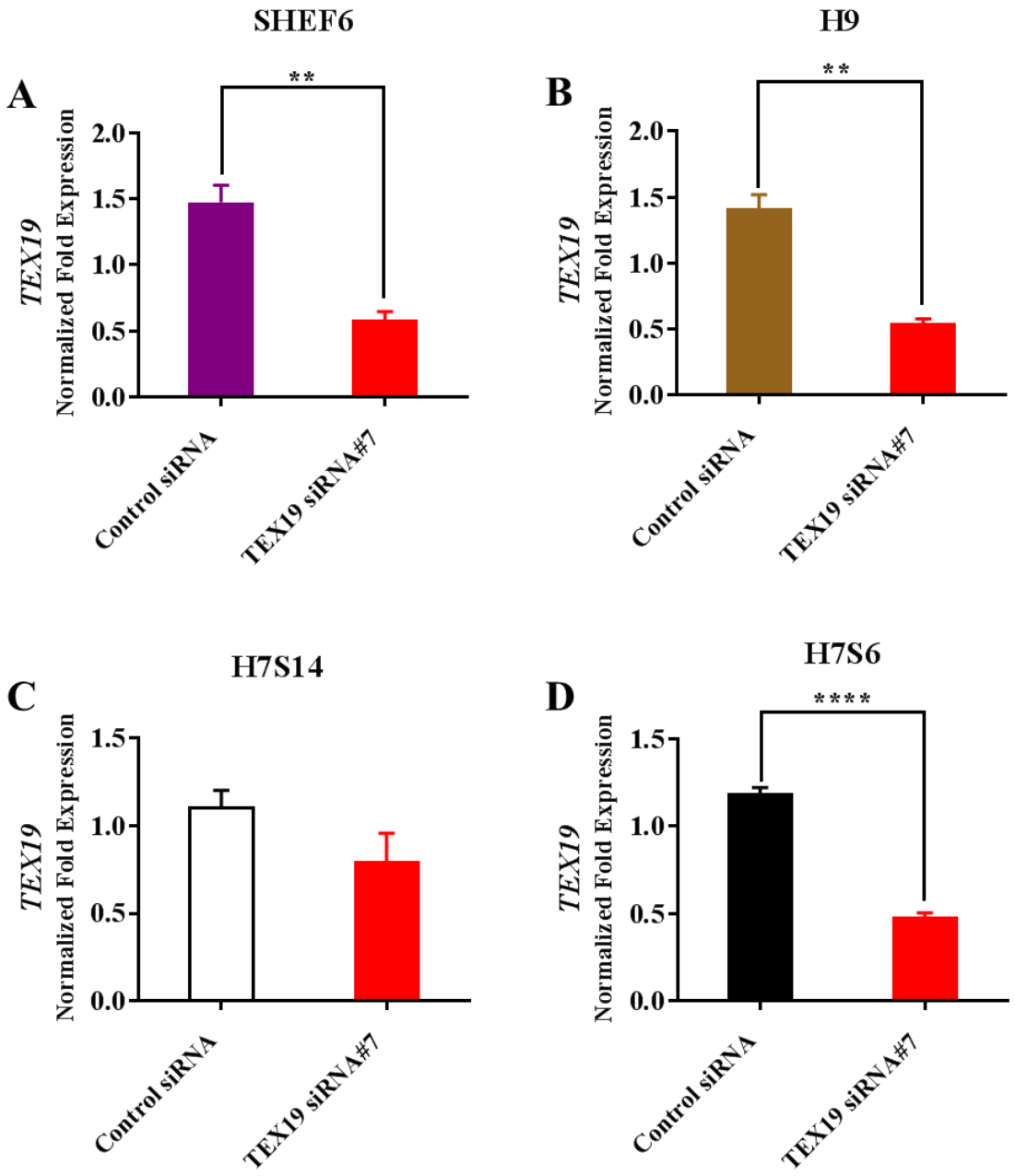

Figure 5-4 Depletion of *TEX19* transcript in the hES cell lines.
Analysis of *TEX19* mRNA levels via RT-qPCR following depletion in the different hES cell lines. *TEX19* siRNA#7 was used for transfection. (A) SHEF6; (B) H9; (C) H7S14; (D) H7S6. Bar charts A, B and D demonstrate a significant reduction in *TEX19* mRNA compared to the control. Asterisks above the bar indicate the *p*-value (**: $p<0.01$;****: $p<0.0001$). *YWHAZ* and *Actin* were used for data normalisation. The error bars show the standard errors of the mean.

5.2.3 The influence of *TEX19* depletion on human embryonic stem cell markers

In order to explore whether *TEX19* expression is correlated with pluripotent markers or if it has a potential function in hESCs, the mRNA of the stem cell markers was evaluated following *TEX19* depletion. Reducing the *TEX19* mRNA level was found to differentially alter the levels of *OCT4* and *NANOG* mRNA. In hES cell line SHEF6, the reduction of *TEX19* mRNA led to significant upregulation in *NANOG* ($p<0.01$), and no significant changes were observed for the rest of the genes of interest (Figure 5.5). In H9, the reduction in the *TEX19* level significantly reduced *OCT4* mRNA ($p<0.05$) and *NANOG* mRNA was substantially reduced ($p<0.001$); however, no effect was observed in the level of *SOX2* mRNA (Figure 5.6). In H7S6, *TEX19* knockdown downregulated *NANOG* mRNA ($p<0.01$), but no effect was detected for *OCT4* and *SOX2* mRNAs (Figure 5.8). According to the *P* value and the statistical significance in H7S14, the difference between the control and *TEX19* siRNA was not statistically significant. Remarkably, this small depletion has significantly downregulated the levels of *NANOG* mRNA ($p<0.001$) (see Figure 5.7). More importantly, *TEX19* depletion has influenced the levels of *NANOG* mRNA in all the hES cell lines examined and the *OCT4* mRNA in an individual hES cell line (H9).

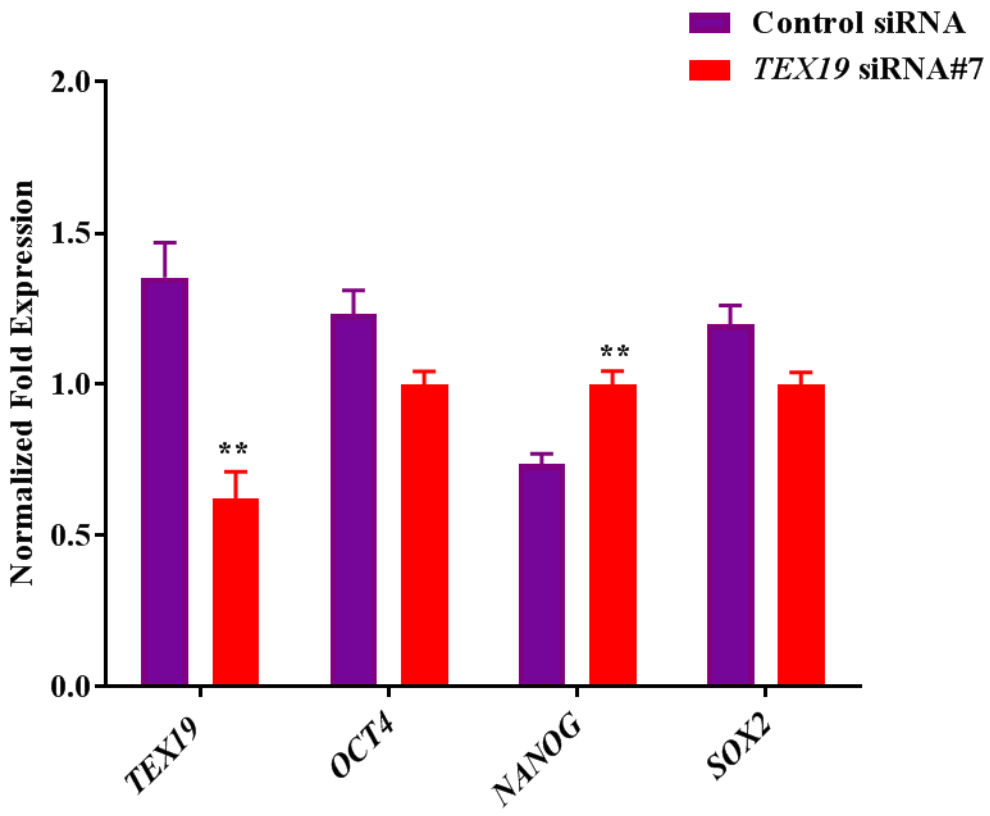

Figure 5-5 RT-qPCR analysis of stem cell marker gene mRNAs following *TEX19* mRNA depletion in SHEF6.
SHEF6 was transfected with *TEX19* siRNA#7 and the results were compared to the control siRNA. The bar charts demonstrate significant *TEX19* transcript depletion and upregulated mRNA for *NANOG*. Asterisks above the bar indicate the *p*-value (**: $p<0.01$). *YWHAZ* and *Actin* were used for data normalisation. The error bars show the standard errors of the mean.

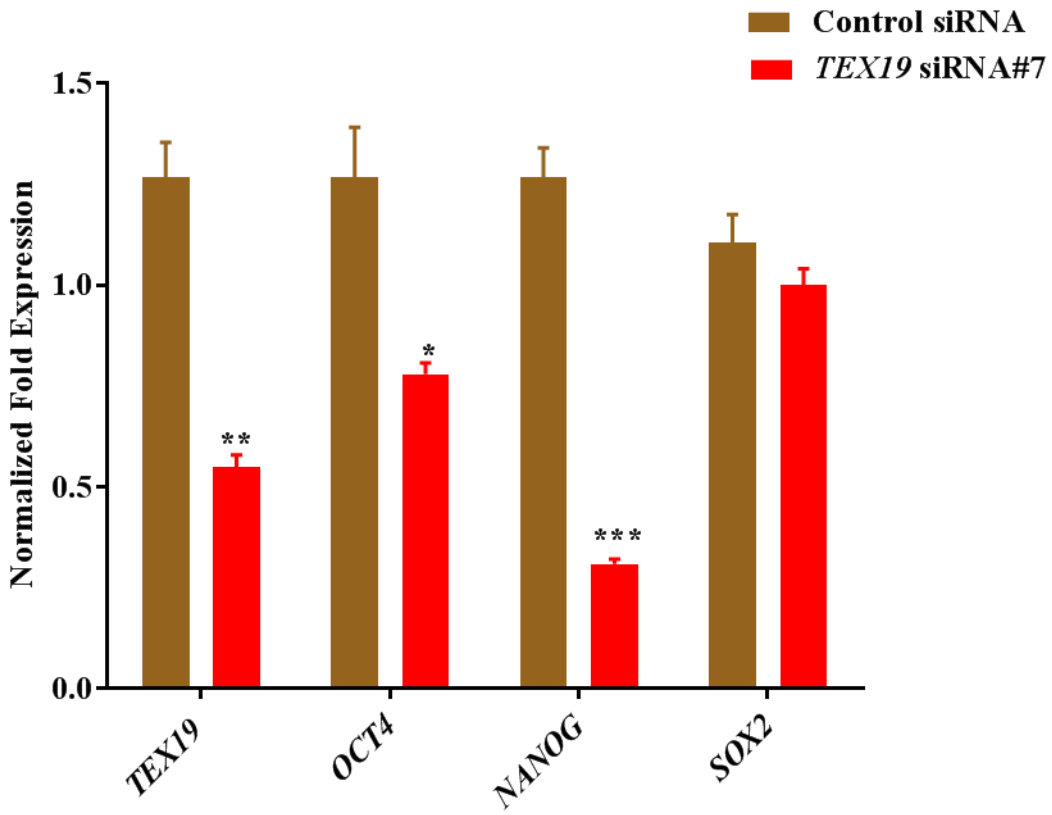

Figure 5-6 RT-qPCR analysis of stem cell marker gene mRNAs following *TEX19* mRNA depletion in H9.
H9 was transfected with *TEX19* siRNA#7 and the results were compared to the control siRNA. The bar charts demonstrate significant *TEX19* transcript depletion and altered mRNAs for the genes of interest. Asterisks above the bar indicate the *p*-value (*: $p<0.05$; **: $p<0.01$;***: $p<0.001$). *YWHAZ* and *Actin* were used for data normalisation. The error bars show the standard errors of the mean.

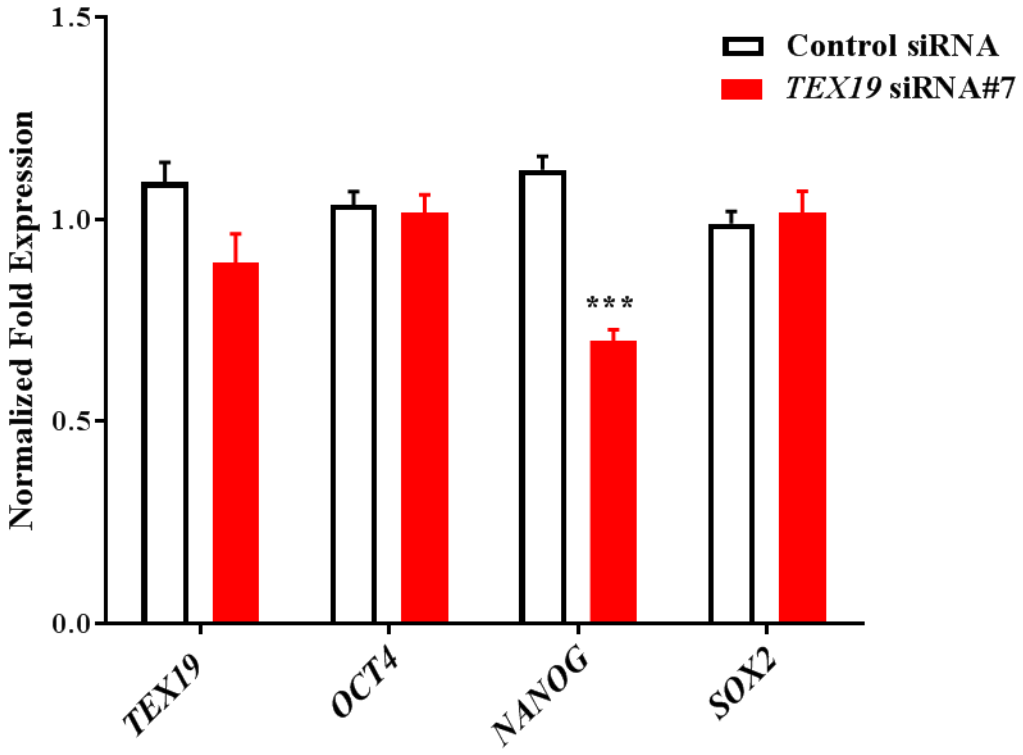

Figure 5-7 RT-qPCR analysis of stem cell marker gene mRNAs following *TEX19* mRNA depletion in H7S14.
H7S14 was transfected with *TEX19* siRNA#7 and the results were compared to the control siRNA. The bar charts demonstrate the mRNA levels of *TEX19* and the genes of interest. Asterisks above the bar indicate the *p*-value (***: $p<0.001$). *YWHAZ* and *Actin* were used for data normalisation. The error bars show the standard errors of the mean.

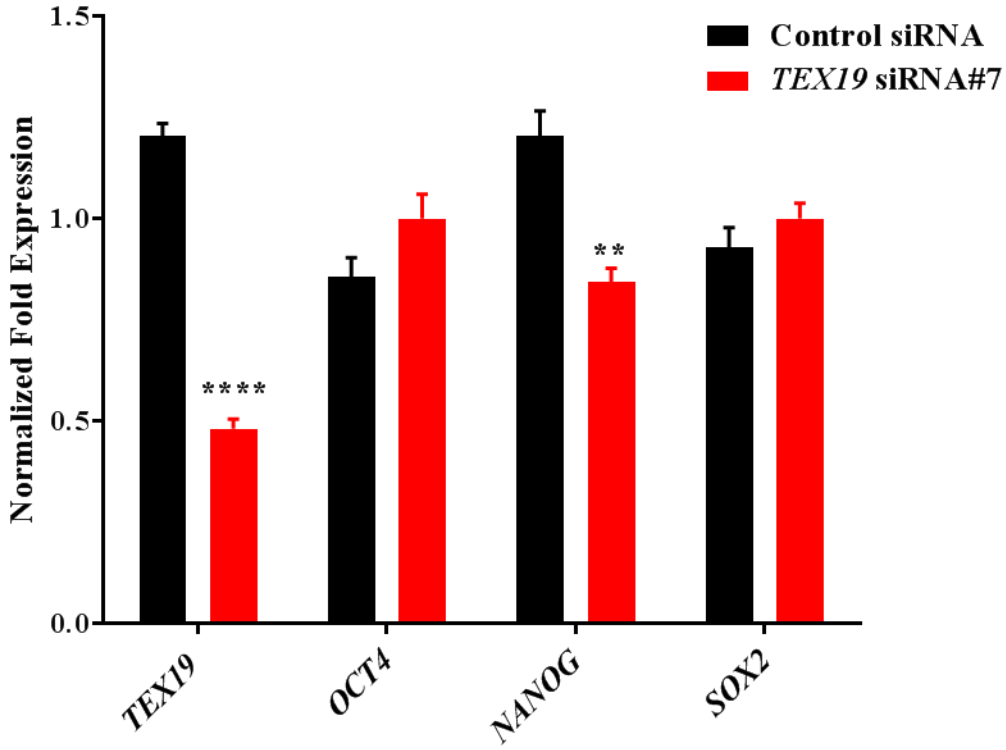

Figure 5-8 RT-qPCR analysis of stem cell marker gene mRNAs following *TEX19* mRNA depletion in H7S6.
H7S6 was transfected with *TEX19* siRNA#7 and the results were compared to the control siRNA. The bar charts demonstrate significant *TEX19* transcript depletion and downregulated mRNA for *NANOG*. Asterisks above the bar indicate the *p*-value (**: $p<0.01$;****: $p<0.0001$). *YWHAZ* and *Actin* were used for data normalisation. The error bars show the standard errors of the mean.

5.2.4 The influence of *TEX19* depletion on *PIWI* genes in hES cell lines

In Chapter 4, *TEX19* expression was found to be controlling *PIWI* gene transcripts in cancer cells and cancer stem-like cells. Based on this, the influence of the *TEX19* knockdown on *PIWI* gene transcripts was investigated in hES cell lines. At the beginning, the transcript levels of *PIWIL1*, *PIWIL2*, *PIWIL3* and *PIWIL4* were evaluated via RT-qPCR in SHEF6, H9, H7S14 and H7S6. The hES cell lines were found to negatively express *PIWIL1* and *PIWIL3* (not shown). In contrast, both *PIWIL2* and *PIWIL4* were detected with significant transcripts in SHEF6, H9, H7S14 and H7S6 (Figure 5.9A, B). *PIWIL2* and *PIWIL4* were further investigated.

The reduction of the *TEX19* mRNA levels in hES cell lines was found to alter the levels of *PIWIL2* and *PIWIL4* mRNAs in H9, H7S14 and H7S6. However, no significant change was observed for *PIWIL2* and *PIWIL4* mRNAs in SHEF6 (Figure 5.10.A). In H9, *PIWIL2* and *PIWIL4* mRNAs were downregulated after *TEX19* knockdown, and a significant change ($p<0.05$; $p<0.01$, respectively) was observed (Figure 5.10.B). In H7S14, the limited depletion of knockdown was found to reduce *PIWIL2* transcripts ($p<0.05$), and no significant change was detected for *PIWIL4* transcripts (Figure 5.10.C). *TEX19* mRNA depletion was found to inhibit the *PIWIL4* transcript levels in H7S6 ($p<0.01$), while no effect was observed for *PIWIL2* (Figure 5.10.D).

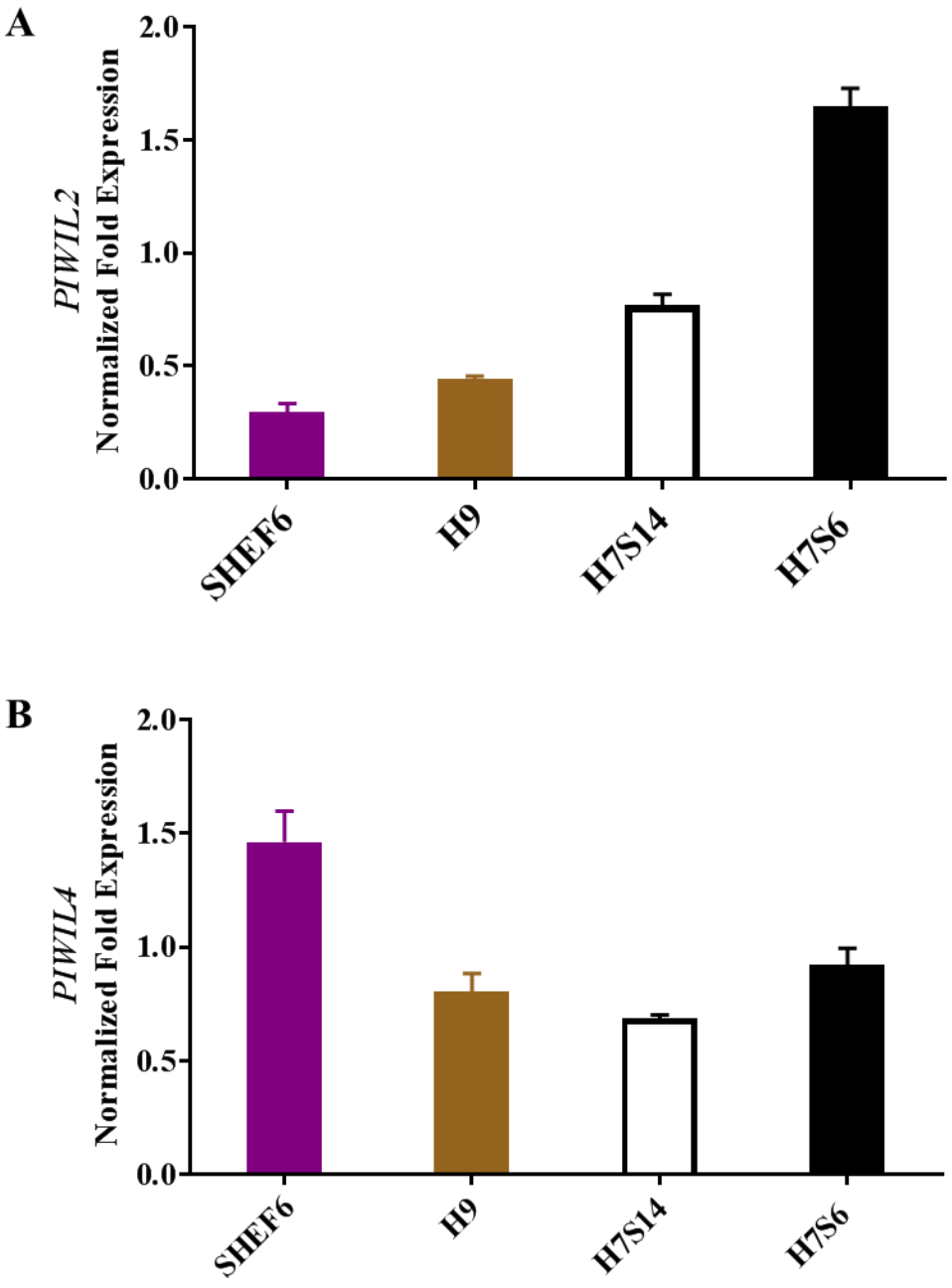

Figure 5-9 RT-qPCR analysis of the *PIWI* genes expression in distinct hES cell lines. (A) Bar chart presenting the expression levels of the *PIWIL2* gene in the hES cell lines. (B) Bar chart showing the expression level of the *PIWIL4* gene in the hES cell lines. The obtained data were normalised using a combination of two endogenous reference genes, *YWHAZ* and *Actin*. The error bars show the standard errors of the mean.

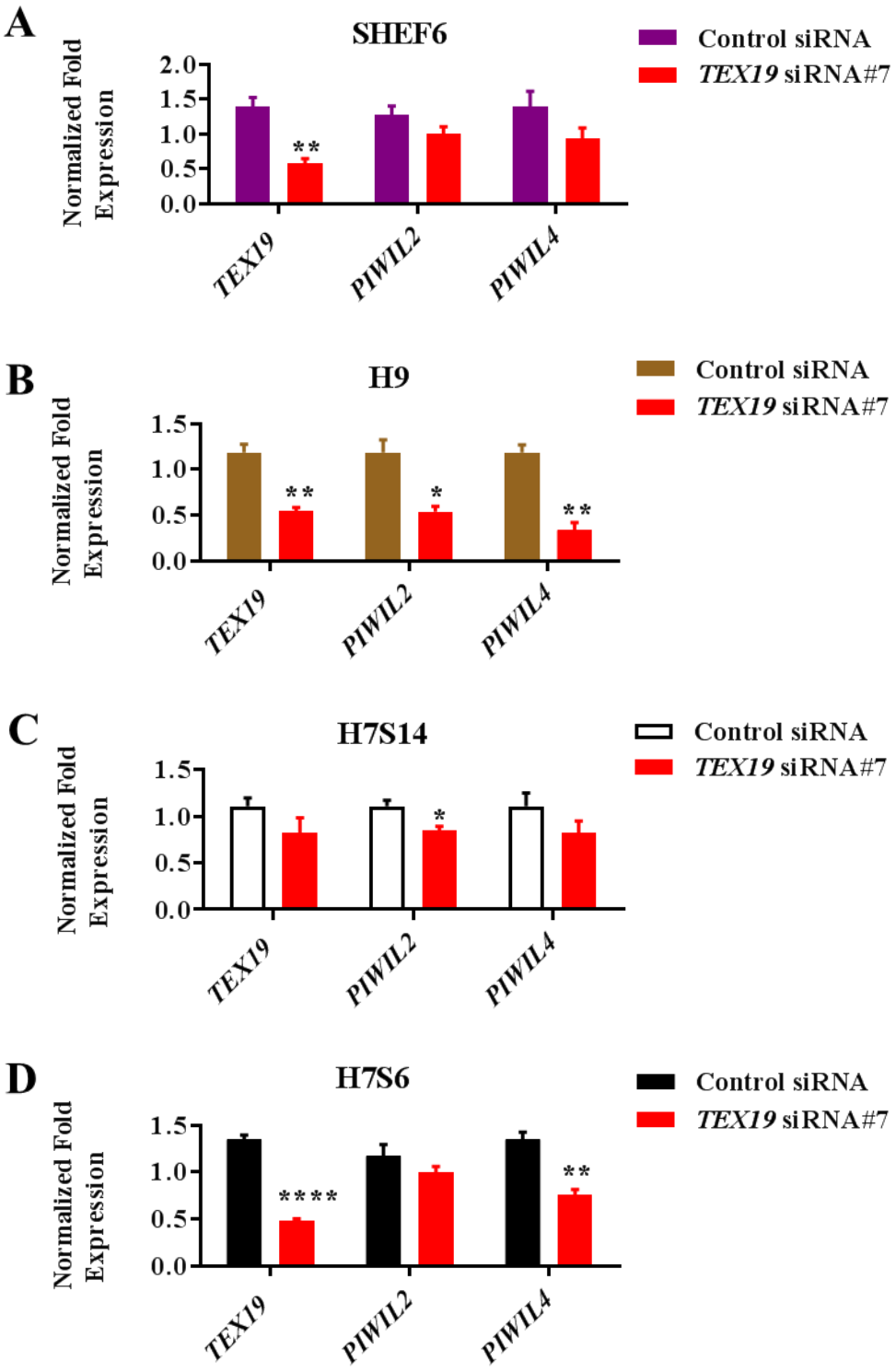

Figure 5-10 RT-qPCR analysis of *PIWI* gene transcripts following *TEX19* mRNA depletion in hES cell lines.

Analysis of *PIWIL2* and *PIWIL4* mRNA levels via RT-qPCR following *TEX19* transcript depletion in different hES cell lines. (A) SHEF6; (B) H9; (C) H7S14; (D) H7S6. Bar charts demonstrate the mRNA levels of *TEX19* and the genes of interest. Asterisks above the bar indicate the *p*-value (*: $p<0.05$;**: $p<0.01$;****: $p<0.0001$). *YWHAZ* and *Actin* were used for data normalisation. The error bars show the standard errors of the mean.

5.2.5 The behaviour of *TEX19* upon differentiation of human embryonic stem cells

In the preliminary results presented in Chapter 3, a significant decrease was observed in the *TEX19* mRNA level when NTERA2 (stem cell model) underwent differentiation. Based on this finding, the behaviour of *TEX19* was monitored in hESCs based on the differentiation time to conclude whether or not it behaved like a stem cell marker. For this purpose, the hES cell lines, SHEF6, H9, H7S14 and H7S6, were differentiated using an inducer agent, retinoic acid, which direct the hESCs to their neuronal lineage. Moreover, the differentiation process was carried out for different times for each hES cell line: day 1, day 3, day 7 and day 10. By day 10, the hESCs showed strong differentiation and morphological changes (see example image in Figure 5.11). Untreated cells were used as a positive control, *OCT4* was used as a stem cell marker and *PAX6* was used as a neuronal marker. The transcript levels of *OCT4*, *PAX6* and *TEX19* were analysed according to the differentiation time using RT-qPCR.

In SHEF6, the analysis of the *OCT4* levels showed a significant decline in *OCT4* mRNA from day 1, and the *OCT4* mRNA levels began to be unmeasurable at day 7 (Figure 5.12 A). This indicates that the SHEF6 cells became differentiated. On day 1, day 3, day 7 and day 10, a significant reduction was detected in *OCT4* transcripts in comparison to the control ($p<0.05$, $p<0.001$, $p<0.001$ and $p<0.001$, respectively). Appearance of *PAX6* mRNA began at day 3, indicating the start of direction to the neuronal linage (Figure 5.12 B). In addition, the analysis of the *TEX19* mRNA levels showed significant reductions on day 3 and day 7 ($p<0.05$; $p<0.05$, respectively). The *TEX19* mRNA level was observed to increase on day 10 ($p<0.05$) (Figure 5.12 C).

The behaviour of H9 was found to be very similar to the behaviour observed in SHEF6. The analysis of the *OCT4* mRNA levels showed a significant decline from day 1, and the *OCT4* mRNA could not be detected from day 7 (Figure 5.13 A). This indicates differentiation of the H9 cells. On day 1, day 3, day 7 and day 10, a significant reduction in *OCT4* mRNA was detected in comparison to the control ($p<0.05$, $p<0.001$, $p<0.001$ and $p<0.001$, respectively). *PAX6* mRNA started to be apparent on day 1, indicating the direction of cells to neuronal linage (Figure 5.13 B). In addition, analysis of the

TEX19 mRNA levels showed significant reductions on day 3 and day 7 ($p<0.05$; $p<0.01$, respectively), increasing again on day 10 ($p<0.05$) (Figure 5.13 C).

The H7S14 analysis, showed a significant decline in *OCT4* mRNA from day 1, and on day 7 was undetectable (Figure 5.14 A). This indicates that the H7S14 cells became differentiated. On day 1, day 3, day 7 and day 10, a significant reduction in *OCT4* mRNA was detected in comparison to the control ($p<0.05$, $p<0.0001$, $p<0.0001$ and $p<0.0001$, respectively). *PAX6* mRNA was apparent on day 1, indicating the start of direction to neuronal linage (Figure 5.14 B). In addition, no significant changes in *TEX19* transcript levels were observed on day 3, day 7 and day 10. However, the *TEX19* mRNA level increased on day 1 ($p<0.05$) (Figure 5.14 C).

In H7S6, the *OCT4* mRNA could not be detected at day 7 and beyond (Figure 5.15 A). This indicates that the H7S6 cells underwent differentiation. On day 7 and day 10, a significant reduction in *OCT4* mRNA was detected in comparison to the control ($p<0.001$; $p<0.001$, respectively). *PAX6* mRNA became apparent on day 7, indicating the beginning of direction to neuronal linage (Figure 5.15 B). In addition, significant reductions in the *TEX19* mRNA levels were observed on day 10 ($p<0.01$) (Figure 5.15 C).

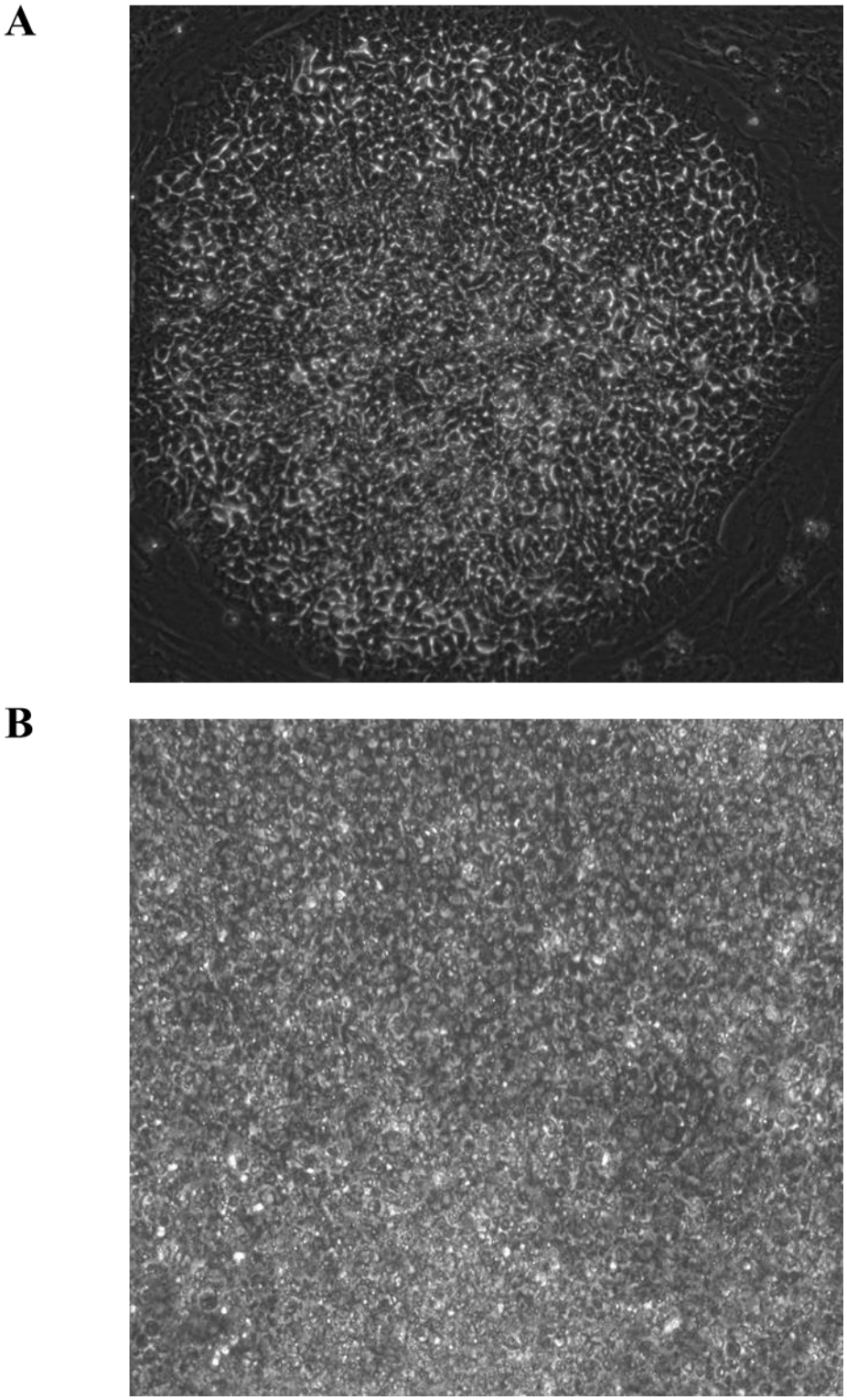

Figure 5-11 Human embryonic stem cell morphology.
(A) Light microscopy image of the normal morphology of the hES cell line (SHEF6). (B) An image of the hES cell line (SHEF6) treated with a retinoic acid inducer for 10 days showing strong differentiation.

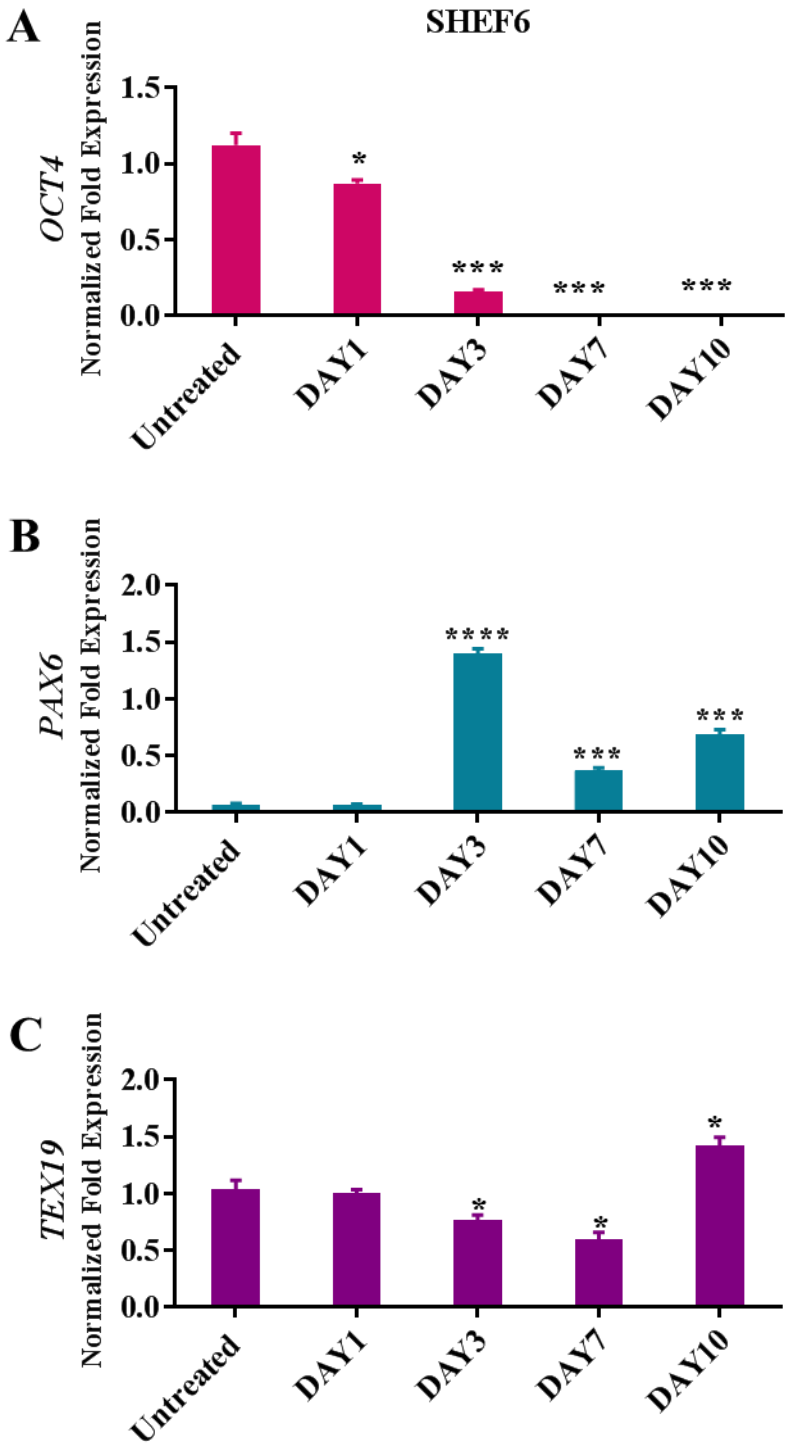

Figure 5-12 RT-qPCR analysis of the *TEX19* mRNA levels in SHEF6 treated with retinoic acid.

(A) Bar chart showing the mRNA levels of the *OCT4* gene in SHEF6 treated with retinoic acid on the selected days. (B) Bar chart showing the mRNA levels of *PAX6*. *OCT4* was used as a stem cell marker and *PAX6* as a neuronal marker. (C) Bar chart elucidating the mRNA levels of the *TEX19* gene upon differentiation. *YWHAZ* and *Actin* were used for data normalisation. The error bars show the standard errors of the mean. Asterisks above the bars indicate the *p*-values (*: $p<0.05$; ***: $p<0.001$; ****: $p<0.0001$).

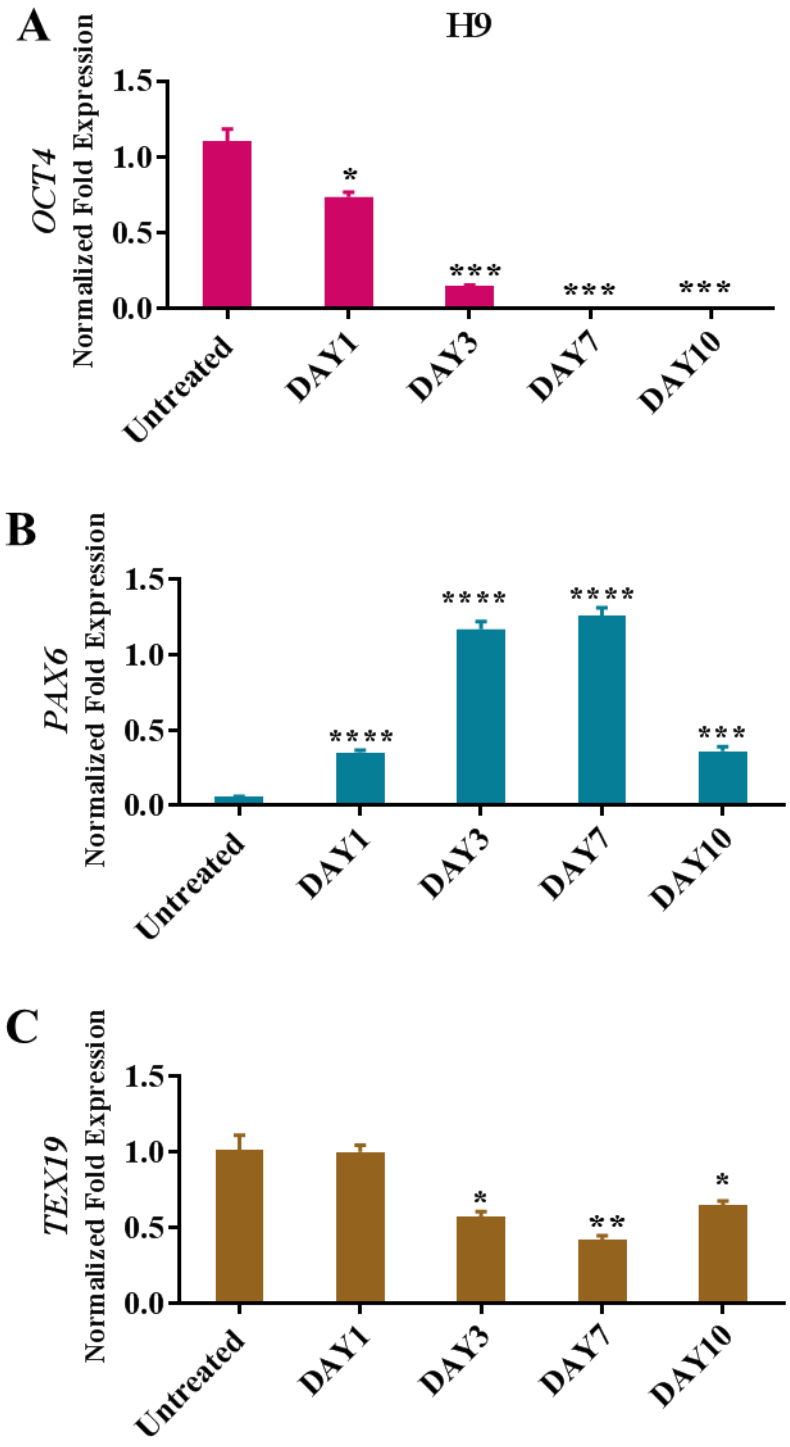

Figure 5-13 RT-qPCR analysis of the *TEX19* mRNA levels in H9 treated with retinoic acid.

(A) Bar chart presenting the mRNA levels of the *OCT4* gene in H9 treated with retinoic acid on the selected days. (B) Bar chart showing the mRNA levels of *PAX6*. *OCT4* was used as a stem cell marker and *PAX6* as a neuronal marker. (C) Bar chart elucidating the mRNA levels of the *TEX19* gene upon differentiation. *YWHAZ* and *Actin* were used for data normalisation. The error bars show the standard errors of the mean. Asterisks above the bars indicate the *p*-values (*: $p<0.05$; **: $p<0.01$;***: $p<0.001$; ****: $p<0.0001$).

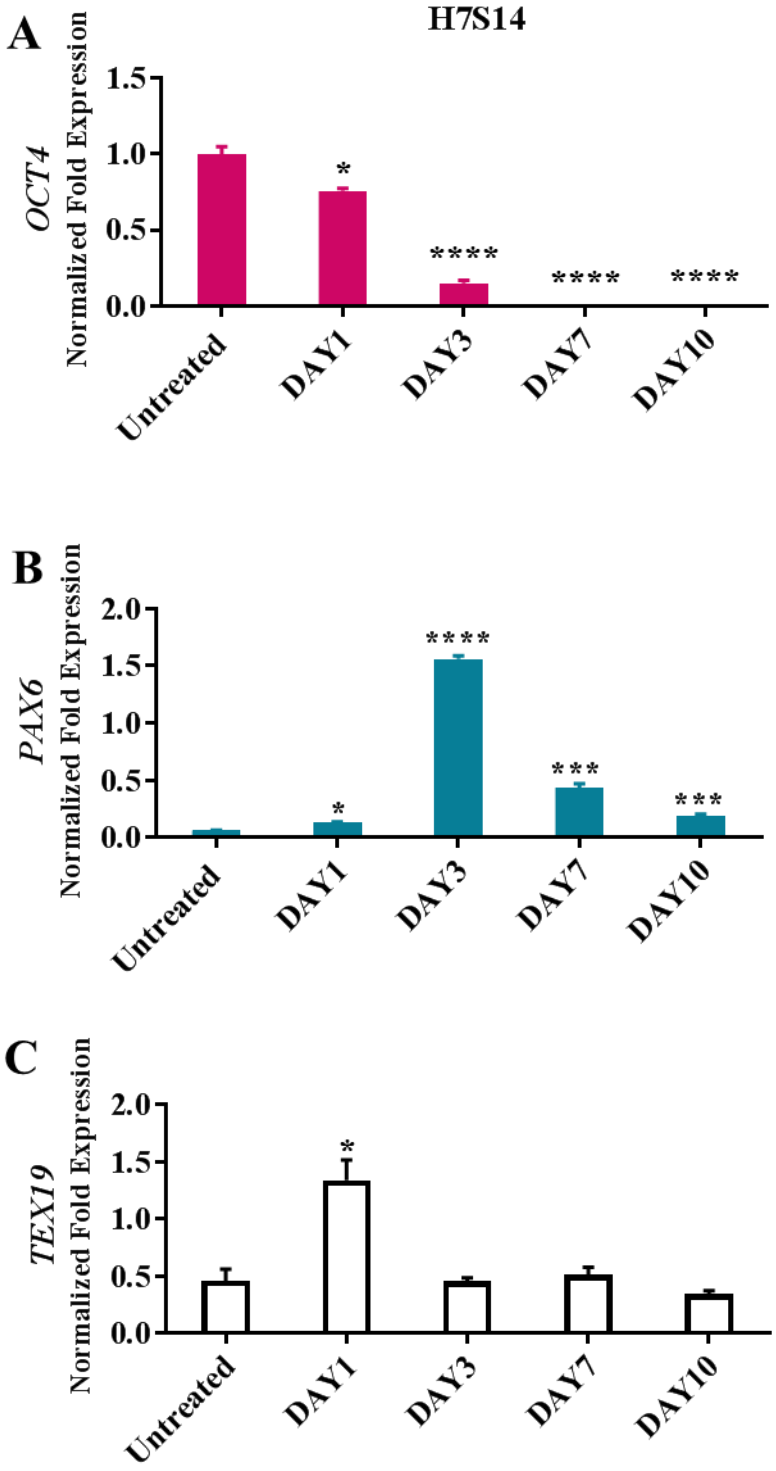

Figure 5-14 RT-qPCR analysis of the *TEX19* mRNA levels in H7S14 treated with retinoic acid.

(A) Bar chart presenting the mRNA levels of the *OCT4* gene in H7S14 treated with retinoic acid on the selected days. (B) Bar chart showing the mRNA levels of *PAX6*. *OCT4* was used as a stem cell marker and *PAX6* as a neuron marker. (C) Bar chart elucidating the mRNA levels of the *TEX19* gene upon differentiation. *YWHAZ* and *Actin* were used for data normalisation. The error bars show the standard errors of the mean. Asterisks above the bars indicate the *p*-values (*: $p<0.05$; ***: $p<0.001$; ****: $p<0.0001$).

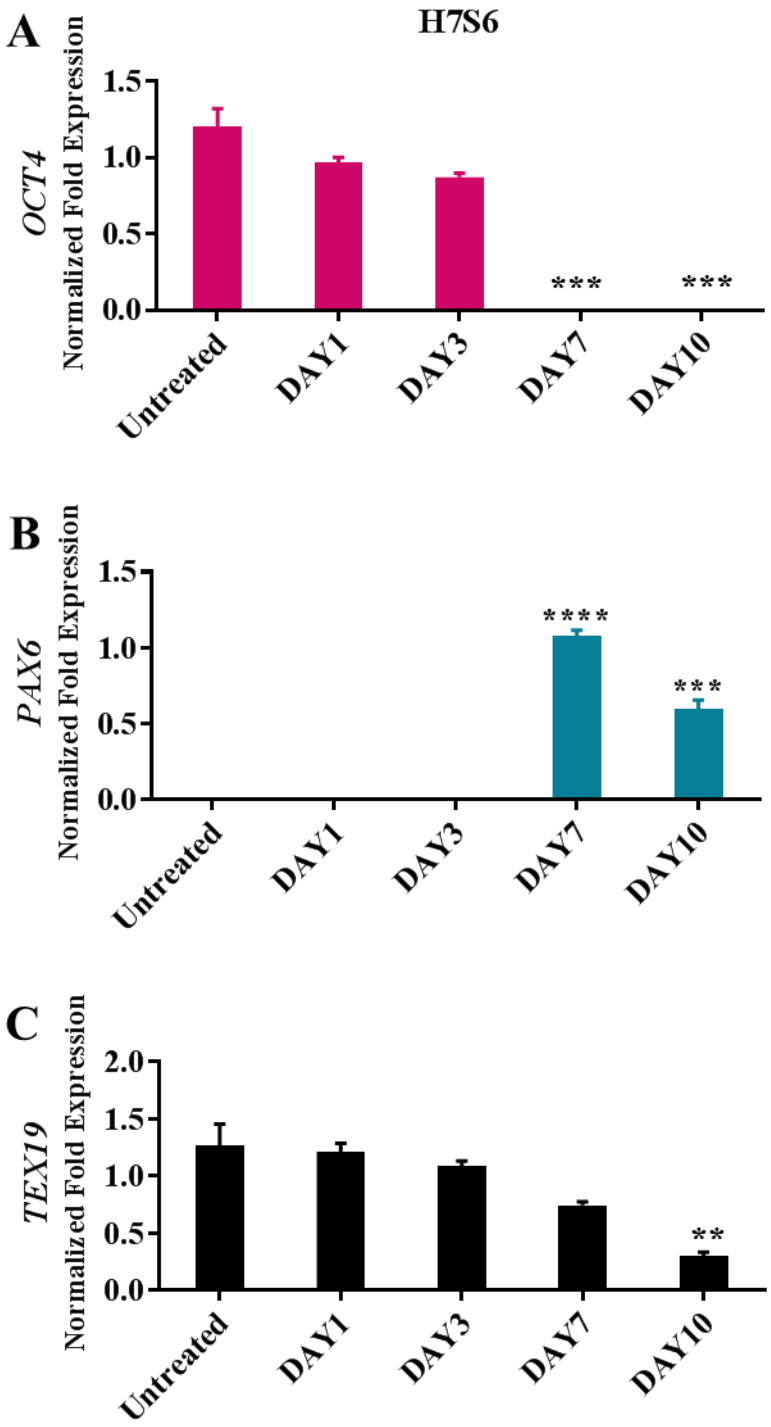

Figure 5-15 RT-qPCR analysis of the *TEX19* mRNA levels in H7S6 treated with retinoic acid.

(A) Bar chart presenting the mRNA levels of the *OCT4* gene in H7S6 treated with retinoic acid on the selected days. (B) Bar chart showing the mRNA levels of *PAX6*. *OCT4* was used as a stem cell marker and PAX6 as a neuron marker. (C) Bar chart elucidating the mRNA levels of the *TEX19* gene upon differentiation. *YWHAZ* and *Actin* were used for data normalisation. The Y axis is linear. The error bars show the standard errors of the mean. Asterisks above the bars indicate the *p*-values (**: $p<0.01$; ***: $p<0.001$; ****: $p<0.0001$).

5.3 Discussion

TEX19 has been hypothesised to be linked to pluripotency (Kuntz et al., 2008). In this study, a set of hES cell lines were examined, and the results have confirmed the presence of *TEX19* transcripts in hESCs. This is a significant sign that *TEX19* is a stemness factor and it may have a functional connection to stem cell biology and pluripotent markers. The mechanism behind the ability of hESCs to remain pluripotent and undifferentiated has not yet been fully explored. To date, few key factors have been identified as being critical for maintaining pluripotency in hESCs (Fong et al., 2008). Several functional studies have elucidated that *OCT4* and *NANOG* encode indispensable transcription factors required to maintain self-renewal and pluripotency, and they critically regulate the cell fate in hESCs. Moreover, these studies have confirmed that a reduction in the expression of *OCT4* and *NANOG* is responsible for differentiation and losing the pluripotency in hESCs (Hay et al., 2004; Hyslop et al., 2005; Matin et al., 2004; Zaehres et al., 2005). In line with this, *TEX19* transcript depletion in distinct hES cell lines has significantly altered the mRNAs of stem cell markers at different levels. In the examined hES cell lines (SHEF6, H9, H7S14 and H7S6), the reducing of *TEX19* mRNA was found to significantly decrease the mRNA levels of *NANOG* in H9 and H7S6, while *NANOG* mRNA level was elevated in SHEF6. Interestingly, the limited *TEX19* transcript depletion in H7S14 has led to a significant reduction in the levels of mRNA of *NANOG*. These observations strongly infer that *TEX19* controls the expression of *NANOG*. *OCT4* was another stem cell marker that was found to be downregulated in H9 after *TEX19* mRNA knockdown. In the H9 hES cell line, *TEX19* mRNA depletion substantially reduced *NANOG* transcripts. This opens up two possibilities. First, *TEX19* transcript depletion has directly reduced *OCT4* expression; second, the significant inhibition in the *NANOG* level has downregulated *OCT4* expression. However, this could indicate that TEX19 may also control *OCT4* expression either directly or indirectly. Therefore, this key finding supports the idea that TEX19 is speculated to play a role in maintaining pluripotency. Moreover, *TEX19* might be required for hESCs to regulate crucial stem cell markers, NANOG in particular. In addition, in the present study TEX19 is emerging evidence to act as a stem cell marker. However, further research is required to conclude if TEX19 has a definitive function in controlling stem cell markers and sustaining the pluripotency in hESCs.

The investigation of the influence of *TEX19* mRNA depletion on hESCs was further extended to include the *PIWI* genes. Those genes encode proteins that contribute to maintaining germline stem cells (Gu et al., 2010). Of the four *PIWI* genes only the transcripts of *PIWIL2* and *PIWIL4* were found to be significant, while all the examined hES cell lines did not appear to express *PIWIL1* and *PIWIL3*. In H9, the transcript levels of both *PIWIL2* and *PIWIL4* were inhibited. This comprehensive inhibition could be due to either the influence of TEX19 or the reduction in *NANOG* and *OCT4* following TEX19 depletion. Moreover, in H7S6 and H7S14 the reduction in the *PIWI* transcripts could be either due to TEX19 depletion or the reduction in the *NANOG* level. No significant change was observed in the transcript levels of *PIWIL2* and *PIWIL4* in SHEF6, and this might be because TEX19 has no influence on those genes or it might be due to the *NANOG* behaviour, as it was elevated in contrast to the other hES cell lines. More importantly, these observations indicate the potential function for TEX19 in terms of regulating *PIWI* genes in hESCs either through its depletion or its influence on the stem cell markers.

The expression of murine *Tex19.1* has been found to be inhibited upon differentiation in parallel with *Oct4*, thereby speculating its function as a pluripotent marker (Kuntz et al., 2008). In line with this, retinoic acid was used to differentiate the hESCs and the subsequent inhibition of *OCT4* expression was monitored. Retinoic acid is a vitamin A metabolite that is required for several processes during the embryonic development, such as differentiation and proliferation. Moreover, retinoic acid stimulates differentiation, promotes stem cell neural lineage specification and reduces the markers of pluripotency (Zhang et al., 2015a). In this present study, applying retinoic acid to the hES cell lines led to the cessation of *OCT4* expression and the activation of the ectoderm marker gene *PAX6*, thereby indicating successful differentiation. The *TEX19* mRNA level decreased on day 3 and day 7 in SHEF6 and H9, suggesting a possible link to *OCT4* expression. The elevation of the *TEX19* transcript levels on day 10 might be attributed to the role of retinoic acid in controlling germ line genes. Hong et al. (2012) elucidated the power of retinoic acid in regulating the expression of germ genes in stem cells. In the present study, differentiation of H7S14 did not lead to reduction in the *TEX19* transcript levels, indicating that different hES cell lines display different behaviours for *TEX19*. The differentiation in H7S6 was found to reduce the *TEX19* mRNA for all of the days, showing significant inhibition on day 10. This hES cell line

provides a very good example of a case in which the *TEX19* transcript level was reduced when hESCs lose pluripotency. In a broad spectrum, *TEX19* could be a stemness factor that requires pluripotency for its stable expression in hESCs. Moreover, using an approach that further investigates hESC differentiation is a valuable way to confirm the behaviour of *TEX19* in hESCs because retinoic acid may modulate the expression of germ genes during the differentiation process.

To summarize, *TEX19* is a specific stemness factor gene found to express in all of the examined hES cell lines, and it might be required for the expression of *OCT4* and *NANOG*. TEX19 depletion was found to alter the expression of *PIWIL2* and *PIWIL4* in hESCs, indicating that it has a potential role in regulating the PIWI pathway. To some extent, differentiation of hESCs was found to reduce the expression level of *TEX19*, and it produced changeable behaviour. More in depth, this study's findings postulate that TEX19 could play a functional role, thereby contributing to stem cell biology and pluripotent markers.

Chapter 6

TEX19 regulates transposable elements (TEs) in cancer cells and human embryonic stem cells (hESCs)

6. *TEX19* regulates transposable elements (TEs) in cancer cells and human embryonic stem cells (hESCs)

6.1 Introduction

The changes in DNA sequences and epigenetic modifications play a key role as a cause of variation in genomes. Alterations in the DNA sequence can be generated by different factors, such as errors in DNA replication/repair or insertion of mobile DNAs. These mobile DNAs are also called transposable elements (TEs), and their DNA sequences can be inserted elsewhere in a genome (Elbarbary et al., 2016). TEs are distinct sequences of DNA that can move from a certain locus to another either in their host genome or among different genomes (Haren et al., 1999). With rare exceptions, TEs have been found in all eukaryotic genomes sequenced to date (Huang et al., 2012), and their ability to modify the genome structure and alter gene expression has been recognised (Cordaux & Batzer, 2009; Huang et al., 2012; Elbarbary et al., 2016). Sequences of TEs inhabit approximately half of the human genome; this means that the human genome has one of the highest levels of TE content among mammals (Belancio et al., 2009).

TEs are broadly divided into two main sets based on the transposition mechanism, namely RNA-based retrotransposons (Class I) and DNA transposons (Class II). Class I TEs, or retrotransposons, use an RNA intermediate for their mobilisation; the sequences of those retrotransposons are transcribed from the genome using cellular RNA polymerases and then integrated into a new site via a transposon-encoded reverse transcriptase. Class II TEs, or DNA transposons, use a DNA-based cut-and-paste transposition (Wicker et al., 2007; Panaud, 2016). The activity of human DNA transposons subsided millions of years ago; consequently, this TE group is no longer contribute considerably to the continuing mutagenesis in humans (Belancio et al., 2009).

Retrotransposons (Class I) participate to form up to approximately 40% of the human genome, and they have been further subdivided into two major groups, namely long terminal repeats (LTRs) and non–long terminal repeats (non-LTRs). LTR

retrotransposons encompass the human endogenous retroviruses (HERVs), while non-LTR Retrotransposons encompass long interspersed element (LINE) and short interspersed elements (SINE) (Piégu et al., 2015).

HERVs represent DNA sequences derived from viruses, and they comprise up to 8% of the human genome (Kurth & Bannert, 2010). Four families of HERVs are known, namely HERV-K, HERV-W, HERV-H and HERV-R; these contain the basic viral genes (Kim, 2012). In addition, HERVs are initiated due to infection in the germline cells by ancient and exogenous retroviruses; later, these HERVs become unable to encapsulate the viral genome, and they continued to be integrated as parts of the human genome. Therefore, the genetic material of HERVs still contain the typical (basic) retroviral genes, including *pro*, *pol*, *gag* and *env* (Dewannieux & Heidmann, 2013; Kurth & Bannert, 2010; Stoye, 2012). In the human genome, studies have indicated an inactive condition for most of TEs, and HERVs have been found to be unable to produce functional viruses. Moreover, some of these elements are found to contribute to the normal physiology of the host species. Syncytin-1 and Syncytin-2 are proteins encoded by the gene *env* from the HERV group, and they have been found to contribute to the development of placental trophoblasts (Lokossou et al., 2014). The retrovirus HERV-H, which belongs to the H family – found to be preferentially expressed in hESCs – is associated with stem cell markers and is required to maintain pluripotency. All of this suggests a potential functional role for HERVs, and thus, they should be considered in research (Lu et al., 2014).

LINE-1 and SINE are mobile elements, and clear evidence has been found that they are active in the human genome. LINE-1 is an autonomous member that forms up to about 17% of the human genome. Its sequence is about 6 kb long, and it encodes the activation of several enzymes, including reverse transcriptase and endonuclease; these enzymes are essential for the integration of the DNA copy into the genome (Belancio et al., 2009; Piskareva et al., 2013). In contrast, SINE is a non-autonomous member comprising more than 10% of some genomes. Its sequence is approximately 700 bp long, and it does not encode any enzymes; instead, it relies on the presence of the functional LINE-1, and it is therefore referred to as the LINE-1 parasite (Vassetzky & Kramerov, 2013).

TEs have intrinsic features in terms of their mobilisation, which may enable them to cause reshuffling of sequences, genetic reorganisation, gene structure alterations and modifications in the expression patterns of the cells. This suggests that the dysregulation of TEs may lead to their activation or translocation, which could result in the accumulation of a prospective oncogenic outcome (Dhivya & Premkumar, 2016). Moreover, analysis of protein level and mRNA for active TEs has revealed their activation in various types of cancer (Downey et al., 2015). The main reason for the activation of TEs in cancer relates to their control by epigenetic processes. TE DNA is methylated in normal conditions and subsequently silenced in normal human cells; TE DNA methylation is eliminated in cancer cells, providing the opportunity for these TEs to be triggered and to disturb the integrity of the cell (Grégoire et al., 2016). In line with this, some TEs have been linked with oncogenesis; for example, the human endogenous retrovirus HERV-K (HML-2) has been detected at a high level in the plasma of lymphoma patients. Remarkably, the patients responding successfully to treatment showed either low or undetectable HERV-K (HML-2) levels, demonstrating that this element is a potential biomarker for lymphoma (Contreras-Galindo et al., 2008). Likewise, this endogenous viral element has been found to be overexpressed in breast cancer, suggesting that its expression plays a role in breast cancer pathogenesis (Wang-Johanning et al., 2001). Moreover, changes in the expression of *LINE-1* due to hypomethylation are linked with various type of cancers, such as colon cancer and breast cancer, and its activation has been found to induce genomic instability in tumour cells. (Kemp & Longworth, 2015).

Öllinger and his co-workers (2008) were the first group to report that murine *Tex19.1* is associated with TE activity. The deletion of *Tex19.1* in testis samples has elevated the expression of a particular ERV, MMERVK10C. A few years after this initial report, Reichmann and his colleagues (2013) showed the elevation of the *LINE-1* transcript level when *Tex19.1* is deleted in the placenta; therefore, these researchers postulated that *Tex19.1* is required to repress TEs. The aim of the present work to examine whether human *TEX19* is linked to TE activity and if it controls TEs expression in cancer stem-like cells, cancer cells and hESCs.

6.2 Results

6.2.1 *TEX19* regulates transposable elements in cancer stem-like cells and cancer cells

The level of *TEX19* mRNA was depleted in cancer stem-like cells (NTERA2) and cancer cells (H460, SW480) using *TEX19* siRNA#7 (see Chapter 4). To inspect the link between *TEX19* and TEs, RT-qPCR was carried to determine the alteration in RNA levels for multiple TEs in NTERA2, H460 and SW480 following *TEX19* transcript depletion. Different groups of TEs were examined, including non-LTR retrotransposons (*LINE-1*and *SINE*) and LTR retrotransposon (HERVs). The multiple TEs belonging to HERVs group were *HERV K pro*, *HERV K 107*, *HERV K 10*, *HERV K HML2 rec*, *HERV K env*, *HERV K pol* and *HERV K gag*. The obtained results via RT-qPCR showed differing alterations in the TE RNA levels based on each examined cancer cell line (Figures 6.1-6.3).

The *TEX19* transcript knockdown in NTERA2 resulted in upregulation of the *HERV K 107* transcript level ($p<0.05$). The other HERV, *SINE* and *LINE-1*transcripts, were not affected, and they exhibited no significant change (Figure 6.1). In H460, the reducing of *TEX19* mRNA resulted in a significant increase for multiple HERV transcript levels, namely *HERV K pro* ($p<0.05$), *HERV K 107*($p<0.05$), *HERV K gag* ($p<0.05$) and *HERV K env* ($p<0.05$; Figure 6.2). Likewise, *LINE-1* transcript level was upregulated, showing a significant change ($p<0.05$). The mRNA levels for the remaining TEs were detected with no significant alteration. In SW480, the depletion of *TEX19* transcript substantially elevated the mRNA levels of most TEs, namely *HERV K 107* ($p<0.001$), *HERV K 10* ($p<0.001$), *HERV K pro* ($p<0.001$), *HERV K pol* ($p<0.001$) and *HERV K env* ($p<0.001$; Figure 6.3). Likewise, both *LINE-1* and *SINE* transcript levels showed significant upregulation ($p<0.001$ and $p<0.001$, respectively). Interestingly, *HERV K 107* was a common TE found with the similar alteration (upregulation) in all examined cancer cells. Correspondingly, in the H460 and SW480 cancer cell lines, two common HERVs were found to be upregulated, namely *HERV K pro* and *HERV K env*. Moreover, the retrotransposon *LINE-1* also found to be elevated in both cancer cell lines (Figure 6.8).

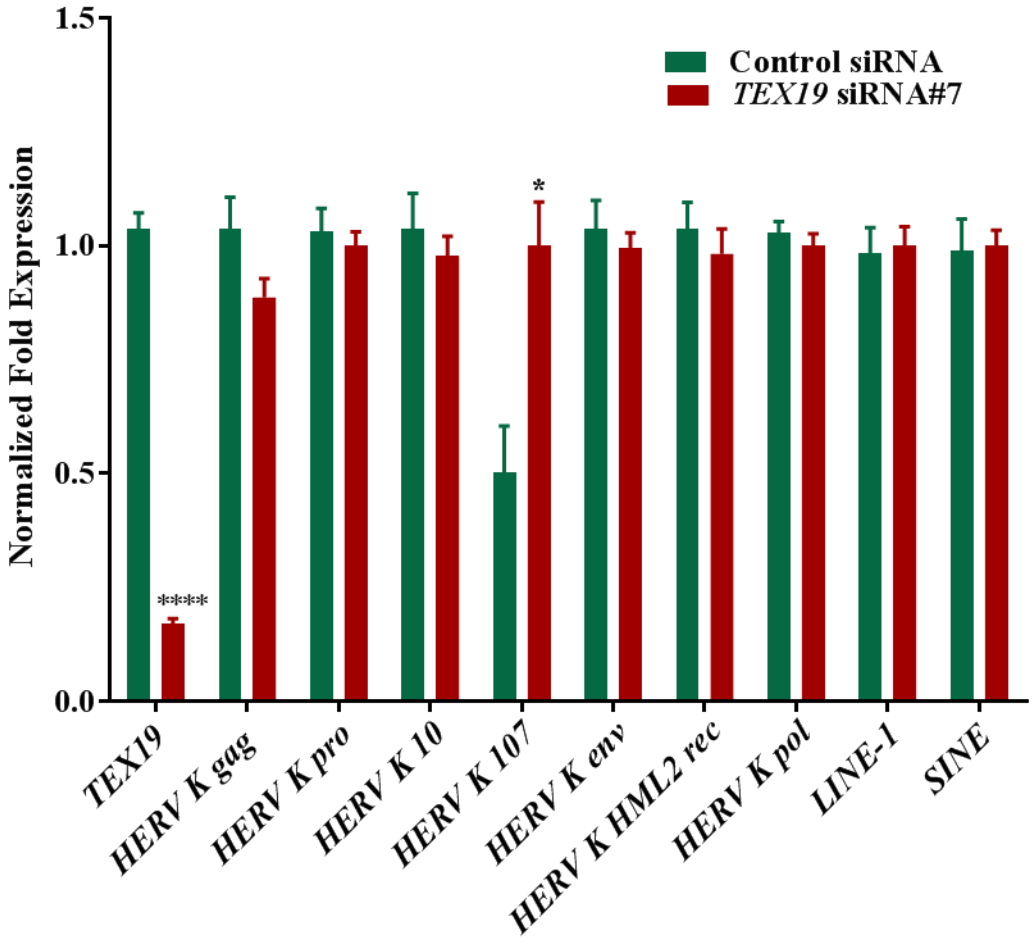

Figure 6-1 RT-qPCR analysis of TEs mRNA levels following *TEX19* transcript depletion in NTERA2.

The bar chart demonstrates the alteration in mRNA levels of various TEs in NTERA2 after *TEX19* transcript knockdown. *LINE-1* and *SINE* belong to the non-LTR retrotransposon group, while the other TEs belong to the LTR retrotransposons group (HERVs). Asterisks above the bars indicate the *p*-value (*: $p<0.05$; ****: $p<0.0001$). *TUBA1C* and *GAPDH* were used for data normalisation. The error bars show the standard errors of the mean.

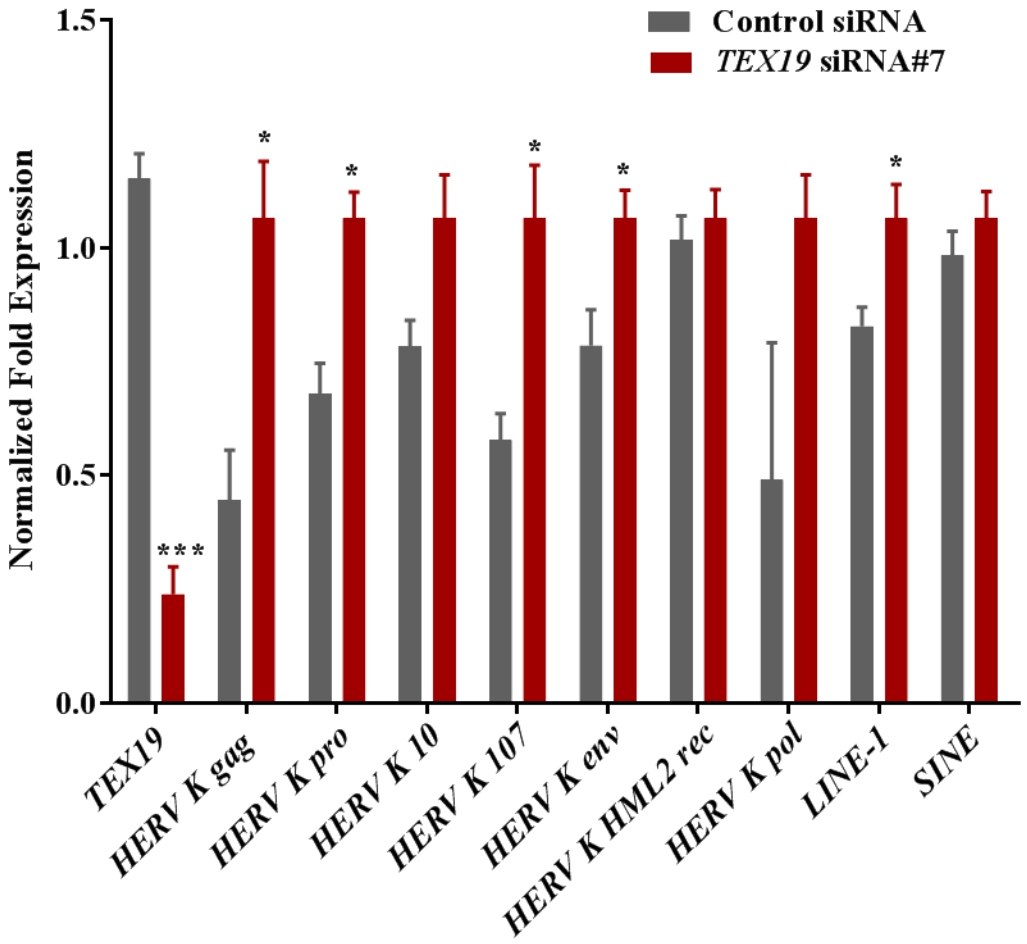

Figure 6-2 RT-qPCR analysis of TEs mRNA levels following *TEX19* transcript depletion in H460.

The bar chart demonstrates the alteration in mRNA levels of various TEs in H460 after *TEX19* transcript knockdown. *LINE-1* and *SINE* belong to the non-LTR retrotransposons group, and the other TEs belong to the LTR retrotransposon group (HERVs). Asterisks above the bars indicate the *p*-value (*: $p<0.05$; ***: $p<0.001$). *TUBA1C* and *GAPDH* were used for data normalisation. The error bars show the standard errors of the mean.

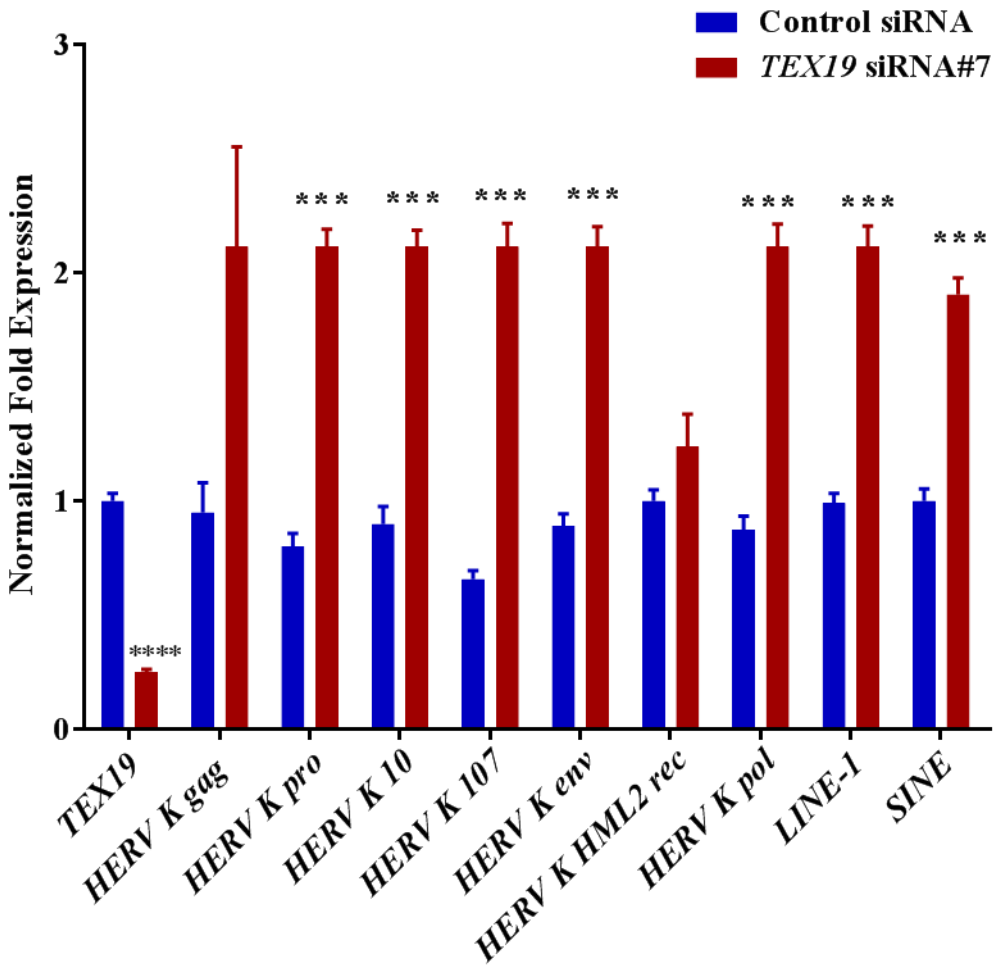

Figure 6-3 RT-qPCR analysis of TEs mRNA levels following *TEX19* transcript depletion in SW480.

The bar chart demonstrates the alteration in mRNA levels of various TEs in SW480 after *TEX19* knockdown. *LINE-1* and *SINE* belong to the non-LTR retrotransposons group, and the other TEs belong to the LTR retrotransposon group (HERVs). Asterisks above the bars indicate the *p*-value (***: $p<0.001$, ****: $p<0.0001$). *TUBA1C* and *GAPDH* were used for data normalisation. The error bars show the standard errors of the mean.

6.2.2 *TEX19* regulates transposable elements in human embryonic stem cells (hESCs)

TEX19 mRNA level was reduced in distinct hES cell lines SHEF6, H9, H7S14 (normal karyotype) and H7S6 (abnormal karyotype, specified in Chapter 5) using *TEX19* siRNA#7. All hES cell lines showed a significant reduction in *TEX19* transcript except for H7S14, which showed a limited reduction; this was illustrated in Chapter 5. As the reduction of the *TEX19* mRNA level resulted in significant alteration for multiple TEs transcript levels in distinct cancer cell lines, this motivated the investigation of whether *TEX19* expression is required to control TEs in hESCs. To inspect the association of *TEX19* with TEs in hESCs, RT-qPCR was carried out to determine the TE mRNA level alterations in SHEF6, H9, H7S14 and H7S6 following *TEX19* transcript knockdown. Different groups of TEs were examined, including non-LTR retrotransposons (*LINE-1* and *SINE*) and LTR retrotransposon (HERVs). Moreover, multiple TEs belonging to the HERV group were employed, namely *HERV K pro*, *HERV K 107*, *HERV K 10*, *HERV K HML2 rec*, *HERV K env*, *HERV K pol* and the *HERV K gag*. The analysed results via RT-qPCR showed different alterations in the TE mRNA level according to each hES cell line (Figures 6.4-6.7).

The depletion of *TEX19* transcript in SHEF6 resulted in significant increases in HERV transcript levels, including those of *HERV K pro* ($p<0.05$) and *HERV K env* ($p<0.05$), while the transcript level of *HERV K HML2 rec* was reduced ($p<0.05$). The other HERVs were not affected, and they showed no significant alteration. Both *LINE-1* and *SINE* transcript levels found to be upregulated ($p<0.01$ and $p<0.05$, respectively; Figure 6.4). In H9, the reducing of *TEX19* transcript reduced the mRNAs of *HERV K pro* ($p<0.05$) and *HERV K pol* ($p<0.01$). The other HERVs were detected with no significant change in their mRNAs. *LINE-1* and *SINE* transcript levels were downregulated ($p<0.05$ and $p<0.05$, respectively; Figure 6.5). In H7S14, the limited reduction in the *TEX19* mRNA level significantly decreased *HERV K pro* transcript level ($p<0.01$). More interestingly, the reduction in *TEX19* transcript activated *HERV K env* expression ($p<0.0001$). No significant alteration was observed for the other HERVs. Moreover, *LINE-1* and *SINE* transcript levels were found to be downregulated ($p<0.001$ and $p<0.01$, respectively; Figure 6.6). In the adapted hES cell line (H7S6), *TEX19* mRNA knockdown downregulated *HERV K gag* ($p<0.05$) and *HERV K HML2 rec* ($p<0.05$).

Remarkably, the reduction in the *TEX19* transcript level activated *HERV K env* expression (p<0.0001). No significant change was detected for the other HERVs. Moreover, *LINE-1* and *SINE* mRNAs exhibited significant downregulation (p<0.001 and p<0.001, respectively; Figure 6.7). No common TE was found to exhibit similar alteration among the examined hESC lines, but both *LINE-1* and *SINE* were found to exhibit significant downregulation in three hES cell lines (H9, H7S14 and H7S6; Figure 6.8).

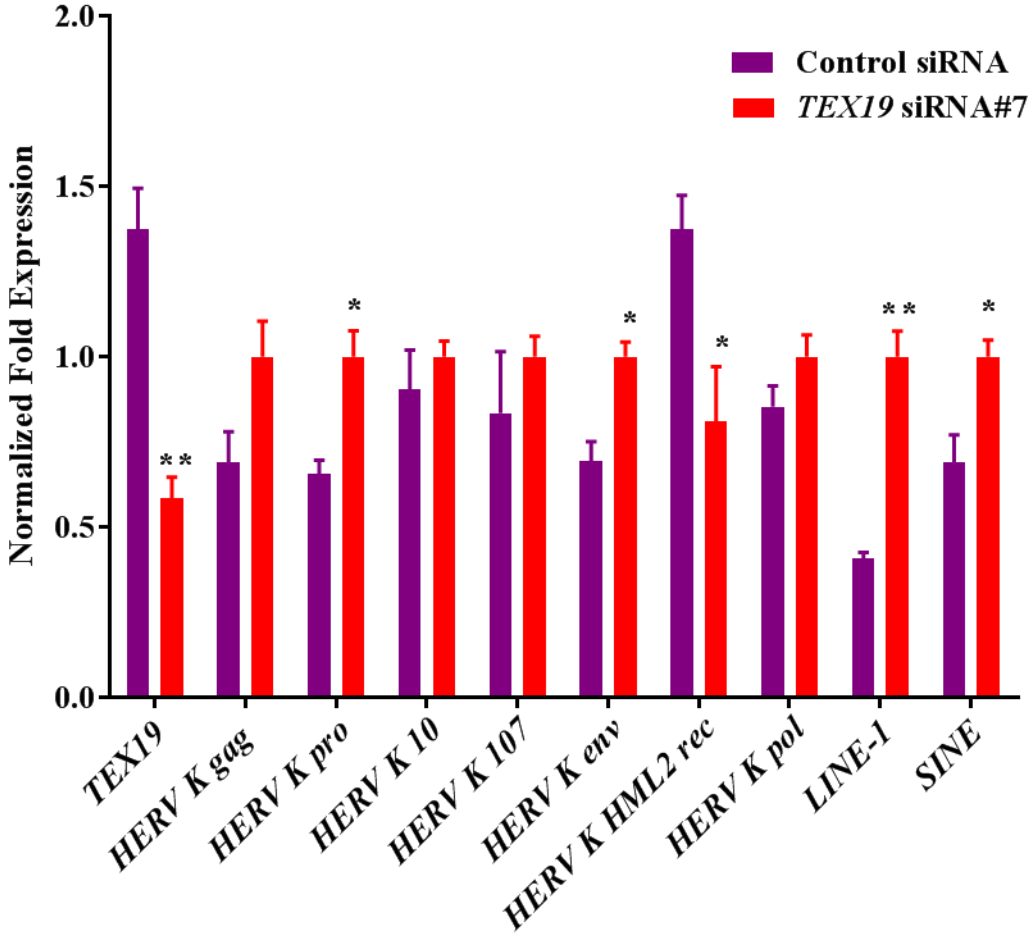

Figure 6-4 RT-qPCR analysis of TEs mRNA levels following *TEX19* transcript depletion in SHEF6.
The bar chart demonstrates the alteration in mRNA levels of various TEs in SHEF6 after *TEX19* transcript knockdown. *LINE-1* and *SINE* belong to the non-LTR retrotransposons group, and the other TEs belong to the LTR retrotransposon group (HERVs). Asterisks above the bars indicate the p-value (*: p<0.05; **: p<0.01). *YWHAZ* and *Actin* were used for data normalisation. The error bars show the standard errors of the mean.

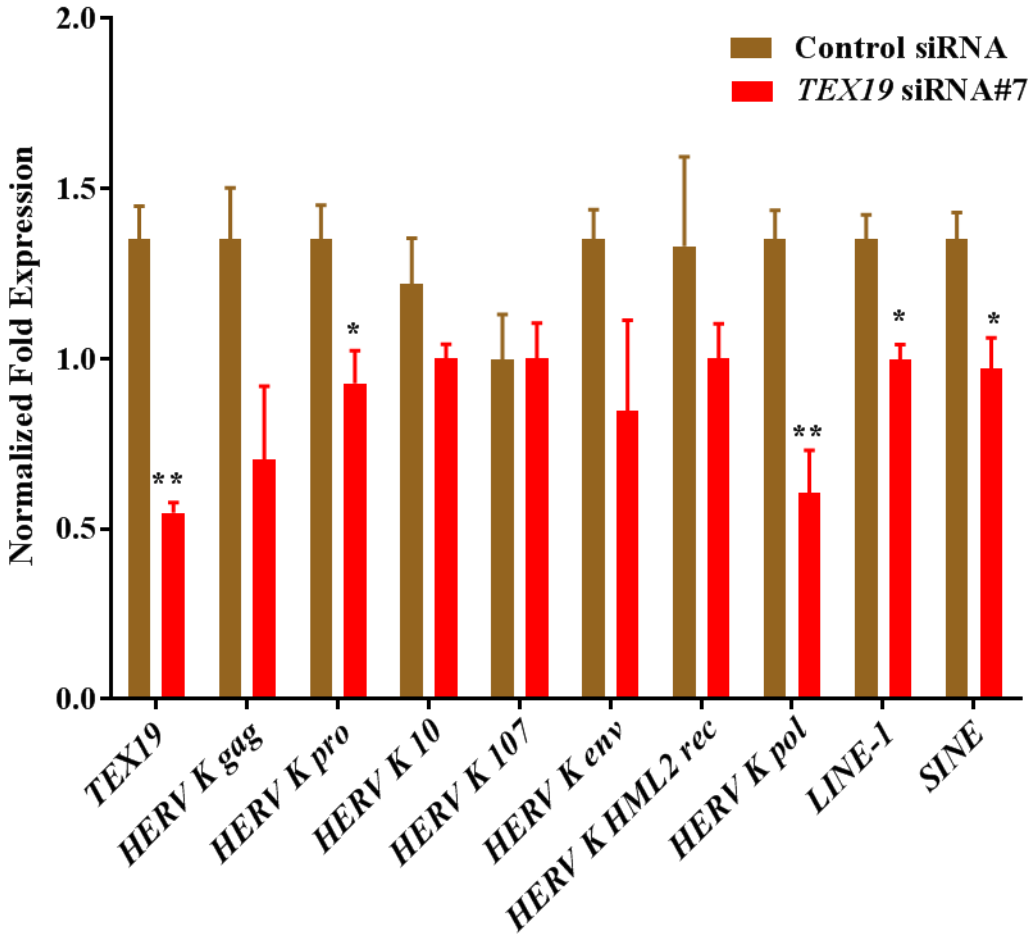

Figure 6-5 RT-qPCR analysis of TEs mRNA levels following *TEX19* transcript depletion in H9.

The bar chart demonstrates the alteration in mRNA levels of various TEs in H9 after *TEX19* transcript knockdown. *LINE-1* and *SINE* belong to the non-LTR retrotransposons group, and the other TEs belong to the LTR retrotransposon group (HERVs). Asterisks above the bars indicate the *p*-value (*: $p<0.05$; **: $p<0.01$). *YWHAZ* and *Actin* were used for data normalisation. The error bars show the standard errors of the mean.

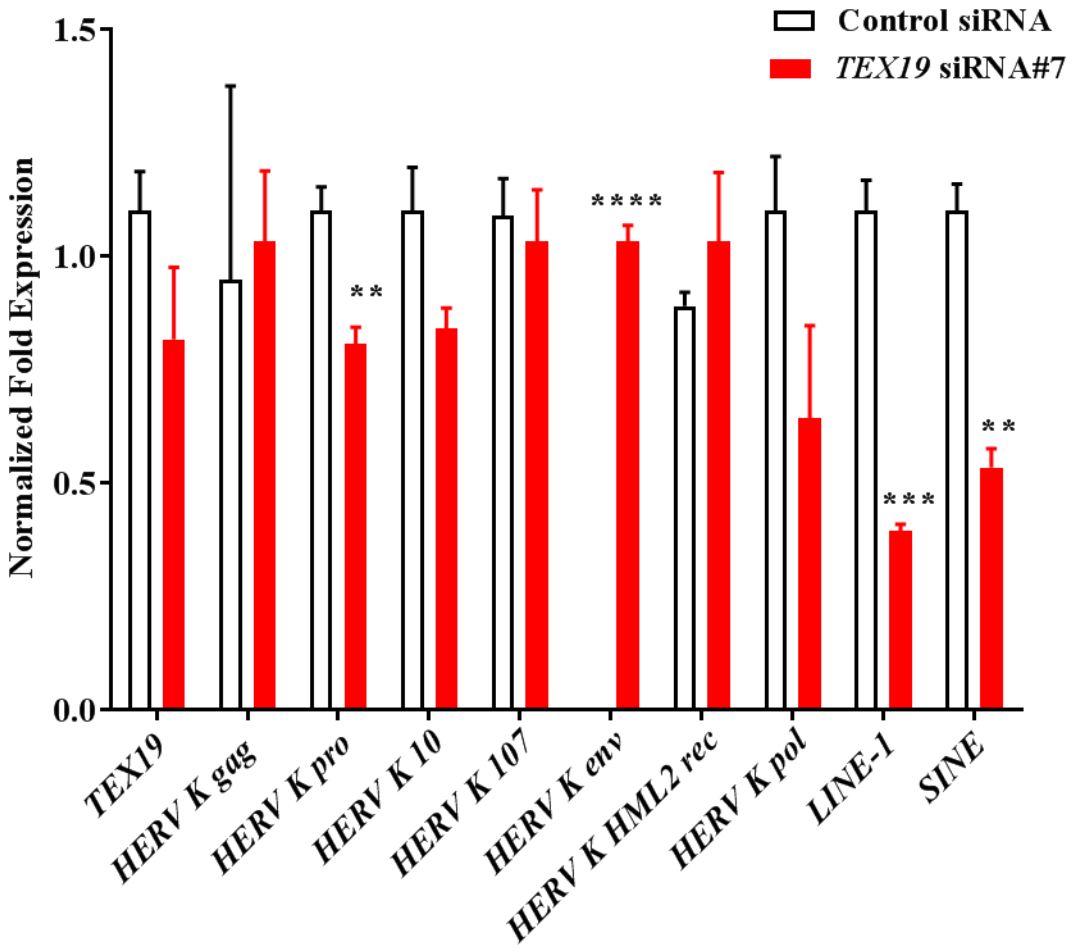

Figure 6-6 RT-qPCR analysis of TEs mRNA levels following *TEX19* transcript depletion in H7S14.

The bar chart demonstrates the alteration in mRNA levels of various TEs in H7S14 after *TEX19* transcript knockdown. *LINE-1* and *SINE* belong to the non-LTR retrotransposons group, and the other TEs belong to the LTR retrotransposon group (HERVs). Asterisks above the bars indicate the *p*-value (**: $p<0.01$, ***: $p<0.001$; ****: $p<0.0001$). *YWHAZ* and *Actin* were used for data normalisation. The error bars show the standard errors of the mean.

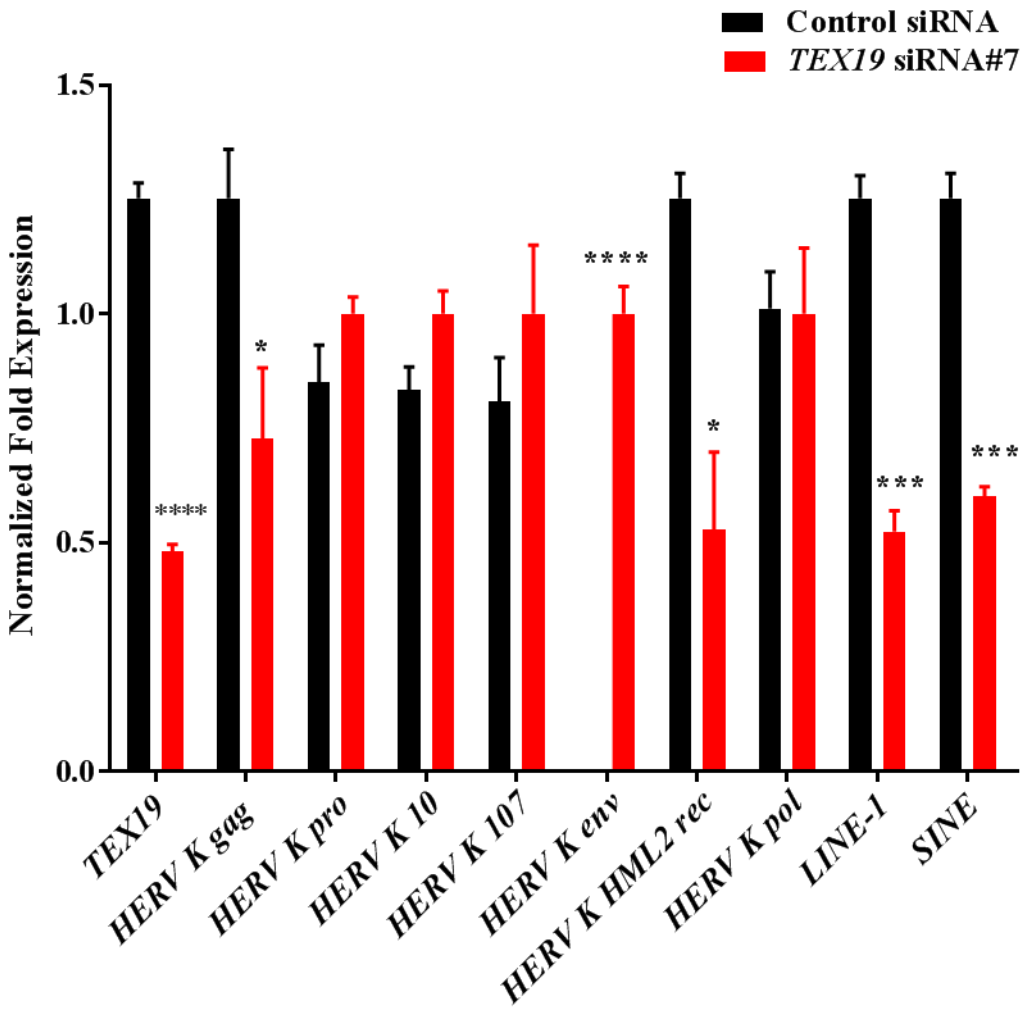

Figure 6-7 RT-qPCR analysis of TEs mRNA levels following *TEX19* transcript depletion in H7S6.

The bar chart demonstrates the alteration in mRNA level of various TEs in H7S6 after *TEX19* transcript knockdown. *LINE-1* and *SINE* belong to the non-LTR retrotransposons group, and the other TEs belong to the LTR retrotransposon group (HERVs). Asterisks above the bars indicate the *p*-value (*: $p<0.05$, ***: $p<0.001$; ****: $p<0.0001$). *YWHAZ* and *Actin* were used for data normalisation. The Y-axis is linear. The error bars show the standard errors of the mean.

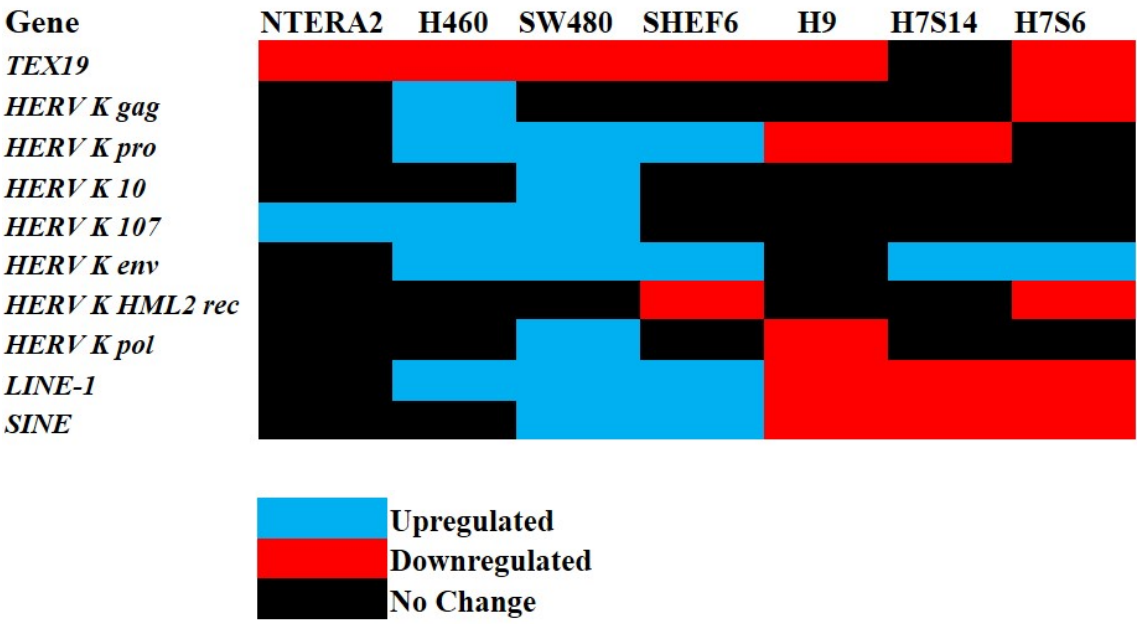

Figure 6-8 A summary of TEs expression following *TEX19* transcript depletion in human cancer cell lines and hES cell lines.
The grid plot illustrates the comparison of differentially expressed TEs following *TEX19* depletion. Results are obtained from RT-qPCR analysis. *LINE-1* and *SINE* belong to the non-LTR retrotransposons group, and the other TEs belong to the LTR retrotransposon group (HERVs).

6.3 Discussion

Deletion of murine *Tex19.1* has been reported to alter expression levels of TEs in the testis and placenta, suggesting that it has an important function in controlling TEs (Öllinger et al., 2008; Reichmann et al., 2013). Despite the growing evidence that *TEX19* is linked to TEs, no previous study has investigated this issue in human cells. In this study, a screening analysis of TEs was performed for a range of TEs belonging to the HERVs and non-LTR (*LINE-1* and *SINE*) groups in distinct cancer cells and hESCs. The depletion of *TEX19* transcript upregulated the mRNA levels of multiple TEs in cancer cell lines H460 and SW480. Remarkably, a specific *HERV K 107* was found to be a common TE upregulated in all examined cancer cells (NTERA2, H460 and SW480). These key findings reveal a strong link between TEX19 function and control of TEs. Öllinger and his co-workers (2008) demonstrated that the deletion of *Tex19.1* increased a specific ERV *MMERVK10C* transcript level in mice. The analysis in this present study has achieved a similar result for human cells, where *TEX19* transcript depletion enhanced the mRNA level of numerous HERVs in cancer cell lines (H460, SW480); the findings indicate that TEX19 might be required to control HERV expression. Moreover, in this study, the elevation level of *HERV K 107* transcript in all cancer cells suggested that its function most likely involves interaction with *TEX19* expression. Likewise, the *LINE-1* transcript level was upregulated in distinct human cells, which is consistent with Reichmann and his colleagues (2013) report that murine *Tex19.1* knockout in the placenta elevates *LINE-1* expression.

Piwi genes express in germ lineage cells and play a key part in repression of retrotransposons in the mammalian germline (Aravin et al., 2007; Lim et al., 2014). Correspondingly, the silencing of *Piwil1* has been found to repress TEs in the male *Drosophila* germline (Kalmykova et al., 2005). Based on the SW480 RNA sequence data and RT-qPCR analysis (see Chapter 4), human *PIWIL1* was found to be particularly upregulated in SW480 and H460 after *TEX19* transcript knockdown. In addition, in these cancer cell lines, screening analysis showed upregulation for most TEs. This suggests that TEX19 may control TEs either through its depletion influence or upregulation of the *PIWI* transcripts, *PIWIL1* in particular. However, it is not yet clear whether there is a direct fundamental association between TEX19 depletion and regulation of the TE mechanism. More importantly, TE activation has been linked with

triggering oncogenic pathways, resulting in the development of different cancer types in humans; this elucidates an important etiological factor in oncogenesis (Solyom et al., 2012; Chénais, 2013; Shukla et al., 2013; Paterson et al., 2015). This opens the possibility that *TEX19* causes carcinogenesis in human tissues through the dysregulation of TE expression.

The expression of TEs has been documented in various stages during embryonic development in mammals. However, the function of TE expression remains unclear in species-specific ESCs (Hutchins & Pei, 2015). Screening analysis of TEs following *TEX19* transcript depletion in distinct hES cell lines (SHEF6, H9, H7S14, H7S6) revealed changes in the mRNA level of multiple TEs, either through upregulation (SHEF6) or downregulation (H9, H7S14, H7S6). This alteration has two possible sources, namely the influence of TEX19 or the effect of NANOG. In Chapter 5, *TEX19* transcript knockdown resulted in *NANOG* mRNA level upregulation in SHEF6 but *NANOG* transcript downregulation for the other hES cell lines. However, this observation opens another view that TEX19 could mediate TE regulation by influencing the stem cell markers, particularly *NANOG*. More importantly, *TEX19* mRNA reduction was found to alter the non-LTR retrotransposon group (*SINE* and *LINE-1*) in all tested hES cell lines, suggesting that it is required to maintain this group's expression. Remarkably, the depletion of *TEX19* transcript activated a specific HERV, namely *HERV K env*, in H7S14 and H7S6 indicating that hESCs may require TEX19 for the repression/deactivation of retrotransposons (HERVs). Correspondingly, the activation HERVs and dysregulation of TEs in pluripotent stem cells and germ cells has been posited to contribute to tumorigenesis and the development of a number of human genetic diseases (Bronson et al., 1984; Chen et al., 2005a; Galli et al., 2005).

In closing, different studies have reported that the alteration of TEs can change the genome sequences, resulting in the development of cancer and genetic disorders. Research focussing on these elements can be exceptionally valuable, as they are potential tumour biomarkers, and a deep understanding of their activation/repression may open new prospects for emerging clinical applications. The outcomes in this work elucidated a potential function for TEX19 in terms of controlling TEs either in cancer cells or in hESCs. Further studies are needed to explain the mysteries behind the dysregulation of TEs and the mechanism responsible for these elements. Another

important avenue of investigation whether the restricted *TEX19* expression in the testis and pluripotent stem cells aims to control TEs expression.

Chapter 7

Summary and general discussion

7. Summary and general discussion

Cancer is a leading cause of death worldwide, threatening the lives of many people; as a result, it is crucial to find a definitive treatment for this disease (Ferlay et al., 2015). Different biomarkers have been discovered that play key roles in detecting cancer and developing clinical applications (Joshi et al., 2016). CTA genes are tumour antigens with a potential function as cancer biomarkers/drug targets due to their exceptional expression, which is largely restricted to testis/germ tissues, and their production in different cancer types (Whitehurst, 2014). *TEX19* is a human-specific gene that was identified as a CTA gene in 2012 via conventional RT-PCR (Feichtinger et al., 2012), recently, this identification has been verified by Zhong and his co-workers (2016). In the current study, screening for this gene was advanced using different approaches, namely RT-PCR, RT-qPCR, WB and IHC to address whether *TEX19* expression is cancer specific. In line with this, our study confirmed that *TEX19* expression in the testis and numerous cancer cells supporting the definition of *TEX19* as a CTA gene. Correspondingly, murine *Tex19.1* expression was detected in mESCs (Kuntz et al., 2008). Our study investigated the expression of *TEX19* in hESCs, reprogrammed iPSCs and cancer stem-like cells, and the findings showed its positive presence. Taking all these results together, we can suggest that *TEX19* has a potential function in cancer and stem cells.

In a previous study, Kuntz and his colleagues elucidated the presence of murine Tex19.1 in the nucleus (Kuntz et al., 2008). Tex19.1 has also been detected in the cytoplasm during spermatogenesis (Öllinger et al., 2008). A recent study reported that human TEX19 is present as a cytoplasmic protein in Sertoli cells (Zhong et al., 2016). In line with this, our study showed that the cellular localisation of TEX19 involved dual localisation, as the TEX19 protein was detected in both the cytoplasm and the nucleus. This finding supports previous work showing that TEX19 does not have a specific cellular localisation and suggesting that it may act as a dynamic protein.

Several studies have linked the function of CTA genes to the promotion of proliferation in different cancer cells, such as breast cancer and melanoma cells (Lajmi et al., 2015; Maxfield et al., 2015; Wang et al., 2016b). Our study demonstrated that *TEX19* is

required for cancer cells, where its depletion drops the cell count and significantly reduces the self-renewal of cancer stem-like cells and cancer cells; this suggests a potential function for TEX19 to act as an oncogenic driver. Hence, this intrinsic feature could make *TEX19* a candidate therapeutic target for different cancer types.

TEX19 mRNA depletion in distinct cancer cells altered the transcript levels of multiple genes. Remarkably, a specific gene, *GPR137B*, was found to be substantially downregulated in two different cancer cell lines. In previous studies, the *GPR137B* gene was reported to promote cancer cell proliferation, and depletion of its expression inhibited cell proliferation in multiple cancer types (Zhang et al., 2014; Zong et al., 2014; Cui et al., 2015). Therefore, TEX19 depletion may contribute to reduce the proliferation in those cancer cells by reducing *GPR137B* transcript level. Furthermore, *TEX19* transcript depletion influenced the mRNAs of genes required for maintaining spermatogenesis, namely *PIWIL1* and *SEPT12*, indicating a possible role for TEX19 that is linked to the spermatogenesis process. Moreover, our analysis demonstrated that human PIWI orthologues (*PIWIL1-4*) require *TEX19* to control their expression, suggesting a potential function for TEX19 in maintaining the PIWI pathway. Hence, *TEX19* is a candidate transcription factor gene, but more investigations are required to determine whether it plays a definitive role in transcriptional regulation.

The function of CTA genes has been associated with stemness, and these genes are expressed in pluripotent stem cells (Costa et al., 2007; Yang et al., 2015). Our results demonstrated that human *TEX19* was significantly expressed in all examined hES cell lines, supporting the idea that CTA genes are linked to stemness. The transcription factor genes *OCT4*, *NANOG* and *SOX2* are essential to maintain the stemness features and self-renewal in hESCs, and their depletion leads to the loss of stemness characteristics (Singh et al., 2016). Our results demonstrated that the depletion of *TEX19* transcripts in hES cell lines resulted in altered mRNA levels of the pluripotent markers *OCT4* and *NANOG*, while the transcript level of *SOX2* did not change; this suggests a possible role of TEX19 in the regulation of stem cell markers. Furthermore, the depletion of *TEX19* influenced the mRNAs of human PIWI orthologues (*PIWIL2* and *PIWIL4*) in hESCs; to some extent, this confirms the results obtained in cancer cell lines, where TEX19 might be required to control the expression of *PIWI* transcripts.

In a previous study, murine *Tex19.1* expression was found to decline in parallel with *Oct4* when mESCs undergo differentiation, suggesting its function as a pluripotent marker (Kuntz et al., 2008). Our analysis showed a non-stable *TEX19* transcript levels in hES cell lines undergoing the differentiation process. The differentiation of the H7S6 hES cell line and NTERA2 (Stem cell model) showed a reduction in *TEX19* levels upon the decline/ceasing of *OCT4* mRNA. Taking these results together, we can suggest that *TEX19* could be linked to *OCT4* and that it may be required for pluripotency.

It has been previously reported that *Tex19.1* regulates TEs in mice (Öllinger et al., 2008; Reichmann et al., 2013). In line with previous studies, our analysis demonstrated alteration in TE transcript levels in cancer cell lines and hES cell lines, providing evidence that TEX19 can act as a TE regulator. A specific *HERV K 107* was found to be a common element upregulated in all tested cancer cell lines, indicating a possible interface function with *TEX19*. In hESCs, our study demonstrated that *NANOG* expression is linked to the upregulation/downregulation of TE transcript levels following *TEX19* transcript reduction, indicating the possibility that TEX19 could alter TEs through its influence on pluripotent markers. More interestingly, our data demonstrated the *TEX19*'s ability to activate a specific *HERV K ENV* expression in two hES cell lines, indicating a potential influence whereby hESCs need *TEX19* to suppress HERV expression. However, further exterminations are necessary to conclusively determine whether TEX19 regulate TEs directly or by influencing other involved genes.

In closing, we believe TEX19 could prove valuable in developing clinical applications due to its cancer-associated properties and its emergence as an anti-cancer therapeutic target. Moreover, our findings in the present study suggest that TEX19 may have a pivotal role in pluripotent stem cells, as well. Taken together, these characteristics indicate that *TEX19* is a gene worthy of further pursuit in human cancer cells and stem cells.

8. References

Abdel-Aziz, M.M., Elshal, M.F., Abass, A.T., El-Kafrawy, S., Ezzat, S. & Abdel-Wahab, M. 2016. Comparison of AFP-L3 and p53 Antigen Concentration with Alpha-Fetoprotein as Serum Markers for Hepatocellular Carcinoma. *Clinical laboratory.* 62 (6). pp. 1121-1129.

Abeyta, M.J., Clark, A.T., Rodriguez, R.T., Bodnar, M.S., Pera, R.A. & Firpo, M.T. 2004. Unique gene expression signatures of independently-derived human embryonic stem cell lines. *Human molecular genetics.* 13 (6). pp. 601-608.

Adams, S., Greeder, L., Reich, E., Shao, Y., Fosina, D., Hanson, N., Tassello, J., Singh, B., Spagnoli, G.C. & Demaria, S. 2011. Expression of cancer testis antigens in human BRCA-associated breast cancers: potential targets for immunoprevention? *Cancer immunology, immunotherapy.* 60 (7). pp. 999-1007.

Ajani, J.A., Song, S., Hochster, H.S. & Steinberg, I.B. 2015. Cancer stem cells: the promise and the potential. *Seminars in oncology.* Elsevier: pp. S3.

Akers, S.N., Odunsi, K. & Karpf, A.R. 2010. Regulation of cancer germline antigen gene expression: implications for cancer immunotherapy. *Future oncology.* 6 (5). pp. 717-732.

Andrews, R.G., Singer, J.W. & Bernstein, I.D. 1989. Precursors of colony-forming cells in humans can be distinguished from colony-forming cells by expression of the CD33 and CD34 antigens and light scatter properties. *The Journal of experimental medicine.* 169 (5). pp. 1721-1731.

Aravin, A.A., Sachidanandam, R., Girard, A., Fejes-Toth, K. & Hannon, G.J. 2007. Developmentally regulated piRNA clusters implicate MILI in transposon control. *Science (New York, N.Y.).* 316 (5825). pp. 744-747.

Assanga, I. & Lujan, L. 2013. Cell growth curves for different cell lines and their relationship with biological activities. *International Journal of Biotechnology and Molecular Biology Research.* 4 (4). pp. 60-70.

Autier, P. 2016. Age at cancer diagnosis and interpretation of survival statistics. *The Lancet Oncology.*

Bagci, O. & Kurtgöz, S. 2015. Amplification of cellular oncogenes in solid tumors. *North American journal of medical sciences.* 7 (8). pp. 341.

Baum, C.M., Weissman, I.L., Tsukamoto, A.S., Buckle, A.M. & Peault, B. 1992. Isolation of a candidate human hematopoietic stem-cell population. *Proceedings of the National Academy of Sciences of the United States of America.* 89 (7). pp. 2804-2808.

Baxter, D. 2014. Active and passive immunization for cancer. *Human vaccines & immunotherapeutics.* 10 (7). pp. 2123-2129.

Beaupre, D.M. & Kurzrock, R. 1999. RAS and leukemia: from basic mechanisms to gene-directed therapy. *Journal of clinical oncology : official journal of the American Society of Clinical Oncology.* 17 (3). pp. 1071-1079.

Belancio, V.P., Deininger, P.L. & Roy-Engel, A.M. 2009. LINE dancing in the human genome: transposable elements and disease. *Genome medicine.* 1 (10). pp. 1.

Berlin, A., Lalonde, E., Sykes, J., Zafarana, G., Chu, K.C., Ramnarine, V.R., Ishkanian, A., Sendorek, D.H., Pasic, I. & Lam, W.L. 2014. NBN gain is predictive for adverse outcome following image-guided radiotherapy for localized prostate cancer. *Oncotarget.* 5 (22). pp. 11081-11090.

Bianchetti, L., Tarabay, Y., Lecompte, O., Stote, R., Poch, O., Dejaegere, A. & Viville, S. 2015. Tex19 and Sectm1 concordant molecular phylogenies support co-evolution of both eutherian-specific genes. *BMC evolutionary biology.* 15 (1). pp. 1.

Bianco, P. 2014. "Mesenchymal" stem cells. *Annual Review of Cell and Developmental Biology.* 30 pp. 677-704.

Bianco, P., Kuznetsov, S.A., Riminucci, M. & Robey, P.G. 2006. [6]-Postnatal Skeletal Stem Cells. *Methods in enzymology.* 419 pp. 117-148.

Bianco, P. & Robey, P.G. 2015. Skeletal stem cells. *Development (Cambridge, England).* 142 (6). pp. 1023-1027.

Bieback, K. & Netsch, P. 2016. Isolation, Culture, and Characterization of Human Umbilical Cord Blood-Derived Mesenchymal Stromal Cells. *Mesenchymal Stem Cells: Methods and Protocols.* pp. 245-258.

Bonini, C. & Mondino, A. 2015. Adoptive T-cell therapy for cancer: The era of engineered T cells. *European journal of immunology.* 45 (9). pp. 2457-2469.

Borovski, T., De Sousa E Melo, F., Vermeulen, L. & Medema, J.P. 2011. Cancer stem cell niche: the place to be. *Cancer research.* 71 (3). pp. 634-639.

Boyer, L.A., Lee, T.I., Cole, M.F., Johnstone, S.E., Levine, S.S., Zucker, J.P., Guenther, M.G., Kumar, R.M., Murray, H.L. & Jenner, R.G. 2005. Core transcriptional regulatory circuitry in human embryonic stem cells. *Cell.* 122 (6). pp. 947-956.

Braam, S.R., Zeinstra, L., Litjens, S., Ward-van Oostwaard, D., van den Brink, S., van Laake, L., Lebrin, F., Kats, P., Hochstenbach, R. & Passier, R. 2008. Recombinant Vitronectin Is a Functionally Defined Substrate That Supports Human Embryonic Stem Cell Self-Renewal via αVβ5 Integrin. *Stem cells.* 26 (9). pp. 2257-2265.

Brábek, J., Mierke, C.T., Rösel, D., Veselý, P. & Fabry, B. 2010. The role of the tissue microenvironment in the regulation of cancer cell motility and invasion. *Cell Communication and Signaling.* 8 (1). pp. 1.

Bray, F. 2014. Transitions in human development and the global cancer burden. *World cancer report.* pp. 54-68.

Bright, R.K., Bright, J.D. & Byrne, J.A. 2014. Overexpressed oncogenic tumor-self antigens: New vaccine targets. *Human vaccines & immunotherapeutics.* 10 (11). pp. 3297-3305.

Bronson, D.L., Saxinger, W., Ritzi, D.M. & Fraley, E.E. 1984. Production of virions with retrovirus morphology by human embryonal carcinoma cells in vitro. *Journal of general virology.* 65 (6). pp. 1043-1051.

Burger, M., Catto, J.W., Dalbagni, G., Grossman, H.B., Herr, H., Karakiewicz, P., Kassouf, W., Kiemeney, L.A., La Vecchia, C. & Shariat, S. 2013. Epidemiology and risk factors of urothelial bladder cancer. *European urology.* 63 (2). pp. 234-241.

Caballero, O.L. & Chen, Y. 2009. Cancer/testis (CT) antigens: potential targets for immunotherapy. *Cancer science.* 100 (11). pp. 2014-2021.

Cavaleri, F. & Schöler, H.R. 2003. Nanog: a new recruit to the embryonic stem cell orchestra. *Cell.* 113 (5). pp. 551-552.

Celebi, C., Van Montfoort, A., Skory, V., Kieffer, E., Kuntz, S., Mark, M. & Viville, S. 2012. Tex 19 paralogs exhibit a gonad and placenta-specific expression in the mouse. *Journal of Reproduction and Development.* 58 (3). pp. 360-365.

Chadwick, K., Wang, L., Li, L., Menendez, P., Murdoch, B., Rouleau, A. & Bhatia, M. 2003. Cytokines and BMP-4 promote hematopoietic differentiation of human embryonic stem cells. *Blood.* 102 (3). pp. 906-915.

Chalmel, F., Rolland, A.D., Niederhauser-Wiederkehr, C., Chung, S.S., Demougin, P., Gattiker, A., Moore, J., Patard, J.J., Wolgemuth, D.J., Jegou, B. & Primig, M. 2007. The conserved transcriptome in human and rodent male gametogenesis. *Proceedings of the National Academy of Sciences of the United States of America.* 104 (20). pp. 8346-8351.

Chambers, I., Colby, D., Robertson, M., Nichols, J., Lee, S., Tweedie, S. & Smith, A. 2003. Functional expression cloning of Nanog, a pluripotency sustaining factor in embryonic stem cells. *Cell.* 113 (5). pp. 643-655.

Chambers, I., Silva, J., Colby, D., Nichols, J., Nijmeijer, B., Robertson, M., Vrana, J., Jones, K., Grotewold, L. & Smith, A. 2007. Nanog safeguards pluripotency and mediates germline development. *Nature.* 450 (7173). pp. 1230-1234.

Chamling, X., Sluch, V.M. & Zack, D.J. 2016. The Potential of Human Stem Cells for the Study and Treatment of GlaucomaHuman Stem Cell for Treatment of

Glaucoma. *Investigative ophthalmology & visual science.* 57 (5). pp. ORSFi1-ORSFi6.

Cheema, Z., Hari-Gupta, Y., Kita, G., Farrar, D., Seddon, I., Corr, J. & Klenova, E. 2014. Expression of the cancer-testis antigen BORIS correlates with prostate cancer. *The Prostate.* 74 (2). pp. 164-176.

Chen, J., Stenson, P.D., Cooper, D.N. & Férec, C. 2005a. A systematic analysis of LINE-1 endonuclease-dependent retrotranspositional events causing human genetic disease. *Human genetics.* 117 (5). pp. 411-427.

Chen, K., Huang, Y. & Chen, J. 2013. Understanding and targeting cancer stem cells: therapeutic implications and challenges. *Acta Pharmacologica Sinica.* 34 (6). pp. 732-740.

Chen, Y., Venditti, C.A., Theiler, G., Stevenson, B.J., Iseli, C., Gure, A.O., Jongeneel, C.V., Old, L.J. & Simpson, A.J. 2005b. Identification of CT46/HORMAD1, an immunogenic cancer/testis antigen encoding a putative meiosis-related protein. *Cancer Immunity Archive.* 5 (1). pp. 9.

Chen, J., Gao, W., Zhou, P., Ma, X., Tschudy-Seney, B., Liu, C., Zern, M.A., Liu, P. & Duan, Y. 2016. Enhancement of hepatocyte differentiation from human embryonic stem cells by Chinese medicine Fuzhenghuayu. *Scientific reports.* 6 pp. 18841.

Chen, Y.T., Scanlan, M.J., Sahin, U., Tureci, O., Gure, A.O., Tsang, S., Williamson, B., Stockert, E., Pfreundschuh, M. & Old, L.J. 1997. A testicular antigen aberrantly expressed in human cancers detected by autologous antibody screening. *Proceedings of the National Academy of Sciences of the United States of America.* 94 (5). pp. 1914-1918.

Chénais, B. 2013. Transposable elements and human cancer: a causal relationship? *Biochimica et Biophysica Acta (BBA)-Reviews on Cancer.* 1835 (1). pp. 28-35.

Cheng, Y., Wong, E.W. & Cheng, C.Y. 2011. Cancer/testis (CT) antigens, carcinogenesis and spermatogenesis. *Spermatogenesis.* 1 (3). pp. 209-220.

Chiriva, M., Yu, Y., Mirandola, L., Jenkins, M., Chapman, C., Cannon, M., Cobos, E. & Kast, W.M. 2010. Effective prevention and therapy of ovarian cancer with sperm protein 17 vaccination (95.7). *The Journal of Immunology.* 184 (1 Supplement). pp. 95.7-95.7.

Chomez, P., De Backer, O., Bertrand, M., De Plaen, E., Boon, T. & Lucas, S. 2001. An overview of the MAGE gene family with the identification of all human members of the family. *Cancer research.* 61 (14). pp. 5544-5551.

Chu, C. & Liaw, Y. 2016. Natural History of Hepatitis B Virus Infection. In: *Hepatitis B Virus in Human Diseases.* Springer: pp. 217-247.

Civin, C.I., Strauss, L.C., Brovall, C., Fackler, M.J., Schwartz, J.F. & Shaper, J.H. 1984. Antigenic analysis of hematopoiesis. III. A hematopoietic progenitor cell surface antigen defined by a monoclonal antibody raised against KG-1a cells. *Journal of immunology (Baltimore, Md.: 1950).* 133 (1). pp. 157-165.

Clarke, M. & Frampton, J. 2016. Hematopoietic Stem Cells. In: *Regenerative Medicine-from Protocol to Patient.* Springer: pp. 111-143.

Clevers, H. 2015. STEM CELLS. What is an adult stem cell? *Science (New York, N.Y.).* 350 (6266). pp. 1319-1320.

Collins, A.T., Berry, P.A., Hyde, C., Stower, M.J. & Maitland, N.J. 2005. Prospective identification of tumorigenic prostate cancer stem cells. *Cancer research.* 65 (23). pp. 10946-10951.

Condic, M.L. 2013. Totipotency: what it is and what it is not. *Stem cells and development.* 23 (8). pp. 796-812.

Contreras-Galindo, R., Kaplan, M.H., Leissner, P., Verjat, T., Ferlenghi, I., Bagnoli, F., Giusti, F., Dosik, M.H., Hayes, D.F., Gitlin, S.D. & Markovitz, D.M. 2008. Human endogenous retrovirus K (HML-2) elements in the plasma of people with lymphoma and breast cancer. *Journal of virology.* 82 (19). pp. 9329-9336.

Cordaux, R. & Batzer, M.A. 2009. The impact of retrotransposons on human genome evolution. *Nature Reviews Genetics.* 10 (10). pp. 691-703.

Costa, F.F., Le Blanc, K. & Brodin, B. 2007. Concise review: cancer/testis antigens, stem cells, and cancer. *Stem cells.* 25 (3). pp. 707-711.

Croce, C.M. 2008. Oncogenes and cancer. *New England journal of medicine.* 358 (5). pp. 502-511.

Cronwright, G., Le Blanc, K., Gotherstrom, C., Darcy, P., Ehnman, M. & Brodin, B. 2005. Cancer/testis antigen expression in human mesenchymal stem cells: down-regulation of SSX impairs cell migration and matrix metalloproteinase 2 expression. *Cancer research.* 65 (6). pp. 2207-2215.

Cui, X., Liu, Y., Wang, B., Xian, G., Liu, X., Tian, X. & Qin, C. 2015. Knockdown of GPR137 by RNAi inhibits pancreatic cancer cell growth and induces apoptosis. *Biotechnology and applied biochemistry.* 62 (6). pp. 861-867.

Damdimopoulou, P., Rodin, S., Stenfelt, S., Antonsson, L., Tryggvason, K. & Hovatta, O. 2016. Human embryonic stem cells. *Best Practice & Research Clinical Obstetrics & Gynaecology.* 31 pp. 2-12.

Davies, H., Bignell, G.R., Cox, C., Stephens, P., Edkins, S., Clegg, S., Teague, J., Woffendin, H., Garnett, M.J. & Bottomley, W. 2002. Mutations of the BRAF gene in human cancer. *Nature.* 417 (6892). pp. 949-954.

De Backer, O., Arden, K.C., Boretti, M., Vantomme, V., De Smet, C., Czekay, S., Viars, C.S., De Plaen, E., Brasseur, F., Chomez, P., Van den Eynde, B., Boon, T. & van der Bruggen, P. 1999. Characterization of the GAGE genes that are expressed in various human cancers and in normal testis. *Cancer research.* 59 (13). pp. 3157-3165.

de Lima, M., McNiece, I., Robinson, S.N., Munsell, M., Eapen, M., Horowitz, M., Alousi, A., Saliba, R., McMannis, J.D. & Kaur, I. 2012. Cord-blood engraftment with ex vivo mesenchymal-cell coculture. *New England Journal of Medicine.* 367 (24). pp. 2305-2315.

De Mot, L., Gonze, D., Bessonnard, S., Chazaud, C., Goldbeter, A. & Dupont, G. 2016. Cell fate specification based on tristability in the inner cell mass of mouse blastocysts. *Biophysical journal.* 110 (3). pp. 710-722.

de Vries, F.A., de Boer, E., van den Bosch, M., Baarends, W.M., Ooms, M., Yuan, L., Liu, J.G., van Zeeland, A.A., Heyting, C. & Pastink, A. 2005. Mouse Sycp1 functions in synaptonemal complex assembly, meiotic recombination, and XY body formation. *Genes & development.* 19 (11). pp. 1376-1389.

DE, E., VAN DEN, B., Knuth, A. & BOONT, T. 1991. A gene encoding an antigen recognized by cytolytic T lymphocytes on a human melanoma.

Delaney, C., Heimfeld, S., Brashem-Stein, C., Voorhies, H., Manger, R.L. & Bernstein, I.D. 2010. Notch-mediated expansion of human cord blood progenitor cells capable of rapid myeloid reconstitution. *Nature medicine.* 16 (2). pp. 232-236.

Demetris Iacovides, S.M., Achilleos, C. & Strati, K. 2014. Shared mechanisms in stemness and carcinogenesis: lessons from oncogenic viruses. *Model organisms in inflammation and cancer.*

Dennis, J.E., Carbillet, J., Caplan, A. & Charbord, P. 2001. The STRO-1 marrow cell population is multipotential. *Cells Tissues Organs.* 170 (2-3). pp. 73-82.

Dewannieux, M. & Heidmann, T. 2013. Endogenous retroviruses: acquisition, amplification and taming of genome invaders. *Current opinion in virology.* 3 (6). pp. 646-656.

Dhivya, S. & Premkumar, K. 2016. Nomadic genetic elements contribute to oncogenic translocations: Implications in carcinogenesis. *Critical reviews in oncology/hematology.* 98 pp. 81-93.

Dick, D. 1997. Human acute myeloid leukemia is organized as a hierarchy that originates from a primitive hematopoietic cell. *Nature Med.* 3 pp. 730-737.

Ding, D., Shyu, W. & Lin, S. 2011. Mesenchymal stem cells. *Cell transplantation.* 20 (1). pp. 5-14.

Downey, R.F., Sullivan, F.J., Wang-Johanning, F., Ambs, S., Giles, F.J. & Glynn, S.A. 2015. Human endogenous retrovirus K and cancer: Innocent bystander or tumorigenic accomplice? *International Journal of Cancer.* 137 (6). pp. 1249-1257.

Dragon, F., Pogacic, V. & Filipowicz, W. 2000. In vitro assembly of human H/ACA small nucleolar RNPs reveals unique features of U17 and telomerase RNAs. *Molecular and cellular biology.* 20 (9). pp. 3037-3048.

Draper, J.S., Pigott, C., Thomson, J.A. & Andrews, P.W. 2002. Surface antigens of human embryonic stem cells: changes upon differentiation in culture. *Journal of anatomy.* 200 (3). pp. 249-258.

Durairajanayagam, D., Rengan, A.K., Sharma, R.K. & Agarwal, A. 2015. Introduction to the Male Reproductive System. *Unexplained Infertility: Pathophysiology, Evaluation and Treatment.* pp. 29.

Elbarbary, R.A., Lucas, B.A. & Maquat, L.E. 2016. Retrotransposons as regulators of gene expression. *Science.* 351 (6274). pp. aac7247.

Evans, M.J. & Kaufman, M.H. 1981. Establishment in culture of pluripotential cells from mouse embryos. *Nature.* 292 (5819). pp. 154-156.

Feichtinger, J., Aldeailej, I., Anderson, R., Almutairi, M., Almatrafi, A., Alsiwiehri, N., Griffiths, K., Stuart, N., Wakeman, J.A., Larcombe, L. & McFarlane, R.J. 2012. Meta-analysis of clinical data using human meiotic genes identifies a novel cohort of highly restricted cancer-specific marker genes. *Oncotarget.* 3 (8). pp. 843-853.

Feichtinger, J., McFarlane, R.J. & Larcombe, L.D. 2014. CancerEST: a web-based tool for automatic meta-analysis of public EST data. *Database : the journal of biological databases and curation.* 2014 (0). pp. bau024.

Felfly, H. & Haddad, G.G. 2014. Hematopoietic stem cells: potential new applications for translational medicine. *Journal of stem cells.* 9 (3). pp. 163.

Ferguson, L.R., Chen, H., Collins, A.R., Connell, M., Damia, G., Dasgupta, S., Malhotra, M., Meeker, A.K., Amedei, A. & Amin, A. 2015. Genomic instability in human cancer: Molecular insights and opportunities for therapeutic attack and prevention through diet and nutrition. *Seminars in cancer biology.* Elsevier: pp. S5.

Ferlay, J., Soerjomataram, I., Dikshit, R., Eser, S., Mathers, C., Rebelo, M., Parkin, D.M., Forman, D. & Bray, F. 2015. Cancer incidence and mortality worldwide: sources, methods and major patterns in GLOBOCAN 2012. *International journal of cancer.* 136 (5). pp. E359-E386.

Fong, H., Hohenstein, K.A. & Donovan, P.J. 2008. Regulation of self-renewal and pluripotency by Sox2 in human embryonic stem cells. *Stem cells.* 26 (8). pp. 1931-1938.

Fratta, E., Coral, S., Covre, A., Parisi, G., Colizzi, F., Danielli, R., Nicolay, H.J.M., Sigalotti, L. & Maio, M. 2011. The biology of cancer testis antigens: putative function, regulation and therapeutic potential. *Molecular oncology.* 5 (2). pp. 164-182.

Friedmann-Morvinski, D. & Verma, I.M. 2014. Dedifferentiation and reprogramming: origins of cancer stem cells. *EMBO reports.* 15 (3). pp. 244-253.

Fu, T., Hsieh, I., Cheng, J., Tsai, M., Hou, Y., Lee, J., Liou, H., Huang, S., Chen, H. & Yen, L. 2016. Association of OCT4, SOX2, and NANOG expression with oral squamous cell carcinoma progression. *Journal of Oral Pathology & Medicine.* 45 (2). pp. 89-95.

Fukuda, K. 2016. *Human IPS Cells in Disease Modelling.* Springer: .

Galli, U.M., Sauter, M., Lecher, B., Maurer, S., Herbst, H., Roemer, K. & Mueller-Lantzsch, N. 2005. Human endogenous retrovirus rec interferes with germ cell development in mice and may cause carcinoma in situ, the predecessor lesion of germ cell tumors. *Oncogene.* 24 (19). pp. 3223-3228.

Gaskell, T., Englund, M.C. & Hyllner, J. 2016. Human Embryonic Stem Cells. In: *Regenerative Medicine-from Protocol to Patient.* Springer: pp. 27-49.

Gaugler, B., Van den Eynde, B., van der Bruggen, P., Romero, P., Gaforio, J.J., De Plaen, E., Lethe, B., Brasseur, F. & Boon, T. 1994. Human gene MAGE-3 codes for an antigen recognized on a melanoma by autologous cytolytic T lymphocytes. *The Journal of experimental medicine.* 179 (3). pp. 921-930.

Ghafouri-Fard, S. 2015. Expression of cancer-testis antigens in stem cells: is it a potential drawback or an advantage in cancer immunotherapy. *Asian Pacific journal of cancer prevention : APJCP.* 16 (7). pp. 3079-3081.

Ghafouri-Fard, S. & Modarressi, M.H. 2009. Cancer-testis antigens: potential targets for cancer immunotherapy. *Archives of Iranian medicine.* 12 (4). pp. 395-404.

Gjerstorff, M.F., Andersen, M.H. & Ditzel, H.J. 2015. Oncogenic cancer/testis antigens: prime candidates for immunotherapy. *Oncotarget.* 6 (18). pp. 15772-15787.

Goodell, M.A., Nguyen, H. & Shroyer, N. 2015. Somatic stem cell heterogeneity: diversity in the blood, skin and intestinal stem cell compartments. *Nature Reviews Molecular Cell Biology.* 16 (5). pp. 299-309.

Grégoire, L., Haudry, A. & Lerat, E. 2016. The transposable element environment of human genes is associated with histone and expression changes in cancer. *BMC genomics.* 17 (1). pp. 588.

Greve, K.B., Lindgreen, J.N., Terp, M.G., Pedersen, C.B., Schmidt, S., Mollenhauer, J., Kristensen, S.B., Andersen, R.S., Relster, M.M. & Ditzel, H.J. 2015. Ectopic

expression of cancer/testis antigen SSX2 induces DNA damage and promotes genomic instability. *Molecular oncology.* 9 (2). pp. 437-449.

Grizzi, F., Mirandola, L., Qehajaj, D., Cobos, E., Figueroa, J. & Chiriva-Internati, M. 2015. Cancer-testis antigens and immunotherapy in the light of cancer complexity. *International reviews of immunology.* 34 (2). pp. 143-153.

Groth, S Fazekas de St 1982. The evaluation of limiting dilution assays. *Journal of immunological methods.* 49 (2). pp. R11-R23.

Grube, M., Holler, E., Weber, D., Holler, B., Herr, W. & Wolff, D. 2016. Risk Factors and Outcome of Chronic Graft-versus-Host Disease after Allogeneic Stem Cell Transplantation—Results from a Single-Center Observational Study. *Biology of Blood and Marrow Transplantation.*

Gu, A., Ji, G., Shi, X., Long, Y., Xia, Y., Song, L., Wang, S. & Wang, X. 2010. Genetic variants in Piwi-interacting RNA pathway genes confer susceptibility to spermatogenic failure in a Chinese population. *Human reproduction (Oxford, England).* 25 (12). pp. 2955-2961.

Gupta, S., Termini, J.M., Rivas, Y., Otero, M., Raffa, F.N., Bhat, V., Farooq, A. & Stone, G.W. 2015. A multi-trimeric fusion of CD40L and gp100 tumor antigen activates dendritic cells and enhances survival in a B16-F10 melanoma DNA vaccine model. *Vaccine.* 33 (38). pp. 4798-4806.

Guzel, E., Karatas, O.F., Duz, M.B., Solak, M., Ittmann, M. & Ozen, M. 2014. Differential expression of stem cell markers and ABCG2 in recurrent prostate cancer. *The Prostate.* 74 (15). pp. 1498-1505.

Haeckel, E. 1874. Anthropogenie. Leipzig.

Hanahan, D. & Coussens, L.M. 2012. Accessories to the crime: functions of cells recruited to the tumor microenvironment. *Cancer cell.* 21 (3). pp. 309-322.

Hanahan, D. & Weinberg, R.A. 2011. Hallmarks of cancer: the next generation. *Cell.* 144 (5). pp. 646-674.

Hanahan, D. & Weinberg, R.A. 2000. The hallmarks of cancer. *Cell.* 100 (1). pp. 57-70.

Haren, L., Ton-Hoang, B. & Chandler, M. 1999. Integrating DNA: transposases and retroviral integrases. *Annual Reviews in Microbiology.* 53 (1). pp. 245-281.

Hastreiter, S. & Schroeder, T. 2016. Nanog dynamics in single embryonic stem cells. *Cell Cycle.* 15 (6). pp. 770-771.

Hay, D.C., Sutherland, L., Clark, J. & Burdon, T. 2004. Oct-4 knockdown induces similar patterns of endoderm and trophoblast differentiation markers in human and mouse embryonic stem cells. *Stem cells.* 22 (2). pp. 225-235.

Heidenreich, A., Bastian, P.J., Bellmunt, J., Bolla, M., Joniau, S., van der Kwast, T., Mason, M., Matveev, V., Wiegel, T. & Zattoni, F. 2014. EAU guidelines on prostate cancer. Part 1: screening, diagnosis, and local treatment with curative intent—update 2013. *European urology.* 65 (1). pp. 124-137.

Henschler, R. 2016. Hematopoietic Stem Cells. *Encyclopedia of Immunotoxicology.* pp. 364-369.

Hirko, K.A., Chen, W.Y., Willett, W.C., Rosner, B.A., Hankinson, S.E., Beck, A.H., Tamimi, R.M. & Eliassen, A.H. 2016. Alcohol consumption and risk of breast cancer by molecular subtype: Prospective analysis of the nurses' health study after 26 years of follow-up. *International Journal of Cancer.* 138 (5). pp. 1094-1101.

Hirohashi, Y., Torigoe, T., Tsukahara, T., Kanaseki, T., Kochin, V. & Sato, N. 2016. Immune responses to human cancer stem-like cells/cancer-initiating cells. *Cancer science.* 107 (1). pp. 12-17.

Hofmann, O., Caballero, O.L., Stevenson, B.J., Chen, Y.T., Cohen, T., Chua, R., Maher, C.A., Panji, S., Schaefer, U., Kruger, A., Lehvaslaiho, M., Carninci, P., Hayashizaki, Y., Jongeneel, C.V., Simpson, A.J., Old, L.J. & Hide, W. 2008. Genome-wide analysis of cancer/testis gene expression. *Proceedings of the National Academy of Sciences of the United States of America.* 105 (51). pp. 20422-20427.

Hong, N., Li, M., He, B. & Hong, Y. Retinoic Acid Regulates Germ Gene Transcription In Vitro and Spermatogenesis in Testicular Organ Culture. *Biological Systems: Open Access.*

Hu, K. 2014. All roads lead to induced pluripotent stem cells: the technologies of iPSC generation. *Stem cells and development.* 23 (12). pp. 1285-1300.

Hu, Y. & Smyth, G.K. 2009. ELDA: extreme limiting dilution analysis for comparing depleted and enriched populations in stem cell and other assays. *Journal of immunological methods.* 347 (1). pp. 70-78.

Huang, C.R., Burns, K.H. & Boeke, J.D. 2012. Active transposition in genomes. *Annual Review of Genetics.* 46 pp. 651-675.

Hunder, N.N., Wallen, H., Cao, J., Hendricks, D.W., Reilly, J.Z., Rodmyre, R., Jungbluth, A., Gnjatic, S., Thompson, J.A. & Yee, C. 2008. Treatment of metastatic melanoma with autologous CD4 T cells against NY-ESO-1. *New England Journal of Medicine.* 358 (25). pp. 2698-2703.

Hung, M.C. & Link, W. 2011. Protein localization in disease and therapy. *Journal of cell science.* 124 (Pt 20). pp. 3381-3392.

Hutchins, A.P. & Pei, D. 2015. Transposable elements at the center of the crossroads between embryogenesis, embryonic stem cells, reprogramming, and long non-coding RNAs. *Science bulletin.* 60 (20). pp. 1722-1733.

Hyslop, L., Stojkovic, M., Armstrong, L., Walter, T., Stojkovic, P., Przyborski, S., Herbert, M., Murdoch, A., Strachan, T. & Lako, M. 2005. Downregulation of NANOG induces differentiation of human embryonic stem cells to extraembryonic lineages. *Stem cells.* 23 (8). pp. 1035-1043.

Ishiguro, K., Kim, J., Fujiyama-Nakamura, S., Kato, S. & Watanabe, Y. 2011. A new meiosis-specific cohesin complex implicated in the cohesin code for homologous pairing. *EMBO reports.* 12 (3). pp. 267-275.

Issaragrisil, S. & Kunacheewa, C. 2016. Matched sibling donor hematopoietic stem cell transplantation for thalassemia. *Current opinion in hematology.*

Jagadish, N., Parashar, D., Gupta, N., Agarwal, S., Sharma, A., Fatima, R., Suri, V., Kumar, R., Gupta, A. & Lohiya, N.K. 2016. A novel cancer testis antigen target a-kinase anchor protein (AKAP4) for the early diagnosis and immunotherapy of colon cancer. *OncoImmunology.* 5 (2). pp. e1078965.

Jager, E., Chen, Y.T., Drijfhout, J.W., Karbach, J., Ringhoffer, M., Jager, D., Arand, M., Wada, H., Noguchi, Y., Stockert, E., Old, L.J. & Knuth, A. 1998. Simultaneous humoral and cellular immune response against cancer-testis antigen NY-ESO-1: definition of human histocompatibility leukocyte antigen (HLA)-A2-binding peptide epitopes. *The Journal of experimental medicine.* 187 (2). pp. 265-270.

Jemal, A., Bray, F., Center, M.M., Ferlay, J., Ward, E. & Forman, D. 2011. Global cancer statistics. *CA: a cancer journal for clinicians.* 61 (2). pp. 69-90.

Jez, M., Ambady, S., Kashpur, O., Grella, A., Malcuit, C., Vilner, L., Rozman, P. & Dominko, T. 2014. Expression and differentiation between OCT4A and its pseudogenes in human ESCs and differentiated adult somatic cells. *PloS one.* 9 (2). pp. e89546.

Jiang, Y., Vaessen, B., Lenvik, T., Blackstad, M., Reyes, M. & Verfaillie, C.M. 2002. Multipotent progenitor cells can be isolated from postnatal murine bone marrow, muscle, and brain. *Experimental hematology.* 30 (8). pp. 896-904.

Jones, R.E. & Lopez, K.H. 2013. *Human reproductive biology.* Academic Press: .

Joshi, G., Kaur, R. & Kaur, H. 2016. Biomarkers in cancer.

Jung, Y. & A Nolta, J. 2016. BMI1 regulation of self-renewal and multipotency in human mesenchymal stem cells. *Current stem cell research & therapy.* 11 (2). pp. 131-140.

Jungbluth, A.A., Busam, K.J., Kolb, D., Iversen, K., Coplan, K., Chen, Y., Spagnoli, G.C. & Old, L.J. 2000. Expression of MAGE-antigens in normal tissues and cancer. *International journal of cancer.* 85 (4). pp. 460-465.

Kalervo Väänänen, H. 2005. Mesenchymal stem cells. *Annals of Medicine.* 37 (7). pp. 469-479.

Kalmykova, A.I., Klenov, M.S. & Gvozdev, V.A. 2005. Argonaute protein PIWI controls mobilization of retrotransposons in the Drosophila male germline. *Nucleic acids research.* 33 (6). pp. 2052-2059.

Kandoth, C., McLellan, M.D., Vandin, F., Ye, K., Niu, B., Lu, C., Xie, M., Zhang, Q., McMichael, J.F. & Wyczalkowski, M.A. 2013. Mutational landscape and significance across 12 major cancer types. *Nature.* 502 (7471). pp. 333-339.

Karley, D., Gupta, D. & Tiwari, A. 2011. Biomarker for cancer: A great promise for future. *World Journal of Oncology.* 2 (4). pp. 151-157.

Kaufhold, S., Garbán, H. & Bonavida, B. 2016. Yin Yang 1 is associated with cancer stem cell transcription factors (SOX2, OCT4, BMI1) and clinical implication. *Journal of Experimental & Clinical Cancer Research.* 35 (1). pp. 1.

Kehler, J., Tolkunova, E., Koschorz, B., Pesce, M., Gentile, L., Boiani, M., Lomeli, H., Nagy, A., McLaughlin, K.J., Scholer, H.R. & Tomilin, A. 2004. Oct4 is required for primordial germ cell survival. *EMBO reports.* 5 (11). pp. 1078-1083.

Kelland, K. 2014, Archaeologists discover earliest example of human with cancer, Reuters, London.

Kelderman, S. & Kvistborg, P. 2016. Tumor antigens in human cancer control. *Biochimica et Biophysica Acta (BBA)-Reviews on Cancer.* 1865 (1). pp. 83-89.

Keller, G. & Gadue, P. 2016. *Mesoderm and definitive endoderm cell populations.*

Keller, G. 2005. Embryonic stem cell differentiation: emergence of a new era in biology and medicine. *Genes & development.* 19 (10). pp. 1129-1155.

Kemp, J.R. & Longworth, M.S. 2015. Crossing the LINE Toward Genomic Instability: LINE-1 Retrotransposition in Cancer. *Frontiers in chemistry.* 3.

Kim, H. 2012. Genomic impact, chromosomal distribution and transcriptional regulation of HERV elements. *Molecules and cells.* 33 (6). pp. 539-544.

Kim, S. 2015. New and emerging factors in tumorigenesis: an overview. *Cancer management and research.* 7 pp. 225.

Kim, Y., Park, H., Park, D., Lee, Y.S., Choe, J., Hahn, J.H., Lee, H., Kim, Y.M. & Jeoung, D. 2010. Cancer/testis antigen CAGE exerts negative regulation on p53 expression through HDAC2 and confers resistance to anti-cancer drugs. *The Journal of biological chemistry.* 285 (34). pp. 25957-25968.

Kirby, R. 2014. Optimising the management of early prostate cancer. *The Practitioner.* 258 (1770). pp. 15-8, 2.

Kisiel, J.B., Limburg, P.J. & Boardman, L.A. 2016. Colonic Polyps and Colorectal Cancer. *Practical Gastroenterology and Hepatology Board Review Toolkit.* pp. 349.

Kiss, T., Fayet-Lebaron, E. & Jády, B.E. 2010. Box H/ACA small ribonucleoproteins. *Molecular cell.* 37 (5). pp. 597-606.

Koenecke, C., Heim, D., van Biezen, A., Heuser, M., Aljurf, M., Kyrcz-Krzemien, S., Volin, L., de Souza, C., Gedde-Dahl, T. & Sengeloev, H. 2016. Outcome of patients with chronic myeloid leukemia and a low-risk score: allogeneic hematopoietic stem cell transplantation in the era of targeted therapy. A report from the EBMT Chronic Malignancies Working Party. *Bone marrow transplantation.*

Konishi, H., Asano, N., Imatani, A., Kimura, O., Kondo, Y., Jin, X., Kanno, T., Hatta, W., Ara, N., Asanuma, K., Koike, T. & Shimosegawa, T. 2016. Notch1 directly induced CD133 expression in human diffuse type gastric cancers. *Oncotarget.*

Kosaka, T., Mikami, S., Yoshimine, S., Miyazaki, Y., Daimon, T., Kikuchi, E., Miyajima, A. & Oya, M. 2016. The prognostic significance of OCT4 expression in patients with prostate cancer. *Human pathology.* 51 pp. 1-8.

Kozlov, A. 2016. Expression of evolutionarily novel genes in tumors. *Infectious Agents and Cancer.* 11 (1). pp. 34.

Kozłowska, A., Mackiewicz, J. & Mackiewicz, A. 2013. Therapeutic gene modified cell based cancer vaccines. *Gene.* 525 (2). pp. 200-207.

Krishnadas, D.K., Bai, F. & Lucas, K. 2013. Cancer testis antigen and immunotherapy. *ImmunoTargets and Therapy.* 2 pp. 11-19.

Krishnakumar, R., Chen, A.F., Pantovich, M.G., Danial, M., Parchem, R.J., Labosky, P.A. & Blelloch, R. 2016. FOXD3 regulates pluripotent stem cell potential by simultaneously initiating and repressing enhancer activity. *Cell stem cell.* 18 (1). pp. 104-117.

Kuchenbaecker, K., Simard, J., Offit, K., Couch, F.J., Easton, D.F., Chenevix-Trench, G., Antoniou, A.C. & Consortium of Investigators of Modifiers of BRCA1/2 2016. Predicting breast and ovarian cancer risks for BRCA1 and BRCA2 mutation carriers using polygenic risk scores. *Cancer research.* 76 (14 Supplement). pp. 2598-2598.

Kuntz, S., Kieffer, E., Bianchetti, L., Lamoureux, N., Fuhrmann, G. & Viville, S. 2008. Tex19, a mammalian-specific protein with a restricted expression in pluripotent stem cells and germ line. *Stem cells.* 26 (3). pp. 734-744.

Kuo, K., Chou, T., Hsu, H., Chen, W. & Wang, L. 2012a. Prognostic significance of NBS1 and Snail expression in esophageal squamous cell carcinoma. *Annals of surgical oncology.* 19 (3). pp. 549-557.

Kuo, Y., Lin, Y., Chen, H., Wang, Y., Chiou, Y., Lin, H., Pan, H., Wu, C., Su, S. & Hsu, C. 2012b. SEPT12 mutations cause male infertility with defective sperm annulus. *Human mutation.* 33 (4). pp. 710-719.

Kurth, R. & Bannert, N. 2010. Beneficial and detrimental effects of human endogenous retroviruses. *International journal of cancer.* 126 (2). pp. 306-314.

Kuttler, F. & Mai, S. 2006. c-Myc, Genomic Instability and Disease. *Genome dynamics.* 1 pp. 171-190.

Ladomery, M. 2013. Aberrant alternative splicing is another hallmark of cancer. *International journal of cell biology.* 2013 pp. 463786.

Lai, D., Wang, Y., Sun, J., Chen, Y., Li, T., Wu, Y., Guo, L. & Wei, C. 2015. Derivation and characterization of human embryonic stem cells on human amnion epithelial cells. *Scientific reports.* 5.

Lai, J., Robbins, P.F., Raffeld, M., Aung, P.P., Tsokos, M., Rosenberg, S.A., Miettinen, M.M. & Lee, C.R. 2012a. NY-ESO-1 expression in synovial sarcoma and other mesenchymal tumors: significance for NY-ESO-1-based targeted therapy and differential diagnosis. *Modern Pathology.* 25 (6). pp. 854-858.

Lai, Q., Melandro, F., Pinheiro, R.S., Donfrancesco, A., Fadel, B.A., Levi Sandri, G.B., Rossi, M., Berloco, P.B. & Frattaroli, F.M. 2012b. Alpha-fetoprotein and novel tumor biomarkers as predictors of hepatocellular carcinoma recurrence after surgery: a brilliant star raises again. *International journal of hepatology.* 2012.

Lai, T., Wu, Y., Wang, Y., Chen, M., Wang, P., Chen, T., Wu, Y., Chiang, H., Kuo, P. & Lin, Y. 2016. SEPT12–NDC1 Complexes Are Required for Mammalian Spermiogenesis. *International Journal of Molecular Sciences.* 17 (11). pp. 1911.

Lajmi, N., Luetkens, T., Yousef, S., Templin, J., Cao, Y., Hildebrandt, Y., Bartels, K., Kröger, N. & Atanackovic, D. 2015. Cancer-testis antigen MAGEC2 promotes proliferation and resistance to apoptosis in Multiple Myeloma. *British journal of haematology.* 171 (5). pp. 752-762.

Langer, R. & Vacanti, J. 2016. Advances in tissue engineering. *Journal of pediatric surgery.* 51 (1). pp. 8-12.

Lawrence, M.S., Stojanov, P., Mermel, C.H., Robinson, J.T., Garraway, L.A., Golub, T.R., Meyerson, M., Gabriel, S.B., Lander, E.S. & Getz, G. 2014. Discovery and saturation analysis of cancer genes across 21 tumour types. *Nature.* 505 (7484). pp. 495-501.

Lee, S., Oh, S., Do, S., Lee, H., Kang, H., Rho, Y., Bae, W. & Lim, Y. 2014. SOX2 regulates self-renewal and tumorigenicity of stem-like cells of head and neck squamous cell carcinoma. *British journal of cancer.* 111 (11). pp. 2122-2130.

Lee, J. & Hirano, T. 2011. RAD21L, a novel cohesin subunit implicated in linking homologous chromosomes in mammalian meiosis. *The Journal of cell biology.* 192 (2). pp. 263-276.

Levine, A.J., Puzio-Kuter, A.M., Chan, C.S. & Hainaut, P. 2016. The Role of the p53 Protein in Stem-Cell Biology and Epigenetic Regulation. *Cold Spring Harbor perspectives in medicine.*

Li, J., Chen, J., Zeng, T., He, F., Chen, S., Ma, S., Bi, J., Zhu, X. & Guan, X. 2016a. CD133 liver cancer stem cells resist interferon-gamma-induced autophagy. *BMC cancer.* 16 (1). pp. 1.

Li, Y., Liu, B., Lukin, K., Finkelman, F., Hagman, J., Roers, A. & Huang, H. 2016b. GATA2 is critical for mast cell differentiation and maintenance. *The Journal of Immunology.* 196 (1 Supplement). pp. 202.4-202.4.

Lim, R.S., Anand, A., Nishimiya-Fujisawa, C., Kobayashi, S. & Kai, T. 2014. Analysis of Hydra PIWI proteins and piRNAs uncover early evolutionary origins of the piRNA pathway. *Developmental biology.* 386 (1). pp. 237-251.

Lokossou, A.G., Toudic, C. & Barbeau, B. 2014. Implication of human endogenous retrovirus envelope proteins in placental functions. *Viruses.* 6 (11). pp. 4609-4627.

López-Lázaro, M. 2015a. The migration ability of stem cells can explain the existence of cancer of unknown primary site. Rethinking metastasis. *Oncoscience.* 2 (5). pp. 467.

López-Lázaro, M. 2015b. Stem cell division theory of cancer. *Cell Cycle.* 14 (16). pp. 2547-2548.

Lord, C.J. & Ashworth, A. 2016. BRCAness revisited. *Nature Reviews Cancer.*

Lu, X., Sachs, F., Ramsay, L., Jacques, P., Göke, J., Bourque, G. & Ng, H. 2014. The retrovirus HERVH is a long noncoding RNA required for human embryonic stem cell identity. *Nature structural & molecular biology.* 21 (4). pp. 423-425.

Lu, Y. Robbins, P.F. 2016. Cancer immunotherapy targeting neoantigens. *Seminars in immunology.* Elsevier: pp. 22.

Luo, G., Liu, C., Guo, M., Cheng, H., Lu, Y., Jin, K., Liu, L., Long, J., Xu, J. & Lu, R. 2016. Potential Biomarkers in Lewis Negative Patients With Pancreatic Cancer. *Annals of Surgery.*

Mak, A.B., Schnegg, C., Lai, C., Ghosh, S., Yang, M.H., Moffat, J. & Hsu, M. 2014. CD133-targeted niche-dependent therapy in cancer: a multipronged approach. *The American journal of pathology.* 184 (5). pp. 1256-1262.

Makarova-Rusher, O.V., Strauss, J., Ulahannan, S., Kim, C., Del Rivero, J., Duffy, A. & Greten, T.F. 2016. Pretreatment carcinoembryonic antigen levels predict survival in patients with rectal adenocarcinoma. *Cancer research.* 76 (14 Supplement). pp. 5015-5015.

Maluszek, M. 2015. Multifunctionality of MDM2 protein and its role in genomic instability of cancer cells. *Postepy biochemii.* 61 (1). pp. 42-51.

Mansouri, K., Mostafie, A., Rezazadeh, D., Shahlaei, M. & Modarressi, M.H. 2016. New function of TSGA10 gene in angiogenesis and tumor metastasis: a response to a challengeable paradox. *Human molecular genetics.* 25 (2). pp. 233-244.

Marcar, L., Maclaine, N.J., Hupp, T.R. & Meek, D.W. 2010a. Mage-A cancer/testis antigens inhibit p53 function by blocking its interaction with chromatin. *Cancer research.* 70 (24). pp. 10362-10370.

Marcar, L., Maclaine, N.J., Hupp, T.R. & Meek, D.W. 2010b. Mage-A cancer/testis antigens inhibit p53 function by blocking its interaction with chromatin. *Cancer research.* 70 (24). pp. 10362-10370.

Marión, R.M., Strati, K., Li, H., Murga, M., Blanco, R., Ortega, S., Fernandez-Capetillo, O., Serrano, M. & Blasco, M.A. 2009. A p53-mediated DNA damage response limits reprogramming to ensure iPS cell genomic integrity. *Nature.* 460 (7259). pp. 1149-1153.

Martin-Moreno, J.M., Soerjomataram, I. & Magnusson, G. 2008. Cancer causes and prevention: a condensed appraisal in Europe in 2008. *European journal of cancer.* 44 (10). pp. 1390-1403.

Marusyk, A. & Polyak, K. 2010. Tumor heterogeneity: causes and consequences. *Biochimica et Biophysica Acta (BBA)-Reviews on Cancer.* 1805 (1). pp. 105-117.

Mason, P.J. & Bessler, M. 2011. The genetics of dyskeratosis congenita. *Cancer genetics.* 204 (12). pp. 635-645.

Matin, M.M., Walsh, J.R., Gokhale, P.J., Draper, J.S., Bahrami, A.R., Morton, I., Moore, H.D. & Andrews, P.W. 2004. Specific Knockdown of Oct4 and β2-microglobulin Expression by RNA Interference in Human Embryonic Stem Cells and Embryonic Carcinoma Cells. *Stem cells.* 22 (5). pp. 659-668.

Maxfield, K.E., Taus, P.J., Corcoran, K., Wooten, J., Macion, J., Zhou, Y., Borromeo, M., Kollipara, R.K., Yan, J. & Xie, Y. 2015. Comprehensive functional characterization of cancer-testis antigens defines obligate participation in multiple hallmarks of cancer. *Nature communications.* 6.

McFarlane, R.J., Feichtinger, J. & Larcombe, L. 2015. Germline/meiotic genes in cancer: new dimensions. *Cell cycle (Georgetown, Tex.).* 14 (6). pp. 791-792.

McFarlane, S., Coulter, J.A., Tibbits, P., O'Grady, A., McFarlane, C., Montgomery, N., Hill, A., McCarthy, H.O., Young, L.S., Kay, E.W., Isacke, C.M. & Waugh, D.J. 2015. CD44 increases the efficiency of distant metastasis of breast cancer. *Oncotarget.* 6 (13). pp. 11465-11476.

Medvedev, S., Shevchenko, A. & Zakian, S. 2010. Induced pluripotent stem cells: problems and advantages when applying them in regenerative medicine. *Acta Naturae (англоязычная версия).* 2 (2 (5)).

Meek, D.W. & Marcar, L. 2012. MAGE-A antigens as targets in tumour therapy. *Cancer letters.* 324 (2). pp. 126-132.

Melero, I., Gaudernack, G., Gerritsen, W., Huber, C., Parmiani, G., Scholl, S., Thatcher, N., Wagstaff, J., Zielinski, C. & Faulkner, I. 2014. Therapeutic vaccines for cancer: an overview of clinical trials. *Nature reviews Clinical oncology.* 11 (9). pp. 509-524.

Mellman, I., Coukos, G. & Dranoff, G. 2011. Cancer immunotherapy comes of age. *Nature.* 480 (7378). pp. 480-489.

Meng, H., Zheng, P., Wang, X., Liu, C., Sui, H., Wu, S., Zhou, J., Ding, Y. & Li, J. 2010. Over-expression of Nanog predicts tumor progression and poor prognosis in colorectal cancer. *Cancer biology & therapy.* 9 (4). pp. 295-302.

Mishra, A. & Verma, M. 2010. Cancer biomarkers: are we ready for the prime time? *Cancers.* 2 (1). pp. 190-208.

Mitalipov, S. & Wolf, D. 2009. Totipotency, pluripotency and nuclear reprogramming. In: *Engineering of stem cells.* Springer: pp. 185-199.

Moller, H., Flatt, G. & Moran, A. 2011. High cancer mortality rates in the elderly in the UK. *Cancer Epidemiology.* 35 (5). pp. 407-412.

Montagnani, S., Rueger, M.A., Hosoda, T. & Nurzynska, D. 2016. Adult Stem Cells in Tissue Maintenance and Regeneration. *Stem cells international.* 2016.

Mooney, S.M., Rajagopalan, K., Rangarajan, G. & Kulkarni, P. 2016. Cancer/testis antigens and obligate participation in multiple hallmarks of cancer: an update. *Asian Journal of Andrology.* 18 (5). pp. 711-712.

Morris, L.G. & Chan, T.A. 2015. Therapeutic targeting of tumor suppressor genes. *Cancer.* 121 (9). pp. 1357-1368.

Motavaf, M., Pakravan, K., Babashah, S., Malekvandfard, F., Masoumi, M. & Sadeghizadeh, M. 2016. Therapeutic application of mesenchymal stem cell-derived exosomes: A promising cell-free therapeutic strategy in regenerative medicine. *Cellular and molecular biology (Noisy-le-Grand, France).* 62 (7). pp. 74-79.

Muñoz, P., Iliou, M.S. & Esteller, M. 2012. Epigenetic alterations involved in cancer stem cell reprogramming. *Molecular oncology.* 6 (6). pp. 620-636.

Nagata, T., Shimada, Y., Sekine, S., Hori, R., Matsui, K., Okumura, T., Sawada, S., Fukuoka, J. & Tsukada, K. 2014. Prognostic significance of NANOG and KLF4 for breast cancer. *Breast cancer.* 21 (1). pp. 96-101.

Nakagawa, M., Koyanagi, M., Tanabe, K., Takahashi, K., Ichisaka, T., Aoi, T., Okita, K., Mochiduki, Y., Takizawa, N. & Yamanaka, S. 2008. Generation of induced pluripotent stem cells without Myc from mouse and human fibroblasts. *Nature biotechnology.* 26 (1). pp. 101-106.

Nardiello, T., Jungbluth, A.A., Mei, A., Diliberto, M., Huang, X., Dabrowski, A., Andrade, V.C., Wasserstrum, R., Ely, S., Niesvizky, R., Pearse, R., Coleman, M., Jayabalan, D.S., Bhardwaj, N., Old, L.J., Chen-Kiang, S. & Cho, H.J. 2011. MAGE-A inhibits apoptosis in proliferating myeloma cells through repression of Bax and maintenance of survivin. *Clinical cancer research : an official journal of the American Association for Cancer Research.* 17 (13). pp. 4309-4319.

Negri Jr, W.J., Phillips, J.M. & Cree, C. 2016. Review-SI 2016; 2016: e00120 ft. *Science.* 2016.

Negrini, S., Gorgoulis, V.G. & Halazonetis, T.D. 2010a. Genomic instability—an evolving hallmark of cancer. *Nature reviews Molecular cell biology.* 11 (3). pp. 220-228.

Negrini, S., Gorgoulis, V.G. & Halazonetis, T.D. 2010b. Genomic instability—an evolving hallmark of cancer. *Nature reviews Molecular cell biology.* 11 (3). pp. 220-228.

Nelson, P.T., Zhang, P.J., Spagnoli, G.C., Tomaszewski, J.E., Pasha, T.L., Frosina, D., Caballero, O.L., Simpson, A.J., Old, L.J. & Jungbluth, A.A. 2007. Cancer/testis (CT) antigens are expressed in fetal ovary. *Cancer immunity.* 7 pp. 1.

Nguyen, L.V., Vanner, R., Dirks, P. & Eaves, C.J. 2012. Cancer stem cells: an evolving concept. *Nature Reviews Cancer.* 12 (2). pp. 133-143.

Nichols, J., Zevnik, B., Anastassiadis, K., Niwa, H., Klewe-Nebenius, D., Chambers, I., Schöler, H. & Smith, A. 1998. Formation of pluripotent stem cells in the mammalian embryo depends on the POU transcription factor Oct4. *Cell.* 95 (3). pp. 379-391.

Niwa, H., Miyazaki, J. & Smith, A.G. 2000. Quantitative expression of Oct-3/4 defines differentiation, dedifferentiation or self-renewal of ES cells. *Nature genetics.* 24 (4). pp. 372-376.

Novo, C.L., Tang, C., Ahmed, K., Djuric, U., Fussner, E., Mullin, N.P., Morgan, N.P., Hayre, J., Sienerth, A.R., Elderkin, S., Nishinakamura, R., Chambers, I., Ellis, J., Bazett-Jones, D.P. & Rugg-Gunn, P.J. 2016. The pluripotency factor Nanog regulates pericentromeric heterochromatin organization in mouse embryonic stem cells. *Genes & development.* 30 (9). pp. 1101-1115.

Nussler, A. & Sajadian, S.O. 2014. Adult Stem Cells. *Stem Cell Nanoengineering.* pp. 1.

Oba-Shinjo, S.M., Caballero, O.L., Jungbluth, A.A., Rosemberg, S., Old, L.J., Simpson, A.J. & Marie, S.K. 2008. Cancer-testis (CT) antigen expression in medulloblastoma. *Cancer immunity.* 8 pp. 7.

Ohnishi, T., Muroi, M. & Tanamoto, K. 2003. MD-2 is necessary for the toll-like receptor 4 protein to undergo glycosylation essential for its translocation to the cell surface. *Clinical and diagnostic laboratory immunology.* 10 (3). pp. 405-410.

Okamoto, K., Okazawa, H., Okuda, A., Sakai, M., Muramatsu, M. & Hamada, H. 1990. A novel octamer binding transcription factor is differentially expressed in mouse embryonic cells. *Cell.* 60 (3). pp. 461-472.

Okita, K. & Yamanaka, S. 2011. Induced pluripotent stem cells: opportunities and challenges. *Philosophical transactions of the Royal Society of London.Series B, Biological sciences.* 366 (1575). pp. 2198-2207.

Öllinger, R., Childs, A.J., Burgess, H.M., Speed, R.M., Lundegaard, P.R., Reynolds, N., Gray, N.K., Cooke, H.J. & Adams, I.R. 2008. Deletion of the pluripotency-associated Tex19. 1 gene causes activation of endogenous retroviruses and defective spermatogenesis in mice. *PLoS Genet.* 4 (9). pp. e1000199.

Oltean, S. & Bates, D. 2014. Hallmarks of alternative splicing in cancer. *Oncogene.* 33 (46). pp. 5311-5318.

Orkin, S.H., Nathan, D.G., Ginsburg, D., Look, A.T., Fisher, D.E. & Lux IV, S. 2014. *Nathan and Oski's Hematology and Oncology of Infancy and Childhood.* Elsevier Health Sciences: .

Ouyang, L., Shi, Z., Zhao, S., Wang, F., Zhou, T., Liu, B. & Bao, J. 2012. Programmed cell death pathways in cancer: a review of apoptosis, autophagy and programmed necrosis. *Cell proliferation.* 45 (6). pp. 487-498.

Panaud, O. 2016. Horizontal transfers of transposable elements in eukaryotes: The flying genes. *Comptes rendus biologies.*

Park, B., Yoo, K.H. & Kim, C. 2015. Hematopoietic stem cell expansion and generation: the ways to make a breakthrough. *Blood research.* 50 (4). pp. 194-203.

Park, C.S., Shen, Y., Suppipat, K., Tomolonis, J., Puppi, M., Mistretta, T., Ma, L., Green, M. & Lacorazza, D. 2016. KLF4 promotes self-renewal by repressing DYRK2-mediated degradation of c-Myc in leukemic stem cells: development of targeted therapy. *Cancer research.* 76 (14 Supplement). pp. 3334-3334.

Park, T.S., Bhutto, I., Zimmerlin, L., Huo, J.S., Nagaria, P., Miller, D., Rufaihah, A.J., Talbot, C., Aguilar, J., Grebe, R., Merges, C., Reijo-Pera, R., Feldman, R.A., Rassool, F., Cooke, J., Lutty, G. & Zambidis, E.T. 2014. Vascular progenitors from cord blood-derived induced pluripotent stem cells possess augmented capacity for regenerating ischemic retinal vasculature. *Circulation.* 129 (3). pp. 359-372.

Parka, L.S., Hernandez-Ramirez, R.U., Silverberg, M.J., Crothers, K.A. & Dubrow, R. 2016. Prevalence of non-HIV cancer risk factors in persons living with HIV/AIDS. *AIDS.* 30 (2). pp. 273-291.

Passier, R. & Mummery, C. 2003. Origin and use of embryonic and adult stem cells in differentiation and tissue repair. *Cardiovascular research.* 58 (2). pp. 324-335.

Passweg, J., Baldomero, H., Bader, P., Bonini, C., Cesaro, S., Dreger, P., Duarte, R., Dufour, C., Kuball, J. & Farge-Bancel, D. 2016. Hematopoietic stem cell transplantation in Europe 2014: more than 40 000 transplants annually. *Bone marrow transplantation.* 51 (6). pp. 786-792.

Paterson, A.L., Weaver, J.M., Eldridge, M.D., Tavaré, S., Fitzgerald, R.C. & Edwards, P.A. 2015. Mobile element insertions are frequent in oesophageal adenocarcinomas and can mislead paired-end sequencing analysis. *BMC genomics.* 16 (1). pp. 1.

Pfau, S.J. & Amon, A. 2012. Chromosomal instability and aneuploidy in cancer: from yeast to man. *EMBO reports.* 13 (6). pp. 515-527.

Piégu, B., Bire, S., Arensburger, P. & Bigot, Y. 2015. A survey of transposable element classification systems–a call for a fundamental update to meet the challenge of their diversity and complexity. *Molecular phylogenetics and evolution.* 86 pp. 90-109.

Piskareva, O., Ernst, C., Higgins, N. & Schmatchenko, V. 2013. The carboxy-terminal segment of the human LINE-1 ORF2 protein is involved in RNA binding. *FEBS open bio.* 3 (1). pp. 433-437.

Plaks, V., Kong, N. & Werb, Z. 2015. The cancer stem cell niche: how essential is the niche in regulating stemness of tumor cells? *Cell stem cell.* 16 (3). pp. 225-238.

Por, E., Byun, H.J., Lee, E.J., Lim, J.H., Jung, S.Y., Park, I., Kim, Y.M., Jeoung, D.I. & Lee, H. 2010. The cancer/testis antigen CAGE with oncogenic potential stimulates cell proliferation by up-regulating cyclins D1 and E in an AP-1- and E2F-dependent manner. *The Journal of biological chemistry.* 285 (19). pp. 14475-14485.

Prabhu, V.V., Hong, B., Allen, J.E., Zhang, S., Lulla, A.R., Dicker, D.T. & El-Deiry, W.S. 2016. Small-Molecule Prodigiosin Restores p53 Tumor Suppressor Activity in Chemoresistant Colorectal Cancer Stem Cells via c-Jun-Mediated DeltaNp73 Inhibition and p73 Activation. *Cancer research.* 76 (7). pp. 1989-1999.

Praud, D., Rota, M., Rehm, J., Shield, K., Zatoński, W., Hashibe, M., La Vecchia, C. & Boffetta, P. 2016. Cancer incidence and mortality attributable to alcohol consumption. *International Journal of Cancer.* 138 (6). pp. 1380-1387.

Prince, M.E., Sivanandan, R., Kaczorowski, A., Wolf, G.T., Kaplan, M.J., Dalerba, P., Weissman, I.L., Clarke, M.F. & Ailles, L.E. 2007. Identification of a subpopulation of cells with cancer stem cell properties in head and neck

squamous cell carcinoma. *Proceedings of the National Academy of Sciences of the United States of America.* 104 (3). pp. 973-978.

Rahman, M., Jamil, H.M., Akhtar, N., Rahman, K., Islam, R. & Asaduzzaman, S. 2016. STEM CELL AND CANCER STEM CELL: A Tale of Two Cells. *Progress in Stem Cell.* 3 (2). pp. 97-108.

Ramalho-Santos, M. & Willenbring, H. 2007. On the origin of the term "stem cell". *Cell stem cell.* 1 (1). pp. 35-38.

Ravasio, R., Ceccacci, E. & Minucci, S. 2016. Self-renewal of tumor cells: epigenetic determinants of the cancer stem cell phenotype. *Current opinion in genetics & development.* 36 pp. 92-99.

Reichmann, J., Reddington, J.P., Best, D., Read, D., Ollinger, R., Meehan, R.R. & Adams, I.R. 2013. The genome-defence gene Tex19.1 suppresses LINE-1 retrotransposons in the placenta and prevents intra-uterine growth retardation in mice. *Human molecular genetics.* 22 (9). pp. 1791-1806.

Ren, B., Wei, X., Zou, G., He, J., Xu, G., Xu, F., Huang, Y., Zhu, H., Li, Y. & Ma, G. 2016. Cancer testis antigen SPAG9 is a promising marker for the diagnosis and treatment of lung cancer. *Oncology reports.* 35 (5). pp. 2599-2605.

Restifo, N.P., Dudley, M.E. & Rosenberg, S.A. 2012. Adoptive immunotherapy for cancer: harnessing the T cell response. *Nature Reviews Immunology.* 12 (4). pp. 269-281.

Rizzino, A. & Wuebben, E.L. 2016. Sox2/Oct4: A delicately balanced partnership in pluripotent stem cells and embryogenesis. *Biochimica et Biophysica Acta (BBA)-Gene Regulatory Mechanisms.* 1859 (6). pp. 780-791.

Robles, V., Herráez, P., Labbé, C., Cabrita, E., Pšenička, M., Valcarce, D.G. & Riesco, M.F. 2016. Molecular basis of spermatogenesis and sperm quality. *General and comparative endocrinology.*

Rodenhuis, S. 1992. Ras and Human Tumors. *Seminars in cancer biology.* 3 (4). pp. 241-247.

Rosner, M.H., Vigano, M.A., Ozato, K., Timmons, P.M., Poirie, F., Rigby, P.W. & Staudt, L.M. 1990. A POU-domain transcription factor in early stem cells and germ cells of the mammalian embryo. *Nature.* 345 (6277). pp. 686-692.

Rousseaux, S., Debernardi, A., Jacquiau, B., Vitte, A.L., Vesin, A., Nagy-Mignotte, H., Moro-Sibilot, D., Brichon, P.Y., Lantuejoul, S., Hainaut, P., Laffaire, J., de Reynies, A., Beer, D.G., Timsit, J.F., Brambilla, C., Brambilla, E. & Khochbin, S. 2013. Ectopic activation of germline and placental genes identifies aggressive metastasis-prone lung cancers. *Science translational medicine.* 5 (186). pp. 186ra66.

Roy, S., K Narang, B., K Rastogi, S. & K Rawal, R. 2015. A novel multiple tyrosine-kinase targeted agent to explore the future perspectives of anti-angiogenic therapy for the treatment of multiple solid tumors: cabozantinib. *Anti-Cancer Agents in Medicinal Chemistry (Formerly Current Medicinal Chemistry-Anti-Cancer Agents).* 15 (1). pp. 37-47.

Sahin, U., Türeci, Ö & Pfreundschuh, M. 1997. Serological identification of human tumor antigens. *Current opinion in immunology.* 9 (5). pp. 709-716.

Salmaninejad, A., Zamani, M.R., Pourvahedi, M., Golchehre, Z., Bereshneh, A.H. & Rezaei, N. 2016. Cancer/Testis Antigens: Expression, Regulation, Tumor Invasion, and Use in Immunotherapy of Cancers. *Immunological investigations.* pp. 1-22.

Sammut, S.J., Feichtinger, J., Stuart, N., Wakeman, J.A., Larcombe, L. & McFarlane, R.J. 2014. A novel cohort of cancer-testis biomarker genes revealed through meta-analysis of clinical data sets. *Oncoscience.* 1 (5). pp. 349-359.

Sato, N., Sanjuan, I.M., Heke, M., Uchida, M., Naef, F. & Brivanlou, A.H. 2003. Molecular signature of human embryonic stem cells and its comparison with the mouse. *Developmental biology.* 260 (2). pp. 404-413.

Sato, S., Tang, Y.J., Wei, Q., Hirata, M., Weng, A., Han, I., Okawa, A., Takeda, S., Whetstone, H. & Nadesan, P. 2016. Mesenchymal Tumors Can Derive from Ng2/Cspg4-Expressing Pericytes with β-Catenin Modulating the Neoplastic Phenotype. *Cell reports.* 16 (4). pp. 917-927.

Saunders, A., Faiola, F. & Wang, J. 2013. Concise review: pursuing self-renewal and pluripotency with the stem cell factor Nanog. *Stem cells.* 31 (7). pp. 1227-1236.

Savage, P.A., Leventhal, D.S. & Malchow, S. 2014. Shaping the repertoire of tumor-infiltrating effector and regulatory T cells. *Immunological reviews.* 259 (1). pp. 245-258.

Scadden, D.T. 2006. The stem-cell niche as an entity of action. *Nature.* 441 (7097). pp. 1075-1079.

Scanlan, M.J., Simpson, A.J. & Old, L.J. 2004. The cancer/testis genes: review, standardization, and commentary. *Cancer Immunity Archive.* 4 (1). pp. 1.

Scarola, M., Comisso, E., Pascolo, R., Chiaradia, R., Marion, R.M., Schneider, C., Blasco, M.A., Schoeftner, S. & Benetti, R. 2015. Epigenetic silencing of Oct4 by a complex containing SUV39H1 and Oct4 pseudogene lncRNA. *Nature communications.* 6.

Schoenhals, M., Kassambara, A., De Vos, J., Hose, D., Moreaux, J. & Klein, B. 2009. Embryonic stem cell markers expression in cancers. *Biochemical and biophysical research communications.* 383 (2). pp. 157-162.

Scholer, H.R. 2004. The potential of stem cells. An inventory. *BUNDESGESUNDHEITSBLATT GESUNDHEITSFORSCHUNG GESUNDHEITSSCHUTZ.* 47 (6). pp. 565-577.

Scholer, H.R., Dressler, G.R., Balling, R., Rohdewohld, H. & Gruss, P. 1990. Oct-4: a germline-specific transcription factor mapping to the mouse t-complex. *The EMBO journal.* 9 (7). pp. 2185-2195.

Schramm, S., Fraune, J., Naumann, R., Hernandez-Hernandez, A., Höög, C., Cooke, H.J., Alsheimer, M. & Benavente, R. 2011. A novel mouse synaptonemal complex protein is essential for loading of central element proteins, recombination, and fertility. *PLoS Genet.* 7 (5). pp. e1002088.

Schuster, M., Nechansky, A. & Kircheis, R. 2006. Cancer immunotherapy. *Biotechnology journal.* 1 (2). pp. 138-147.

Schütze, M., Boeing, H., Pischon, T., Rehm, J., Kehoe, T., Gmel, G., Olsen, A., Tjønneland, A.M., Dahm, C.C. & Overvad, K. 2011. Alcohol attributable burden of incidence of cancer in eight European countries based on results from prospective cohort study. *BMJ: British Medical Journal.* 342.

Schwartz, S.D., Regillo, C.D., Lam, B.L., Eliott, D., Rosenfeld, P.J., Gregori, N.Z., Hubschman, J., Davis, J.L., Heilwell, G. & Spirn, M. 2015. Human embryonic stem cell-derived retinal pigment epithelium in patients with age-related macular degeneration and Stargardt's macular dystrophy: follow-up of two open-label phase 1/2 studies. *The Lancet.* 385 (9967). pp. 509-516.

Schwarzenbach, H., Eichelser, C., Steinbach, B., Tadewaldt, J., Pantel, K., Lobanenkov, V. & Loukinov, D. 2014. Differential regulation of MAGE-A1 promoter activity by BORIS and Sp1, both interacting with the TATA binding protein. *BMC cancer.* 14 (1). pp. 1.

Seipel, K., Marques, M.T., Bozzini, M.A., Meinken, C., Mueller, B.U. & Pabst, T. 2016. Inactivation of the p53-KLF4-CEBPA Axis in Acute Myeloid Leukemia. *Clinical cancer research : an official journal of the American Association for Cancer Research.* 22 (3). pp. 746-756.

Seita, J. & Weissman, I.L. 2010. Hematopoietic stem cell: self-renewal versus differentiation. *Wiley Interdisciplinary Reviews: Systems Biology and Medicine.* 2 (6). pp. 640-653.

Selvaraj, V., Plane, J.M., Williams, A.J. & Deng, W. 2010. Switching cell fate: the remarkable rise of induced pluripotent stem cells and lineage reprogramming technologies. *Trends in biotechnology.* 28 (4). pp. 214-223.

Shang, B., Gao, A., Pan, Y., Zhang, G., Tu, J., Zhou, Y., Yang, P., Cao, Z., Wei, Q. & Ding, Y. 2014. CT45A1 acts as a new proto-oncogene to trigger tumorigenesis and cancer metastasis. *Cell death & disease.* 5 (6). pp. e1285.

Sharma, S., Javadekar, S., Pandey, M., Srivastava, M., Kumari, R. & Raghavan, S. 2015. Homology and enzymatic requirements of microhomology-dependent alternative end joining. *Cell death & disease.* 6 (3). pp. e1697.

Sharma, S., Kelly, T.K. & Jones, P.A. 2010. Epigenetics in cancer. *Carcinogenesis.* 31 (1). pp. 27-36.

She, Z. & Yang, W. 2015. SOX family transcription factors involved in diverse cellular events during development. *European journal of cell biology.* 94 (12). pp. 547-563.

Shi, G. & Jin, Y. 2010. Role of Oct4 in maintaining and regaining stem cell pluripotency. *Stem cell research & therapy.* 1 (5). pp. 1.

Shirai, H. & Mandai, M. 2016. Retinal regeneration by transplantation of retinal tissue derived from human embryonic or induced pluripotent stem cells. *Inflammation and Regeneration.* 36 (1). pp. 1.

Shono, Y., Docampo, M.D., Peled, J.U., Perobelli, S.M., Velardi, E., Tsai, J.J., Slingerland, A.E., Smith, O.M., Young, L.F. & Gupta, J. 2016. Increased GVHD-related mortality with broad-spectrum antibiotic use after allogeneic hematopoietic stem cell transplantation in human patients and mice. *Science translational medicine.* 8 (339). pp. 339ra71-339ra71.

Shufaro, Y. & Reubinoff, B.E. 2004. Therapeutic applications of embryonic stem cells. *Best Practice & Research Clinical Obstetrics & Gynaecology.* 18 (6). pp. 909-927.

Shukla, R., Upton, K.R., Muñoz-Lopez, M., Gerhardt, D.J., Fisher, M.E., Nguyen, T., Brennan, P.M., Baillie, J.K., Collino, A. & Ghisletti, S. 2013. Endogenous retrotransposition activates oncogenic pathways in hepatocellular carcinoma. *Cell.* 153 (1). pp. 101-111.

Siegel, R., Naishadham, D. & Jemal, A. 2013. Cancer statistics, 2013. *CA: a cancer journal for clinicians.* 63 (1). pp. 11-30.

Silva, J., Nichols, J., Theunissen, T.W., Guo, G., van Oosten, A.L., Barrandon, O., Wray, J., Yamanaka, S., Chambers, I. & Smith, A. 2009. Nanog is the gateway to the pluripotent ground state. *Cell.* 138 (4). pp. 722-737.

Simpson, A.J., Caballero, O.L., Jungbluth, A., Chen, Y. & Old, L.J. 2005. Cancer/testis antigens, gametogenesis and cancer. *Nature Reviews Cancer.* 5 (8). pp. 615-625.

Singh, A., Singh, D.K. & Bhoria, U. 2015. Induced pluripotent stem cells: An update. *International Journal of Blood transfusion and Immunohematology.* 5 pp. 6-13.

Singh, V.K., Saini, A., Kalsan, M., Kumar, N. & Chandra, R. 2016. Describing the Stem Cell Potency: The Various Methods of Functional Assessment and In silico Diagnostics. *Frontiers in Cell and Developmental Biology.* 4.

Siu, M., Wong, E., Kong, D., Chan, H., Jiang, L., Wong, O., Lam, E.W., Chan, K., Ngan, H. & Le, X. 2013. Stem cell transcription factor NANOG controls cell migration and invasion via dysregulation of E-cadherin and FoxJ1 and contributes to adverse clinical outcome in ovarian cancers. *Oncogene.* 32 (30). pp. 3500-3509.

Slotkin, E., de Stanchina, E., Cartegni, L., Ladanyi, M. & Spraggon, L. 2016. Abstract B26: Therapeutic targeting of sarcomas driven by EWSR1 fusion oncogenes by modulation of the fusion oncogene pre-mRNA. *Cancer research.* 76 (5 Supplement). pp. B26-B26.

Solit, D.B., Garraway, L.A., Pratilas, C.A., Sawai, A., Getz, G., Basso, A., Ye, Q., Lobo, J.M., She, Y. & Osman, I. 2006. BRAF mutation predicts sensitivity to MEK inhibition. *Nature.* 439 (7074). pp. 358-362.

Solyom, S., Ewing, A.D., Rahrmann, E.P., Doucet, T., Nelson, H.H., Burns, M.B., Harris, R.S., Sigmon, D.F., Casella, A., Erlanger, B., Wheelan, S., Upton, K.R., Shukla, R., Faulkner, G.J., Largaespada, D.A. & Kazazian, H.H.,Jr 2012. Extensive somatic L1 retrotransposition in colorectal tumors. *Genome research.* 22 (12). pp. 2328-2338.

Song, M., Kim, Y., Lee, J., Lee, C. & Lee, S. 2016. Cancer/testis antigen NY-SAR-35 enhances cell proliferation, migration, and invasion. *International journal of oncology.* 48 (2). pp. 569-576.

Song, M. & Giovannucci, E.L. 2015. Cancer risk: many factors contribute. *Science (New York, N.Y.).* 347 (6223). pp. 728-729.

Sonnenschein, C. & Soto, A.M. 2013. The aging of the 2000 and 2011 Hallmarks of Cancer reviews: a critique. *Journal of Biosciences.* 38 (3). pp. 651-663.

Souhami, R.L. & Tobias, J.S. 2005. *Cancer and its management.* 5th ed. Blackwell Pub: Malden, Mass.

Srivastava, P., Paluch, B.E., Matsuzaki, J., James, S.R., Collamat-Lai, G., Blagitko-Dorfs, N., Ford, L.A., Naqash, R., Lubbert, M., Karpf, A.R., Nemeth, M.J. & Griffiths, E.A. 2016. Induction of cancer testis antigen expression in circulating acute myeloid leukemia blasts following hypomethylating agent monotherapy. *Oncotarget.* 7 (11). pp. 12840-12856.

Stevenson, B.J., Iseli, C., Panji, S., Zahn-Zabal, M., Hide, W., Old, L.J., Simpson, A.J. & Jongeneel, C.V. 2007. Rapid evolution of cancer/testis genes on the X chromosome. *Bmc Genomics.* 8 (1). pp. 1.

Stoltz, J., de Isla, N., Li, Y., Bensoussan, D., Zhang, L., Huselstein, C., Chen, Y., Decot, V., Magdalou, J. & Li, N. 2015. Stem cells and regenerative medicine: myth or reality of the 21th century. *Stem Cells Int.* 2015 (3). pp. 734731.

Story, E. & Johnston, D. 2016. Multiple Metastatic Somatic Tissue Ganglioneuroma from a Primary Adrenal Ganglioneuro blastoma in a Pediatric Patient. *Cancer Res Oncol.* 2 (005).

Stoye, J.P. 2012. Studies of endogenous retroviruses reveal a continuing evolutionary saga. *Nature Reviews Microbiology.* 10 (6). pp. 395-406.

Stratton, M.R., Campbell, P.J. & Futreal, P.A. 2009a. The cancer genome. *Nature.* 458 (7239). pp. 719-724.

Stratton, M.R., Campbell, P.J. & Futreal, P.A. 2009b. The cancer genome. *Nature.* 458 (7239). pp. 719-724.

Sulek, J., Goliadze, E., Zhou, S., Manjili, M.H., Toor, A. & Guruli, G. 2016. The Expression of Cancer/Testis Antigens in Kidney and Bladder Malignancies. *Archives of Medicine.*

Surani, A. & Tischler, J. 2012. Stem cells: a sporadic super state. *Nature.* 487 (7405). pp. 43-45.

Surget, S., Khoury, M.P. & Bourdon, J. 2014. Uncovering the role of p53 splice variants in human malignancy: a clinical perspective. *Onco Targets Ther.* 7 pp. 57-68.

Tabar, V.S. 2016. 133 The Development of Human Embryonic Stem Cell-Derived Dopamine Neurons for Clinical Use in Parkinson Disease. *Neurosurgery.* 63 pp. 154-155.

Takahashi, K., Tanabe, K., Ohnuki, M., Narita, M., Ichisaka, T., Tomoda, K. & Yamanaka, S. 2007. Induction of pluripotent stem cells from adult human fibroblasts by defined factors. *Cell.* 131 (5). pp. 861-872.

Takahashi, K. & Yamanaka, S. 2006. Induction of pluripotent stem cells from mouse embryonic and adult fibroblast cultures by defined factors. *Cell.* 126 (4). pp. 663-676.

Takebe, T., Sekine, K., Enomura, M., Koike, H., Kimura, M., Ogaeri, T., Zhang, R., Ueno, Y., Zheng, Y. & Koike, N. 2013. Vascularized and functional human liver from an iPSC-derived organ bud transplant. *Nature.* 499 (7459). pp. 481-484.

Tarabay, Y., Kieffer, E., Teletin, M., Celebi, C., Van Montfoort, A., Zamudio, N., Achour, M., El Ramy, R., Gazdag, E., Tropel, P., Mark, M., Bourc'his, D. & Viville, S. 2013. The mammalian-specific Tex19.1 gene plays an essential role in spermatogenesis and placenta-supported development. *Human reproduction (Oxford, England).* 28 (8). pp. 2201-2214.

Tarnowski, M., Czerewaty, M., Deskur, A., Safranow, K., Marlicz, W., Urasińska, E., Ratajczak, M.Z. & Starzyńska, T. 2016. Expression of Cancer Testis Antigens in Colorectal Cancer: New Prognostic and Therapeutic Implications. *Disease markers.* 2016.

Taswell, C. 1987. Limiting dilution assays for the separation, characterization, and quantitation of biologically active particles and their clonal progeny. *Cell separation: methods and selected applications.* 4 (6). pp. 109-145.

Tauchi, H. 2000. Positional cloning and functional analysis of the gene responsible for Nijmegen breakage syndrome, NBS1. *Journal of radiation research.* 41 (1). pp. 9-17.

Thoma, C.R., Toso, A., Meraldi, P. & Krek, W. 2011. Mechanisms of aneuploidy and its suppression by tumour suppressor proteins. *Swiss medical weekly.* 141 pp. w13170.

Thomson, J.A., Itskovitz-Eldor, J., Shapiro, S.S., Waknitz, M.A., Swiergiel, J.J., Marshall, V.S. & Jones, J.M. 1998. Embryonic stem cell lines derived from human blastocysts. *Science (New York, N.Y.).* 282 (5391). pp. 1145-1147.

Tiernan, J., Perry, S., Verghese, E., West, N., Yeluri, S., Jayne, D. & Hughes, T. 2013. Carcinoembryonic antigen is the preferred biomarker for in vivo colorectal cancer targeting. *British journal of cancer.* 108 (3). pp. 662-667.

Till, J.E. & McCulloch, E.A. 1961. A direct measurement of the radiation sensitivity of normal mouse bone marrow cells. *Radiation research.* 14 (2). pp. 213-222.

Tiwari, A., Moeneclaey, G., Jenkin, G. & Kirkland, M.A. 2016. Exploring Life Saving Potential of Umbilical Cord Blood Derived Hematopoietic Stem Cells. *Insights in Stem Cells.*

Tomasetti, C., Vogelstein, B. & Parmigiani, G. 2013. Half or more of the somatic mutations in cancers of self-renewing tissues originate prior to tumor initiation. *Proceedings of the National Academy of Sciences of the United States of America.* 110 (6). pp. 1999-2004.

Trego, K.S., Groesser, T., Davalos, A.R., Parplys, A.C., Zhao, W., Nelson, M.R., Hlaing, A., Shih, B., Rydberg, B. & Pluth, J.M. 2016. Non-catalytic Roles for XPG with BRCA1 and BRCA2 in Homologous Recombination and Genome Stability. *Molecular cell.* 61 (4). pp. 535-546.

TUreci, O., Chen, Y., Sahin, U., GUre, A.O., Zwick, C., Villena, C., Tsang, S., Seitz, G., Old, L. & Pfreundschuh, M. 1998. Expression of SSX genes in human tumors. *International Journal of Cancer.* 77 (1). pp. 19-23.

Tureci, O., Sahin, U., Zwick, C., Koslowski, M., Seitz, G. & Pfreundschuh, M. 1998. Identification of a meiosis-specific protein as a member of the class of cancer/testis antigens. *Proceedings of the National Academy of Sciences of the United States of America.* 95 (9). pp. 5211-5216.

Ullah, N., Liaqat, S., Fatima, S., Zehra, F., Anwer, M. & Sadiq, M. 2016. Stem cells and cancer: A review. *Asian Pacific Journal of Tropical Disease.* 6 (5). pp. 406-419.

Valastyan, S. & Weinberg, R.A. 2011. Tumor metastasis: molecular insights and evolving paradigms. *Cell.* 147 (2). pp. 275-292.

van der Bruggen, P. & Traversari, C. 1991. A gene encoding an antigen recognized by cytolytic T lymphocytes on a human melanoma. Science. 254 (5038). pp. 1643.

Vassetzky, N.S. & Kramerov, D.A. 2013. SINEBase: a database and tool for SINE analysis. *Nucleic acids research.* 41 (Database issue). pp. D83-9.

Vatolin, S., Abdullaev, Z., Pack, S.D., Flanagan, P.T., Custer, M., Loukinov, D.I., Pugacheva, E., Hong, J.A., Morse, H.,3rd, Schrump, D.S., Risinger, J.I., Barrett, J.C. & Lobanenkov, V.V. 2005. Conditional expression of the CTCF-paralogous transcriptional factor BORIS in normal cells results in demethylation and derepression of MAGE-A1 and reactivation of other cancer-testis genes. *Cancer research.* 65 (17). pp. 7751-7762.

Vidal, S., Rodriguez-Bravo, V., Galsky, M., Cordon-Cardo, C. & Domingo-Domenech, J. 2014. Targeting cancer stem cells to suppress acquired chemotherapy resistance. *Oncogene.* 33 (36). pp. 4451-4463.

Vigneron, N. 2015. Human tumor antigens and cancer immunotherapy. *BioMed research international.* 2015.

Vogelstein, B. & Kinzler, K.W. 2004. Cancer genes and the pathways they control. *Nature medicine.* 10 (8). pp. 789-799.

Vogelstein, B., Papadopoulos, N., Velculescu, V.E., Zhou, S., Diaz, L.A.,Jr & Kinzler, K.W. 2013. Cancer genome landscapes. *Science (New York, N.Y.).* 339 (6127). pp. 1546-1558.

Walmsley, G.G., Ransom, R.C., Zielins, E.R., Leavitt, T., Flacco, J.S., Hu, M.S., Lee, A.S., Longaker, M.T. & Wan, D.C. 2016. Stem Cells in Bone Regeneration. *Stem Cell Reviews and Reports.* pp. 1-6.

Wang, C., Gu, Y., Zhang, K., Xie, K., Zhu, M., Dai, N., Jiang, Y., Guo, X., Liu, M. & Dai, J. 2016a. Systematic identification of genes with a cancer-testis expression pattern in 19 cancer types. *Nature communications.* 7.

Wang, D., Wang, J., Ding, N., Li, Y., Yang, Y., Fang, X. & Zhao, H. 2016b. MAGE-A1 promotes melanoma proliferation and migration through C-JUN activation. *Biochemical and biophysical research communications.* 473 (4). pp. 959-965.

Wang, Y., Li, M., Long, J., Shi, X., Li, Q., Chen, J., Tong, W., Jia, J. & Huang, J. 2014. Clinical significance of increased expression of Nijmegen breakage syndrome gene (NBS1) in human primary liver cancer. *Hepatology international.* 8 (2). pp. 250-259.

Wang, Z., Oron, E., Nelson, B., Razis, S. & Ivanova, N. 2012. Distinct lineage specification roles for NANOG, OCT4, and SOX2 in human embryonic stem cells. *Cell stem cell.* 10 (4). pp. 440-454.

Wang, B.B., Li, Z.J., Zhang, F.F., Hou, H.T., Yu, J.K. & Li, F. 2016c. Clinical significance of stem cell marker CD133 expression in colorectal cancer. *Histology and histopathology.* 31 (3). pp. 299-306.

Wang, C. & Meier, U.T. 2004. Architecture and assembly of mammalian H/ACA small nucleolar and telomerase ribonucleoproteins. *The EMBO journal.* 23 (8). pp. 1857-1867.

Wang-Johanning, F., Frost, A.R., Johanning, G.L., Khazaeli, M.B., LoBuglio, A.F., Shaw, D.R. & Strong, T.V. 2001. Expression of human endogenous retrovirus k envelope transcripts in human breast cancer. *Clinical cancer research : an official journal of the American Association for Cancer Research.* 7 (6). pp. 1553-1560.

Ward, A., Hopkins, J., Mckay, M., Murray, S. & Jordan, P.W. 2016. Genetic Interactions Between the Meiosis-Specific Cohesin Components, STAG3, REC8, and RAD21L. *G3 (Bethesda, Md.).* 6 (6). pp. 1713-1724.

Washio, M., Mori, M., Mikami, K., Miki, T., Watanabe, Y., Nakao, M., Kubo, T., Suzuki, K., Ozasa, K., Wakai, K. & Tamakoshi, A. 2016. Risk Factors for Upper and Lower Urinary Tract Cancer Death in a Japanese Population: Findings from the Japan Collaborative Cohort Study for Evaluation of Cancer Risk (JACC Study). *Asian Pacific journal of cancer prevention : APJCP.* 17 (7). pp. 3545-3549.

Weinberg, R. 2013. *The biology of cancer.* Garland science: .

Weon, J.L. & Potts, P.R. 2015. The MAGE protein family and cancer. *Current opinion in cell biology.* 37 pp. 1-8.

Whitehurst, A.W. 2014. Cause and consequence of cancer/testis antigen activation in cancer. *Annual Review of Pharmacology and Toxicology.* 54 pp. 251-272.

Wicker, T., Sabot, F., Hua-Van, A., Bennetzen, J.L., Capy, P., Chalhoub, B., Flavell, A., Leroy, P., Morgante, M. & Panaud, O. 2007. A unified classification system for eukaryotic transposable elements. *Nature Reviews Genetics.* 8 (12). pp. 973-982.

Wodarz, D. & Zauber, A.G. 2015. Cancer: Risk factors and random chances. *Nature.* 517 (7536). pp. 563-564.

Woo, D., Hwang, H.S. & Shim, J.H. 2016. Comparison of adult stem cells derived from multiple stem cell niches. *Biotechnology Letters.* 38 (5). pp. 751-759.

Wright, A.J. & Andrews, P.W. 2009. Surface marker antigens in the characterization of human embryonic stem cells. *Stem cell research.* 3 (1). pp. 3-11.

Wu, G. & Schöler, H.R. 2014. Role of Oct4 in the early embryo development. *Cell Regeneration.* 3 (1). pp. 1.

Wu, L. & Qu, X. 2015. Cancer biomarker detection: recent achievements and challenges. *Chemical Society Reviews.* 44 (10). pp. 2963-2997.

Xu, H., Wu, Q., Dang, S., Jin, M., Xu, J., Cheng, Y., Pan, M., Wu, Y., Zhang, C. & Zhang, Y. 2011. Alteration of CXCR7 expression mediated by TLR4 promotes tumor cell proliferation and migration in human colorectal carcinoma. *PloS one.* 6 (12). pp. e27399.

Yamada, R., Takahashi, A., Torigoe, T., Morita, R., Tamura, Y., Tsukahara, T., Kanaseki, T., Kubo, T., Watarai, K. & Kondo, T. 2013. Preferential expression of cancer/testis genes in cancer stem-like cells: proposal of a novel sub-category, cancer/testis/stem gene. *Tissue antigens.* 81 (6). pp. 428-434.

Yamada, T. & Ohta, K. 2013. Initiation of meiotic recombination in chromatin structure. *Journal of Biochemistry.* 154 (2). pp. 107-114.

Yang, F., Cheng, Y., An, J.Y., Kwon, Y.T., Eckardt, S., Leu, N.A., McLaughlin, K.J. & Wang, P.J. 2010. The ubiquitin ligase Ubr2, a recognition E3 component of the N-end rule pathway, stabilizes Tex19. 1 during spermatogenesis. *PloS one.* 5 (11). pp. e14017.

Yang, P., Huo, Z., Liao, H. & Zhou, Q. 2015. Cancer/testis antigens trigger epithelial-mesenchymal transition and genesis of cancer stem-like cells. *Current pharmaceutical design.* 21 (10). pp. 1292-1300.

Yang, X.A., Dong, X.Y., Qiao, H., Wang, Y.D., Peng, J.R., Li, Y., Pang, X.W., Tian, C. & Chen, W.F. 2005. Immunohistochemical analysis of the expression of FATE/BJ-HCC-2 antigen in normal and malignant tissues. *Laboratory investigation.* 85 (2). pp. 205-213.

Ye, S., Zhang, D., Cheng, F., Wilson, D., Mackay, J., He, K., Ban, Q., Lv, F., Huang, S., Liu, D. & Ying, Q.L. 2016. Wnt/beta-catenin and LIF-Stat3 signaling pathways converge on Sp5 to promote mouse embryonic stem cell self-renewal. *Journal of cell science.* 129 (2). pp. 269-276.

Yoshida, K. & Miki, Y. 2004. Role of BRCA1 and BRCA2 as regulators of DNA repair, transcription, and cell cycle in response to DNA damage. *Cancer science.* 95 (11). pp. 866-871.

Young, R.A. 2011. Control of the embryonic stem cell state. *Cell.* 144 (6). pp. 940-954.

Yu, J., Hu, K., Smuga-Otto, K., Tian, S., Stewart, R., Slukvin, I.I. & Thomson, J.A. 2009. Human induced pluripotent stem cells free of vector and transgene sequences. *Science (New York, N.Y.).* 324 (5928). pp. 797-801.

Zaehres, H., Lensch, M.W., Daheron, L., Stewart, S.A., Itskovitz-Eldor, J. & Daley, G.Q. 2005. High-efficiency RNA interference in human embryonic stem cells. *Stem cells.* 23 (3). pp. 299-305.

Zafarana, G., Avery, S.R., Avery, K., Moore, H.D. & Andrews, P.W. 2009. Specific knockdown of OCT4 in human embryonic stem cells by inducible short hairpin RNA interference. *Stem cells.* 27 (4). pp. 776-782.

Zamuner, F.T., Karia, B.T., de Oliveira, C.Z., Santos, C.R., Carvalho, A.L. & Vettore, A.L. 2015. A Comprehensive Expression Analysis of Cancer Testis Antigens in Head and Neck Squamous Cell Carcinoma Revels MAGEA3/6 as a Marker for Recurrence. *Molecular cancer therapeutics.* 14 (3). pp. 828-834.

Zavala, V.A. & Kalergis, A.M. 2015. New clinical advances in immunotherapy for the treatment of solid tumours. *Immunology.* 145 (2). pp. 182-201.

Zhang, J., Gao, Y., Yu, M., Wu, H., Ai, Z., Wu, Y., Liu, H., Du, J., Guo, Z. & Zhang, Y. 2015a. Retinoic acid induces embryonic stem cell differentiation by altering both encoding RNA and microRNA expression. *PloS one.* 10 (7). pp. e0132566.

Zhang, W., Barger, C.J., Eng, K.H., Klinkebiel, D., Link, P.A., Omilian, A., Bshara, W., Odunsi, K. & Karpf, A.R. 2016. PRAME expression and promoter hypomethylation in epithelial ovarian cancer. *Oncotarget.* 7 (29). pp. 45352-45369.

Zhang, K., Shen, Z., Liang, X., Liu, T., Wang, T. & Jiang, Y. 2014. Down-regulation of GPR137 expression inhibits proliferation of colon cancer cells. *Acta biochimica et biophysica Sinica.* 46 (11). pp. 935-941.

Zhang, S., Zhou, L., Hong, B., van den Heuvel, A.P., Prabhu, V.V., Warfel, N.A., Kline, C.L., Dicker, D.T., Kopelovich, L. & El-Deiry, W.S. 2015b. Small-Molecule NSC59984 Restores p53 Pathway Signaling and Antitumor Effects against Colorectal Cancer via p73 Activation and Degradation of Mutant p53. *Cancer research.* 75 (18). pp. 3842-3852.

Zhong, J., Chen, Y., Liao, X., Li, J., Wang, H., Wu, C., Zou, X., Yang, G., Shi, J. & Luo, L. 2016. Testis expressed 19 is a novel cancer-testis antigen expressed in bladder cancer. *Tumor Biology.* pp. 1-9.

Zong, G., Wang, H., Li, J., Xie, Y., Bian, E. & Zhao, B. 2014. Inhibition of GPR137 expression reduces the proliferation and colony formation of malignant glioma cells. *Neurological Sciences.* 35 (11). pp. 1707-1714.

9. Appendix

"Human germ/stem cell-specific gene *TEX19* influences cancer cell proliferation and cancer prognosis". (Published in BIOMED-MOLECULAR CANCER- 2017)